DAFNE JÁCOME SANZ

Proprotein Convertase Subtilisin/kexin Type 9 (PCSK9) Enzyme in Immunity and Cancer

DAFNE JÁCOME SANZ

Proprotein Convertase Subtilisin/kexin Type 9 (PCSK9) Enzyme in Immunity and Cancer

ACADEMIC DISSERTATION
To be presented, with the permission of
the Faculty of Medicine and Health Technology
of Tampere University,
for public discussion in the Yellow Hall (F025)
of the Arvo building, Arvo Ylpön katu 34, 33520 Tampere,
on 13th of October, at 12 o'clock.

The originality of this thesis has been checked using the Turnitin OriginalityCheck service.

Cover design: Roihu Inc.

HIILINEUTRAALI PAINOTUOTE

ClimateCalc CC-000025/FI
PunaMusta Printing

Carbon dioxide emissions from printing Tampere University dissertations have been compensated.

« *Nemo nascitur sapiens, sed fit* »

- Seneca

Kukaan ei ole seppä syntyessään
Ningú no neix ensenyat

ABSTRACT

The first and best characterized physiological function of PCSK9 enzyme has been the regulation of the low-density lipoprotein receptors (LDLR) turn-over in the liver, affecting the circulating cholesterol uptake, and contributing eventually to the development of cardiovascular events. Recently it has been reported that PCSK9 controls the turn-over of other cellular receptors, such as the major histocompatibility complex class I (MHC-I). However, its participation in the immune responses against infections and cancer, is not fully understood, in part, due to the diverse results obtained in bacterial infections studies, and in part because little research has been done in certain malignancies with altered lipid metabolism, such ovarian cancer.

In the present study, circulating PCSK9 protein levels were explored in bacteremic patients. Interestingly, those with lower PCSK9 levels, but still over the normal range, had worse prognosis. Thus, to study *in vivo* the effects of PCSK9 gene knockout upon pneumococcal infection, two zebrafish mutant lines were generated using a genetic modification method called CRISPR/Cas9. Both, in humans and zebrafish, PCSK9 gene and protein levels are upregulated upon systemic infection, especially due to *Streptococcus pneumoniae*, where it resembles an acute-phase reactant correlating with the levels of infection-associated marker C-reactive protein (CRP). In zebrafish, PCSK9 protein is dispensable for the correct neurogenesis during ontogeny, and also for adult host survival against *Streptococcus pneumoniae* infections. However, certain immune related genes were downregulated, whereas lipid-metabolism related genes were upregulated, suggesting a conserved hepatic immunoregulatory function.

Lastly, the expression and putative role of PCSK9 protein in epithelial ovarian cancer cells was explored in selected cell lines. It was found that PCSK9 protein is expressed and secreted by immortalized cell lines and patient derived cancer cell cultures, suggesting a paracrine modulation. PCSK9 protein was also detected at low concentrations in patients' ascites fluids. Furthermore, to study its effects on cell proliferation, PCSK9 gene expression was modulated. When PCSK9 gene was silenced, cancer cell survival was impaired, suggesting a pro-survival role for PCSK9 protein, in line with previous studies in other malignancies. When PCSK9 protein

expression was transiently induced, intracellular signaling activation was observed, reinforcing the pro-survival role for PCSK9.

In conclusion, PCSK9 plays a role in immunity and cancer. However, some aspects remain ambiguous, and more research would be needed to determine its roles and its usefulness as a therapeutic target to treat bacterial infections or cancer.

TIIVISTELMÄ

PCSK9 entsyymin ensimmäisenä löydetty ja parhaiten tunnettu fysiologinen rooli on alhaisen tiheyden lipoproteiinireseptorin (engl. low density lipoprotein receptor, LDLR) ilmentämisen säätely maksassa, mikä vaikuttaa verenkierrossa olevan kolesterolin kulkeutumiseen soluihin ja lopulta sydän- ja verisuonitautien kehittymiseen. Hiljattain on näytetty, että PCSK9 kontrolloi myös muiden solureseptoreiden, kuten esimerkiksi MHCI:n (engl. major histocompatibility complex I), uudelleenkiertoa. PCSK9:n merkitystä infektioita ja syöpää vastaan suuntautuvassa immuunivasteessa ei täysin ymmärretä, – osittain sen vuoksi, että, bakteeri-infektioiden tutkimuksista on saatu vaihtelevia ja toisistaan poikkeavia tuloksia. Toisaalta pahanlaatuisia kasvaimia, joilla esiintyy poikkeavaa lipidiaineenvaihduntaa, on toistaiseksi tutkittu vain vähän. Esimerkkinä tällaisesta kasvaimesta on munasarjasyöpä.

Tässä tutkimuksessa selvitettiin PCSK9:n määrää verenkierrossa bakteremiapotilailla. Tulokset osoittivat matalampien PCSK9 tasojen olevan yhteydessä huonompaan taudin ennusteeseen. Lisäksi pcsk9-geenin poistamisen vaikutusta pneumokokki-infektiossa tutkittiin *in vivo* luomalla kaksi seeprakalan mutanttilinjaa käyttäen CRISPR/Cas9-menetelmää. Sekä ihmisessä että seeprakalassa PCSK9- proteiinin ja geenin tasot nousevat systeemisessä infektiossa, etenkin *Streptococcus pneumoniae* infektiossa, ja se käyttäytyy akuutin vaiheen proteiinin tavoin korreloiden infektioihin liittyvän C-reaktiivisen proteiinin (CRP) tasojen kanssa. *Pcsk9*-geeni ei ollut seeprakalassa välttämätön yksilönkehityksen aikaiselle neurogeneesille eikä aikuisen kalan selviytymiskyvylle streptokokin aiheuttamassa keuhkoinfektiossa. Poistogeenisessä kalassa tietyt immuunipuolustukseen liittyvät geenit kuitenkin ilmentyivät alentuneesti ja toisaalta lipidimetaboliaan liittyvien geenien ilmentyminen oli koholla. Tämä viittaa pcsk9:llä olevan evoluutiossa säilynyt immuunijärjestelmän säätelijän rooli maksassa.

Lopuksi PCSK9 proteiinin ilmentämistä ja merkitystä epiteliaalisessa munasarjasyövässä tutkittiin hyödyntäen valikoituja solulinjoja. Immortalisoidut solulinjat ja potilaiden syöpäkasvaimista viljellyt solut ilmensivät ja erittivät PCSK9:ää, mikä viittaa parakriiniseen säätelyyn. PCSK9:ää havaittiin myös matalina pitoisuuksina potilaiden vastaontelon nesteessä. PCSK9:n ilmentämistä muokattiin, jotta sen vaikutusta solujen jakaantumiseen voitaisiin selvittää. Kun PCSK9

ilmentymistä hiljennettiinvähennettiin, syöpäsolujen selviytymiskyky huonontui. Tämä tulos on samansuuntainen aiempien pahanlaatuisten kasvainten tutkimusten kanssa ja viittaa PCSK9:n parantavan syöpäsolujen selviytymistä. Kun PCSK9:n ilmentymistä lisättiin soluissa ohimenevästi, havaittiin solunsisäistä signaaliaktivaatiota, mikä vahvistaa hypoteesia PCSK9:n merkityksestä solujen selviytymisen paranemisessa.

Yhteenvetona, PCSK9:llä on merkitystä immuunipuolustuksessa ja syövässä. Kuitenkin jotkin asiat jäävät moniselitteisiksi, ja lisää tutkimuksia tarvitaan selvittämään PCSK9:n toimintaa sekä sen hyödyllisyyttä terapeuttisena kohteena bakteeri-infektioiden ja syövän hoidossa.

CONTENTS

List of Figures

List of Tables

ABBREVIATIONS

A2780cis	Cis-platin resistant A2780
APO	Apolipoprotein
APR	Acute-phase reactant protein
BRAF	V-raf murine sarcoma viral oncogene homolog B1
C	Complement component
CFU	Colony forming unit
CRISPR/Cas9	Clustered Regularly Interspaced Short Palindromic Repeats and CRISPR-associated protein 9
DEPTOR	DEP domain containing mTOR interacting protein
dpf	Days post fertilization
dpi	Days post infection
DSS	Drug sensitivity score
EOC	Epithelial ovarian cancer
gDNA	Genomic DNA
GO	Gene ontology
gRNA	Guide RNA
GTP	Guanosine triphosphate
HAMP	Hepcidin antimicrobial peptide
HDL	High-density lipoprotein
HeLa	Henrietta Lacks' cervical carcinoma cell line
HepG2	Hepatoma G2
HGSOC	High-grade serous ovarian cancer
hpf	Hours post fertilization
hpi	Hours post infection
HR(D)	Homologous recombination (deficiency)
KO	Knock-out
KRAS	Kirsten Rat Sarcoma Viral Proto-Oncogene
LDLR	Low-density lipoprotein receptor
LGSOC	Low-grade serous ovarian cancer
MAPK	Mitogen-Activated Protein Kinase
MHC-I	Major histocompatibility complex class I (aka human leukocyte antigen, HLA, complex)

mTOR(C)	Mammalian target of Rapamycin (Complex)
NARC-1	Neural Apoptosis-Regulated Convertase 1 (aka PCSK9)
OC	Ovarian cancer
OVCAR3cis	Cisplatin resistant OVCAR3
PARPis	Poly (ADP-ribose) polymerase inhibitors
PBS	Phosphate-buffered saline
PCA	Principal components analysis
PCs	Proprotein convertases
PCSK	Proprotein convertase subtilisin/kexin
PCSK9	Proprotein convertase subtilisin/kexin type 9
PDCs	Patient-derived cancer cell cultures (*ex vivo* tumor cells)
PD-1	Programmed Cell Death 1
PD-L1	Programmed Cell Death Ligand 1
PI3K	Phosphoinositide 3-kinase
PIKK	Phosphoinositide 3-kinase-related kinase family
PTMs	Post translational modifications
qPCR	Quantitative PCR
RNA	Ribonucleic acid
ROS	Reactive oxygen species
RT-qPCR	Real time quantitative polymerase chain reaction
siRNA	Small interference RNA
SOCS3	Suppressor of cytokine signaling 3
SREBP	Sterol regulatory element-binding protein
TAMs	Tumour-associated macrophages
TNF	Tumour necrosis factor
TP53	Cellular Tumor Antigen P53
WT	Wild type

LIST OF ORIGINAL PUBLICATIONS

This thesis is based on three original publications, which are referred to by their Roman numerals (I-III). The original publication I was used in the doctoral thesis of Juha Rannikko (Tampere University, 2019). The articles have been reproduced with the permission of the copyright holders.

Publication I   Juha Rannikko, <u>Dafne Jacome Sanz</u>, Zsuzsanna Ortutay, Tapio Seiskari, Janne Aittoniemi, Reetta Huttunen, Jaana Syrjänen, Marko Pesu. **Reduced plasma PCSK9 response in patients with bacteraemia is associated with mortality.** Journal of Internal Medecine, 2019; 286(5):553-561.

Publication II   <u>Dafne Jacome Sanz</u>, Anni K. Saralahti[1], Meeri Pekkarinen[1], Juha Kesseli, Matti Nykter, Mika Rämet, Markus J.T. Ojanen[2], Marko Pesu[2]. **The Proprotein Convertase Subtilisin/Kexin Type 9 (PCSK9) Regulates the Production of Acute Phase Reactants from the Liver.** Liver International, 2021; 41(10):2511-2522.

Publication III   <u>Dafne Jacome Sanz</u>[3], Juuli Raivola[3], Hanna Karvonen, Mariliina Arjama, Harlan Barker, Astrid Murumägi, Daniela Ungureanu. **Evaluating targeted therapies in ovarian cancer metabolism: novel role for PCSK9 and second generation of mTOR inhibitors.** Cancers (Basel), 2021; 24;13(15):3727.

[1, 2, 3] Equal contribution.

THE AUTHOR'S CONTRIBUTION

Publication I   MSc Dafne Jacome Sanz and PhD Zsuzsanna Ortutay curated the patient samples and performed the ELISA experiments together. Acquired data was analysed and discussed together. The manuscript was mainly prepared by MD, PhD Juha Rannikko and MD, PhD Marko Pesu, but Sanz also partly contributed.

Publication II   MSc Dafne Jacome Sanz and PhD Markus Ojanen performed all the animal experiments with zebrafish together, having an important role in acquiring and analysing the data. Sanz optimized some methods (qPCR and western blotting). Sanz designed and performed the HepG2 *in vitro* experiments. Sanz participated in analysing and interpreting the results and drafting and revising the manuscript together with PhD Markus Ojanen and the main supervisor MD, PhD Marko Pesu.

Publication III   The experiments needed for the third original publication were performed in Tampere University (Faculty of Medicine and Health Technology, MET) and the University of Helsinki (Institute for Molecular Medicine Finland, FIMM). Sanz participated in the design of the main experiments and performed the experiments at Tampere University. Sanz analysed the data together with the co-authors and the main supervisor PhD, Associate Professor Daniela Ungureanu. The manuscript was mainly written by the supervisor.

1   INTRODUCTION

The pro-protein convertase subtilisin kexin enzyme PCSK9, formerly known as neural apoptosis-regulated convertase 1 (NARC-1), is widely expressed during ontogeny and in the adulthood. Since its discovery in 2003, the impact and relevance of PCSK9 in biomedical research and clinical practice has been undeniable. In the past decade, interest towards PCSK9 has rapidly increased (90% of the published literature has been generated after 2013), and much research and patenting have expanded the focus to understand the roles of PCSK9 beyond cholesterol homeostasis. The main biological function of PCSK9 is non-enzymatic and it is related to escorting low-density lipoprotein receptors (LDLR) into intracellular acidic compartments for degradation.

PCSK9 is a class of its own regarding the pro-protein convertases subtilisin/kexin type, since to be functionally mature needs to be autocleaved. It is an interesting protein linking cholesterol homeostasis (via LDLR degradation) with innate immunity, bacterial lipid clearance (via TLR2) and cellular apoptosis (via TLR4 and TLR2). Moreover, recently it was demonstrated that PCSK9 acts in bridging the two branches of the immune system, the innate with the adaptive immunity. PCSK9 is responsible for the modulation of the major histocompatibility complex class I (MHC-I), in a similar non-enzymatic fashion as that for LDLR. Also, PCSK9 contributes in an LDLR-dependent way to cytotoxic T-cell activation. Interestingly, despite early reports on PCSK9 expression in organs such as the spleen and thymus, its functions in these regulatory immune tissues have not been exhaustively studied until recently.

The clinical relevance and potential of PCSK9 has received increasing interest, especially since the approval of PCSK9 inhibitors (PCSK9i) for treating hypercholesterolemia and atherosclerosis under the scope of the global market in July 2015. The long-term benefits, especially for patients that had developed statin resistance, suggested that PCSK9i could also be used for treating other diseases, such as sepsis or cancer. This was inferred, in part, from the fact that bacterial lipids are cleared by the host immune system under the same pathway as cholesterol. This is possible because innate immune host responses and the housekeeping lipid

metabolism share common trafficking pathways (in mammals) and underlying reciprocal mechanisms. Additionally, it has been explored if PCSK9 levels could be used as a biomarker for several conditions.

Pneumococcal infection and ovarian cancer, characterized by altered lipid metabolism, are two diseases with high incidence, responsible for significant mortality worldwide, every year. Despite clinical advance, overcoming the drug resistance generated against conventional treatments and medications remains challenging, and the diseases have a significant socioeconomic impact. Thus, new candidates for drugs are in high demand, to improve diagnosis, treatment, and prognosis.

Despite the undoubtedly increased interest towards PCSK9 and the consequent intensive research and scientific efforts, the mechanisms of PCSK9 in immunity and cancer are not fully understood yet. Thus, it is still elusive how PCSK9 acts in streptococcal infections, and very little is known regarding the role of PCSK9 in epithelial ovarian cancer.

Therefore, the purpose of this study was to contribute to a better understanding of PCSK9 participation in these two diseases. To this end, first we explored *ex vivo* the plasma PCSK9 levels of patients suffering from bacteraemia with a positive blood-culture. Second, we investigated *in vivo* the host immune responses to a *Streptococcus pneumoniae* infection in a zebrafish pcsk9 knockout model. To create our *pcsk9*-knockout zebrafish mutant lines were employed CRISPR/Cas9 tools. Third, we characterized *in vitro* the expression and putative role of PCSK9 in different human ovarian cancer cell lines and patient-derived cancer cell cultures. Additionally, low- and high-grade subtypes of EOC show metabolic heterogeneity with different drug vulnerabilities, which could be of clinical interest. We screened for metabolic vulnerabilities using drugs that could offer enhanced efficacy when combined with existing therapies, such as the combination of the anti-metabolic drug AVN944 with the commonly used cisplatin.

2 REVIEW OF THE LITERATURE

2.1 Proteases

The Central Dogma of molecular biology concerns about how genetic information flow within a biological system, with one gene generating one RNA, which in turn generates one protein (Crick 1958; Crick 1970). Since then, scientific evidence has vastly accumulated, displaying that biological systems are far more complex. The human genome is estimated to comprise about 20,000 protein-coding genes, whereas the human proteome comprises a larger number of elements (López-Otín & Overall, 2002; The Human Protein Atlas). This diversity is not achieved by direct translation from protein-coding genes, but is due to different events, such as genomic recombination, transcription termination, alternative splicing (AS), polymorphisms (single-amino acid or single-nucleotide) or post-translation modifications (PTMs) (Pruitt et al., 2007; Smith et al., 2013; The Consortium for Top-Down Proteomics).

More than 200 types of PTMs have been identified, including the addition of a phosphoryl, sugar, acetyl, or methyl group (Walsh et al., 2005). Customarily, how an enzyme competes for a substrate defines its specificity, depending mostly on the acylation steps (Hedstrom, 2002).

Proteases (also referred to as peptidases in the literature) are enzymes that regulate the localization, activity, and fate of many proteins, primarily via hydrolytic cleavage of their peptide bonds (Ward, 2011). They are involved in many processes, such as replication and transcription, cell proliferation, extracellular matrix remodelling or hormone activation. An alteration in their amino acid composition, structure, or activity might lead to pathological conditions such as autoimmunity, cardiovascular diseases, or even cancer. It is noteworthy that many infectious organisms use proteases as virulence factors to produce mechanical damage or to evade the host's immune responses. Consequently, protease inhibitors have medical relevance and wide clinical applicability (Abbenante & Fairlie, 2006).

It is assumed that proteases arose in primitive organisms as simple enzymes intended for protein catabolism and amino acids generation. Most proteases are substrate specific, but others, such as proteinase-K, target multiple substrates indiscriminately (Neurath & Walsh, 1976).

The sizes of proteases range from 20kDa, up to 6MDa (Bertenshaw et al., 2003). In humans so far, thousands of proteases have been identified, encoded by over 600 genes[1]. Proteases such as pepsin, papain, or trypsin, were already discovered and characterized during the 1800s and crystallized a century later (Northrop 1930; Northrop and Kunitz 1931; Kimmel and Smith 1954).

Typically, proteases have been organized (see Figure 1) into five catalytic classes (i.e., metallo, aspartic, cysteine, serine, and threonine) and into 63 different families (Puente et al., 2003; Seidah & Chretien, 1999). Also, a classification into six catalytic classes (adding glutamic) is often used (Rawlings & Barrett, 2013).

Figure 1. Classification of proteases. The 9 mammalian proprotein convertase members (referred to here as PC) were classified according to the degree of identity of the primary sequences of their catalytic domain. (Adapted from Puente et al. 2003; Siezen and Leunissen 1997).
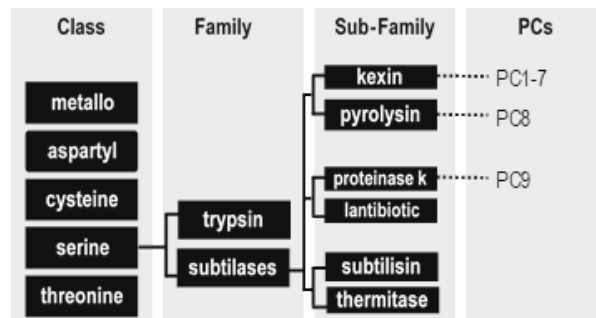
The overall process to hydrolyse peptide bonds is essentially the same for all classes of proteases and follows a general three-step kinetic mechanism: a) destabilize an amide bond by nucleophilic attack, b) activate water, since it is a poor nucleophile, and c) protonate an amine to force its expulsion (Erez et al., 2009). Serine, cysteine, and threonine proteases use their eponymous residue, located in the active site, to endorse pairing with a proton-withdrawing group of a peptide bond. Aspartyl and metalloproteases use their own amino acid and employ an activated water molecule serving as the nucleophile (Erez et al., 2009).

Serine proteases, including granzymes, plasminogen activators and type II transmembrane proteinases, are very efficient in performing these three-steps (Hedstrom, 2002). Commonly, they cleave extracellular proteins and contribute to the host defence against bacteria through inflammation and tissue remodelling. However, when their activity or structure (specially at the so called "catalytic triad") is dysregulated, may contribute to the pathogenesis of several diseases (Polgár, 2013).

---

[1] A useful research tool is the MEROPS Peptidase database of proteolytic enzymes, their substrates, and inhibitors, available online at http://merops.sanger.ac.uk (Rawlings & Barrett, 2013).

Serine proteases have at least four independent evolutionary origins with similarities in the reaction mechanisms (Rawlings & Barrett, 1994), accounting for a wide distribution in all natural kingdoms including viruses (Cera, 2009); Stroud 1974). They constitute one third of all known proteolytic enzymes, with nearly 50 families based on their amino acid sequences (Rawlings & Barrett, 2013). The type of reaction catalysed by serine proteases has proven to be suitable for controlling a wide range of biological processes, as demonstrated by their ubiquity and multiple independent evolutions. Abundance is one measure of success (Hedstrom, 2002).

Therefore, serine proteases can be organized into two main subclasses, depending on how close they are to trypsin/chymotrypsin or to the bacterial subtilisin and the yeast Kexin, also referred to as subtilases (Siezen & Leunissen, 1997). The trypsin/chymotrypsin-like proteases are the most abundant in nature. The subtilases family is the second largest serine protease family characterized to date, with over 200 members identified. Most of them are endopeptidases, although there are also exopeptidases and a tripeptidyl peptidase (Rawlings & Barrett, 1994).

2.2   Pro-protein convertases (PCs)

2.2.1   The Prohormone Theory

Five decades ago, the Prohormone Theory stated that biologically active peptides are derived from larger inactive precursors after enzymatic proteolytic cleavage (Steiner 1967; Levine 1967). The theory was simultaneously proposed by two independent research groups, based on two different experimental models: proinsulin (the prohormone precursor to insulin in the pancreas), and pro-opiomelanocortin (POMC) (precursor of adrenocorticotropin (ACTH) and the β-lipotropin (β-LPH) in the pituitary gland) (Steiner 1967; Levine 1967; Chrétien et al 1976).

Later, during the 1970s and 1980s, the Prohormone Theory was proven to be true for many other molecules, such as neuropeptides and neurotrophins (Benjannet et al., 1977; Chrétien et al., 1983). Since then, in all kinds of organisms and in different tissues, it has been demonstrated that many molecules go through post-translational maturation, involving one or more rounds of proteolytic cleavage (not necessarily at one site) in order to become functional (López-Otín & Overall, 2002). Since this theory implied the existence of specific mediators, it can be considered seminal for the research on PCs.

2.2.2   Subtilases

Subtilases are also known as subtilisin-like proteases. As schematized in Figure 1, the subtilase family of serine proteins is divided into six sub-families based on their sequence homology: 1) kexin, 2) pyrolysin, 3) proteinase K, 4) lantibiotic peptidases, 5) subtilisin and 6) thermitase. Based on the homology of the structure of their catalytic domains, the first seven proprotein convertase members were considered to belong to the Kexin subfamily (Siezen and Leunissen 1997).

PCs themselves are products of secretory precursor proteins. During the 1980s, the criteria that an enzyme had to meet in order to be considered a proprotein convertase were revised (Lazure et al 1983). Also, during that time another important molecule was discovered in the secretory granules of neuroendocrine cells, the pituitary peptide 7B2 (Hsi et al., 1982). Two decades later it was found that 7B2 interacts with PCSK1/PCSK2 (PC1/PC2 in the Figure 1), in a chaperone-like fashion, contributing to their activation and trafficking (Mbikay et al., 2001).

PCs have conserved catalytic domains and thus they are thought to originate from a common ancestor through events such as translocations, insertions, duplications, or deletions at least eighty million years ago (Seidah & Chretien, 1999).

2.2.3   Pro-protein convertase subtilisin/kexin (PCSKs) family

The pro-protein convertases subtilisin/kexin belong to a class of serine-proteases, of the subtilases family. The members belong to different sub-families, termed subtilisin/kexin type (See Figure 1). Their ancient phylogenetically conserved proteolytic mechanism allows them to generate a myriad of products, from precursors, in a calcium-dependent fashion (Seidah et al., 2008, 2017).

Identification of the yeast convertase Kexin (Kex2p), responsible for cleaving the pro-K1 killer toxin precursor and the pro-α-factor of *Saccharomyces cerevisiae*, lead to the identification of the mammalian PCSKs (Julius et al. 1984), which are related to bacterial subtilases rather than eukaryotic trypsin-like enzymes (Mizuno et al. 1988).

In less than two decades, nine PCSKs were found to be encoded by the mammalian genome, termed PCSK 1–9 (i.e., *Proprotein Convertase Subtilisin-Kexin*) based on the recommendation of the Human Gene Nomenclature Committee (HUGO, https://www.genenames.org). The first PCSK to be discovered was FURIN, thanks to the high degree of homology it shares with the yeast Kexin (Roebroek et al 1986; Mizuno et al. 1988; Henrich et al 2003). During the years 1991-1996, six more PCSKs were discovered (Kiefer et al. 1991; Lusson et al. 1993; Seidah

et al. 1990; Seidah et al., 1996; Smeekens & Steiner, 1990). PCSK8 and PCSK9, were the last to be identified (Seidah et al., 1999; Seidah et al., 2003). (See Table 1 and Figure 2). All *PCSK* are located on different chromosomes, except for *PCSK3* and *PCSK6*, which are closely positioned on chromosome 15 (Seidah & Chretien, 1999).

Table 1. **PCSKs family characterization.** Human genes. *V stands for number of variants.

Gene ID Ensembl ID	Protein ID	V	Protein length	Tissue location	Subcellular location
PCSK1 ENSG00000175426	PC1 PC3, PC1/3	3	83kDa, 753aa **84kDa, *66kDa	Neuronal, Endocrine	Secretory granules
PCSK2 ENSG00000125851	PC2	3	71kDa, 638aa **70kDa, *55kDa	Neuronal, Endocrine	Secretory granules
PCSK3 (FURIN) ENSG00000140564	FURIN, Pace	6	88kDa, 794aa **100kDa, *94kDa	Ubiquitous	Cell surface, *Trans*-Golgi, Endosomes (shed)
PCSK4 ENSG00000115257	PC4	2	83kDa, 755aa *50kDa	Germinal	Cell surface (shed)
PCSK5 ENSG00000099139	PC5, PC6, PC5/6	5	205kDa, 1860aa	Wide	Cell surface (PC5B, shed), extracellular (PC5A, secreted)
PCSK6 ENSG00000140479	PACE4	1 4	107kDa, 975aa **106kDa	Wide	Cell surface, extracellular (secreted)
PCSK7 ENSG00000160613	PC7 PC8	6	87kDa, 785aa **89kDa, *64kDa	Ubiquitous	Cell surface, *Trans*-Golgi, endosomes (not secreted)
PCSK8 (MBTPS1) ENSG00000140943	SKI-1, S1P, Mbtps1	4	116kDa, 1052aa **120kDa, *51kDa	Ubiquitous	*Cis-*. and *Medial-* Golgi (not secreted)
PCSK9 ENSG00000169174	PCSK9 NARC-1, HCHOLA3	1	75kDa, 692aa **72kDa, *63kDa, *55kDa	Wide	*Trans*-Golgi, extracellular (secreted)

*PCSK*s are expressed differently across time, cell types and subcellular compartments and synthesized as inactive zymogens. All are secreted, freely or inside granules, into the extracellular milieu, except for FURIN, isoform PC5B, PC7 and SKI-1, which are type 1 membrane-bound proteases (Seidah et al., 2006). PC2 undergo autocatalytic processing in the secretory granules, whereas the rest, in the endoplasmatic reticulum (ER) (Seidah et al., 2006).

After cleavage, the prosegment remains attached, forming a heterodimer, exerting inhibitory properties. Then, can exit the ER heading to specific subcellular compartment, wherein a second autocatalytic cleavage of the prosegment might follow to be fully functional. This multi-step process ensures that each convertase is only active at the intracellular site/s where the conditions of pH and calcium are optimal for conducting its main function. PCSKs main role is the post-translational activation of precursor protein via proteolytic cleavage (Seidah et al., 2013).

Figure 2. **Primary structures of human protein convertases**. A schematic representation. The signal peptide (SP), pro-peptide and catalytic domain are common to all convertases having the catalytic triad residues Asp-His-Ser. The seven first convertases have a stabilizer β-barrel P domain after the catalytic domain. The carboxy-terminal domain contains unique sequences for each convertase to sort them to their cellular localization. PC5 and PACE4 contain a Cysteine-rich (Cys-rich) domain. FURIN, PC4, PC5B, PC7 and SKI-1 have a trans-membrane domain. PCSK9 has a Cysteine-Histidine rich (CHRD) domain required for escorting the PCSK9-LDLR complex to endosomes/lysosomes. Primary (black arrow) and secondary (grey) autocleavage sites are indicated. (Adapted from Seidah and Prat 2012; Siegfried et al 2020).
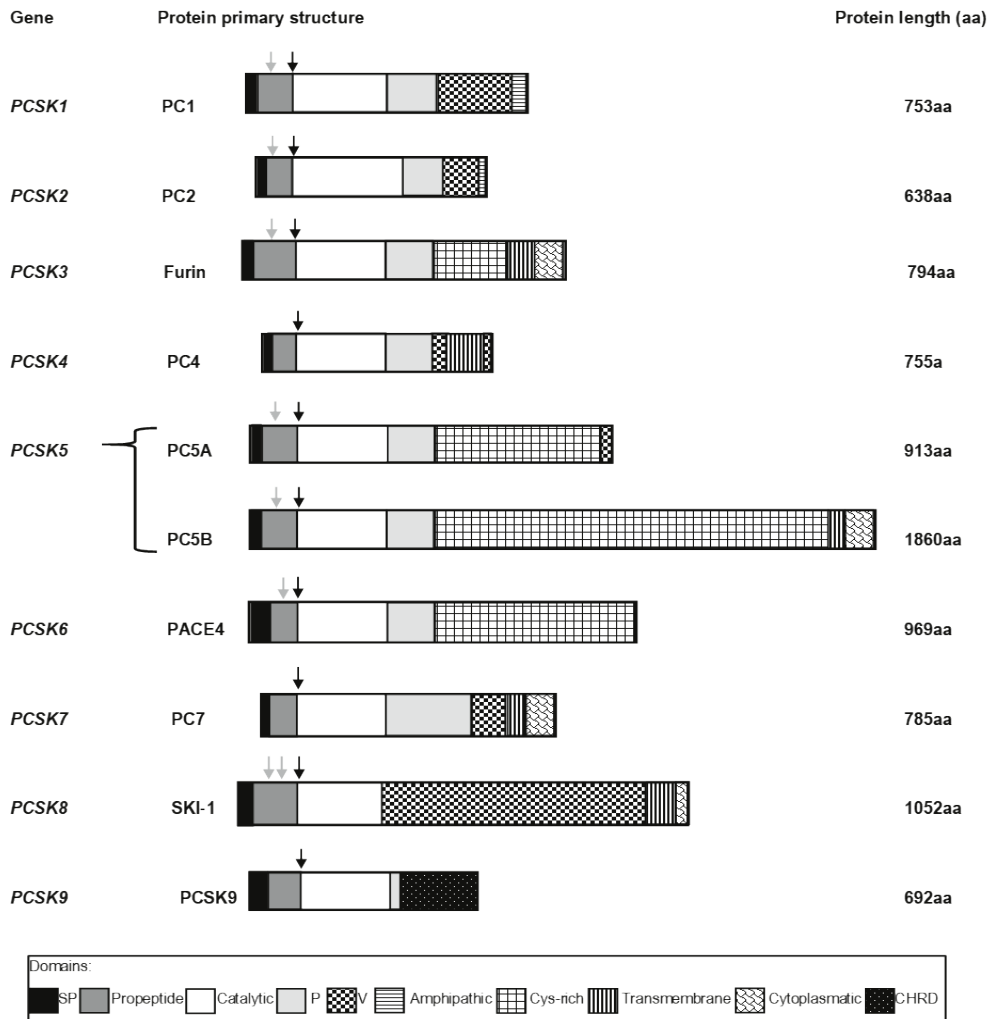
Although a certain degree of synergistic functional redundancy was observed when they were overexpressed in cell lines, *in vivo* studies have revealed that each PCSK has a specific phenotype and functions. Many lessons were derived from: a) knocking-out *PCSK* genes (tissue-specific or whole organism) in animal models, b) overexpressing *PCSK* genes in transgenic mice and c) identifying patients lacking functional alleles (≥1). In addition, clinical cases and genome-wide association studies corroborated the observations gathered from *in vitro* and *in vivo* studies. The clinical relevance of animal models has increased since the evaluation and approval of the use of specific PCSK inhibitors (Creemers & Khatib, 2008; Scamuffa et al, 2006; Seidah, 2011; Seidah et al., 2013). Murine PCSK phenotypes and *in vivo* defects are diverse, ranging from non-apparent to lethal: a) loss of anxiety (*PCSK7*), b) obesity, hyperproinsulinaemia, retarded growth and endocrinal disorders (*PCSK1, PCSK2*) (Furuta et al., 1997; Jackson et al., 1997; Shen et al., 2004), c) disrupted cholesterol metabolism (*PCSK8, PCSK9*), d) craniofacial abnormalities (*PCSK6*), e) impaired fertility (*PCSK4*) (Mbikay et al., 1997), and f) embryonic malformities (*PCSK3, PCSK5, PCSK6, PCSK8*) (Scamuffa et al., 2006; Szumska et al., 2017).

According to the array of substrates activated by PCSKs, numerous clinical implications have been predicted (Duckert et al., 2004), and research has been conducted over the years in order to identify and characterize the many substrates cleaved (see Table 2) (Artenstein & Opal, 2011).

PCSKs' substrates contain a consensus sequence needed for recognition and cleavage. The first seven members cleave precursor proteins at single or paired basic amino acids after the general motif (K/R)-(X)-(K/R)↓ (where X stands for a given number/s of aa/s) (Creemers & Khatib, 2008). Although all proproteins activate molecules by limited intracellular proteolysis before trafficking within the secretory pathway, PCSK9 has a distinct mode of action, since its main known role is non-enzymatic (Seidah & Chretien, 1999).

Table 2.   Selection of the main known substrates cleaved by PCSKs.

Gene ID	Precursor proteins (PMID of references)
PCSK1 PCSK2	Proopiomelanocortin (POMC) Insulin Glucagon-like peptides Corticotropin β-lipotropin Melanocyte-stimulating hormones Met-enkephalin β-endorphin Somatostatin (2023902, 10816641, 22204726)
PCSK3	Murine β-nerve growth factor (2269657) Human neurotophin-3 (neutrophins) (8603699) Human parathyroid hormone (7721880, 9242622) Insulin-like growth factor 1 (IGF-1), IGF-1R (15358140, 18064302) Platelet-derived growth factor A and B (PDGF-) (12670890, 16007151) Transforming growth factor β (TGF-β) (7737999, 17516499) Vascular endothelial growth factor C (VEGF-C) (12782675) Human integrins (15756593) Human albumin (1482351, 10050053) Human blood factor X (10688334) Human von Willebrand factor (2094803) Human stromelysin-3 (7746327) Membrane type matrix metalloproteinase (8804434) Disintegrin and metalloproteinase (ADAM) (14744861) Human FURIN prodomain (9130696) Mouse 7B2 chaperone (8034690) Anthrax toxin protective antigen (1644824) Diphtheria toxin (8253774) Shiga toxin (7738018, 17407762) HIV-1, Ebola, influenza, coronavirus (9576958, 10816641) PCSK9 (16912035, 33429337) BAFF, APRIL (21889147)
PCSK4	Human insulin-like growth factor I and II (16040806) Pituitary adenylate cyclase activating polypeptide (9493858) Enkephalins (17012247) GHRH-related peptides (17012247) Nerve growth factors (17012247) Fertilins (17012247)
PCSK5	Human neurotophin-3 (PC5B) (8603699) Insulin-like growth factor 1 (IGF-1) (15358140, 18064302) Platelet-derived growth factor A and B (PDGF-) (16007151) Vascular endothelial growth factor C (VEGF-C) (12782675) Growth differentiation factor 11 (GDF11) (18378898) Human insulin receptor (PC5A) (8226974) Human blood factor X (PC5) (10688334) PCSK9 (PC5A) (16912035) Neural adhesion molecule L1 (12529374)
PCSK6	Human insulin-like growth factor-I (7615562, 11402025) Platelet-derived growth factor A and B (PDGF-) (16007151) Mouse proopiomelanocortin (POMC) (10816641) Human von Willebrand factor (2094803) Human MT-MMP1 (8804434) Human FURIN prodomain (9130696) Bone morphogenic proteins (BMPs) (10633867, 9885250) Shiga toxin (7738018)
PCSK7	Platelet-derived growth factor A and B (PDGF-) (16007151) Vascular endothelial growth factor C (VEGF-C) (12782675) Mouse proopiomelanocortin (POMC) (10816641) Human αv integrin (15756593) Human von Willebrand factor (2094803) TGFβ1a (24178295)
PCSK8	Crimean-Congo virus glycoprotein precursor (16352575) Lassa virus glycoprotein C (GP-C) (11943176, 12633879) Aarenavirus GP precursor (GPC) (22357276) Lymphocytic choriomeningitis virus (LCMV) (12584310) Sterol regulatory-element--binding proteins (SREBP) (10701998) Brain- derived neurotrophic factor (9990022)
PCSK9	LDLR, VLDLR, LRP1, LRP8, ApoER2 (24144304, 18039658) HDL (lipoprotein metabolism, immunity...) (34601896) CD36 (long chain FA and TAG storage) (26494228) CD81 (HCV receptor) (26195630, 19489072) Annexin A2 (ANXA2) (LDLR regulation) (18799458, 22848640) ABCA-1 (LDL-c efflux in macrophages) (27940374) NPC1L1 (LDL-c intestinal absorption) (23422832) ENaC (Blood pressure) (22493497) BACE1 (Alzheimer) (18660751) MHC-I receptor (immune regulation) (33177715)

PCSK1 and PCSK2

The *PCSK1* is associated with monogenic obesity together with leptin (Jackson et al., 1997). Both proteins play a role in (neuro)endocrine tissues, where they are highly expressed, but also, activity within immune cells was suspected (Refaie et al., 2012).

Shortly after being synthesized in the ER, proPCSK1 cleaves itself after the prosegment, becoming PCSK1 and moving forward to the trans Golgi network (TGN), where the prosegment is released after a second cleavage, and the enzyme becomes functionally active. Both can process substrates in the secretory granules, but PCSK1 also in the TGN (Seidah, 2011). Only one of them is needed to process proinsulin into insulin, although the synergistic activity of both leads to enhanced outcomes (Bailyes et al., 1992; Bennett et al., 1992; Zhu et al., 2002).

PCSK3

The third member of the family, FURIN, is a type I transmembrane protein, mainly localized and activated in the TGN, and secondarily in the endosomal subcellular compartment and on the cell surface (Thomas, 2002). It was initially found in the upstream region of the feline sarcoma oncogene (FES) (Roebroek et al., 1986). It has functional redundancy with other PCSKs, such as PCSK5 and PCSK7 (Remacle et al., 2008). FURIN has many implications in development, viral infections (including the recently emerged SARS-COV-2) and cancer (Johnson et al., 2020; Seidah et al., 2017). Its role it is explained in more detail in the following subchapters.

PCSK4

The fourth member of the PCSK family is mainly expressed in the reproductive organs and plays a relevant role in fertility (Seidah et al., 2017; Seidah & Prat, 2012). It does not undergo secondary autocleavage and limited functional overlap with other PCSKs has been reported in the testis and related to fertility (Seidah and Prat 2012). Of note, the C-terminus of *PCSK4* is species, suggesting a possible cross-species fertilization prevention function (Seidah et al., 1992).

PCSK5 and PCSK6

The fifth and sixth members of the PCSK family become active on the cell surface, upon binding to heparin sulfate proteoglycans, exerting their function mainly on the cell surface and in the extracellular matrix (Malfait et al., 2008). They play critical

roles during development regulating the body axis (Seidah, 2011). PCSK5 is the only known convertase that encodes for two functional isoforms generated by alternative splicing: PC5/A and PC5/B. The 21st exon of the C-terminal variant *PCSK5* has been replaced by 18 additional exons in the PC5B variant (Nakagawa et al., 1993). The isoforms are sorted to different subcellular compartments (De Bie et al. 1996).

PCSK7

PCSK7 it is related to the other members of the PCSK family but diverged from the common ancestor earlier than others (Seidah et al., 1996). It is a type 1 membrane-bound protease, and like PCSK4, it does not undergo a second cleavage event. Data derived from *in silico* analyses (e.g., genome-wide association), suggested a role for PCSK7 in dyslipidemias related to triglycerides (TA) regulation (Ashraf et al., 2020; Kurano, Tsukamoto and Kamitsuji, 2016), complementing the knowledge of its main role related to iron metabolism and depression disorders (Seidah et al., 2017).

PCSK8

SKI-1 is the most ancient PCSK, related to eubacteria and plant subtilases rather than mammalian PCSKs and the yeast Kexin (Sakai et al., 1998; Seidah et al., 1999). It is found in parasites and in the entire plant kingdom (Barale et al., 1999). *PCSK8* encodes for a type 1 membrane-bound protease with a cytosolic tail, located in the *cis/medial*-Golgi and acidic compartments but not at the cell surface (Pullikotil et al., 2007). It cleaves molecules at the consensus motif R-X-(hydrophobic)-Z↓ (where X is any residue except for proline and cysteine, and Z stands for any amino acid except for valine, proline, cysteine, and glutamine) (Pasquato et al., 2006). SKI-1 can cleave and process viral glycoproteins, soluble precursors, and transmembrane transcription factors (e.g., SREBPs, regulators of cholesterol and fatty acids), and regulates the lysosomal targeting of proteins (Marschner et al., 2011; Pullikotil et al., 2007; Seidah et al., 1999).

PCSK9

Browsing results from a search with the criterion "PCSK9" in PubMed[2], retrieves 4,684 entries. Only during the time to took to carry out this PhD research, around

---

2500 new publications were added to the literature. Also, 240 clinical trials are ongoing; exemplifying the outpour of data and increased interest toward this protein since its discovery (see Figure 3).

Figure 3.   Main events related to PCSK9 from bench-to-bedside. Almost two decades of research in a nutshell. (Adapted from Seidah, 2021).

1990s	PCSK1-PCSK8 discovery	
2003	PCSK9 discovery (FH): S127R and F216L GOF variants associated PCSK9 completed sequence (human, rat, mouse)	**Fundamental research**
2004	PCSK9 enhances LDLR degradation reported D374Y GOF variant discovered: effect on LDL and upregulation by statins	
2005	PCSK9 LOF associated with hypercholesterolemia: 1st healthy mouse KO	**Target validation**
2006	PCSK9 LOF healthy women (lower plasma PCSK9 levels and CAD risk)	
2007	PCSK9: 3D protein structure reported 1st evidence of non-enzymatic activity of PCSK9 to regulate LDLR (EDF-A binding)	
2008	More targets identified: VLDLR, ApoER2 (LRP8) Liver specific PCSK9 KO	
2009	Intra- and extracellular pathways to enhance LDLR degradation used by PCSK9 1st PCSK9 mAb: LDL decreased in animals	**Drug discovery**
2010	PCSK9 mAb Phase I clinical trials	
2011	Phase II clinical trials PCSK9-LDLR complex: 3D structure reported Circulating PCSK9 degrades visceral adipose VLDLR (in mice)	
2012	PCSK9 KO: reduced atherosclerosis and cancer (and/or with metastasis)	
2013	Phase III Clinical Trials siRNA preclinical Trials	
2014	siRNA Phase I trials 1st evidence: PCSK9 inhibition improves sepsis treatment	
2015	FDA approval: PCSK9 mAb treatment (Evolocumab and Alirocumab)	**Clinical practice**
2017	PCSK9 siRNA usage: long duration of the LDL-lowering effect	
2018	PCSK9 siRNA Phase II Clinical Trials	
2019	PCSK9 siRNA Phase III Clinical Trials	
2020	EU marketing authorization: liver-targeted nanoparticle PCSK9 siRNA (Inclisiran)	
2021	CRISPR/Cas9 PCSK9 deletion in primates (PMID : 34012082)	

PCSK9 was originally identified in the brain during ontogeny, and in proliferating tissues. Genomic annotation evidenced that the human *PCSK9/NARC-1* gene was located close to a major locus for autosomal dominant hypercholesterolemia (ADH), and consequently identified as the third gene related to ADH (Abifadel et al., 2003), together with *ApoB* (Innerarity et al., 1987), and *LDL* (Sakai et al., 1998) (Brown & Goldstein, 1974) genes.

The evolutionary history of PCSK9 gene

The *PCSK9* gene comprises 12 exons in human (Ensembl ID: ENSG00000169174), mouse (ENSMUSG00000044254) and zebrafish (ENSDARG00000074185). In human (2n=46) and zebrafish (2n=50), it is located in the forward strand of chromosome 1 (Seidah et al., 2003) and 20, respectively. In mouse (2n=40) it is in the reverse strand of chromosome 4.

The evolutionary history of the *PCSK9* gene includes several events that led to the loss of the *PCSK9* gene in many species such as pigs, cows, whales, camels, and bears. In the light of this evidence, a dispensable role for *PCSK9* was suggested in the mammalian lineage (Murphy et al., 2001; van Asch & Teixeira da Costa, 2021).

In humans, at least 48 genetic variants have been reported to date. Among them, 27 are gain-of-function (GOF) and 21 loss-of-function mutations (LOF). Sixteen are in the prodomain (8 GOF and 8 LOF), 15 in the catalytic domain (9 GOF and 6 LOF) and 17 in the CHRD (10 GOF and 7 LOF) (Awan et al., 2014).

These genetic mutations can modify the amino acid structure of the protein, having functional consequences over posttranslational modifications (Dewpura et al., 2008), activation or affinity for substrates (e.g., LDLR) (Cesaro et al., 2020).

Ascertaining whether LOF variants were detrimental for our own evolutionary lineage as a species has been partially based on evidence based on the archaic hominids Denisovans. They had these gene variants regardless of having a suspected low cholesterol diet (Mikaeeli et al., 2020). Also, they have a unique homozygous mutation never found in any other hominids (Seidah et al., 2017).

PCSK9 protein and its expression

At the transcriptional level, PCSK9 expression is mainly (down)regulated by SREBP2 (Dubuc et al., 2004; Lebeau et al., 2022). The length of the PCSK9 protein is 692aa (human), 694aa (mouse) and 667aa (zebrafish). The protein has four domains in its structure, not all of them equally conserved. Residues involved in protein–protein interactions are more evolutionarily conserved than other surface-exposed residues. PCSK9 has a large conserved protrusion on the surface of the catalytic domain, whereas the C-terminal domain is poorly conserved (Cameron et al., 2008; Holla et al., 2011).

After cleavage of the signal peptide (SP) (1-30aa), the PCSK9 precursor form (proPCSK9) displays three structural domains: 1) prodomain (PRO) between 31-152aa, 2) catalytic domain (152-421aa) and 3) C-terminal cysteine and histidine rich domain (CHRD, 453-692aa) (see Figure 4, and Figure 2 for a schematic comparison with other PCSKs) (Cunningham et al., 2007; Piper et al., 2007). As summarized in Figure 1, PCSK9 belongs to the proteinase K family of subtilases, and its catalytic domain is 25% identical to the sequence of SKI-1(Seidah et al., 2003).

In healthy humans, the normal range of PCSK9 circulating in the plasma is between 170-220 ml (Boyd et al., 2016), depending on certain factors such as diet, age, gender and ethnicity (Lakoski et al., 2009).

Figure 4. **Structure of PCSK9 and its binding to three main molecules.** A schematic presentation. PCSK9 is composed of its prodomain (P), catalytic domain (C) and CHRD C-terminus (formed by three tandem repeats: M1-M3-M2). The LDL receptor (LDLR) binds by its extracellular EGF-A domain to PCSK9 by its catalytic domain. The MHC-I complex binds to PCSK9's M2 repeat of the cysteine and histidine rich C-terminus, whereas the cytosolic adenyl cyclase-associated protein 1 (CAP1) binds to the M1-M3 repeats of the C-terminus of PCSK9 when complexed with LDLR, enhancing their degradation into the lysosomal compartment. (Adapted from Seidah and Prat, 2021).
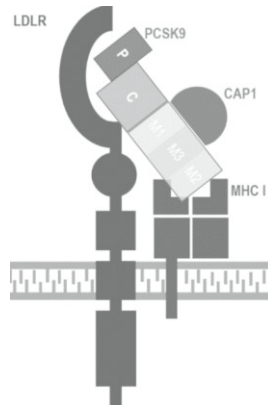
PCSK9 is widely expressed (see Figure 5), and predominantly synthesized in organs such as the liver, lungs, and small intestine, according to *in situ* hybridization and cellular analyses (Seidah et al., 2003).

Figure 5. **Bulk tissue gene expression for PCSK9, both genders.** Manual selection of fifteen main tissues. Data processing and normalization: expression values are shown in the logarithmic scale of TPM (log10(Transcripts Per Million+1) and calculated from a gene model with isoforms collapsed to a single gene. Box plots are shown as the median and 25th and 75th percentiles and sorted according to their median values. Points are displayed as outliers if they are above or below 1.5 times the interquartile range (Query ID for PCSK9 is ENSG00000169174.10 at GTEx, Broad Institute of MIT and Harvard©. Analysis Release V8 dbGaP Accession phs000424.v8p2. (https://www.gtexportal.org/).
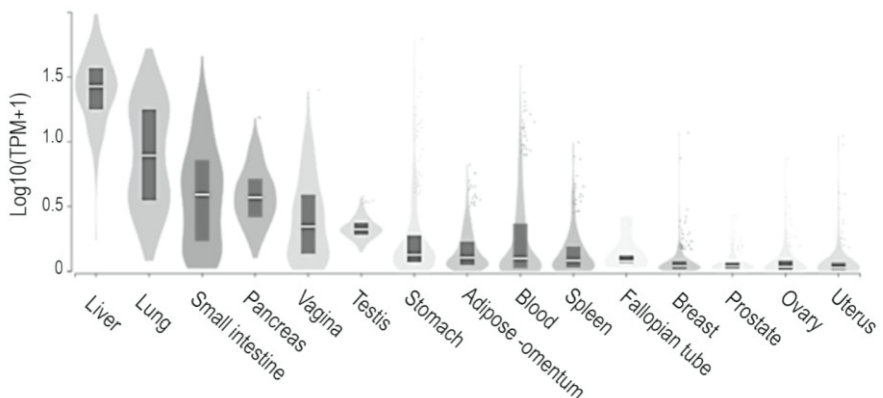
The tissue distribution and expression of PCSK9 depend on several factors: a) the gene methylation state (Lohoff et al., 2018; Yu et al., 2015), b) the abundance and variety of transcriptional factors such as hepatic nuclear factor 1-alpha (HNF1α) (Wang et al., 2020), SREBP-2 (Dong et al., 2010) or FoxO3/SIRT6 complex (Tao et al., 2013), c) mRNA degradation factors, d) translational efficiency, and e) protein stability (Seidah et al., 2018).

PCSK9 follows a diurnal circadian rhythm, synchronized with cholesterol synthesis, with a peak at 4:30h and a nadir between 15-21h (Persson et al., 2010). Other studies reported a peak close to midnight instead (Chen et al., 2014). There are different agents that regulate the transcription and expression of PCSK9 (Krysa et al., 2017). It has been studied, both in humans and mice, how the metabolic and nutritional state, including fasting regulate PCSK9 expression (Browning & Horton, 2010). Insulin levels, via SREBP proteins and hepatocyte nuclear factor 1α regulate PCSK9 expression as well (Costet et al., 2006; Persson et al., 2010). Murine experiments showed how a high fat diet downregulates PCSK9 transcription (Maxwell et al., 2003). Certain conisoforms

ntrations of caffeine (I.e., 1,3,7-trimethylxanthine) suppress SREBP2-induced hepatic PCSK9 expression in liver hepatocytes (Lebeau et al., 2022). Moreover, some drugs used to control lipid homeostasis, like statins, inhibit 3-hydroxy-3-methyl-glutaryl-CoA reductase (HMG-CoA) and consequently activate SREBPs, which in turns increases PCSK9 transcription (Horton et al., 2003).

It is worth noting, FURIN and PC5/6 exert an inhibitory effect over the function of the PCSK9 protein (Benjannet et al., 2006; Essalmani et al., 2011; Lipari et al., 2012), leading to the circulation of different forms (Oleaga et al., 2021).

More recently, it was reported that cytosolic adenyl cyclase-associated protein 1 (CAP1) is a positive regulator of PCSK9 function regarding low density lipoprotein receptors. CAP1 binds to the M1-M3 repeats of the C-terminus of PCSK9 once complexed with LDLR, (see Figure 4) enhancing their transport into the lysosomal compartment for degradation (Jang et al., 2020).

Known biological functions of PCSK9

As was previously introduced, PCSK9 is synthesized as a precursor like are other PCSKs but does not undergo secondary cleavage. After the first autocatalytic cleavage, the prodomain is not released, but remains fastened, conforming the prodomain-PCSK9 complex. This complex, after a conformational modification of

the N-terminal α helix of the catalytic domain, is ready to exit the ER (Cunningham et al., 2007; Seidah et al. 2003).

To date, PCSK9s only known enzymatic substrate is itself and its own prosegment region is autocatalytically cleaved at sequence VFAQ152↓ (Benjannet et al., 2004; Naureckiene et al., 2003).

The best characterized biological function of PCSK9 is non-enzymatic, related to the control of the turn-over of LDLR (see Figure 6) in the liver (Benjannet et al., 2004). More recently, it has been reported its role related to immune checkpoints (Crunkhorn, 2021), platelet co-activation (Camera et al., 2018; Petersen-Uribe et al., 2021), epithelial sodium channels (ENaC) expression in renal cells (Sharotri et al., 2012), modulation of insulin secretion in pancreatic β-cells (Ramin-Mangata et al., 2021), CNS development (Poirier et al., 2006), the regulation of plasma triglyceride-rich lipoproteins in intestinal cells (Levy et al., 2013), the regulation of the accumulation of foam cells in vessels and atherosclerotic plaques (Ferri et al., 2012; Tang et al., 2017b), and aiding in tumor growth (Bassi et al., 2005).

Figure 6. Schematic overview of the intracellular regulation of cholesterol, LDLR and PCSK9.
Sterol responsive element-binding protein (SRBP) and Liver X receptor (LXR) are the major transcriptional mechanisms that regulate the intracellular concentrations of sterols, as a response to a deficit or excess of cellular cholesterol, respectively. LXR exerts its regulation through Idol-dependent ubiquitination of the LDL receptor, targeting genes related to ATP-binding cassette transporter A1 and G1 (e.g., ABCA1 and ABCG1) to promote the flowing out of cellular cholesterol (Zelcer et al., 2009). It has been suggested that IDOL ubiquitinates the LDLR-PCSK9 complex, targeting it into the lysosomal compartment for degradation, via a clathrin-independent pathway (Scotti et al., 2013). The cholesterol lowering drug statin inhibits the hydroxymethylglutaryl (HMG)-CoA reductase, and consequently reduces the concentration of LDL cholesterol in the plasma. (Adapted from Stancu & Sima, 2001;Sawamura, 2009).
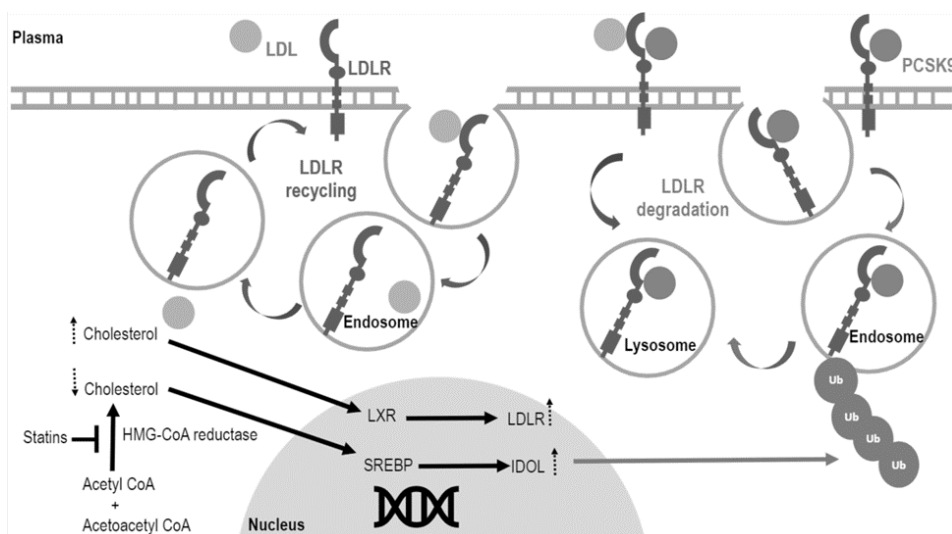
Mechanistically, circulating PCSK9 can escort certain surface receptors (e.g., LDLR and MHC-I receptor) towards the endosomal/lysosomal compartment for degradation through clathrin-coated pits (Benjannet et al., 2004; Liu et al., 2020; Nassoury et al., 2007).

Moreover, PCSK9 is responsible for the degradation of other close family members such as VLDLR and ApoER2 (Poirier et al., 2008), as well as the membrane antigen CD36 responsible for internalizing fatty acids and TA into the cells (Demers et al., 2015) and CD81(Le et al., 2015; Levy et al., 1998).

The first evidence for this mechanism of action, which mainly relays on the C-terminus (Cameron et al., 2009; Zhang et al., 2008), was published shortly after the discovery of PCSK9. By overexpressing PCSK9, the protein levels of LDLR were reduced (but not its mRNA) via intracellular degradation (Maxwell et al., 2005; Maxwell & Breslow, 2004). Thus, positioned PCSK9 as a novel pharmacological candidate for treating hypercholesterolemia and atherosclerosis (Cariou et al., 2011).

Therapies targeting PCSK9

Since 2015, when the US Food and Drug Administration (FDA) approved the first PCSK9i, a monoclonal antibody (mAb), many strategies to therapeutically target and inhibit PCSK9 activity, at several levels, have been developed: a) at the expression level to affect gene integrity and the translation or stability of the mRNA (using CRISPR methodology, antisense drugs, or small molecules), b) at the secretion level to block cell exit (inhibitors), and c) at the plasmatic free circulating level (using antibodies, EGF-A mimetics and vaccines)(Seidah, 2015; Seidah et al., 2019).

In primates, PCSK9 levels were downregulated, in tissue-specific manner, by using CRISPR and adeno-associated virus (AAV)-delivered meganuclease. The effects lasted up to 8 months (Musunuru et al., 2021; Wang et al., 2021).

To date, the most successful strategies for treating hypercholesterolemia in humans (and the only approved treatment by the regulatory agencies) has been those that target the processes related to the PCSK9-LDLR interaction (with injectable mAb) and mRNA stability (with a small interfering RNA called Inclisiran). The two used mAb are known by their generic names Alirocumab and Evolocumab, or their trade name Praluent (manufactured by Sanofi-Aventis) and Repatha (manufactured by Amgen) (Seidah et al. 2019).

PCSK9 treatments revealed to be as an effective substitute (or co-treatment) for statins' users. These statins are HMG-CoA reductase inhibitors, and have been used to treat hypercholesterolemia since the early 1990s (Endo, 2010). They function by

interrupting the cholesterol biosynthesis pathway, specifically avoiding the conversion of HMG-coA into mevalonate, a precursor of cholesterol (Sirtori, 2014). Interestingly, many patients have developed side-effects and resistance to this treatment (Reiner, 2014), a circumstance defined as the "statin paradox". This is because statins increase, at the same time, the expression and activity of LDLR (and consequently, lower the circulating LDL) and the expression and activity of PCSK9 (which degrades LDLR contributing to reduce the LDL uptake) (Dubuc et al., 2004).

In 2014, anti-PCSK9 agents were proposed for the treatment of septicemia, because patients carrying genetic mutations that cause hypocholesterolemia have shown resistance to bacterial septic shocks (Walley et al., 2014).

2.2.4   PCSKs and immunity

Many infections are due to bacteria that reside in their host as part of the normal commensal microbiota (e.g., *Streptococcus pneumoniae*), whereas other infections are caused by external pathogens (e.g., *Mycobacterium tuberculosis*). Certain components of the immune system exert a selective pressure on the commensal microbes, which may result in selection of more virulent strains resulting in a clinical infection, such as invasive group A streptococci infections (Walker et al., 2007). Also, pathogens can acquire new resistance mechanisms towards drugs and treatments, leading to antimicrobial resistance, which has been considered a serious global health threat (WHO, 2017). Both in cancer and infections, a therapeutic endeavor is to promptly detect emergent resistance (Waldetoft et al., 2017).

As was previously stated, PCSKs orchestrate many biological processes, and although many uncharacterized functions in the immune system need to be further addressed, PCSKs can be defined as modulators of the immune system (see Table 3). The activity of PCSK can favor the host immune response and the establishment and progression of infectious agents (Norata et al., 2016; Seidah et al., 2021).

PCSK1, PCSK2, FURIN, PCSK5 and *PCSK7* are expressed in several lymphoid organs (mainly the lymph nodes, the thymus, and the spleen) and immune cells, (such as macrophages and lymphocytes) (Lansac et al., 2006). All these, excluding *PCSK2*, regulate the mechanisms of antigen presentation and many other functions of macrophages and lymphocytes (Rose et al., 2021).

Table 3.   PCSKs in immunity.

ID	Implication | References
PCSK1	Innate immunity regulation: macrophage activity, TLR4 and TLR9 Adaptive immunity: T-cells, Foxp3 processing
	(Lansac et al, 2006), (Rodet et al, 2019), (Refaie et al, 2012), (Duhamel et al, 2015; 2016), (Gagnon et al, 2013), (Lansac et al, 2006), (de Zoeten et al, 2009)
PCSK2	Innate immunity : TLRs
	(Lansac et al, 2006)
PCSK3	Innate immunity : hepcidin activation, macrophage activity regulation Adaptive immunity: essential for T-cell mediated peripheral tolerance, Th1/2 cell balance Antigen presentation and recognition: TLR7 activation, processing peptides for MHC1 Viral infections: HIV envelope glycoprotein processing
	(Hipp et al, 2013), (Gil-Torregrosa et al, 2000), (Medina et al, 2009), (Pesu et al, 2008), (Guillemot et al, 2013), (Pesu et al, 2006), (Ortutay et al, 2021), (Decroly et al, 1997)
PCSK4	Immunocontraception: in males
	(Dahril et al, 2019)
PCSK5	Inflammation : in brain tissue Antigen presentation and recognition : TLR activation
	(Rose et al, 2021), (Ito et al, 2021)
PCSK6	Viral infections: activation of hemaglutinin from avian influenza
	(Hotimoto et al, 1994)
PCSK7	Antigen presentation and recognition Adaptive immunity: T-cells, Foxp3 processing, MHC-I Viral infections: HIV envelope glycoprotein processing
	(Leonhardt et al, 2010), (Turpeinen et al, 2011), (Pesu et al, 2008), (de Zoeten et al, 2009), (Decroly et al, 1997)
PCSK8	Innate immunity: dendritic cells in persistent arenavirus infections
	(Popkin et al, 2011)
PCSK9	Infectious diseases clearance: hepatitis C, sepsis, septic shock Innate immunity: inflammation, monocyte/macrophage activation, TLR4 activation Adaptive immunity: MHC-I Autoimmunity: lupus, rheumatoid arthritis
	(Labonté et al, 2009), (Walley et al, 2014), (Scalise et al, 2021), (Liu et al, 2020,2), (Liu et al, 2020), (Arida et al, 2021)

An important component of the innate immune system is the Toll-like Receptors (TLRs), a type of the host's innate pattern recognition receptors (PRRs), accounting for 10 different ones in humans and 13 in mice. Each of these type I transmembrane receptors recognizes one or more microbial molecular patterns, present on the surface of microorganisms. In humans, four are located in the endosome membrane (i.e., TLR-3, TLR-7, TLR-8 and TLR-9), whereas TLR-2/TLR-6, TLR-1/TLR-2, TLR-5 and TLR-4 are in the plasma membrane (Medzhitov & Janeway, 2000).

TLRs engage with major adaptor molecules (MyD88, TRIF, MAL, and TRAM) triggering signaling pathways heading to the activation of several transcription factors, such as NF-kB, which in turn leads to the induction of inflammatory type I interferon (O'Neill & Bowie, 2007). The orchestrated responses enhance pneumococcal phagocytosis and the intracellular clearance of leucocytes (Koppe et al., 2012; Letiembre et al., 2005).

Pathogens, such as *Streptococcus pneumoniae*, have microbe-associated molecular patterns (MAMPs) or danger-associated molecular patterns (DAMPs) which can be recognized by TLRs. For example, bacterial lipids such as LTA and LPS are detected

by TLR-1/TLR-2 or TLR-2/TLR-6 and TLR-4, respectively (Yoshimura et al., 1999), bacterial pneumolysin is detected by TLR4 (Malley et al., 2003), and bacterial unmethylated CpG DNA by TLR9 (Albiger et al., 2007).

Several studies have shown that PCSKs regulate the function of TLRs, controlling the activity of the immune cells (Hipp et al., 2013; Ishii et al., 2014). This association between TLR and PCSKs is relevant for regulating inflammatory responses; ergo, TLR agonists have therapeutic potential as immunomodulators, as they are able to train the immune system via epigenetic modifications and metabolic reprograming (Janeway, 2001).

While PCSK1 is associated with TLR4 and TLR9 trafficking, FURIN interacts with TLR7, TLR8, and TLR9, having a role in their processing. Also it is known that FURIN cleaves TGFβ, regulates IFN- ɣ, and is essential for maintaining peripheral immune tolerance, as it is expressed in differentiated Th1 cells (Dubois et al., 2001; Pesu et al., 2006, 2008). PCSK7 participates in TLR7 processing (Rose et al., 2021). Also, it has been reported that the proinflammatory effects of PCSK9 are dependent on the activation of TLR4/NF-kB signaling (Badimon et al., 2021; Lei et al., 2020; Scalise et al., 2021; Tang et al., 2017b).

Experiments mimicking pathogen-like infections, such as challenging cells with LPS, demonstrated the plasticity of PCSK expression in immune cells, through the activation of Toll-like receptors (TLRs), being able to coordinate innate and acquired immune responses (Lansac et al., 2006).

Among the components of the innate immune system, dendritic cells (DCs) are a key player in linking both branches of the immune system. During maturation, DCs lose their endocytic functions and express cell-surface molecules, such as the major histocompatibility complex class I (MC-I) and class II (MC-II), similar in structure and function. These receptors have an important role in discriminating between what is self and what isn't, and detecting intracellular bacteria, parasites, and viruses (Coutant & Miossec, 2016; Janeway, 200). MHC also referred to as human leukocyte antigen (HLA), a family of cell-surface glycoproteins essential for antigen presentation to T-cells and thereby for bridging the innate and the adaptive branches of the immune system (Janeway, 2001).

PCSK9, and also PCSK7 interact with MHC-I (Bassi et al., 2005; Liu et al., 2020). Mechanistically, PCSK9 can disrupt the recycling of MHC-I to the cell surface by binding to it for lysosomal escorting and degradation (Liu et al., 2020). A genome-wide expression correlation analysis in humans, demonstrated a correlation between PCSK7 and MHC-class genes (Turpeinen et al., 2011). Also, it has been suggested that PCSK7 participates in stabilizing the expression of MHC-I (Rose et al., 2021).

2.2.5   PCSKs and cancer

According to the International Agency for Research on Cancer (https://gco.iarc.fr/), only in 2020 more than 4 million new cases of cancer were diagnosed in Europe alone (all ages, both genders).

A proper host response against pathogens and tumor cells stems from the precise activation of both branches of the immune system, the innate and the adaptive (Chaplin, 2010). The relationship between the immune system and cancer has been extensively reviewed, elucidating the anti- and pro-tumorigenic dynamics provided by the different components of the immune system (Bashford, 1910; Garner & de Visser, 2020; Hiam-Galvez et al., 2021). Cancers can arise in any multicellular organism (Albuquerque et al., 2018), including invertebrates (Scharrer & Lochhead, 1950), and plants (Doonan & Sablowski, 2010), in diverse tissues (liquids or solids), and can be caused by different agents (endogenous or exogenous), implying a wide range of mutations, characterized by common features such as unrestricted growth or metabolic reprogramming (Hanahan, 2000; Hanahan & Weinberg, 2011). Drugs as poly (ADP-ribose) polymerase inhibitors (PARPi) have been extensively used to treat some cancers, such as OC, since they exploit certain mutations and genetic instabilities (e.g., DNA double stranded break repair deficiency) (Amé et al., 2004).

Already in the 1990s, PCSKs were associated with cancer, when it was found that PCSK1, PCSK2 and FURIN are overexpressed in certain malignancies (Smeekens and Steiner 1990). Afterward, many *ex vivo*, *in vitro* and *in vivo* studies have addressed the role of PCSKs in neoplastic transformation (Mbikay et al., 1997), proliferation, vascular remodeling mainly via TGFβ and pro-VEGF processing, invasiveness (Pei & Weiss, 1995), and cell metastasis (through processing several types of matrix metalloproteinases, collagen and integrins) (Mbikay et al., 1993) (See Table 4).
PCSK1 and PCSK2 have been studied mainly in the context of neuroendocrine tumors, pituitary adenomas, thyroid and lung (Creemers et al., 1992). FURIN, PCSK5, PACE4 and PCSK7 in breast, prostate (D'Anjou et al., 2011), lung and head/neck cancers (Bassi et al., 2001; Mbikay et al., 1997).

FURIN is the most studied PCSK due to its action over TGFβ (Dubois et al., 2001; Pesu et al., 2006), with seven studies (four of them focusing on OC). For instance, Vigil (NCT03842865) is an shRNA-based blocker of FURIN that together with granulocyte-macrophage colony-stimulating factor (GM-CSF) causes DC-mediated immune activation against cancer. This is achieved because GM-CSF is a myelopoietic growth factor and pro-inflammatory cytokine that promotes DC

activation and maturation (Fleetwood et al., 2005; Hamilton, 2008) and blocks immunotolerance via the down-regulation of FURIN-mediated TGF-β processing.

PCSK9 regulates several pathways in cancer, such as JNK, NF-κB, and the mitochondrial-mediated apoptotic pathway (Singh et al., 2021). PCSK9 contributes, in an LDLR-dependent way, to the activation of CD8+ T-cells (Yuan et al., 2021). Moreover, PCSK9 disrupts the recycling of MHC-I in an LDLR-independent fashion (Liu et al., 2020). PCSK9-deficient tumor cells have an increased response to immune checkpoint blockade therapy by promoting mature T-cell intertumoral infiltration. The molecular mechanism behind is related to the interaction of PCSK9 with MHC-I rather than with LDLR. PCSK9 is responsible to bind and escort MHC-I for lysosomal degradation (in a similar fashion as for LDLR). Thus, by inhibiting or silencing PCSK9, the expression of MHC-I on the surface of tumor cells, increases. Therefore, T-cells via their T-cell receptors (TCRs) can recognize surface MHC-I, and effectively counteract tumor cells. Moreover, was proven that induced LDLR-deficiency in the tumor cells, did not have any significant consequent on tumor growth (Liu et al., 2020). Additionally, downregulating PCSK9 expression showed a synergistic effect with anti-PD-1 antibodies (Crunkhorn, 2021).

Table 4. **PCSKs in cancer.** (In brackets, referenced other relevant diseases).

Gene ID	Disease (implication)
PCSK1	Human colorectal liver metastasis, pituitary adenomas. [Diabetes (insulin processing), obesity (humans)]
	PMID: 21437630, 25784503, 9207799,16293189, 11081197, 33299884, 32346297
PCSK2	Human colorectal liver metastasis (abnormal expression and processing) [Alzheimer, diabetes (insulin processing), obesity]
	PMID: 16293189, 14614908
PCSK3	Cancer (processing growth factors), tumorigenesis (VEGF-C activation), onco-immune response [Bone endocrine functions (osteocalcin regulation), atherosclerosis, Infections]
	PMID: 28972540, 21889147, 17909005, 12360192, 15899807, 12782675, 25624351, 32300641, 28369813, 26167473, 4127186, 32057769, 33432808, 17972346, 33995401
PCSK4	[Fertility]
	PMID: 9192653
PCSK5	Cancer (neuro and glioblastoma, tumorigenesis (VEGF-C activation) [Developmental defects (in humans), LDL-c metabolism]
	PMID: 20031622, 19737405, 12782675, 18519639, 28446132
PCSK6	Cancer (prostate, breast), tumorigenesis (vascular remodeling), [Osteoarthritis pain (in humans), blood pressure (Corin enzyme activation)]
	PMID: 25682874, 28993410, 17909005, 26838312
PCSK7	Cancer (invasiveness), tumorigenesis (VEGF-C activation), [Anxiety/depression, iron and lipid metabolism (TAG), Alzheimer (alpha-secretase pathway)]
	PMID: 26341526, 12782675, 21149283, 34565765, 26763881, 24558110, 10537065
PCSK8	[Infections (viral), lipid disorders (LDL-c and TAG synthesis regulation)]
	PMID: 11606739, 30655525
PCSK9	Cancer [LDL-c metabolism, Infections (Dengue), Sepsis (bacteremia and septic shock)]
	PMID: 24518357, 32644974, 33995401, 34144130,33262511

Several drugs and biologicals are being evaluated, whether they can be used on cancer patients, to inhibit or block the different PCSKs members (see Table 5). For PCSK9 there are two ongoing studies assessing whether the use of drugs might be beneficial for patients suffering from pancreatic cancer and glioblastomas. Additionally, one study for evaluating whether PACE4 isoforms can be used as biomarkers in thyroid cancer has been completed, and eight studies are ongoing centered on PCSK1 to treat obesity and diabetes.

Table 5. **Clinical trials based on inhibiting PCSKs in cancer.** As December 2021 (https://clinicaltrials.gov/).

NIH ID	Drug/Biological	Target	Malignancy	Country	Status
NCT04937413	Evolocumab	PCSK9	Glioblastoma	U.S.	Recruiting
NCT04862260	LDL-c disruption, FOLFIRINOX	PCSK9	Pancreatic cancer	Canada	Not yet recruiting
NCT 01867086	Salvage Ovarian FANG™Vaccine, Carboplatinum	FURIN	OC stage III and IV	U.S.	Completed
NCT01551745	Salvage Ovarian FANG™Vaccine, Bevacizumab	FURIN	OC stage III and IV	U.S.	Completed
NCT03073525	Atezolizumab and Vigil	FURIN	Gynecological cancers (OC included)	U.S.	Active, not yet recruiting
NCT03842865	Vigil	FURIN	Five solid tumors (OC included)	U.S.	N/A
NCT03495921	Vigil, Irinotecan, Temozolomide	FURIN	Ewing tumors family	U.S.	Active, not yet recruiting
NCT03160482	Isoforms as biomarkers	PACE4	Thyroid cancer	Canada	Completed

2.3   Pneumococcal infections

The *Streptococcus pneumoniae* is a facultative anaerobic Gram-positive organism with a heterogeneous and plastic genome, which confers the ability to adapt and change (Kadioglu et al., 2008). As of the year 2020, 100 serotypes have been documented, with different prevalence depending on the area or age group (Kroger et al., 2015). The extracellular pneumococcus uses a combination of different virulence factors, which confers the capability of intracellular invasion and survival, such as toxins (e.g., pneumolysin), enzymes (e.g., pyruvate oxidase or metalloproteases), proteins (e.g., PspA, PavB), the external capsule itself or the formation of biofilms (Kadioglu et al., 2008; Subramanian et al., 2019).

Pneumococci can be found as single bacteria, but hey tend to form duplets and biofilms, to avoid phagocytosis and complement-mediated immunity (Domenech et al., 2013). Another important virulence factor is the surface capsule that may or may be not present, conferring resistance against opsonization, phagocytosis and complement activity (Dalia et al., 2010; Hyams et al., 2010). Surface capsules contain polysaccharides, most of which are covalently attached to the outer surface of the cell wall peptidoglycan, and which can used to classify *S. pneumoniae* into serotypes (MacLeod & Krauss, 1950; Sorensen et al., 1988). Also, there are cell-surface proteins associated with adhesion and antigenicity, making them promising vaccine candidates (Marquart, 2021).

The bacterial toxin pneumolysin (ply) belongs to the family of cholesterol-dependent cytolysins, essential for pneumococci in evading intracellular degradation in the lysosomal compartment and thus, successfully trafficking across the blood brain barrier and invading the brain (Surve et al., 2018). It is produced as a soluble protein, which oligomerizes in the membrane of target cells and the formation of pores in the transmembrane (Tilley et al., 2005). Ply has three main functions: 1) as a cell modulator, 2) as an activator of the classical complement pathway (Mitchell et al., 1991), and 3) as an inflammation inducer via TLR signaling (Marquart, 2021). It has been reported that ply has a function as activator of TLR signaling, since TLR4 on host macrophages, has evolved to recognize it (Malley et al., 2003).

Recently, four pneumococcal serine proteases, belonging to the category of trypsin-like or subtilisin-like family proteins (i.e., HtrA, SFP, PrtA, and CbpG), have received increased attention due to their immunogenicity, acting as a key players covering different stages of the invasion and pathogenesis of pneumonia and sepsis (Ali et al., 2021; Marquart, 2021).

2.3.1   Host immune response to *Streptococcus pneumoniae*

The molecular basis of a *Streptococcus pneumoniae* infection remains unclear, as do individual susceptibilities and the genetic factor of the host that affect the disease outcome (Brown, Hammerschmidt, & Orihuela, 2015). In the recent decades, associations between blood types and various diseases (e.g., bacterial infections, hypercholesterolemia, Covid-19) have been gaining more attention (Deng et al., 2021; Goel et al., 2021; Paquette et al., 2018)). The possible relationship between a streptococcal infection and the ABO group has been studied, concluding that blood type B is strongly associated with an increased streptococcal infection incidence (Abegaz, 2021). Infectious agents (i.e., bacteria, viruses, and parasites) attach to cell surface glycoconjugates. Thus, blood type glycosylation polymorphisms may affect the individual vulnerability to infections (Zoldoš et al., 2013).

Every bacterial colonization starts when the bacteria irrupt the mechanical barriers, the first line of defense. Epithelial cells have mucosa rich in lysozyme, an enzyme able to degrade the peptidoglycan in the cell wall of *S. pneumoniae* (Henriques-Normark & Normark, 2010). Innate immune responses are triggered by Pattern Recognition Receptors (PRRs), a set of proteins capable of recognizing pathogenic elements, otherwise known as Pathogen-Associated Molecular Pattern (PAMPs), or molecules released by damaged cells (Damage-Associated Molecular Patterns or DAMPs) (Takeuchi & Akira, 2010). These receptors have a conserved function and an ancient evolutionary history, since they emerged phylogenetically prior to the emergence of the adaptive immunity (Janeway, 1989). Upon PAMP ligation to PRR, a cascade of signals is triggered, leading to the production and secretion of soluble mediators such as cytokines and chemokines (see Figure 7).

Figure 7.   Representation of the host response to a *Streptococcus pneumoniae* infection. As explained in the text, the schematic illustration summarizes the main players involved in pneumococcal infections at the cellular level. *S. pneumoniae* components in dark red.
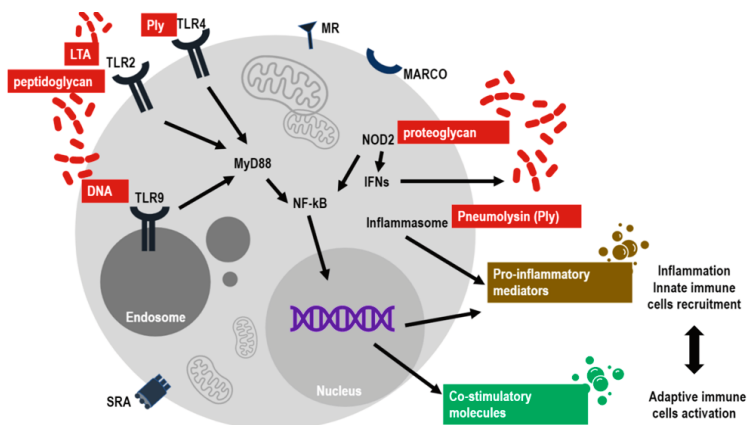
A subset of membrane-bound PRR, the Toll-like Receptors (TLRs), is responsible for the activation of transcription factors such as those of the NF-kB and IRF families (Kawai & Akira, 2010). The TLR signals are mediated by adaptors such as MyD88 or TRIF (Medzhitov et al., 1998). In the context of a *S. pneumoniae* infection, the principal TLRs involved are the cell membrane harbored TLR2 and TLR4; as well as the intracellular (endosome membrane harbored) TLR9 (Takeda & Akira, 2015). TLR2 has the ability to bind a vast range of ligands (e.g., bacterial lipopeptides, LTA) via heterodimerizing with other TLRs (either TLR1 or TLR6) (Malley et al., 2003). The main LPS detector, TLR4 in turn, recognizes pneumolysin, a cytolytic toxin produced by most clinical *S.pneumoniae* isolates, stimulating TNF-α and IL-6 release in macrophages (Malley et al., 2003). TLR9 detects unmethylated CpG motifs (Hemmi et al., 2000). In the airways, upon a pneumococcal infection, TLR9 activates the resident macrophages via MyD88. *In vivo* experiments showed that TLR9-deficient mice are more vulnerable to develop a respiratory tract pneumococcal infection than their wild-type controls (Albiger et al., 2007).

Another family of receptors with an important role is the cytoplasmatic Nucleotide-binding Oligomerization Domain-containing (NOD2) receptors. Upon recognition of bacterial peptidoglycan, they activate transcription factors to produce pro-inflammatory soluble mediators (e.g., CCL2) and type I interferon responses (Nakamura et al., 2011). In the affected tissue, recruited monocytes differentiate into macrophages, to phagocyte bacteria (Davis et al., 2011).

Pneumolysin (Ply) activates a intracellular complex of proteins, the NLRP3 inflammasome, leading either to the production of proinflammatory cytokines (e.g., interleukins IL-1b and IL-18), independently of TLR4 (McNeela et al., 2010), or to the induction of pyroptosis, a form of cell death (Man et al., 2017; D. Xu et al., 2021).

The complement system is a set of plasma proteins, that act synergistically to increase the opsonization of pathogens by antibodies, while engaging with the inflammatory response (Winkelstein, 1981) (Murphy & Weaver, 2016). It has been proven that *S. pneumoniae* resistance to complement-mediated immunity is dependent on the capsular serotype (Hyams et al., 2010; Winkelstein, 1981). *In vitro* studies shown that *S. pneumoniae* can activate the terminal components of the complement (i.e., C3-C9), via the classical and alternative pathways (Winkelstein, 1981).

The adaptive immune system is not critical in the pneumococcal clearance. Murine experiments have shown that animals lacking mature B-cells, therefore failed to produce antibodies, had no detrimental consequences compared with controls (McCool & Weiser, 2004).

2.3.2 Pathogenesis and clinical aspects

Streptococcus pneumoniae (aka pneumococcus) is an old acquaintance of human beings (Loughran et al., 2019), and its etiology is well known (Dion & Ashurst, 2021). Although it is a resident commensal bacterium of the flora of the nasopharynx (Cole et al., 2008), it is the main causative agent of opportunistic local and systemic infections (Krzyściak et al., 2013), such as otitis media, bacteremia, meningitis, or community-acquired pneumonia worldwide (Steel et al., 2013).

Bacteremia is a clinical term for describing the illness derived from having bacteria in the bloodstream, whereas sepsis refers to a clinical diagnosis defined by organ dysfunction and a dysregulated host response to an infection. Thus, not all infections progress to sepsis or septic shock, which still is the leading cause of death due to an infection (Napolitano, 2018).

Sepsis is a life-threatening organ failure condition extensively reviewed and characterized for the activation of many pathways, including those related to cytokine storms, the coagulation cascade, cellular apoptosis, and mitochondrial collapse (Huerta & Rice, 2019).

So far, not a single robust biomarker is available for the early diagnosis of sepsis, but high levels of C-reactive protein (CRP), procalcitonin, and lactic acid are indicative of sepsis. Thus, in order to recognize patients at risk of sepsis early (and to confer consistency for epidemiologic studies and clinical trials), the parameters, definitions (of sepsis and septic shock) and clinical criteria were revised in 2016, resulting in what is known as the SEPSIS-3 criterion (Singer et al., 2016). This definition, like the previous one, does not necessarily imply that septic patients would also have bacteraemia or *vice versa*.

The person-to-person transmission of *S. pneumoniae* is via respiratory droplets or autoinoculation. A seasonal or temporal pattern for *S. pneumoniae* has been reported, infections being more common during winter and early spring. Humans are the main reservoir, and both healthy adults and children are asymptomatic carriers of *S. pneumoniae* (O'Brien et al., 2009; Regev-Yochay et al., 2004).

According to the Centers for Disease Control and Prevention (CDC), diagnosis is based on the isolation of *S. pneumoniae* from sterile body sites (e.g., blood, pleural fluid or cerebrospinal fluid). Additionally, the presence of pneumococcal antigens in body fluids can be tested. For a diagnostic evaluation in adults, a urinary antigen is also available. In general terms, a clinical criterion for suspecting pneumococcal

pneumonia is to find polymorphonuclear leukocytes, epithelial cells and Gram-positive diplococci in a sputum or any sterile fluid[3].

Extensive research has been conducted over the years to prevent and find new treatments against pneumococcal infections. During the last decade, efforts have focused on enhancing the host immune system (e.g., by administering selective antibodies), targeting the virulence factors, and overcoming increased pneumococcal resistance. Moreover, a few experimental therapies have progressed into clinical trials, mainly based on the use of liposomes, such as Ply inhibitors. These novel therapies interfere with pneumococcal survival mainly through the inhibition of transcription, translation and enzyme elongation (Cools et al., 2021). Another important resource are vaccines against pneumococcus. They have been developed since 1911. The fist vaccine was approved for use in the U.S., containing a purified capsular polysaccharide antigen from 14 different serotypes (Smeall, 1948).

2.3.3 Epidemiology and societal impact

Estimations from the WHO state that *S. pneumoniae* is responsible for at least half a million deaths among children under 5 years old, annually worldwide. Its impact is so high that pneumococci received the title of "The Forgotten Killer of Children". Asia and Africa are by far the most affected continents. For instance, in 2013 only in Africa, 1milion children died of pneumonia (O'Brien et al., 2009).

The high burden of disease together with an increased antibiotics/penicillin resistance, placed *S. pneumoniae* on the priority pathogens' list by the WHO in 2017. The societal burden and economic costs are not only caused by lethal outcomes, but also non-lethal long-term morbidities (Prina et al., 2015). In Finland, 18,513 cases of *Streptococcus pneumoniae* were recorded between 1995 and 2021 (Finnish Institute of Health and Welfare[4]). There are close to 800 cases every year, except for the years 2020 and 2021 (only 318 and 235 cases registered). From 21 Hospital Districts, Helsinki and Pirkanmaa had the most cases.

---

[3] available at https://www.cdc.gov

[4]https://sampo.thl.fi/pivot/prod/fi/ttr/shp/fact_shp?row=reportgroup-12416&column=time-12059.

2.3.4 PCSK9's mechanism of action in pneumococcal infection

Innate immune host responses and housekeeping lipid metabolism share ancient connections, as they have evolved from a single common system (Azzam & Fessler, 2012).

Lipids have many roles related to organization and structure (including cellular trafficking), energy storage and cellular signaling. Cholesterol (LDL-c) and bacterial lipids (e.g. LPS, LTA) are cleared under common pathways. LPS is a phosphorylated glycolipid, with a similar structure compared to some host lipids (e.g., ceramides and phosphatidic acid). The reverse cholesterol transport (RCT) mobilizes the LDL-c from peripheral tissues to the liver and gut, involving TLRs. This has an impact on atherosclerosis and potentially on endotoxemia. RCT and sterol networks are examples of an ancient regulatory part of the innate immune system. There are other alternative pathways, such as the transintestinal cholesterol efflux (TICE), for the elimination of serum LDL-c into the intestinal lumen (Azzam & Fessler, 2012).

The main proteins involved in the clearance of both self and bacterial lipids are: CD14 (Schmitz & Orsó, 2002), TLR4 (Bae et al., 2009; Poltorak et al., 1998), ABCA1 (Thompson et al., 2010; Yin et al., 2010), scavenger receptors (Vishnyakova et al., 2003), and Annexins (Eberhard & Vandenberg, 1998; Lemmon, 2008). For example, it has been reported that TLR4 interacts with both host lipids and with microbial lipids (Bae et al., 2009; Poltorak et al., 1998), as well as with PCSK9 (Badimon et al., 2021; Lei et al., 2020; Scalise et al., 2021; Tang et al., 2017).

Experimental evidence has shown that PCSK9 and lipoproteins have a role in the innate immune responses and inflammation albeit contradictory results (Abbas et al., 2019; Barnett & Kagan, 2020; Walley et al., 2014). Generally significant changes in cholesterol levels have been reported from infection or cancer, and often has implications on the prognosis and outcome (Brantley et al., 2020; Dos Santos & Marshall, 2014; Kamińska et al., 1983; Lee et al., 2015; Munir et al., 2014). Interestingly, it has been reported that plasma levels of PCSK9 correlate with plasma levels of cholesterol, but only explains part of its variation (Lakoski et al, 2009).

More recently, plasma PCSK9 levels have been used as a reference of infection (Innocenti et al., 2021). During inflammation, infection and sepsis, it is common to find disturbances in cholesterol metabolism (Lee et al., 2015). Reduction in cholesterol levels correlates with severity of the infection (Barlage et al., 2001).

PCSK9 is linked to the regulation of the innate immunity primarily due to its LDLR-mediated pathogen clearance. Experiments in mice showed that LPS triggered inflammation. LPS is able to upregulate PCSK9 expression, leading to

increased LDLR degradation. Thereby, the authors hypothesized that increased circulating LDL might have possible beneficial effects on the host defense (Feingold et al., 2008). Often, during an infection, the levels of liver-produced circulating PCSK9 are increased compared with healthy controls (Boyd et al., 2016). Moreover, it has been reported recently that PCSK9 induces transcription factors expression through the activation of TLR4/NFkB signaling in different animal experiments (Lei et al., 2020; Scalise et al., 2021; Tang et al., 2017a).

Clinical trials indicate that PCSK9i reduced LDL-c levels up to 70% as a monotherapy or as a co-treatment with statins (Lepor & Kereiakes, 2015). Thus, it has been proposed that PCSK9i could be used to treat also other diseases beyond hypercholesterolemia; like cancer, infections, inflammation or even allergy, at an affordable cost (Almeida et al., 2021). Two decades of clinical research endorse the protective effect of having lower PCSK9 levels/activity associated with a lesser risk of experiencing a cardiovascular event, but also with a reduced risk of complications upon sepsis or inflammation (Walley et al., 2015).

Nowadays, out of 240 registered studies at the NIH, two ongoing clinical trials are evaluating the feasibility of the use of PCSK9i for treating sepsis patients with Evolocumab or Alirocumab (NCT03869073 and NCT03634293, respectively). In addition, there are two patents related to PCSK9 and sepsis: "Methods and compositions for diagnosis and prognosis of sepsis" (EP-2875347-A1) and "Biomarkers for detection of neonatal sepsis in body fluids" (JP-2012516445-A). However, more research is needed to elucidate the long-term effects of PCSK9i or the permanent silencing of PCSK9 (Seidah & Prat, 2021).

2.4 Ovarian cancer

2.4.1 Ovarian cancer and omental migration

Ovarian cancer (OC) is a complex and heterogeneous disease, with a varying histology, molecular characteristics, grades and clinical outcomes (Lheureux et al., 2019). Primary OC has two main origins: non-epithelial and epithelial (EOC) (Gaona-Luviano et al., 2020; Webb & Jordan, 2017). Non-epithelial OC comprises different subtypes (i.e., stroma, germ cells or fallopian tube epithelia stem-like cells) (O'Shea, 2022; Paik et al., 2012), whereas EOC arises from the ovary epithelium and account for the 90-95% of all malignant tumors (Rojas et al., 2016; Torre et al., 2018). Thus, EOC is a heterogeneous group (see also Table 6), classified as mucinous (3%) and non-mucinous (97%). Non-mucinous tumors comprise different histological types, differing in their origin, pathogenesis, molecular profile, and even risk factors and clinical prognosis: serous (70%), endometroid (10%), clear cell (10%), and unspecified (7%) (Lheureux et al., 2019; Prat, 2012).

For the serous histological type, two groups have been characterized, the high grade serous ovarian cancer (HGSOC), most common, and low grade serous ovarian cancer (LGSOC) (Holschneider & Berek, 2000; Rojas et al., 2016). Genetically, HGSOC is less defined than LGSOC, but as a common feature, almost all HGSOC cases (I.e., ~97%), have a mutated *TP53* gene (Bell et al., 2011).

HGSOC was stratified initially into four (later into 7) signatures or prognostic subtypes according to their gene expression profiles: differentiated, immunoreactive (with better overall survival, OS), mesenchymal (worst OS) and proliferative (Konecny et al., 2014; Tothill et al., 2008). Also, half of HGSOC patients have homologous recombination deficiency (HRD) as a contributing factor (Bell et al., 2011; da Cunha Colombo Bonadio et al., 2018; Saravi et al., 2021), associated with gene defects related to DNA-repair, affecting transcriptional activation. HRD has been successfully targeted using poly (ADP-ribose) polymerase inhibitors (PARPi) particularly for patients harboring *BRCA1/2* mutations (Saravi et al., 2021), and platinum-based chemotherapy (Kroeger & Drapkin, 2017). Although the initial response rate to standard care of treatment is high (i.e., ~80%), relapses and subsequent progression to metastatic invasion of the peritoneum, are high too. This is the main reason why the mortality of HGSOC is high (Kim et al., 2018).

Table 6.   Subtypes of EOC and their main features.

	HGSOC (~70%)	LGSOC (~10%)	Clear cell (~5%)	Endometrioid (~10%)	Mucinous (~3%)
Specific clinical information	15-25% of the diagnoses have inherited predisposition	From borderline tumours	Endometriosis	Synchronous primary ~10% endometriosis	Exclude GI primary
Histology	Large papillae; solid growth; large mononuclear cells; pleomorphic prominent nuclei; mitotic activity.	Small papillae; cells with uniform nuclei and hyalinized stroma; psammoma bodies.	Complex papillae with tubules and solid areas, prominent nucleoli; clear cytoplasm with glycogen present.	Solid; cystic.	Heterogeneous components (invasive and non-invasive).
Molecular Information	↑CNA *TP*53 BRCA1/2 CDK12 HRD	↓CNA MAPK activation KRAS BRAF NRAS HER2	ARID1A PI3K/AKT act. RTK/Ras act. MMR PI3KCA KRAS PTEN TP53	PI3KCA ARID1A KRAS Wnt/β-catenin act. PTEN CTNNB1 PPP2R1α TP53	KRAS *HER2* amplifica-tion.
Platinum Chemotherapy	Sensitive	Resistant (relatively)	Resistant (relatively)	Sensitive	Resistant (relatively)
PARP Inhibitor	Yes	No	No	Yes (high grade)	No

* Abbreviations: AKT:AKT serine/threonine kinase 1; ARID1A: AT-Rich Interaction Domain 1A; BRAF: carcinoma B-Raf proto-oncogene, serine/threonine kinase; BRCA1/2: breast cancer 1/2 gene; CDK12: cyclin dependent kinase 12; CNA: copy number alteration; CTNNB1: catenin beta 1; HER2: human epidermal growth factor receptor 2; HRD: homologous recombination deficiency; KRAS: Kirsten rat sarcoma viral oncogene homologue; MAPK: mitogen-activated protein kinase; MMR: mismatch repair; NRAS: neuroblastoma RAS viral (V-ras) oncogene homologue; OR: oestrogen receptor; PI3K(CA): phosphoinositide 3-ki-nase (catalytic, α polypeptide); PPP2R1α: protein phosphatase 2, subunit A, α isoform; PR: progesterone receptor; PTEN: phosphatase and tensin homologue; RTK: receptor tyrosine kinase; TP53: tumour protein p53; Wnt: wingless-related integration site. Adapted from (Lheureux et al., 2019; Prat, 2012).

Cancerous cells often home into the omentum, an abdominal layer of fatty tissue, covering the intra-peritoneal organs that conforms a proinflammatory microenvironment. It is responsible for fat storage, and other important biological functions such as tissue regeneration and immune regulation. It is a reservoir of both soluble factors and cellular components (Ford et al., 2020). It is also rich in highly vascularized immune structures known as "milky spots", formed mainly of macrophages and lymphocytes. These spots form a niche that supports cancer cell proliferation (Clark et al., 2013; Hagiwara et al., 1993). Advanced OC patients commonly accumulate large quantities of fluid within the abdomen, known as ascites. This fluid is a reservoir of soluble factors and cellular components, which provides a pro-inflammatory and pro-tumoural microenvironment to the OC cells,

and thus facilitates their omental metastasis (Adam & Adam, 2004; Ahmed & Stenvers, 2013). The development of ascites correlates with a significantly decreased 5-year survival rate (5% with ascites vs 45% without ascites) among women with stage III or IV EOC, and thus has prognostic value (Puls et al., 1996).

OC has a different unique metastatic idiosyncrasy compared with the classic pattern of hematogenous metastasis (Lengyel, 2010). It has been suggested that OC cells detach (individually or forming small clusters) from the primary ovarian tumor via a passive mechanism, flowing through the peritoneal fluid (Lengyel, 2010). But, more recently, it was reported that an active neutrophil influx is a prerequisite for cellular migration (Lee et al., 2019). Interestingly, under healthy conditions, neutrophiles are not present in the tissue of the omentum. However, upon the onset of the disease, neutrophiles are recruited to the milky spots (Buscher et al., 2016). Neutrophile stimulation and the ejection of pro-metastatic neutrophil extracellular traps (NETs) are mediated by inflammatory factors derived from tumor cells (e.g., IL-8, GROα/β, G-CSF, and MCP-1) (Lee et al., 2019).

The cellular dynamics that orchestrate this tropism and the resulting accumulation of abnormal abdominal liquid (ascites), a hallmark of OC, are still not fully understood. At the beginning, highly controlled interactions between proteases and adhesion receptors are the main regulators of cancer progression, whereas later steps are characterized by the fast growth of tumor nodules driven by oncogenes (Ford et al., 2020; Lengyel, 2010).

These complex and heterogeneous processes change over time due to the spontaneous clonal evolution of cancer cells or due to an adaptive response to treatment (Zhang et al., 2018).

2.4.2   Pathogenesis and clinical aspects

The clinical management and prognosis of OC depend greatly on its staging and subtype (Bast et al., 2021). OC staging was determined in 1988 by FIGO[5], and updated in 2014 as "The new WHO Classification of Ovarian Cancer" (Kurman et al., 2014).

The OC stage stands for the degree of spreading from its site of origin, and it is determined by a histological examination after the surgical removal of affected tissues (O'Shea, 2022). Currently four stages are defined: I) tumors confined to ovaries, II) involving at least one ovary with pelvic extension, III) further into abdominal cavity and/or lymph nodes, and IV) including distant metastasis.

---

[5] *Fédération Internationale de Gynécologie et d'Obstétrique*, https://www.figo.org/

Currently, only about 1 out of 4 of patients are diagnosed with stage I or II (Bast et al., 2021). OC is commonly referred to as the "silent killer", due to the lack of noticeable symptoms. Typically patients experience only non-specific bloating, fatigue, frequent urination, abdominal and/or pelvic pain, leg pain, digestive alterations, or rarely, vaginal bleeding (Ebell et al., 2016). Therefore, diagnosis is usually confirmed at advanced stages, increasing the probability of poor patient outcome (Gaona-Luviano et al., 2020; Momenimovahed et al., 2019).

Homologous recombination deficiency (HRD) has diagnostic, prognostic and therapeutic implications. Early detection enables curable treatment in 90% of the cases, including the most aggressive histological subtypes (Peres et al., 2019).

The preliminary examinations include ultrasound exploration, computed tomography (CT) scanning, magnetic resonance imaging (MRI), biomarker testing, and biopsy screening (Doubeni et al., 2016; Ebell et al., 2016). Standard treatment relies primarily on debulking surgery, followed by systemic therapy according to the OC subtype and the patient's molecular and clinical data (e.g., platinum-based chemotherapy) (Vergote et al., 2010). It is known that patients harboring *BRCA*-mutated genes are more platinum sensitive than the carriers of non-mutated *BRCA* gene, the former having a better prognosis (Yang et al., 2011).

Although complete remission is achieved in many EOC patients (HGSOC in particular) treated with surgical intervention and posterior first-line platinum-based chemotherapy (carboplatin and paclitaxel/docetaxel/pegylated liposomal doxorubicin altogether), still within 18 months many of these patients will experience recurrence of the cancer (Dogan et al., 2013).

Detection of an OC relapse is based mainly on upregulated levels of the cancer antigen 125 (CA-125) protein in serum. CA-125 is a suitable biomarker for patients who have elevated levels already in the early phases (Buechel et al., 2019). Chemotherapy resistance is a pressing issue (Jiang et al., 2019b) in the treatment of OC. It is a complex and heterogeneous phenomenon, both within and between patients (Christie & Bowtell, 2017). Recurrent cancer is generally incurable, although some subtype specific therapeutic strategies have been suggested. For instance, in recurrent LGSOC patients, the use of MEK-inhibitors has been found beneficial (Lheureux et al., 2019).

Since OC is a disease with several hallmarks related to angiogenesis mediated by the vascular endothelial growth factor (VEGF); bevacizumab -a humanized monoclonal antibody against VEGF-, has proven to be beneficial for treating recurrent OC, especially in combination with PARP inhibitors (PARPis) (Garcia et

al., 2020), which interfere with the NHEJ pathway, causing "synthetic lethality" (Helleday et al., 2008).

Currently, there are 137 studies on PARPis addressing OC, evaluating their efficacy in combination with other drugs and biologicals[6].

PARP enzymes consist of a family of at least 17 members mainly responsible for detecting single-strand breaks (SSBs). Inhibition of the PARP-1 and PARP-2 enzymes leads to the accumulation of SSBs and alterations in the formation of replication forks and subsequently, an increase in double-strand breaks, commonly repaired by HR enzymes. Cells die as consequence of having two or more genes mutated or with loss of function (like *BRCA1, BRCA2*) (Jiang et al., 2019a). Therefore, it has been an important factor, when treating patients with HGSOC subtype (Faraoni & Graziani, 2018; Torre et al., 2018).

Research has focused also on targeting lipid metabolism related genes and enzymes. For example, a study showed that the inhibition of HMG-CoA reductase, also lowers cholesterol (70% of circulating cholesterol is in LDL-c form) levels, which also leads to lower odds of EOC, valid also for *BRCA1/2* carriers (Goldstein & Brown, 2009; Yarmolinsky et al., 2020).

Treatments based on inter-patient variability, employ different diagnostic tools such as cfDNA (Werner et al., 2021) or microRNA (Jiang et al., 2021) from ascites liquid biopsies. Pathological evaluation also considers the presence of tumor infiltrating lymphocytes (TILs), particularly those enriched with CD3-positive T-cells (Zhang et al., 2003). Novel biomarkers for diagnosis and treatment are in great need (Bast et al., 2021).

2.4.3   Epidemiology and societal impact

OC is the seventh most common cancer type and second most common cause of gynecologic cancer death worldwide (Bray et al., 2018). The highest prevalence (cases per 100,000 individuals) of OC is seen in white women (Torre et al., 2018), whereas the mortality has a different pattern. African populations are the most affected (Chornokur et al., 2013). In Finland, five hundred women are diagnosed with OC yearly (Suomen Syöpärekisteri, https://cancerregistry.fi/).

Known risk factors of OC include: a) demographic (e.g., age specially >65 years) (Chan et al., 2006), b) reproductive antecedents (e.g., menarche <12 years, parity and age of childbirth (Adami et al., 1994; Fathalla, 1971), c) gynecologic (e.g., endometriosis, cysts or tub ligation) (Erzen & Kovacic, 1998; Wong et al., 2007), d)

---

[6] According to https://clinicaltrials.gov/

hormonal aspects (e.g., replacement or fertility therapy) (Mørch et al., 2009), e) genetic inherited background (e.g., *BRCA*) (Metcalfe et al., 2005; Nakamura et al., 2014), f) lifestyle (e.g., diet, obesity, exercise, stimulant use, perineal talc use) (Delort et al., 2009; Ong et al., 2016; Penninkilampi & Eslick, 2018). Additional relevant factors are socioeconomic status (Booth et al., 2010) and lactation (Jordan et al., 2010). As a protective role, the most relevant are pregnancy, oral contraceptive drugs, aspirin intake or nonsteroidal anti-inflammatory drugs (Trabert et al., 2019).

2.4.4   PCSK9 mechanism of action in EOC

To date, very little is known about the role of PCSK9, or of other PCSKs, in OC or even in healthy ovarian tissue. For instance, it has been reported that inhibiting PCSK1 promotes the intra-tumoral activation of M1-macrophages (Duhamel et al., 2015). Also, it is known that FURIN, which exerts an inhibitory cleavage over PCSK9 (Essalmani et al., 2011), is highly expressed in HGSOC patients, both in the ovaries and in the omentum, with an inverse correlation with patient survival (Chen et al., 2020). Another member, PACE4, promotes cell proliferation, whereas PCSK5/6 and PCSK7 are highly expressed in OC primary tumors, ascites cells and metastases (Longuespée et al., 2014).

Additionally, several studies, both in rodent models and in human patients, addressed the role of PCSK9 in other non-cancer related ovarian diseases, such as Polycystic Ovary Syndrome (PCOS), metabolically characterized for dyslipidemia (Mondal et al., 2018; Xavier et al., 2018). One study proposed PCSK9 as a novel target for diagnosis and treatment since it was reported that increased PCSK9 levels might contribute similarly to the pathogenesis of PCOS by affecting lipid metabolism and ovarian function, both at the systemic (I.e., blood) and the local (e.g., liver, ovary) level (Wang et al., 2019).

The regulation of PCSK9 levels -among other PCSKs- have been studied in rat ovaries during pregnancy. Unlike other PCSKs, Pcsk9 levels seem to remain steady (Kwok et al., 2013). The putative role of PCSK9 has not been explored before in the context of ovarian cancer. But in the context of other cancer types, it is known that PCSK9 has a role in cell proliferation and apoptosis (Piao et al., 2015; Zhang et al., 2021). Also, it has been reported that PCSK9 is aberrantly expressed in many cancers, contributing to disease prognosis in a lipid-independent manner as well (Liu et al., 2020). Cancer cells can evade the immune system by downregulating MHC-I expression (Cornel et al., 2020; Dong et al., 2018) and upregulating PD-L1

expression (Ohaegbulam et al., 2015). The downregulation of MHC-I has been observed in 40–90% of all human tumors, often correlating with a poor prognosis (Cornel et al., 2020). Recently, it was reported that PCSK9 interacts with MHC-I in a similar way as it does with LDLR (Liu et al., 2020).

2.5   Zebrafish as a research tool for immunological research

Zebrafish (*Danio rerio*), a freshwater fish from south Asia (Parichy, 2015), is a cost-effective alternative to mammalian animal models, being susceptible to infections with Gram-negative and Gram-positive bacteria, mycobacteria, protozoa and viruses (Van Der Sar et al., 2004). This teleost become a popular research tool for the study of development, physiology, immunity and human diseases (Trede et al., 2004).

Zebrafish immune system is quite similar to that of humans. Approximately 70% of all human genes have at least one zebrafish orthologue (Howe et al., 2013), including mammalian counterparts for pathogen recognition receptors (PRRs) and downstream signaling components (Van Der Vaart et al., 2012). Zebrafish have an extraordinary repertoire of NOD-like receptors when compared to humans (I.e., >400 members vs 23 members) (Li et al., 2017). The three pathways of the complement system (I.e., classical, alternative and lectin) are common for both species (Zhang & Cui, 2014).

One relevant shortcoming is the existence of duplicate genes, like those for *FURIN* and *PCSK5* for example (Woods et al., 2000). Gene orthologous of PCSK family members to their mammalian counterparts have been well described for zebrafish, with conserved biological functions: pcsk1 (ENSDARG00000002600), pcsk2 (ENSDARG00000019451), furina (ENSDARG00000062909), furinb (ENSDARG00000070971), pcsk5a (ENSDARG00000067537), pcsk5b (ENSDARG00000060518), pcsk6 (ENSDARG00000104574), pcsk7 (ENSDARG00000069968), mbtps1 (ENSDARG00000014634), pcsk9 (ENSDARG00000074185) (Ensembl IDs).

Pcsk1 and *Pcsk2* were detectable at the mRNA level, after 4-5hpf. PCSK1 expression increases throughout development, but *pcsk2* expression remains the same until 5dpf, when it increases (Morash et al. 2009). Two homologues of *FURIN* have been described in zebrafish, and are involved in craniofacial patterning (Walker et al., 2006). *Pcsk9* is expressed in the brain comparably to *pcsk1* and *pcsk2*. Morpholino-based knockdown of *pcsk9* expression has led to embryonic lethality (Poirier et al., 2006).

Since 1999, zebrafish have drawn attention as a valuable tool for modelling host–pathogen interactions, after it was discovered that all of the adaptive immune cells and APC are present in zebrafish (Lewis et al., 2014), as are almost all innate immune cells (only basophils are not present) (Balla et al., 2010). Adult zebrafish have matured functional components of both the innate and the adaptive immune system, making them a great tool to mimic and study infectious diseases (Sullivan & Kim, 2008). However, it takes up to 4-6 weeks for the adaptive immune responses to fully mature and reach complete functionality and therefore, embryos are useful for studying innate immune responses separately (Lam et al., 2002).

At 22 hours post fertilization (hpf) primitive macrophages appear, developed during embryogenesis before the formation of pluripotent hematopoietic stem cells) (Herbomel et al., 1999). At 36hpf, neutrophiles are ready to join macrophages in the innate host defense (Willett et al., 1999). Already at 2 days post fertilization (dpf), all organs are formed with certain cellular differentiation, achieving full development within 7dpf, except for the reproductive organs (90dpf). Thus, the zebrafish innate immune system can be separately studied since the adaptive system is not yet mature. At 4dpf, the first adaptive immune markers start to appear (Traver et al., 2003), and the recombination-activating genes (i.e., *rag1* and *rag2*) become active (Willett et al., 1997). It takes four weeks for the adaptive immune system to achieve maturation and immune competence (Lam et al., 2002, 2004). A component that is missing from fish compared to human is class switching (Danilova et al., 2005). The immunoglobulin antibody response has less variation in zebrafish when compared to humans (only IgD and IgM, but no IgA, IgG, and IgE) despite having VDJ recombination (Meeker & Trede, 2008; Willett et al., 1997), and somatic hypermutation (Marianes & Zimmerman, 2011).

In addition, zebrafish presents a set of advantages for research: 1) it is relatively cheap to maintain, b) it has external and optically transparent egg fertilization and development, c) its offspring are large, d) its development is fast, e) it shares immunological and physiological similarities with humans (Major & Poss, 2007).

Many human pathogens cause a disease at the temperature of the human body (i.e., 37°C), whereas zebrafish are maintained at a water temperature close to 28°C. This fact prevents the study of certain pathogens, although some can be replaced using fish-specific pathogens. If this is the case, the host–pathogen interactions might be fish-specific. There is a significant lack of tools for conducting studies at the cellular level. For example, until now monoclonal antibodies have not been available for surface antigens of zebrafish immune cells. Moreover, despite the evident physical differences with humans (e.g., lack of lungs, lymph nodes or

hematopoietic sites), the zebrafish is a suitable model to recapitulate and study pneumococcal infections (Rounioja et al., 2012).

Additionally, reverse and forward genetics tools can be used to target specific genes (Fuentes et al., 2018), CRISPR technology is the most promising methodology as it doesn't cause off-target effects, like the ones generated when using morpholinos (Kok et al., 2015; Shah et al., 2015). CRISPR/Cas9 is a more efficient and precise genome editing technique, preventing undesired off-target effects, commonly observed with techniques derived from morpholino-mediated gene silencing (Kok et al., 2015). CRISPR/Cas9 permits targeted gene cleavage and gene editing in a variety of eukaryotic cells, since an RNA sequence guides the endonuclease to virtually any genomic locus. The Cas9 protein is responsible for inducing a double-strand break at the specific genomic region of interest, which can be repaired by the cellular machinery, by either nonhomologous end joining (NHEJ) or homology-directed repair (HDR) (Ran et al., 2013).

Efforts have been made to develop zebrafish models (both, larvae and adult) to study pneumococcal infections (Rounioja et al., 2012; Saralahti et al., 2014). An important point is where to inject streptococcal bacteria. The injection site for juveniles (2-3dpf) is the blood circulation valley or alternatively, the otic vesicle. For adults, intramuscular and intraperitoneal injections are the points of inoculation (Phelps et al., 2009). Few years ago, a meningitis model was established employing live fluorescent *S. pneumoniae* infected zebrafish embryos to monitor pneumococcal meningitis in real-time (Jim et al., 2016). Another well-established zebrafish model is based on *S. agalacticaea*, to study neonatal sepsis. A threatening condition that urges to find early biomarkers and treatments (Keij et al., 2021).

3   AIMS OF THE STUDY

The overall aim of the present study was to better understand the implications of the PCSK9 protein in the host response against pneumococcal infections and in ovarian cancer. Based on the recent evidence that PCSK9 not only participates in cholesterol homeostasis, but also in immunity; we hypothesised a relevant participation for PCSK9 in such diseases commonly related to lipid metabolism. Thus, our main research questions and aims can be organized as follows:

1. To assess and to further explore the plasma PCSK9 levels in blood culture-positive bacteraemia patients. Also, to evaluate the association between the plasma PCSK9 response and patients' clinical factors (**Study I**).

2. To study *in vivo* and *in vitro* the effects of lack of PCSK9 in the context of pneumococcal infections and ovarian cancer (**Studies II, III**)

3. To create a *pcsk9*-deficient zebrafish line using CRISPR/Cas9 methodology, in order to provide a suitable animal model to study *in vivo* the participation of PCSK9 in host immune responses against *Streptococcus pneumoniae* systemic infection (**Study II**).

4. To further assess *in vitro* the putative expression and role of PCSK9 in ovarian cancer, using different cell lines and patient-derived cancer cell cultures (e*x vivo* tumor cells) (**Study III**).

4   MATERIALS AND METHODS

4.1   Ethical aspects (I, II, III) and patient recruitment (I, III)

For aim I, approval was obtained from the Ethics Committee of Tampere University Hospital (permit #R11099). The requirement for informed consent was waived as no additional blood sampling was needed.

Patients' samples were recruited at Tampere University Hospital (TUH), Finland. The control samples (n=17) were collected from patients one year after recovery, during the years 1999-2002 (Huttunen et al., 2010). With an age ranging between 20 and 82 years, 59% were males. The median plasma PCSK9 level was 188ng/ml. The bacteraemia patients' samples (n=481) were collected during the years 2012-2014, under the inclusion criteria of any patient with a blood culture-positive infection admitted to the hospital (Rannikko et al., 2017). The median plasma PCSK9 level on the day of admittance was 376ng/ml and 53% were males. Altogether, 27% of the patients died (n=129), and the rest recovered.

Follow-up blood samples were collected according to treatment-based routine laboratory testing, employing blood culture bottles (I.e., BacT/Alert Aerobic (FA Plus) and Anaerobic (FN Plus)), and placed into an automated microbial detection system (BacT/Alert 3D; bioMerieux, Marcy l'Etoile, France). Clinical data and site of infection were collected and determined retrospectively from their medical records. Clinical diagnoses of severe sepsis and septic shock followed the Sepsis-2 consensus definitions (Levy et al., 2003), and the quick sequential organ failure assessment (qSOFA) score was calculated on the bases of Sepsis-3 definitions, dictating that an adult patient with a suspected infection is more likely to have a fatal outcome if he/she has ≥2 criteria: 1) respiratory rate ≥22 per minute, 2) altered mentation and 3) systolic blood pressure ≤100 mm Hg (Singer et al., 2016). The Pitt Bacteraemia Score was implemented as reported (Korvick et al., 1991).

For aim II, the experiments were approved by the Animal Experiment Board of Finland (permits ESAVI/10079/04.10.06/2015 and ESAVI/2235/04.10.07/2015). The zebrafish maintenance and the experiments followed the European ARRIVE directive guidelines (2010/63/EU) and the Finnish Act on the Protection of Animals Used for Scientific or Educational Purposes (497/2013).

For aim III, informed consent was obtained from all patients. PDCs (n=5) and data were handled following the recommendations approved by the Institutional Ethical Review Board (permit #56/13/03/03/2014) and published protocols (Liu et al., 2012, 2017). Their clinical and genomic characterization are summarized in III, Table 1. PDCs were verified for the identical phenocopy with their original tumour samples by next-generation sequencing (data not shown) and the expression of Müllerian marker paired-box 8 (PAX8), a known marker for the diagnosis of EOC.

Ascites were handled following the Ethics Committee of Tampere University Hospital guidelines (permit #R11137). Samples (n=18) were collected during the years 2018-2020 at TUH. All the samples had a yellow coloration, except for three samples that had a clear read color (patients 4,10 and 14) and four had an orange brownish coloration (patients 9, 13, 16 and 18). Also, all samples were liquid except for four samples that were viscous (patients 9, 14, 17 and 18). Additionally, ten samples were turbid, having some floating particles (patients 1,5,6,7,8,9,12,13,16 and 17). These characteristics were considered when centrifuging and pipetting.

4.2 *Ex vivo* ELISA immunoassays (I, III)

For aim I, prior to the quantification using a commercially available enzyme-linked immunosorbent assay (ELISA) for human PCSK9 (#DPC900, R&D Systems, Minneapolis, MN, USA), 1854 plasma samples were diluted 1:20 following the manufacturer's protocol. Most of the samples were measured as singlets (no technical parallels), whereas 50 samples were measured as duplicates on the same plate, validating the reproducibility of the ELISA kit. The intra and inter-array sample variations were measured, and on average they were 3.5% of the defined final concentration. In any case, each plate had its own standard curve (40 – 0 ng/ml, which is equivalent to 0-800ng/ml.), including an assay buffer without sample or standard for background counting. The optical density was measured using a Perkin Elmer Envision. PCSK9 concentration was calculated based on the standard curve.

For aim III, PCSK9 levels were quantified from unfiltered ascites samples, with no controls available, using a commercially available ELISA for human PCSK9 (#DPC900, R&D Systems, Minneapolis, MN, USA). From each patient, an aliquot was taken and diluted 20-fold, since the standard in the ELISA R&D kit covers a range from 0 to 40ng/ml, which is equivalent to 0-800ng/ml. Another extra 50-fold dilution was prepared. Samples and standards were run as duplicates and the absorbance signal measured at 450 nm, with the correction wavelength set at 540 nm

or 570 nm. The average zero standard optical density was subtracted. The PCSK9 concentration was calculated based on the standard curve.

4.3   *In vivo* experiments (II)

4.3.1   Housing and maintenance

Zebrafish larvae were maintained in E3 medium (5mM NaCl, 0.17mM KCl, 0.33mM CaCl2, 0.33mM MgSO4, 0.0003g/l methylene blue) at 28.5°C until 7dpf. Unchallenged adult fish were maintained in a conventional flow through system (Aquatic Habitats, Florida, USA) with an automated light/dark cycle (14h/10h) and fed once a day with Gemma Micro 500 (Skretting, Stavanger, Norway).

Adult zebrafish infected with *Streptococcus pneumoniae* were kept in a separate flow through system (Aqua Schwarz GMbH, Göttingen, Germany). Conductivity (800µs) and pH (7.6) were adjusted and manually changed twice a day. The water tanks were kept at 28.5°C for the duration of the experiment. An identical light/dark cycle compared to the unchallenged fish was used and the fish fed once a day with Gemma Micro 500 (Skretting).

4.3.2   Reverse genetics

Reverse genetics is a molecular technique used to understand the function of a given gene by examining the phenotypical changes caused by genetically engineered specific changes using nucleic acid sequences. Thus, zebrafish lines carrying nonsense *pcsk9* mutations were created as previously described with slight adjustments (Ojanen et al., 2019; Uusi-Mäkelä et al., 2018). From the generated lines, two were selected for conducting the experiments, since they had the final same number of base pairs (bp), deleted, or added. The mutant lines were named accordingly as *pcsk9*[tpu-13] and *pcsk9*[tpu-2,+15]. In zebrafish, the total length of pcsk9 is 667 amino acids (aa), whereas for the mutant lines, the truncated proteins were 159aa and 173aa, respectively (see II, Figure 1A and 1C).

Recombinant Cas9 protein production

The Cas9 expression plasmid 1xNLS-pMJ915v2 was a gift from Jennifer Doudna (Addgene plasmid #88915; http://n2t.net/addgene:88915). The recombinant Cas9 protein was expressed in house using *Escherichia coli* bacterial cells. The plasmid was

transformed into One Shot® BL21 Star DE3 competent cells (Invitrogen, CA, USA) using a standard heat shock protocol (Staahl et al., 2017).

A single colony was used as a pre-culture seed that was further used to inoculate the culture by diluting it at a ratio of 1:50 in 1000ml of lysogeny broth (LB) supplemented with 5mM glucose and 50µg/ml kanamycin. Bacteria were grown at 37°C under 90rpm shaking until the culture reached an optical density of 0.6 after which the temperature was dropped to 18°C and after 30 minutes the culture was induced with 0.2mM IPTG. Cells were harvested after a 25-hour incubation by centrifugation, washed with 50mM Tris, 0.5 M NaCl, 10mM imidazole (pH 8.0) buffer and frozen at -20°C. Then, cells were lysed in 50mM Tris, 0.5M NaCl, 10mM imidazole (pH 8.0) buffer, and the supernatant clarified with centrifugation at 20,000 x g for 20 minutes. The soluble protein from the cleared supernatant was bound to 4ml of Ni-NTA agarose (Macherey-Nagel) at 4°C. Impurities were washed with 30ml of binding buffer and the bound protein eluted from the column using 50mM Tris, 0.5M NaCl, 500mM imidazole, 10mM EDTA (pH 8.0) buffer. The protein was concentrated and the buffer-changed to 20mM HEPES, 150mM KCl, 1% sucrose (pH 7.5) using PALL MacroSep 30K Ultrafiltration Units.

CRISPR/Cas9 mutagenesis

gRNA and primer design

Susceptible guide RNA (gRNA) target sites were identified using CHOPCHOP v2 (available at https://chopchop.cbu.uib.no/) (Labun et al., 2016). We determined the nucleotide sequence of the gRNA target site located in the zebrafish *pcsk9* gene in exon 3 (ENSDARG00000074185). This corresponded to the following sequence: GCATCCCATGGAACCTGCAG**CGG** (in bold, the Protospacer Adjacent Motif).

The specificity of the target sites was evaluated with a Basic Local Alignment Search Tool (BLAST) analysis (Altschul et al., 1997) . The gRNA synthesis was done following the protocol by Hruscha and Schmid. First, the DNA-oligos (containing the reverse complementary sequence of the gRNA) were annealed to T7-primers. The gRNAs were synthetized using the MEGAshortscript T7 Transcription kit (Ambion Life Technologies, U.S.). The quantity and quality of the gRNAs were evaluated with electrophoresis (1% agarose TAE gel) and NanoDrop or Qubit.

Microinjections

The embryos were aligned on home-made 1.2% agarose and E3-medium plates. To induce target-site mutagenesis, 1.5ng of phenol red (Sigma), 170 ng of *pcsk9* exon 3 gRNA together with 300pg of in-house produced Cas9 protein (Invitrogen, California, U.S.) were injected into one-cell-stage embryos of AB zebrafish in a 1nl nuclease free water suspension. Injections were performed using borosilicate capillary needles (Sutter Instrument Co., California, U.S.), a micromanipulator (Narishige International, London, U.K.) and a PV830 Pneumatic PicoPump (World Precision Instruments, Florida, U.S.).

Working concentrations were described in the original communications. Injections were monitored using a SMZ645 microscope (Nikon, Tokyo, Japan) and the AxioVision software applying filters (excited at 570nm and emitted at 620nm).

Mutation efficiency

The gRNA target sites were amplified by PCR using target site specific primers and the Maxima Hot Start DNA polymerase (ThermoFisher Scientific, Waltham, Massachusetts, U.S.). The PCR products (V=10μl) were denatured and annealed using 1x NEB Buffer (New England Biolabs, U.S.), and incubated with 0.5μl of T7 endonuclease I for 30 minutes at 37°C (VT=20μl). After performing the T7 endonuclease I assay target-loci analysis, T7EI treated PCR products were analysed by electrophoresis (2.5% agarose TAE gel) and imaged. Expected band sizes are 169bp for WT and ~100 and ~70bp for mutated bands. The mutation efficiency was estimated with the following formula: [% mutagenesis = 100 x (1 – (1- fraction of cleavage)$^{1/2}$)] (Ran et al., 2013), and the effects of the indel mutations on the protein sequence using the Translate tool (Expasy; SIB, Swiss Institute of Bioinformatics, https://web.expasy.org/translate/) (Artimo et al., 2012).

4.3.3 Microscopy for phenotype evaluation

Ungenotyped F2-progeny of *pcsk9*tpu-13/+ and *pcsk9*tpu-2+15/+ zebrafish, and their WT sibling controls, were imaged at 1, 4 and 7dpf. For imaging purposes, the larvae were anesthetized with 0.02% of 3-amino benzoic acid ethyl ester (Sigma-Aldrich). Images were taken with Zeiss Lumar V12 fluorescence microscope and Axiocam MRm digital camera using a bright field exposure of 2ms. A 22x-magnification was used at 1dpf and a 17x-magnification at 4 and 7dpf. Fish larvae were euthanized and collected for genotyping (Sanger sequencing and PCR product size) at 7dpf.

4.3.4 Sequencing of zebrafish genotypes

Both *pcsk9*[tpu13] and *pcsk9*[tpu-2,+15] mutant zebrafish lines were genotyped using Sanger sequencing using the primers 5´ AGTAAAGTTGCCCCATGTGG-3´ (forward) and 5´-TAAGTGCAAAGAGTGTGATTTGG-3´(reverse). For heterozygote and mutation detection was the BigDye™ Terminator v3.1 Cycle Sequencing Kit (#4337455, Applied Biosystems™, ThermoFisher Scientific, Waltham, Massachusetts, U.S.) was used, to ensure longer, higher-quality reads, more accurate base assignments, uniform peak heights and optimized signal balance.

4.3.5 Experimental *Streptococcus pneumoniae* infections

The employed methodology has been established by the Experimental Immunology research group at Tampere University. Thus, pneumococcal culturing and infections were performed as before (Rounioja et al., 2012; Saralahti et al., 2014).

Bacterial culture

Zebrafish individuals, both adults and larvae, were inoculated with *S. pneumoniae* serotype 4, sequence type 205. The bacterial culture was kept overnight on 5% lamb blood agar plates at 37°C. The next day, bacteria were transferred into 5ml of Todd Hewitt broth (Becton, Dickinson and Company, New Jersey, USA) supplemented with 0.5% Todd-Hewitt yeast extract (Becton, Dickinson, and Company). The bacteria were cultured until the optical density reached a value of 0.40 at 620nm.

Bacterial preparation and inoculation

Larvae and adults were similarly anesthetized, but the volume and the site of injection varied. For larvae experiments, 2dpf zebrafish were used. They were anesthetized with 0.02% 3-aminobenzoic acid ethyl ester (Sigma-Aldrich, Missouri, USA). The bacterial suspension was prepared adding 2µl of bacteria in 0.2M potassium chloride (KCl) with 7mg/ml of tetramethylrhodamine dextran (Thermo Fisher Scientific, Massachusetts, USA). The site of microinjection was into the blood circulation valley. The survival of the embryos was monitored twice a day during the first 50 hpi and subsequently, once a day until 5dpi (I.e., 7dpf).

Adult zebrafish were injected with 5µl of suspension bacteria in 10mM phosphate-buffered saline (PBS) and 0.3mg/ml phenol red (Sigma-Aldrich). The

injection site was the abdominal cavity using a 30-gauge Omnican 100 insulin needle (Braun, Melsungen, Germany). Colony forming units (CFU) of viable *Streptococcus pneumoniae* were counted afterwards, by culturing inoculates of bacteria on 5% lamb blood agar plates overnight at 37°C with 5% CO2.

4.4   *In vitro* experiments (II, III)

4.4.1   Cell culturing (II, III)

All cell lines were kept and incubated at 37°C and 5% CO$_2$ (see Table 7). Three different media were used: RPMI1640 and DMEM from Lonza (Basel, Switzerland) or DMEM/F-12 from Gibco™ (Thermo Fisher Scientific, Waltham, MA, USA).

Table 7.   **Cell lines and their requirements used in the studies.**

Cell line	Cell type	Culture media	Supplementation
HepG2	Hepatocyte carcinoma	RPMI 1640	FBS (10%), 2mM L-glutamine (1%), penicillin and streptomycin (6mM)
OVCAR3	High grade ovarian serous adeno carcinoma	RPMI 1640	FBS (20%), 2mM L-glutamine (1%), penicillin and streptomycin (6mM)
OVCAR3cis	High grade ovarian serous adenocarcinoma, cisplatin resistant	RPMI 1640	FBS (10%), 2mM L-glutamine (1%), penicillin and streptomycin (6mM), cisplatin (1uM)
A2780	Ovarian endometroid adenocarcinoma	RPMI 1640	FBS (10%), 2mM L-glutamine (1%), Primocin™
A2780cis	Ovarian endometroid adenocarcinoma, cisplatin resistant	RPMI 1640	FBS (10%), 2mM L-glutamine (1%), cisplatin (1uM), Primocin™
Kuramochi	High grade ovarian serous adenocarcinoma	RPMI 1640	FBS (10%), 2mM L-glutamine (1%), Primocin™
OVSAHO	High grade ovarian serous adenocarcinoma	RPMI 1640	FBS (10%), 2mM L-glutamine (1%), Primocin™
JHOS2	High grade ovarian serous adenocarcinoma	DMEMF-12	FBS (10%), MEM-NEAA (1%), Primocin™
COV362	High grade ovarian serous adenocarcinoma	DMEM	FBS (10%), 2mM L-glutamine (1%), Primocin™
HeLa	Cervical carcinoma	DMEM	FBS (10%), 2mM L-glutamine (1%), Primocin™
HEK293T	Embryonic renal	DMEM	FBS (10%), 2mM L-glutamine (1%), Primocin™

Two different antimicrobial agents were used: penicillin and streptomycin mix (Thermo Fisher Scientific, Waltham, MA, USA) and Primocin™ (InvivoGen, San

Diego, CA, USA). Supplements included heat inactivated, sterile-filtered fetal bovine serum (FBS), L-glutamine and MEM-NEAA, all from Thermo Fisher Scientific (Waltham, MA, USA). To maintain the drug resistant phenotype, cisplatin (SelleckChem, Houston, TX, USA) was added to the culturing media.

4.4.2 Cell transfections (II, III)

HepG2 cells (for aim II), and OVCAR3 and HeLa cancer cell lines (for aim III) were transfected with small interference RNA (siRNA) ON-TARGETplus Human PCSK9-SMART pool 10nM (GE Dharmacon, Lafayette, CO, USA), altogether with Transfection Reagent 1 or 4 (GE Dharmacon, Lafayette, CO, USA). Acting as a control was used siRNA ON-TARGETplus Non-targeting Control Pool (GE Dharmacon, Lafayette, CO, USA). The final concentration of siRNA used in the transfection was 6nM for HepG2 and OVCAR3 cells and 25nM for HeLa cells.

The human PCSK9/NARC1 plasmid (HG15813-CM) was transfected into HEK293T and JHOS2 cells with TurboFect™ Transfection Reagent (Thermo Fisher Scientific, Waltham, MA, USA), using Opti-MEM I reduced serum media (Gibco™, Thermo Fisher Scientific, Waltham, MA, USA). The pCINEO expression vector (Promega, Madison, WI, USA) was used as a transfection control.

4.4.3 Cell viability measurements (III)

The CellTiter-Glo (CTG) 2.0 Assay (Promega, Madison, WI, USA) assay was used to measure cell viability, according to the manufacturer's instructions. Cells were plated to 96- or 384-well plates and treated with various drug concentrations, as detailed in the original publication. The luminescence was measured with the Envision plate reader (Perkin-Elmer, Waltham, MA, USA).

4.4.4 Inhibitor treatment (III)

HeLa, OVCAR3, OVCAR3cis, and JHOS2 cells were plated into 96-well plates and untreated or treated with increasing concentrations of the PCSK9 inhibitor (PCSK9i) PF-06446846 hydrochloride (MedChemExpress, Monmouth Junction, USA), and the cell viability was analysed after 48h using CTG. The luminescence was measured with the Envision plate reader (Perkin-Elmer, Waltham, MA, USA).

4.4.5 Western blotting (II, III)

For aim II and III, cells were lysed with 50mM Tris-HCl (pH 7.5) containing 1mM EDTA, 50mM NaF, 150mM NaCl, 1% Triton X-100, 10% glycerol plus 10% phosphatase and a protease inhibitor cocktail (Bimake, Houston, TX, USA). After sample centrifugation, the supernatant fraction was boiled in 4x Laemmli sample buffer (Bio-Rad Laboratories, California, USA) containing 2-Mercaptoethanol (Sigma-Aldrich, Missouri, USA) for 5min at 98°C. Once ready, samples were loaded onto in-house prepared 7.5% or 12% gels for SDS-PAGE. Gels were blotted using Trans-Blot® Turbo™ Midi Nitrocellulose Transfer Packs (Bio-Rad) and the TransBlot® Turbo™ Transfer System (Bio-Rad). Next, the proteins were transferred onto a nitrocellulose membrane (Bio-Rad Laboratories, California, USA), which was blocked using 0.05% Tween, 4% BSA in TBS.

Staining solutions were prepared with 0.05% Tween, 0.5% BSA and 0.02% NaN3 in TBS and proteins were detected using the antibodies summarized in Table 8. The image scan and analysis were done using Odyssey® CLx Imaging System, and Image Studio Lite (LI-COR ™ Lite, Biosciences).

Table 8.   Antibodies used in the current research.

Antibody against	Ab Type	Dilution	Catalog	Manufacturer
PCSK9 (D7U6L)	Primary	1/1,000	# 85813	CST, Massachusetts, US
pERK1/2 (T202/Y204)		1/1000	#9101	
ERK1/2 (L34F12)		1/1000	#4696	
pAKT (Ser473)		1/1000	#4060	
AKT		1/1000	#2920	
pMEK (Ser217/221)		1/1000	#9121	
MEK		1/1000	#4694	
HAMP		1/10	#30760	Abcam, Cambridge, UK
β-tubulin		1/1,000	#166729	Santa Cruz Biotech., Texas, US
Goat anti-Rabbit (IRDye® 680LT)	Secondary	1/10,000	#925-68021	LI-COR, Nebraska, US
Goat anti-Mouse (IRDye® 800CW)		1/10,000	#925-32210	
Donkey anti-Goat IgG (IRDye® 680RD)		1/10,000	#926-68071	
Donkey anti-Mouse IgG (IRDye® 800CW)		1/10,000	# 926-32212	
Donkey anti-Rabbit IgG (IRDye® 680RD)		1/10,000	# 926-68073	

4.4.6 Drug sensitivity and response testing (III)

Drug testing (DSRT) was conducted in the High Throughput Biomedicine and Sequencing Laboratory Units at the Finnish Institute for Molecular Medicine (FIMM, University of Helsinki), as described previously (Pemovska et al., 2013; Yadav et al., 2014). The platform comprises a panel of five hundred clinically approved drugs and experimental drugs against cancer, pre-printed in 384-well culture plates covering a 10,000-fold concentration range (specifically, in five different concentrations). The mechanism or target, and the class of drugs used in aim III are listed in (III, Table 2).

The OC cell lines and PDCs adherent cells were seeded with a dose-dependent concentration of drugs (e.g., 1,000-1,500 cells per well). Then, plates were incubated at 37°C for 72 hours, followed by a cell viability measurement with the CellTiter-Glo assay (Promega), as described in subchapter 4.4.3, with the exception that the plates were read with PHERAstar FS (BMG Labtech, Ortenberg, Germany), and the results were analysed using BREEZE DSRT pipeline (https://breeze.fimm.fi/).

Cell viability was calculated as percentage inhibition, where the lowest drug concentration was given 100% percentage cell survival. Original drug dose-response curves of metabolic and mTOR targeting drugs in OC cell lines and PDCs, were calculated according to five concentrations, represented as log10 values. Dose-response curves were used to calculate a drug sensitivity score (DSS), as has been done before (Yadav et al., 2014). DSS is a measure of the drug-response based on the area under the dose response curve, capturing the potency and the efficacy of the drug's effect. It integrates complementary information extracted by a half-maximal inhibitory concentration (IC50), slope and minimal and maximum asymptotes. Thus, DSS is used for the quantitative scoring of differential drug responses. A DSS $\geq$ 7 in at least one cell line was used as a threshold for the evaluation of the drug's efficacy.

4.4.7 Gene expression analysis (II, III)

RNA isolation

In aim II, adult zebrafish tissues or HepG2 cells were homogenized prior genomic DNA (gDNA) removal or RNA isolation, performed according to manufacturer's instructions using the RNeasy Mini Kit or RNeasy Plus Mini Kit (Qiagen, Hilden, Germany). For aim III, total RNA was isolated from PDCs using the total RNeasy

kit (Qiagen, Germany). The sample quantity and quality were assessed by Qubit (Thermo Fisher Scientific, USA) and Bioanalyzer (Agilent Technologies, USA).

qPCR

The oligonucleotide primer sequences for qPCR analysis used in aim II and III are specified in Table 9. PCR-products specificity and possible contaminations were monitored using as a controls water (non-template) and no-reverse transcriptase. Melt curve analysis and 1.5% agarose TAE gel electrophoresis were performed too.

For aim II, reverse transcriptions were done using the iScript™ cDNA synthesis kit (Bio-Rad Laboratories, California, USA). The relative gene expression of the target genes was determined with qPCR using the PowerUp™ SYBR® master mix (Thermo Fischer Scientific) and either the CFX96™ (Bio-Rad Laboratories) or the QuantStudio™ 12K Flex (Applied Biosystems, California, USA) detection systems. The CFX Manager software (v. 3.1; Bio-Rad Laboratories) and the QuantStudio 12K Flex Software (v.1.2.2; Applied Biosystems) were used for data analyses using the $2^{(\Delta Ct)}$ method. The target gene expression from zebrafish data was normalized to the expression of the eukaryotic translation elongation factor 1 alpha 1, like 1 (*eef1a1l1* or *ef1a*) (Tang et al., 2007), whereas the HepG2 data to glyceraldehyde 3-phosphate dehydrogenase (*GAPDH*).

Table 9. **Oligonucleotide primer sequences for qPCR used for Aim II.** The first five rows belong to the genome of *Danio rerio* and the rest to *Homo sapiens*.

Gene	Ensembl ID	Sequence 5'-3' (F)	Sequence 5'-3' (R)
pcsk9	ENSDARG00000074185	CACAGGCAGGCCAGTCAGTG	GCTGAGAGGCCAGAGATGAC
ldlrap1a	ENSDARG00000004311	GATGAGCATCATGTGGAGAG	AGAACTCGAAGGCCACTCTG
Hamp	ENSDARG00000102175	GATGAGCATCATGTGGAGAG	GTATCCGCAGCCTTTATTGC
socs3a	ENSDARG00000025428	AGCCGAGACTCGACACTCTG	CCTTGGAGCTGAAGGTCTTG
eef1a1l1	ENSDARG00000020850	CTGGAGGCCAGCTCAAACAT	ATCAAGAAGAGTAGTACCGCTAGCATTAC
PCSK9	ENSG00000169174	GACACCAGCATACAGAGTGACC	GTGCCATGACTGTCACACTTGC
HAMP	ENSG00000105697	CTGACCAGTGGCTCTGTTTTCC	AAGTGGGTGTCTCGCCTCCTTC
C7	ENSG00000112936	GTGGTTTGGCTACTGTTGAGGG	TCCAAGAGGACCAGCAACTCCA
SOCS3	ENSG00000184557	CATCTCTGTCGGAAGACCGTCA	GCATCGTACTGGTCCAGGAACT
TNF	ENSG00000232810	CTCTTCTGCCTGCTGCACTTTG	ATGGGCTACAGGCTTGTCACTC
TNFAIP3	ENSG00000118503	CTCAACTGGTGTCGAGAAGTCC	TTCCTTGAGCGTGCTGAACAGC
C6	ENSG00000039537	GTGTCAGAGTGGCACCTATGGT	GTAGCATCACAGGTACTCCAGG
LDLRAP1	ENSG00000157978	CCATCAAGAGGATCGTGGCTAC	GGACACGTTCTCAATGAGCTGG
GAPDH	ENSG00000111640	GTCTCCTCTGACTTCAACAGCG	ACCACCCTGTTGCTGTAGCCAA

RNA sequencing and differential gene expression analysis

In aim II, RNA quality was assessed with the Fragment Analyzer and the Standard Sensitivity RNA Analysis Kit (15nt) (both from Advanced Analytical, Inc, Ankeny, USA). RNA sequencing was performed by Novogene Co. (Hong Kong, Special Administrative Region of the People's Republic of China) and the data were provided in a FASTQ format.

The differential gene expression analysis for RNA sequencing results started with the pre-processing steps: the quality control and the alignment against *GRCz11* (ENSEMBL release 97), performed with Spliced Transcripts Alignment to a Reference (STAR) (Dobin et al., 2013), and Snakemake (v.5.6.0). It was combined modules from the Snakemake-wrapper (release 0.38.0) with in-house scripts (Köster & Rahmann, 2012). Next, the analyses were performed in R (v.3.6.0). The sample clustering and within-group variation were examined by principal component analysis (PCA) using the regularized log (rlog)-transformed gene counts and DESeq2 (v.1.24.0) (Love et al., 2014). The differentially expressed genes (DEGs) between homozygous *pcsk9*[tpu-13/tpu-13] mutant zebrafish and the WT controls within each treatment group were annotated with biomaRt (v.2.40.5) (Durinck et al., 2009). The transcripts were annotated with Benjamini-Hochberg (BH). Those with adjusted P-values less than 0.05 were considered differentially expressed, and chosen for a further analysis (Benjamini & Hochberg,1995). Expression of protein-coding DEGs were visualized with pheatmap using the rlog-transformed gene counts as the input (Raivo, 2019). Gene ontology was examined by using the *Danio rerio* genome assembly and Gorilla (Eden et al., 2007, 2009). Using the standard Hyper Geometric statistics, unranked lists of genes, were analysed with a target list (P-value <0.05), against a background list (P-value ≥0.05). The RNA sequencing results were submitted to the Gene Expression Omnibus (GEO) repository (GSE165508).

In aim III, RNA with an RNA integrity number (RIN) over 8 units, was used to derive libraries. The sequencing was performed with the Illumina HiSeq system as previously described (Kumar et al., 2017). The expression of lipid metabolism and PCSK family genes was derived from the RNA-seq analysis. Hierarchical clustering analysis was performed using a log2 transformation of transcripts per kilobase million (TPM), values derived from RNA-Seq data from samples of five PDCs. Clustering was done on genes involved in the lipid-metabolism pathway and PCSK family based on KEGG pathway definitions (Kanehisa et al., 2009). Clustering was done with the cluster module of the SciPy library (Oliphant, 2007), using a Euclidean

distance metric and Ward linkage variance. Visualization of clusters done with Matplotlib (Hunter, 2007) and Seaborn (Waskom et al., 2014).

4.5 Statistical analysis (I, II, III)

For aim I, data was analysed using either SPSS (version 22.0; IBM Corp., Armonk, NY, USA) or R (version 3.4.4.; https://www.r-project.org). Nonparametric data were analysed using the Mann–Whitney U-test. To test for correlation, Pearson's product moment coefficient was used. P-values less than 0.05 were considered significant. For predictive patient performance, the receiver operating characteristic (ROC) statistic was used, and the Youden index to select an optimal cut-off value. The Kaplan–Meier method was used for calculating the survival curve.

For aim II, sample sizes were decided based on previous experimental observations (Rounioja et al., 2012; Saralahti et al., 2014). Zebrafish and HepG2 cells' qPCR results were analysed according to nonparametric two-tailed Mann-Whitney parameters. Zebrafish survival experiments were analysed using a log-rank (Mantel-Cox) test when comparing the experimental groups. Statistically significancy was considered when the P-value (adjusted P-value in RNA sequencing) was <0.05.

For aim III, an analysis of hierarchical clustering and a similarity matrix were done using the Morpheus software (https://software.broadinstitute.org/morpheus).

5 RESULTS

5.1 Plasma PCSK9 levels in patients with bacteraemia (I)

5.1.1 Plasma PCSK9 is upregulated in patients with blood culture-positive infections

According to Boyd and colleagues, the reference value for a normal plasma PCSK9 level is between 170 and 220 ng/ml (P-value less than 0.001) (Boyd et al., 2016). From 1854 measurements, 19 were beyond the highest concentration of the standard (800ng/ml). Only three were over 1000ng/ml. on the other end, only 20 measuremnets had a value under 100ng/ml. According to Boyd and colleagues, 118 measurements landed within the normal plasma PCSK9 levels reported range.

In general, on day 0, plasma PCSK9 level was elevated in bacteremic patients, being the median plasma PCSK9 level 376 ng/ml (interquartile range (IQR) 293-483), whereas in the control group it was 188 ng/ml (IQR 139-264). The difference between groups is significant (P-value=0.001). In patients with bacteremia the median PCSK9 plasma levels remained high during the sampling period, on days 1, 2, 3 and 4 as follows: 383, 381, 360 and 356 ng/ml, respectively.

The plasma PCSK9 levels were similarly upregulated (P-value < 0.001 for both, Welch's two sample-tests) in infections caused by Gram-positive (median 381ng/ml) and Gram-negative (median 380ng/ml) bacteria. No statistically significant difference in the level of PCSK9 between Gram-positive or Gram-negative bacteria was observed (P-value=0.499) (see I, Figure 1).

5.1.2 Plasma PCSK9 levels associate with certain underlying conditions

On the day of admission (as summarized in I, Table 3), the patients' PCSK9 levels were significantly different (P-value=0.001) according to gender, being lower in male patients (n=253) than in females. Also, patients suffering from liver disease (n=49) and those having a history of alcohol abuse (n=49) had statistically significantly lower

plasma PCSK9 levels. In contrast, patients using statins (n=116) had significantly higher PCSK9 levels than those not using statins. Statin users represented 24% of the bacteremia patient cohort. The most used statins were simvastatin (63% of the users) and atorvastatin (28%), with an average dose of 25 mg and 22 mg, respectively.

No other significant association between PCSK9 and age, or underlying conditions on day 0 such as cardiovascular disease (n=155), diabetes (n=137), kidney disease (n=66), solid tumors (n=55), hematological malignancies (n=45) or use of oral corticosteroids (n=92) was found.

5.1.3   *Streptococcus pneumoniae* upregulates plasma PCSK9 levels the most

The plasma PCSK9 levels in relation to different causative organisms on day 0 are presented in (I, Table 1). If a single microbe type accounted for less than five samples, the corresponding samples were excluded.

The median PCSK9 value for all 481 patients on day 0 was 376 ng/ml (IQR 293-483), whereas patients suffering from a *Streptococcus pneumoniae* infection showed the highest plasma PCSK9 levels (476 ng/mL, IQR 319–561, P-value=0.003). The lowest PCSK9 levels were seen in patients with polymicrobial bacteremia (311 mg/ml, IQR 235–501, NS). For others, the median plasma PCSK9 level was 339 ng/ml (IQR 261-488) and on day 7, the case fatality rate was 23.9%.

For patients with Gram-positive bacterial infections (n=213, 44% of the cohort), the median PCSK9 level was 381 ng/ml (IQR 315-493). The day 7 case fatality rate was 5.6%. For patients suffering from Gram-negative bacteria (n=222, 46%) the median value was 380ng/ml (IQR 306-465) and the day 7 case fatality rate was 9.5%.

5.1.4   Plasma PCSK9 levels and site of infection

Patients were grouped based on the site of infection on day 0 (I, Table 2); 29 cases had two different infection sites. The highest median plasma PCSK9 level was found in patients suffering from a lower respiratory tract infection (472 ng/ml, IQR 315-557), whereas the lowest PCSK9 levels were found in individuals suffering from an unknown (I.e., unclassifiable infection) (352 ng/ml, IQR 262–474, P-value=0.039).

5.1.5   Plasma PCSK9 resembles APR and correlates with CRP

Plasma PCSK9 acts similarly to an acute phase reactant protein (APR); since its expression is induced upon infection. The correlation between plasma PCSK9 levels and infection-associated markers were evaluated using Pearson's product-moment analysis. On day 0, no significant correlation was observed between plasma PCSK9 levels and body temperature, leukocyte numbers or cell-free DNA. But up to 4 days after hospitalization, the upregulated plasma PCSK9 levels showed a significant (P-value<0.001) positive correlation with CRP levels. For correlation on day 0 see (I, Figure 2), and for correlation on day 1-4 after admission to the emergency department see (I, Supp. Figure 1).

5.1.6   Plasma PCSK9 levels are lower in patients with a fatal prognosis

As evidenced in (I, Table 3), PCSK9 levels were not significantly associated with indicators of severity of the bacteremia on day 0. From all the indicators considered, the need for vasopressors was statistically significant. Cases that were moved to the ICU from the ED showed a positive trend. Interestingly, the qSOFA score showed no difference when comparing patients that met the 2 or 3 criteria ("factor present"), against those that had less than 2 ("factor absent column").

Of the bacteremia patients with upregulated plasma PCSK9 levels (compared to the normal range of 170-220 ng/ml), those with lower values had a significant association with a fatal prognosis. It was observed that patients with mortality on day 7, 28 and 90, all had statistically significantly lower plasma PCSK9 levels (P-value<0.001) than the others. The fatality rate on day 7 was 9% (n=45), and the patients that died by day 7 had a median PCSK9 level of 306ng/ml (IQR 257-454). On day 28 and 90, the PCSK9 levels were 308ng/ml and 320ng/ml (IQR 249-442), respectively. Excluding statin users resulted in the same outcome, whereas excluding patients with liver disease as an underlying condition showed no significant relationship between the PCSK9 level and mortality by day 7 and 28 (P-value=0.336 and P-value=0.059, respectively).

When patients are followed beyond the first month from the bacteremia diagnosis, the occurrence of true infection-associated deaths is overcome by underlying disease-based mortality.

5.2 Pcsk9 levels in the zebrafish host defence against *Streptococcus pneumonia* (II)

5.2.1 *Pcsk9* expression is upregulated upon a *Streptococcus pneumoniae* infection in AB-wildtype zebrafish

Evidence from patients and *in vivo* experiments has shown that PCSK9 expression increases in a liver-dependent manner (Feingold et al., 2008; Yuan et al., 2020). From our results from bacteremia patients, we concluded that the bacterial agent that upregulated PCSK9 the most was *Streptococcus pneumoniae.* Thus, we wanted to explore *in vivo* the levels of PCSK9 produced in the liver and whether these are upregulated upon a pneumococcal infection in zebrafish. We injected 635.000CFU *Streptococcus pneumoniae* (SD 276.000 CFU) into the abdominal cavity of adult WT zebrafish from the AB line. The control group was injected with PBS. At 7dpi the experiment was ended. We checked the relative levels of pcsk9 mRNA in the liver (n=5, all males) by qPCR. Gene expression was normalized to *eef1a1l1* expression and *pcsk9* was run once as technical duplicates. The PCSK9 levels of pneumococcus infected zebrafish were increased by 4.5-fold (P-value=0.008) compared to fish injected with PBS, suggesting an evolutionarily conserved induction of hepatic PCSK9 mediated by inflammation (see II, Figure 3A).

5.2.2 CRISPR/Cas9 mutagenesis induces deletions efficiently at target loci in the zebrafish embryo

In the current research, CRISPR/Cas9 tools, derived from the bacterial immune system, were used to create null-like phenotypes already in the parental F0-generation, as reported before (Hruscha & Schmid, 2015; Jao et al., 2013).

Since repairing native gene disruptions often leads to frameshifts or random indel mutations, we aimed to disrupt the open reading frame to knockout the *pcsk9* gene (ENSDARG00000074185) in AB-wildtype zebrafish, based on the Hruscha and Schmid protocol. The entire process takes a minimum of 10 months, and the main steps are schematized in Figure 8 and II, Figure 9.

Figure 8. **Creation of a stable mutant zebrafish line using CRISPR/Cas9.** (A) Design of the gDNA target sequence (I.e., PCSK9 exon3) ordered as a single-strand oligonucleotide and (B) transferred into a gRNA. Pair of primers to amplify the fragment covering the target region were also designed accordingly using online tools. (C) Microinjection into a 1-cell stage zebrafish embryo of gRNA, Cas9 protein and phenol red dye. (D) Induction of a gDNA double strand break by Crispr/Cas9. (E) *In vitro* efficiency validation (by primer testing) and comparison with the *in vivo* efficiency (embryos evaluation). (F) Cross mating and offspring examination until generation F2 along 9-12 months.

A functional gRNA intended to target the third exon of *pcsk9*, induced parental (F0-generation) indel mutations at the target site. The *in vivo* mutagenesis efficiency was estimated in the *pcsk9* gRNA and Cas9 protein injected F0-generation embryos and in the uninjected controls using a T7 endonuclease I (T7EI) assay and 2.5% agarose TAE gel electrophoresis. Results showed a single WT PCR product band of ~169bp for uninjected controls (lanes 8 and 9), and three bands for gRNA and Cas9-injected mutant embryos sized 169bp (WT), ~100bp and ~70bp (lanes 1-7). The average mutagenesis efficiency was around 40% (II, Figure 1B and Figure 14E), which is similar to previous in-house attempts (Ojanen et al., 2019).

Next, by sequencing the mutated loci in the F1 (outcrossed F0-generation × WT Tüpfel long fin), we identified 2 germ-line transmitted nonsense *pcsk9* mutations. One with a deletion of 13bp (AACCTGCAGCGGG) and another with an insertion of 13bp (deletion of 2 bp (TG) and insertion of 15bp (AGCATCCATGCGAAC)). These mutations lead to disrupted reading frames after 147 and 148 amino acids and to premature stop-codons at the beginning of the protein regions at 173 aa and 159 aa, respectively (II, Figure 1C). The pcsk9 KO lines were named accordingly as *pcsk9*[tpu-13] and *pcsk9*[tpu-2,+15].

The expression of Pcsk9 was quantified by qPCR using brain as a starting tissue. Two females and three males from each mutant zebrafish line were used, as well as from WT siblings. Gene expression levels were normalized to eef1a1l1 (in a 2-tailed Mann-Whitney test). Steady-state zebrafish had significantly lower pcsk9 mRNA levels in homozygous *pcsk9*[tpu-13/tpu-13] and *pcsk9*[tpu-2,+15/tpu-2,+15] mutants (residual expression medians of 15.9% and 8.0%; P-value=0.008 in both) compared with their WT siblings (see II, Figure 1D).

Thus, the in-house CRISPR/Cas9 mutagenesis method proved to be an efficient method to induce indel mutations at the gRNA specified target loci in the zebrafish embryos, affecting the protein translation by not allowing the production of intact functional transcripts.

Making use of the advantages of CRISPR/Cas9, and the many available design tools (described in materials and methods) for calculating the probability of an incorrect gRNA binding event and for identifying the target-loci-specific gRNA sites with minimal off-target site recognition, we induced deleterious mutation at the *Pcsk9* target loci in zebrafish embryos (Poirier et al., 2006). Our efforts resulted in a successful frameshift leading to two nonsense mutations (*pcsk9*[tpu-13/tpu-13] and *pcsk9*[tpu-2,+15/tpu-2,+15]), generating truncated protein forms, (see Figure 9 and 10).

Figure 9. **Alignment of Pcsk9 protein sequences.** DNA sequences of WT and KOs zebrafish were obtained by NGS sequencing and translated into their protein sequence using ClustalOmega (https://www.ebi.ac.uk/Tools/msa/clustalo/). The protein sequences were aligned, and the targeted site and the induced mutation identified. The protein structure was determined according to the results obtained after analyzing the sequence with Open SignalP4.1Server (http://www.cbs.dtu.dk/services/SignalP/), and colored as follows: Signal peptide sequence (1-22aa, in yellow), Propeptide region (23-143aa, in green) and Target region (in blue and one aa in yellow corresponding to PAM region coded aa). Zymogen activation predicted at SSIFAQ[143]↓SIPWN), similarly to human and mouse.


```
CLUSTAL O(1.2.4) multiple sequence alignment (PCSK9 protein sequences)

PCSK9tpu-13      MRSVVSVCCLGFLLGLLAVVECDEDYIEDEDEMILSLILQDDTQPEAENRPSAQFYRCTK    60
PCSK9            MRSVVSVCCLGFLLGLLAVVECDEDYIEDEDEMILSLILQDDTQPEAENRPSAQFYRCTK    60
PCSK9tpu-2,+15   MRSVVSVCCLGFLLGLLAVVECDEDYIEDEDEMILSLILQDDTQPEAENRPSAQFYRCTK    60
                 ************************************************************

PCSK9tpu-13      DAWRMPGQYLVVMRNGTHVNQVERTTRRLSAKAAKRGYLIEILQTYSGAFRGFLVKMSSD   120
PCSK9            DAWRMPGQYLVVMRNGTHVNQVERTTRRLSAKAAKRGYLIEILQTYSGAFRGFLVKMSSD   120
PCSK9tpu-2,+15   DAWRMPGQYLVVMRNGTHVNQVERTTRRLSAKAAKRGYLIEILQTYSGAFRGFLVKMSSD   120
                 ************************************************************

PCSK9tpu-13      VLHMAVKLPHVEYIEEDSSIFAQSIPWSFKINMRLENTLHPMT----ELKWECICWT---   173
PCSK9            VLHMAVKLPHVEYIEEDSSIFAQSIPWNLQRVLQNKHEAGKYSPPNDGAKVGVYLLDTSV   180
PCSK9tpu-2,+15   VLHMAVKLPHVEYIEEDSSIFAQSIPWNQHPMEPAGPSK---------------------   159
                 ************************. :

PCSK9tpu-13      ------------------------------------------------------------   173
PCSK9            QLTHREVEDRVMVTDFNRVPEEDGVRVHRQASQCDSHGTHIAGVISGRDSGVARGASVNS   240
PCSK9tpu-2,+15   ------------------------------------------------------------   159

PCSK9tpu-13      ------------------------------------------------------------   173
PCSK9            VRVLNCQGKGTVSGALAGLEYIQSSLASQPVSPVILLLPFVGGFSRTLNTACRKIVESGA   300
PCSK9tpu-2,+15   ------------------------------------------------------------   159

PCSK9tpu-13      ------------------------------------------------------------   173
PCSK9            VLIAAAGNYNDDACLYSPASEPEVITVGAVNFADQPLNRGTTGTNVGRCVDVFAPGDDII   360
PCSK9tpu-2,+15   ------------------------------------------------------------   159

PCSK9tpu-13      ------------------------------------------------------------   173
PCSK9            SASSDCPTCFTTKSGTSQAAAHVAGVAAVLLNLRPNSSSAEVLQQLRYHSVKQVINPESL   420
PCSK9tpu-2,+15   ------------------------------------------------------------   159

PCSK9tpu-13      ------------------------------------------------------------   173
PCSK9            PVMHRLTTPNMVVALPDPTSTLTGEDLLCRSVWSERSASPVFSTAVSRCRSTEEMLSCSS   480
PCSK9tpu-2,+15   ------------------------------------------------------------   159

PCSK9tpu-13      ------------------------------------------------------------   173
PCSK9            FSDNGMRAGERVEERDGQKECVAVNVNGGPGVFAVARCCTGHRAQCQMLEGPERGAGAEC   540
PCSK9tpu-2,+15   ------------------------------------------------------------   159

PCSK9tpu-13      ------------------------------------------------------------   173
PCSK9            PPEHHLTGCSFSSSSGEASDSDRTLHGSRRTCAAKKGMMSYAFCCHTSTLECRLKEHHLN   600
PCSK9tpu-2,+15   ------------------------------------------------------------   159

PCSK9tpu-13      ------------------------------------------------------------   173
PCSK9            TLSQQVEVSCEDSWTLTACEALSRDAVIHGAFAMGNTCVVRTSGVDKDAAAIATCCRNHP   660
PCSK9tpu-2,+15   ------------------------------------------------------------   159

PCSK9tpu-13      -------        173
PCSK9            LHGTQDH        667
PCSK9tpu-2,+15   -------        159
```

Figure 10. Translated wildtype and mutated PCSK9 protein. Generated using Swiss Institute of Bioinformatics resource portal tools (available online at http://expasy.org). Pcsk9 proteins translated in wildtype (a), *pcsk9*tpu-13 (b), and *pcsk9*tpu-2,+15 (c) zebrafish lines.
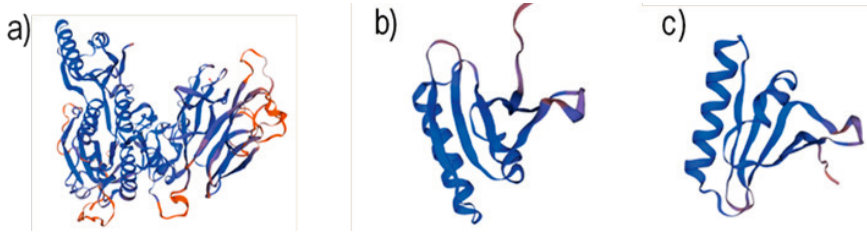
5.2.3 Knocking down *Pcsk9* has no lethal phenotype or detrimental effects on the development of pcsk9-deficient zebrafish

The mortality rates of mutant individuals during development were similar to their wildtype siblings. No severe detrimental development or phenotypic defect, such as a curved body, were observed. The onset of the CRISPR/Cas9 mutagenesis was analyzed by checking the mortality rate after 24hpf and 48hpf in the F0-generation.

The expected mortality rate was ~30% among the controls (uninjected embryos) and ~50% for the injected ones. Although some individuals showed developmental abnormalities, these were ones typically also present in similar numbers in non-manipulated fish. Thus, no severe defects were observed during the first week of life, indicating that the injected RNA and the amounts of other reagents were not toxic for the correct development of the embryos (see also II, Supp.Fig.1).

5.2.4 Pcsk9 is not required for survival against a pneumococcus infection in the *Pcsk9*-deficient zebrafish lines

Previous investigations have demonstrated that zebrafish is a suitable model to model pneumococcal pathogenesis (Rounioja et al., 2012; Saralahti et al., 2014). The host defense against pneumococcus is mainly dependent on the innate immune response (Rounioja et al., 2012). Thus, we wanted to further study if PCSK9 is relevant for the correct innate immune response to pneumococcal infections.

To that end, we carried out specific infection experiments with larvae and adults. In the larval infection experiments, 2-day-old F2-generation progeny of heterozygous *pcsk9*tpu-13/+ and *pcsk9*tpu-2,+15/+ were injected with 240 CFU bacteria (SD 76 CFU) into their yolk sac. Their survival was followed for 5 days (up to 7dpf).

At the end of experiment, the observed mortality percentages were 71% for *pcsk9*$^{tpu-13}$ line and 21% for *pcsk9*$^{tpu-2,+15}$ line (see II, Figure 2C and 2D). In more detail, when comparing survival rates between WT (*pcsk9* $^{tpu-13}$) (17%) and *pcsk9* $^{tpu-13/tpu-13}$ (21%) no significance was observed (P-value=0.57). Although the same was observed between WT larvae (*pcsk9*$^{tpu-2,+15}$) (87%) and *pcsk9*$^{tpu-2,+15/tpu-2,+15}$ (59%) (P-value=0.078), significant differences were observed between *pcsk9*$^{tpu-2,+15/+}$ (88%) and *pcsk9*$^{tpu-2,+15/tpu-2,+15}$ (P-value=0.038).

Statistically significant differences regarding the induced mortality between groups was not observed in the adult fish infection experiments. In the adult (4 to 7-month-old) zebrafish experiments, wild type AB, F2-generation *pcsk9*$^{tpu-13}$ and F3-generation *pcsk9*$^{tpu-2,+15}$ zebrafish were inoculated with 4.700.000 CFU bacteria (SD 990.000 CFU) into the abdominal region. Their survival was followed over 7 days. Mortality percentages at the end of the experiment were 32% for the *pcsk9*$^{tpu-13}$ line and 13% for the *pcsk9*$^{tpu-2,+15}$ line (see Table 10 and II, Figure 2A, 2B).

Table 10. **Zebrafish survival in *Streptococcus pneumoniae* infection experiments.** Adult survival followed for 7 days, and the survival of 2-day old embryos was followed for 5 days. Columns stand for the two different mutant zebrafish lines created with CRISPR/Cas9 tools (pcsk9tpu-13 and pcsk9tpu-2+15). Data from a single experiment. Abbreviations: n stands for group size; F for females; M for males; (s) for survived individuals; m for mortality; WT for wildtype, HT for heterozygous; KO for mutant. Log-rank Mantel Cox test.

ADULTS 4700000CFU SD 990000CFU	pcsk9tpu-13								pcsk9tpu-2+15							
	n	F	M	n (s)	F (s)	M (s)	s (%)	m (%)	n	F	M	n (s)	F (s)	M (s)	s (%)	m (%)
WT	26	5	21	15	4	11	58	42	23	12	11	19	10	9	17	17
HT	24	7	17	17	6	11	71	29	54	10	44	49	9	40	9	9
KO	21	8	13	16	8	8	76	24	20	4	16	16	3	13	20	20
Total	71	20	51	48	18	30	68	32	97	26	71	84	22	62	87	13

LARVAE 240CFU SD 76CFU	pcsk9tpu-13								pcsk9tpu-2+15							
	n	F	M	n (s)	F (s)	M (s)	s (%)	m (%)	n	F	M	n (s)	F (s)	M (s)	s (%)	m (%)
WT	24	-	-	4	-	-	17	83	15	-	-	13	-	-	87	13
HT	48	-	-	19	-	-	40	60	24	-	-	21	-	-	88	13
KO	24	-	-	5	-	-	21	79	17	-	-	10	-	-	59	41
Total	96	-	-	28	-	-	29	71	56	-	-	44	-	-	79	21

When comparing the survival of adult *pcsk9*$^{tpu-13/tpu-13}$ zebrafish (~76%) with their *pcsk9*$^{tpu-13/+}$ heterozygous (~71%) or WT siblings (~58%), we did not observe any statistically significant differences (P-value=0.31 and P-value=0.16, respectively). (See Table 16 and II, Figure 2A). Similar results were observed for adults *pcsk9*$^{tpu-2+15/tpu-2+15}$ zebrafish mutants (80%) with their *pcsk9*$^{tpu-2,+15/+}$ heterozygous (~91%) or WT siblings (~83%) (P-value=0.30 and P-value=0.79, respectively).

Additionally, to confirm the presence of living bacteria in the individuals, we plated blood and brain tissues on blood agar plates, confirming the formation of colony-forming units CFU (data not shown and unpublished).

According to the results, it can be stated that the lack of pcsk9 does not have an impact on the zebrafish survival from a pneumococcal infection.

5.2.5 In the mutant *pcsk9*[tpu-13] zebrafish line, innate immune related genes are downregulated, whereas lipid-metabolism related genes are upregulated upon a *Streptococcus pneumoniae* infection

To further investigate the results obtained from AB-pneumococcal infected fish (see 5.2.1.) regarding the PCSK9-dependent hepatic transcriptional response during pneumococcal infections, we conducted a genome-wide transcriptome analysis in mutant zebrafish lines.

Three treatment groups with WT (*pcsk9*[tpu-13]) and KO (*pcsk9*[tpu-13/tpu-13]) individuals (n=16, all females) were conformed as follows: unchallenged (n=2, both groups), PBS-injected as control (n=3, both groups) and 3.370.000CFU (SD 840.000CFU) *S. pneumoniae*-infected (n=3, both groups). The individuals were euthanized 24h after the infection, and RNA from their liver was isolated.

Next, using a gene ontology (GO) enrichment analysis, we studied the up-and downregulated transcripts in the infected KOs compared with WTs. A target list of differentially expressed genes (P-value<0.05) was compared with a background list (P-value≥0.05). The sample clustering between and within r-log transformed gene counts is depicted using PCA, showing that the experimental group is the variant affecting the sample clustering the most (see II, Suppl.Figure2). Interestingly, WTs and KOs clustered separately within the unchallenged and pneumococcus infected groups. This indicates that *pcsk9*-mediated effects on the global gene expression in the liver.

A comparison of transcript levels between KOs and WTs based on DESeq2, adjusted using the Benjamini-Hochberg method, revealed a total of 828 differentially expressed genes (also see Venn Diagram II, Supp. Figure 3B and Tables S2-S4). Out of the differentially expressed genes, 609 were expressed in unchallenged, 81 in PBS-injected and 241 in *S. pneumoniae*-infected zebrafish. Only a total of 16 genes were expressed by all individuals. Although 87 genes were expressed in at least two different experimental groups, most of the transcripts were treatment-specific: 526

in unchallenged zebrafish, 25 in the PBS-injected and 189 in infected individuals (see the Venn diagram on II, Figure 3B).

We explored the 112 upregulated and the 77 downregulated protein coding genes closer in the infected KOs compared to WTs (II, Suppl. Table 5) (Also, for a list of differentially expressed for each experimental group see Suppl. Tables 2-4). A gene ontology (GO) enrichment analysis of the 189 induced transcripts revealed fifteen enriched processes related to hormonal and lipid responses and six enriched processes related to immune processes and cellular metabolism (II, Table 1-2).

Among the upregulated genes in KOs were the *stearoyl-CoA desaturase* (log 2-fold change 5.1, P-value<0.001), *estrogen receptor 1* (log 2-fold change 3.5, P-value<0,001), *vitellogenin* (log 2-fold change 2.3, P-value<0.010), *lipoprotein receptor adaptor protein 1a* (log 2-fold change 2, P-value<0.049) (see II, Figure 3 and Table S5).

The downregulated genes, 23%, were related to immunological processes, such as *hepcidin antimicrobial peptide* (log 2-fold change –5.8, P<0.001), *complement component 7b* (log 2-fold change –3.53, P-value<0.001), *interleukin-1 receptor-associated kinase 3* (log 2-fold change –3.29, P-value<0.001), *tumour necrosis factor, alpha-induced protein 3* (log 2-fold –3.02, P-value<0.001) and *suppressor of cytokine signaling 3a* (log 2-fold change – 2.97, P-value=0.008). Thus, it was deemed relevant to take a closer look at the association of Pcsk9 with the expression of acute-phase reactants (APR).

We used qPCR to check the relative expression of the following selected APR genes: *ldlrap1a, hamp* and *socs3a*. Gene expression levels were normalized to *eef1a1l1* expression. Target genes were run once as technical duplicates (see II, Figure 3D).

The results indicated that *pcsk9* expression is upregulated *in vivo*, in the zebrafish liver upon a *S. pneumoniae* infection. In addition, the lack of PCSK9 promotes the expression of genes related to lipid and estrogen metabolism (e.g., *ldlrap1, estrogen receptor1*) and downplays several liver acute-phase reaction genes (e.g., *hamp, socs3*). These findings suggest a novel immunoregulatory function for the proprotein convertase PCSK9 in the liver.

### 5.2.6 PCSK9 regulates the expression of innate immunity genes in human HepG2 cells

To study whether PCSK9 controls the expression of the identified innate immunity genes *in vitro* and elucidate if there is a direct regulatory function for PCSK9 in the immune response in the absence of a bacterial challenge, we conducted a functional validation in human HepG2 cells. This is a human hepatocarcinoma cell line, known

to have decreased expression of PCSK9, whereas conversely, LDLR expression is increased, suggesting a modulated local microenvironment to ensure a constant energy supply (Bhat et al., 2015).

The results corroborated the decreased expression of PCSK9 and the notion that hepatocytes secrete PCSK9 extracellularly (see Figure 11C). Despite its peculiarities, the manipulated cell line was suitable for *in vitro* functional studies (see Figure 11D).

Figure 11. PCSK9 characterization in HepG2 cells. (A) Relative HepG2 cell proliferation of steady state cells infected with HKSP (titter from 1-100 million bacterial cells) at 6hpi (exploratory results unpublished), **(B)** PCSK9 expression explored by western blotting at 6 and at 24 hours after insulting steady HepG2 cells with a HKSP titter (the tubulin control is not shown in the first 6 lanes due to a wrong cut of the membrane, exploratory results unpublished), **(C)** PCSK9 expression of steady state HepG2 cells explored by western blotting. PCSK9 secretion of untreated HepG2 cells along 4 days secreted into the supernatant (SN), and PCSK9 expression is decreased in the cell lysate (CL) fraction, **(D)** transiently induced PCSK9 expression (500ng). Western blots of the supernatant (SN) up to three days, and the cell lysate (CL) fraction at 48h, **(E)** Western blotting of silenced PCSK9 expression in a titter experiment, in a supernatant and cell lysate fractions. Annotations as follows: HEK293T- as negative control, HepG2, HeLa, HEK293T+ as positive control induced expression of PCSK9 (250ng), PCSK9** for uncleaved form of PCSK9 (~71kDa), PCSK9* for cleaved form of PCSK9 (~57kDa), β-Tubulin (~50kDa).
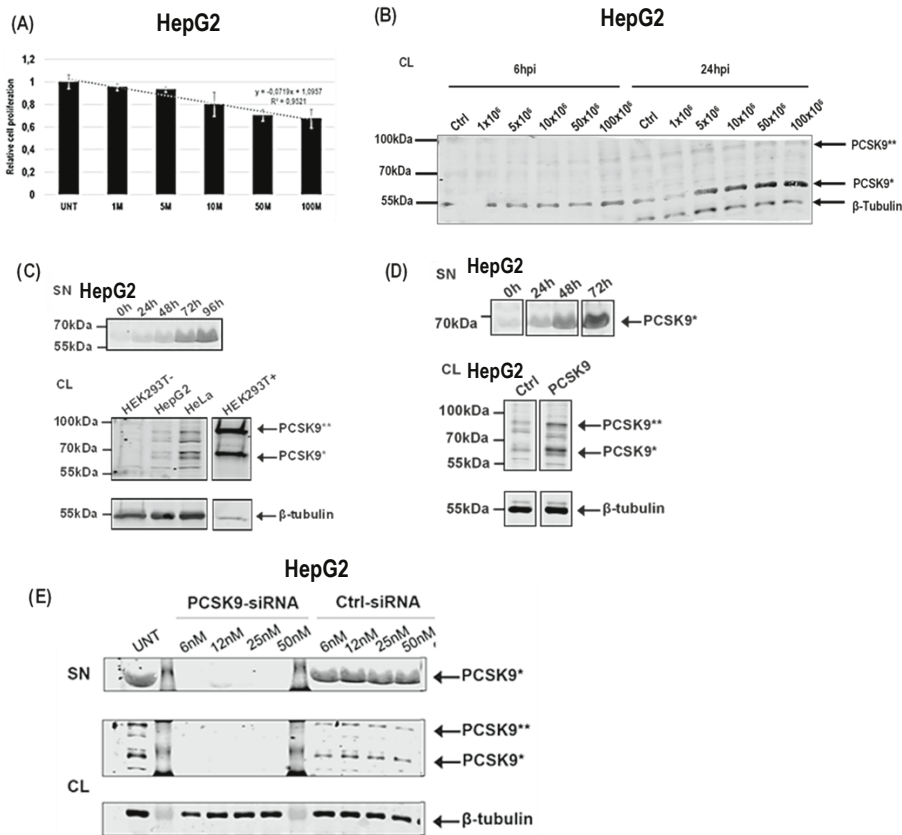
As an explorative assay, steady state HepG2 cells were insulted with cell heat killed *Streptococcus pneumoniae (*HKSP, #tlrl-hksp from InvivoGen). Already at 6 hours, cell proliferation appeared to be downregulated (see Figure 11A). Western blot results showed an alleged upregulation of PCSK9 6 and 24 hours after administering the bacterial insult (Figure 11B). Although results need to be reproduced and further investigated, seems that HepG2 cells do express more PSCK9 as larger amounts of bacteria were administered. Important to mention that the protein bands did not advance evenly in the gel, and thus, when cutting the membrane some information was lost (beta-tubulin bands from 6hpi). Blot was not repeated since it was a preliminary exploration, and data was not included in the original publication, thus, this preliminary data must be further explored and validated before drawing conclusions.

Accordingly to materials and methods chapter, we knocked-down PCSK9 expression (41.8% residual expression median compared with controls) to further quantify the expression of genes expressed in a PCSK9-dependent manner in the zebrafish liver. *HAMP* (-25% in median, P<0.001), *C7* (-1.41-fold in median, P-value=0.008), SOCS3 (-1.29-fold in median, P-value=0.019), *TNF* (-2.52-fold in median, P-value=0.017), *TNFAIP3*, *C6* and *LDLRAP1* genes were quantified by qPCR (see II, Figure 4 and Figure S3A). The relative expression levels were determined in control (n=3) and in pcsk9 siRNA transfected cells (n=3). Gene expression levels were normalized to *GAPDH* expression. Target genes were run once as technical duplicates. Silencing *PCSK9* affects the expression of the innate immune response genes in human HepG2 cells (see II, Figure 4).

We also confirmed the downregulation of PCSK9 and HAMP at the protein level (see western blot images II, Supp. Figure 3). These findings suggest a direct immunoregulatory role for PCSK9 also in the human hepatocarcinoma cell line.

5.3   PCSK9 in human ovarian cancer (III)

5.3.1   PCSK9 is expressed and secreted in OC cell lines and patient samples

Since it is well known that lipid metabolism is altered in OC, we explored whether PCSK9 expression could play a role in the survival of cancerous cells, in both neoplastic primary cell lines and patient derived cells.

Six out of eight cell lines belonged to the HGSOC subtype (JHOS2, Ovsaho, Kuramochi, COV362, OVCAR3 and OVCAR3cis) and two were of the endometroid subtype (A2780 and its cisplatin-resistant pair). No cell lines that represent LGSOC are known to date. PCSK9 protein levels were analyzed with antibodies for western blotting from both cell lines and PDCs. Protein levels were normalized to β-tubulin.

Lysates for OC cell lines showed varying expression levels of PCSK9 isoforms (I.e., uncleaved and cleaved). Compared to the cervical carcinoma HeLa cell line, which is known to express high levels of PCSK9, and which thus serves as a positive control (Wang et al., 2012), the OVCAR3 had the highest PCSK9 levels. Interestingly, the cisplatin-resistant line showed lower PCSK9 levels regarding the parental line. This difference was not observed in the other pair A2780/A2780cis (endometrioid subtype), (see III, Figure 1A, B and Suppl. Figure 1).

Next, we wanted to further analyze if ovarian cancer cells secrete cleaved PCSK9. When we analyzed the supernatant fraction by western blot analysis, we found an enriched expression of PCSK9 in OVCAR3 and HeLa cell lines (see III, Figure 1C and Supp. Figure 1).

Following this, we evaluated the expression of PCSK9 in OC PDCs derived from HGSOC and LGSOC types. PDCs are *ex vivo* representatives of patients' tumors (Kodack et al., 2017). A western blot analysis revealed that PDCs express PCSK9. Moreover, three out of five PDCs (patient 2,4 and 5) cell lysates have an uncleaved form of PCSK9. LGSOC PDCs (I.e., patients 4 and 5) showed also detectable levels of a cleaved PCSK9 form (see III, Figure 1D and 1E). Thus, PCSK9 expression was detected in tumor derived PDCs for the first time. These findings were complemented by analyzing the gene expression of PCSKs together with lipid-associated proteins. Hierarchical Kyoto Encyclopedia of Genes and Genomes (KEGG) clustering of the HGSOC and LGSOC PDCs showed that LGSOC PDCs (patients 4 and 5) clustered together, whereas HGSOC PDCs were more similar to each other. Also, LGSOC PDCs had low expression levels of genes of the apolipoprotein family (*APOA1, APOA4, APOH, APOC3*) and some PCSKs genes *(PCSK2, PCSK6* and *PCSK1)* (see III, Figure 1F, Supp. Figure 1 and Supp. Table 1).

5.3.2   Exploring PCSK9 levels in ascites fluids from OC patients

Although many studies have identified and characterized proteins within the subproteome of ascites fluid from OC patients (Kuk et al., 2009), to our knowledge,

at the time of this study no data or reference values for PCSK9 levels in ascites were available in the existing literature. To better characterize and understand the presence of PCSK9 in ascites fluids, a hallmark of OC (Ford et al., 2020), we measured PCSK9 protein levels using an enzyme-linked immunosorbent assay (ELISA) (data unpublished). Since the omentum is an environment rich in lipids, we expected to find low levels of PCSK9. Patient PCSK9 levels in the ranged from 14 to 79 ng/ml (SD 18.07), with average value of 56ng/ml and median of 62ng/ml (see Figure 12).

Figure 12. PCSK9 levels in ascites fluids from OC patients. PCSK9 levels from 14 to 79ng/ml.
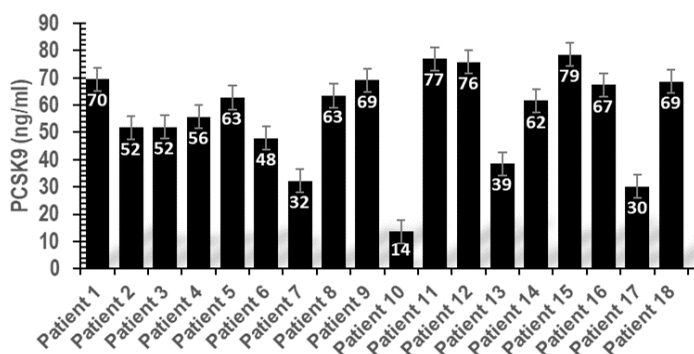
5.3.3   Targeting PCSK9 expression impaired OC cell survival

Once *PCSK9* expression in OVCAR3 and HeLa cell lines was detected, we explored whether targeting *PCSK9* expression with siRNA or with a specific inhibitor (PF-06446846) would have an effect on cell viability.

We first explored if knocking down *PCSK9* expression in OVCAR3 cells using siRNA had a statistically significant effect (P-value<0.05 for both cell lines) on cell viability already after 48h (see also III, Figure 2A). Additionally, we confirmed the reduction of PCSK9 levels by western blotting in cell lysates and the supernatant fractions (see III, Figure 2B and 2C, Supp. Figure 2 and Supp. Table 2). Second, we used an increased concentration of a commercially available PCSK9 inhibitor for 48h, to check if it impaired OC cell survival in a similar fashion as the PCSK9 knockdown. A working concentration of 100µM siRNA had a clear effect on cell proliferation in paired OVCAR3 cell lines (P-value<0.001) as well as in HeLa (P-value<0.01). In JHOS2 cells, which under normal conditions do not express PCSK9, minimal sensitivity was observed and quantified as a 15% reduction in cell growth (P-value<0.05) (see III, Figure 2D).

5.3.4 Anti-apoptotic role of PCSK9 in OC cells mediated by the intracellular activation of AKT/ERK/MEK signalling

To further investigate, whether expressing PCSK9 in JHOS2 cell activates the pro-survival AKT/ERK signaling pathways we overexpressed PCSK9 transiently, and saw an increase in phosphorylated AKT, ERK and MEK levels. Also, the basal expression levels of ERK and MEK were increased (see III, Figure 2E and 2F, Supp. Figure 2B). Thus, we could conclude that PCSK9 overexpression induced robust AKT phosphorylation along with increased expression of ERK1/2 and MEK1/2.

5.3.5 Drug testing revealed marked differences in OC cytotoxic responses

Since targeting PCSK9 with its specific inhibitor had an impact on OC cell survival, we decided to proceed by investigating the cytotoxic effects of other compounds (n=21) involved in lipid-metabolism in both OC cell lines and PDCs (see Table 10 and III, Table 2). The tested compounds belong to two different biochemical classes: metabolic modifiers (n=11), and mTOR inhibitors (n=10, first and second generation). An arbitrary threshold of DSS 7 was chosen according to a moderate median value of overall drug cytotoxicity.

Regarding the panel of metabolic modifiers, OC cell lines and PDCs had different responses (see III, Figure 3A and 3B, and original drug-response curves of anti-metabolic drugs on Supp. Figure 3A and 3B). The anti-metabolic drugs that generated higher DSS values, both in OC cell lines and PDCs were Daporinab, Pevonedistat and AVN944.

OC cell lines (especially A2780 and OVCAR3 pairs and COV362) were sensitive also to methotrexate and pemetrexed.

Among the PDCs, we observed that HGSOC patient PDC#3 and the Kuramochi cell line were highly sensitive to Erastin, both including the HGSOC cell subtype and MYC and KRAS amplification as the main genomic aberrations. Their similar sensitivity to this metabolic modifier was also seen when performing hierarchical clustering of DSS values, showing them grouped together (see III, Figure 3C). Additionally, a similarity matrix (III, Figure 3D) and a principal component analysis plot of combined DSS values from OC cell lines and PDCs (III, Figure 3E) showed that the A2780 and OVCAR3 pairs clustered together, respectively, as did the LGSOC patients (4 and 5) and HGSOC patients (1,2 and 3) altogether with other HGSOC cell lines.

Also, we observed an increase in the cytotoxicity activity of AVN944 when combined with a cisplatin treatment in HGSOC PDC#2 and LGOSC PDC#4 (see III, Supp. Figure 5), evidencing an additive cytotoxic activity with possible clinical relevance.

From our results, the second generation of mTOR inhibitors demonstrated the highest cytotoxic effect when compared with rapalogs. In particular, both OC cell lines and PDCs were more sensitive to AZD8055, Vistusertib, Dactolisib and Sapanisertib. Among the OC cell lines, A2780 and Kuramochi were the most affected, whereas COV362 showed the lowest response to all of the drugs, which is in line with its known drug-resistant phenotype.

Among PDCs, the subtype LGSOC (I.e., patient 4 and 5) were the most sensitive towards mTOR inhibitors, compared to HGSOC PDCs (see III, Figure 4A and 4B, Supp. Figure 4A and 4B). The drug responses were also analyzed based on hierarchical clustering (III, Figure 4C). The similarity matrix (III, Figure 4D) and PCA (III, Figure 4E) revealed that HGSOC PDCs clustered together, whereas LGSOC did not, evidencing a variable drug response profile within the same OC subtype towards mTOR inhibitors.

As a conclusion, the first generation of mTOR inhibitors (aka rapalogs) did not show an enhanced cytotoxic activity in OC cell lines and PDCs, whereas the second generation (tyrosine kinase inhibitors) were able to elicit an efficient cytotoxic response.

The drug testing revealed differences in the responses to the drugs that target the metabolic pathways of HGSOC and LGSOC PDCs. This demonstrates a metabolic heterogeneity related to OC subtypes, and a clinically relevant sensitivity to drugs, an aspect that should be investigated further when developing novel therapeutics.

6 DISCUSSION

6.1 CRISPR/Cas9 methodology can be an effective means for gene-editing in zebrafish and thereby suitable for the generation of non-lethal Pcsk9-KO zebrafish embryos

At the time of starting this research, proper pcsk9-deficient zebrafish lines were not available through the EZRC and ZIRC stock centres for commercial mutant zebrafish lines[7]. According to the Zebrafish Information Network (ZFIN) only one commercial *pcsk9*-mutant line generated with the morpholino methodology was commercially available (Poirier et al., 2006).

Thus, we aimed to create an in-house pcsk9-deficient line using CRISPR/Cas9 as a reliable model for conducting further research. Therefore, for this study we used AB-wild type zebrafish altogether with non-commercially available *pcsk9*[tpu-2+15] and *pcsk9*[tpu-13] mutant zebrafish, to further investigate and better understand the role of pcsk9 in the host immune response against a *Streptococcus pneumoniae* infection.

Genome editing tools have evolved and have been refined quite fast since the discovery of restriction enzymes used by procaryotic cells (Smith & Wilcox, 1970), allowing to manipulate genomes from test tubes to living organisms (Rothstein, 1983). Several different technologies have been developed based on elements of the procaryote immune system; ranging from meganucleases (MN), eukaryotic zinc finger proteins (ZFNs) (Miller et al., 2007), transcription activator-like effector nucleases (TALENs) (Miller et al., 2011), morpholino oligomers (MO) (Summerton & Weller, 1997) to CRISPR/Cas9 (Ishino et al., 1987; Jansen et al., 2002) which has been recently approved for use in clinical trials (Cyranoski, 2016).

The laborious cloning and protein engineering process required for ZFNs and TALENs has prevent their wider use (Adli, 2018). The use of MOs is limited by their immunogenic and off-target side effects (Bedell et al., 2011; Gentsch et al., 2018). In turn, the CRISPR/Cas9 system has proved to be a reliable and precise tool for *in vivo* genome manipulation (Hruscha & Schmid, 2015; Jao et al., 2013), despite the effect of certain factors, such as chromatin accessibility, that might affect the

---

[7] e.g., ZL10859.10 line with one point mutation allele, available at https://zebrafish.org/fish/

efficiency of the cleavage process (Uusi-Mäkelä et al., 2018). Although CRISPR/Cas9 is an efficient method, it can still potentially generate certain unwanted genomic damage and off-target editing effects. The prevention and reduction of side effects are based mainly on the accurate design of the gRNA (Cho et al., 2014), and on leveraging the capabilities of the Cas9 nuclease, which is used not only for genomic editing but also for transcriptional, epigenetic and chromatin engineering (Adli, 2018; Cho et al., 2013; Mali et al., 2013). Cas9 only requires a simple target-specific gRNA for each gene to edit (Yip, 2020). Each Cas9 ortholog has a unique PAM sequence (Ran et al., 2013). Cas9 can be delivered via different means (DNA, mRNA or protein). We decided to use direct transfection of the Cas9 protein after observing a higher gene editing efficiency, in accordance with previous publications (Liang et al., 2015).

One of the most challenging aspects of CRISPR/Cas9 is the optimization of the safe and efficient *in vivo* delivery of the reagents needed, to avoid off-target effects, such as insertional mutagenesis or immunologic responses. In our research, we have used a physical delivery method, since they are known to work better than the chemical ones (Yip, 2020). Microinjection protocol requires careful optimization. In our study, since no severe defects were observed during the first week, and there was no increase in the mortality of injected individuals compared to uninjected controls, we concluded that the procedures and the amounts were correct and not toxic for the proper development of the embryos (See II, Supp.Fig.1).

Posterior research has evidenced that neural toxicity could be the outcome of an unwanted and unexpected off-target effect of MO, and not a gene specific effect. A well-described example is the p53-dependent neural toxicity phenotype, a dose-dependent effect, estimated to be apparent in 15–20% of all MOs (Nasevicius & Ekker, 2000; Robu et al., 2007). This supports the interpretation that the *Pcsk9*-MO phenotype is probably unspecific. All in all, our viable in-house mutant zebrafish phenotype is in line with mammalian model systems and human data.

Zebrafish has been demonstrated to be also a suitable model for studying *Streptococcus pneumoniae* infections, due to its susceptibility to the same virulence factors as mammals (i.e., capsule, pneumolysin, autolysin and pilus) already at 2dpf (Saralahti et al., 2014). According to previous results, it seems that pneumococcus is less virulent in adult zebrafish than in embryos, since a bacterial dose of 2.5×10^6CFU was needed to kill half of the infected adult individuals (Rounioja et al., 2012; Saralahti et al., 2014).

Due to the lack of appropriate commercially available antibodies, we could not confirm the knockdown at the protein level by western blotting but at the genetic

(NGS sequencing) and transcriptional level (qPCR) we could see the depletion of Pcsk9, with an average *in vivo* mutagenesis efficiency ~40% in the F0-generation embryos. This percentage is similar to previous in-house experiments (Ojanen et al., 2019).

Also, it has been shown that a *pcsk9*-deficiency leads to no neuronal defects or lethal phenotype, implying that PSCK9 is dispensable for embryonic development and growth and its absence has no detrimental effects in the *in vivo* zebrafish model. KO individuals are morphologically comparable to WT zebrafish (See also II, Supp.Fig.1). In zebrafish, the neural plate formation start already at 10hpf, being visible at 24hpf (Korzh et al., 2001; Lossi & Merighi, 2003; Schier et al., 1996) at the same time when pcsk9 expression is detected (Poirier et al., 2006), before the formation of the liver (16-18hpf).

Although MO have been used in zebrafish with efficient results (Nasevicius & Ekker, 2000), it has been reported that the MO-based knockdown of the pcsk9 reduced its expression ~60%, resulting in a general disorganization of the CNS and embryonic lethality at 48-96hpf (Poirier et al., 2006). These results are contradictory also to those obtained in mammals. In fact, neurological alterations have not been seen in Pcsk9-KO C57BL/6J mice (Rashid et al., 2005; Seidah et al., 2003), or humans with genetic LOF variants (Mefford et al., 2018; Postmus et al., 2013). Moreover, last year it was reported that primates were healthy and that their hepatic LDL-c uptake increased, after being genetically targeted with CRISPR/Cas9 (Musunuru et al., 2021). Therefore, in any reported case did the lack of PCSK9 manifest as developmental defects or a lethal phenotype. Some impairment in glucose tolerance and pancreatic islet abnormalities were observed in murine models (Mbikay et al., 2010).

It is certainly known that PCSK9 has a dispensable role in the mammalian lineage, since the PCSK9 gene has been lost in many species such as pigs, cows, whales, camels, and bears (Murphy et al., 2001; van Asch & Teixeira da Costa, 2021). Interestingly, these animals share metabolic processes for fat storage, which for example enable bears to spend prolonged times in hibernation. Thus, having no PCSK9 at all might have even been beneficial at some point during the course of the natural history of these animals.

6.2 PCSK9 is upregulated upon infection and acts as an acute-phase reactant protein, both in patients and in zebrafish

The study carried out with bacteremic patients showed a significant upregulation (almost two-fold) of plasma PCSK9 levels in bacteremic patients (376ng/ml) when compared with healed healthy controls (188ng/ml) and with the normal range in healthy individuals (170-220ng/ml). During the first four days of hospitalization PCSK9 levels remained high, ranging from 383ng/ml on day 1 to 356ng/ml on day 4. Also, we observed this upregulation *in vitro* (in HepG2 cells exposed to heat killed whole pneumococcus) and *in vivo* (adult AB zebrafish challenged with pneumococcus had a 4.5-fold increase in PCSK9 levels compared to unchallenged fish).

Interestingly, cases with a poor outcome, had less upregulation of PCSK9. Patients with a fatal prognosis had the lowest plasma PCSK9 levels on the day of admission (although they were still higher than the normal range seen in healthy individuals), when compared to all bacteremia patients.

The patients' age and underlying conditions were similar to those in other studies with bacteremia patients (Diekema et al., 2003; Ortega et al., 2007). Also, the cohort was large, and it was collected individually and prospectively (not from registries). It included only culture-positive cases, which represent true infections, not just cases with suspected infections (as culture-negative with an implied infection).

Gram-positive and Gram-negative causative organisms upregulated plasma PCSK9 levels similarly, and no statistically significant difference between them was observed. This finding is in line with the fact that both types of pathogens have lipidic components (e.g., LTA, LPS) that are able to trigger immune responses (Grin et al., 2018) upon interaction with elements of the innate immune system, such as the TLRs (Savva & Roger, 2013), in a LDLR/PCSK9 dependent pathway (Leung et al., 2019). LPS is a TLR4- ligand (Ciesielska et al., 2021; Poltorak et al., 1998), cleared from the blood almost solely by the liver (Scott et al., 2009), whereas LTA interacts with TLR2, involving the participation of CD14 and CD36 (Hoebe et al., 2005; Schröder et al., 2003; Yoshimura et al., 1999). Murine *in vivo* studies have reported that PCSK9 induces CD36 degradation, affecting the long-chain fatty acid uptake and triglyceride metabolism in adipose and hepatic tissues (Demers et al., 2015).

Also, a significant correlation between PCSK9 and CRP levels was reported, not only on the day of admittance but also during the first four days of hospitalization. This association was noticed and reported already in the context of other diseases (Gao et al., 2018). Another result that can be interpreted as PCSK9 resembling an APR is that patients suffering from liver condition had lower levels of circulating

plasma PCSK9. CRP is a key protein of the innate immune system. It is a pentameric protein synthesized by the liver, primarily induced by cytokines such as IL-6, IL1β and IL-17 after damage (Nehring et al., 2021). Elevated blood CRP levels rise promptly (Sproston & Ashworth, 2018), constituting a biomarker for inflammation (Healy & Freedman, 2006). Unfortunately, CRP does not have value in the prognosis of a patient with bacteremia, like do other factors (e.g., cfDNA). Interestingly, human CRP recognizes and binds specifically to the C-polysaccharide on the surface of *Streptococcus pneumoniae* to promote complement-mediated phagocytosis (Kaplan & Volanakis, 1974; Thomas-Rudolph et al., 2007). In this regard, PCSK9 levels might be better as a prognosis marker than CRP. Further research is needed to elucidate it.

On the day of admittance, patients with lower plasma PCSK9 levels 1) were males, 2) suffered from liver disease, 3) had a history of alcohol abuse, 4) suffered from a polymicrobial infection. This was in accordance with previous investigations. It has been reported that there is a sex difference in PCSK9 levels, women having significantly higher plasma PCSK9 levels than men (Lakoski et al., 2009). The expression of circulating PCSK9 is reduced in patients with liver dysfunction (Schlegel et al., 2017). In turn, the patients with higher plasma PCSK9 levels 1) were on statin medication, 2) suffered from lower respiratory tract infections and 3) suffered from *Streptococcus pneumoniae* infections. In our patient cohort, we observed that statin users had higher levels of circulating PCSK9 and should be addressed specifically in the analysis of any study. This is in line with previous findings. Ever since the discovery of PCSK9 it has been known that PCSK9 expression is enhanced in patients on statins (Davignin & Dubuc, 2009; Dubuc et al., 2004; Mayne et al., 2008). Satins are responsible for inhibiting 3-hydroxy-3-methyl-glutaryl-CoA reductase (HMG-CoA). Consequently, SREBPs are activated, and are responsible of increasing PCSK9 transcription (Horton et al., 2003).

Several studies have been published with opposite and even conflicting results regarding PCSK9 in the clearance of infections. While certain studies are in line with our results (Vecchié et al., 2021), others are not (Boyd et al., 2016; Walley et al., 2014), or did not even find a clear protective effect (Mitchell et al., 2019).

A recent study, part of the ALBIOS trial explored the association between plasma PCSK9 levels (on day 1) and mortality based on 958 ICU patients with sepsis/septic shock. They also concluded that patients with septic shock have lower plasma PCSK9 levels (19–182 ng/mL) on day 1 and showed higher mortality rates in the short (28-) and long term (90-day). They analyzed a larger cohort than we did, and also, the patients were collected from more than one hospital. On the other hand, patients were admitted to the ICU, not the ED. The stage of severity might have

been different, also because in our study 15% of the patients died by day 28, whereas 32% died in the ALBIOS study.

Also, a couple of more points to discuss are that in the ALBIOS study they did not show records on statin therapy. They analyzed the samples without differentiating if the blood culture was positive or negative for infection. We should consider that 33% of their samples were blood culture negative. It could be interesting to independently analyze the data from these 642-blood culture positive samples as well, as was done in the current research. They also did not include a control group. They also found a positive association between PCSK9 and PTX3, a pentraxin (member of CRP family), which is considered to be an APR and has already been evaluated as a biomarker for the severity and outcome of infectious diseases (Bottazzi et al., 1997; Uusitalo-Seppälä et al., 2013). The ALBIOS trial did not screen for LOF variants, so no strong conclusions can be made about this point.

Another study recruited 200 septic patients (Boyd et al., 2016), and concluded that higher plasma PCSK9 levels were associated with increased severity and poor outcomes, correlating with higher risk of organ failure. It is worth mentioning that 85% of the patients had very low levels of cholesterol.

Studies considering genetic PCSK9 variants have also generated contradictory results (Mitchell et al., 2019; Walley et al., 2014). On the one hand, Mitchell and colleagues stated that no association between LOF and the incidence of serious infections can be implied. In their study (REGARDS), of 10,924 individuals only 2.2% carried one of the two *PCSK9* loss-of-function variants considered in the study (n=244). Also, the data used for this publication was a part of a bigger study, collecting data from different racial groups. This might create a bias. It is possible also that a different conclusion would have been drawn with a higher proportion of LOF individuals. On the other hand, Walley and colleagues assessed in two independent cohorts (619 and 408 respectively) the most common missense variants in septic patients: 3 LOF and 1 GOF. They concluded that a lower expression of PCSK9 (especially due to the rs11591147 variant) contributes to a better survival among infectious patients (Walley et al., 2014).

The results of *in vivo* experiments have also been contradictory (Berger et al., 2017; Walley et al., 2014). Walley and colleagues administered LPS to *Pcsk9* knockout (*Pcsk9−/−*) and genetic WT background mice controls. Compared to wildtypes, *Pcsk9* knockout animals had better bacterial lipid clearance (55% lower plasma endotoxin) and survival outcome. Similar outcomes were seen for mice treated with a Pcsk9 blocking antibody in a polymicrobial sepsis experiment (Walley et al., 2014). The authors suggest that having a low level of PCSK9 aids in the uptake of lipids and in

a decreased inflammatory response. In contrast, Berger and colleagues concluded that neither inhibiting PCSK9 nor genetically deleting it (*Pcsk9⁻/⁻*) reduces LPS-induced mortality (Berger et al., 2017).

The results from *in vitro* experiments in HepG2 cell culture have also been varied (Boyd et al., 2016; Walley et al., 2014). This cancer cell line is known for having reduced expression of PCSK9. Also, they used the same purified recombinant human PCSK9 protein (AcroBiosystems PC9-H5223) to induce the transient expression of PCSK9. Boyd et al. evaluated the threshold and dose-response characteristics of the PCSK9 level compared to the rate of LPS clearance from the circulation by the liver. Having whether very low PCSK9 levels or very high, implies poor responses against sepsis. These results might partially explain why patients with very high upregulation of PCSK9 have more difficulties coping with the infection, leading to an eventual organ failure.

Mention that PCSK9 does not significantly affect HDL levels (Abifadel et al., 2003). HDL levels are known to be critical for sepsis patients, as those with declining HDL are at a higher risk of organ failure and death (Trinder et al., 2019). Furthermore, there is the so called "obesity paradox", stating that obese patients have lower mortality due to sepsis (Shimada et al., 2020) than do patients that are not obese. Additionally, it is interesting that VLDLR located in adipose tissues, is a surrogate or alternative agent responsible for sequestering lipopolysaccharides (Roubtsova et al., 2011), suggesting a contribution to patient survival.

There are at least four reported forms of PCSK9 (Seidah, 2021): immature zymogen (~75kDa), autocleaved (~62KDa), FURIN-cleaved (~55KDa) and PC5/6 cleaved (~55KDa) (Dubuc et al., 2010). Many studies have not explored which form was measured. This fact might explain, in part, why results were different or apparently contradictory. Could be of interest to elucidate which are the circulating PCSK9 forms (liver produced), since they are not equally functional (Dubuc et al., 2010; Han et al., 2014; Kuyama et al., 2021). It is known that FURIN-cleaved PCSK9 bound to LDLR with a 2-fold reduced affinity compared with intact PCSK9 but still is able to reduce LDLR levels in HepG2 cells and in mouse liver (Lipari et al., 2012).

As a final commentary, PCSK9 follows a circadian rhythm (Chen et al., 2014), having a higher expression towards the evening (and therefore, less LDL-c/bacterial lipids hepatic clearance). This could also be contributing factor to the differences seen among patients. In our study, the first blood sample was withdrawn in the ED usually within one hour after the arrival of the patient, many of them arriving between noon and 6p.m., but patients were admitted 24/7. After hospitalization, samples were mostly collected between 6a.m. and 10a.m.

6.3 PCSK9 is dispensable for zebrafish survival after a *Streptococcus pneumoniae* infection but has an evolutionarily conserved immunoregulatory function in the liver

In our zebrafish *in vivo* experiments, we observed that PCSK9 had a nonessential role in host survival upon a systemic pneumococcal infection. That was true for both mutant lines and both growth stages. Adults and larvae, which only rely on the innate immunity to cope with a pneumococcus infection, showed similar mortalities. Overall, larvae experienced a higher mortality (-71% for *pcsk9*tpu-13 and -21% for *pcsk9*tpu-2,+15) compared to adults (-32% and –13%, respectively). Also, KOs experienced a similar mortality percentage as WTs, with a non-significant difference observed between *pcsk9*tpu-13 adults and *pcsk9*tpu-2+15 larvae (see Table 16 and II, Fig.2).

We can ascertain that bacterium were viable and active after injecting them into the zebrafish, since we cultured them after euthanizing few representative individuals for each treatment and plating their tissues (blood and brain). After an overnight incubation at 37 °C and 5.0% CO_2, bacterial colony forming units were counted to determine the bacterial load. Bacterial expansion in the blood was rapid, evidencing the ability of pneumococcus to replicate in zebrafish and cause an acute infection and bacteremia. Moreover, pneumococcus can invade the brain, having the potential to induce meningitis, mimicking the common route of infection in humans. It also includes the induction of proinflammatory cytokines, in line with previous research (Rounioja et al., 2012).

The amount of bacteria (240CFU for larvae and 4,7x10^{6}CFU for adults) inoculated was calculated according to previous results (Rounioja et al., 2012; Saralahti et al., 2014). It has been reported that the WT pneumococcus strain T4 is less virulent in adult zebrafish when compared to other streptococci-zebrafish models, and thus a dose larger than 2.5x10^{6}CFU is needed to elicit a notable infection (Neely et al., 2002; Saralahti et al., 2014). In our experiments, individuals that were alive after 96hpi most likely overcame the infection. It has been observed that zebrafish can clear the infection within 4 days, thus, the protective immune response mainly relies on the innate immune system (Saralahti et al., 2014).

Interestingly, we noticed that fish lacking *Pcsk9* when compared to their WT siblings, experienced an upregulation of lipid metabolism and estrogen related genes upon a pneumococcal infection. The most relevant and apparent were the upregulation of *ldlrap1* (low density lipoprotein receptor adapter protein 1), required for efficient endocytosis of the LDLR in hepatocytes, and of *estrogen receptor1*. To mention that *PCSK9* has two estrogen response elements (EREs) in its promoter

region (Maarouf et al., 2020), as predicted by an *in silico* MatInspector analysis (https://www.genomatrix.de/). This finding is in line with the finding that females have higher levels of PCSK9 than men (Lakoski et al., 2009; Mayne et al., 2008).

Several genes related to innate immune responses were downregulated. The most relevant genes were *hamp* (hepcidin antimicrobial peptide), *socs3* (suppressor of cytokine signaling 3). *Hamp* is a liver produced antimicrobial peptide. It is part of the acute phase response against microbes, and it is involved in iron homeostasis (Park et al., 2001). Its expression is upregulated in response to several stimuli, including proinflammatory cytokines (Wrighting & Andrews, 2006). *Socs3* is a negative regulator of the JAK/STAT pathway activated by proinflammatory cytokines (e.g., TNF-α). Also, it is implicated in hypertriglyceridemia associated with insulin resistance. It has been reported that SOCS3 induces PCSK9 expression in the hepatic HepG2 cell line, confirmed by silencing *SOCS3* with its specific siRNA, which reduced PCSK9 mRNA levels (Ruscica et al., 2016). In our research, we observed that when *PCSK9* was silenced, the expression of *SOCS3* increased (P=0.019).

We investigated a selection of the genes differentially expressed in zebrafish involved in the human HepG2 cell line, confirming some of the findings. Additionally, treating HepG2 cells *in vitro* with an infectious insult, had a slight effect on cell viability at 6h (see Figure 14A), but not at 24h (data not shown). Thus, this reinforces the statement that a lack of or reduced expression of Pcsk9 does not have a detrimental effect on survival. Consequently, the evidence suggested a novel immunoregulatory function for PCSK9 in the liver.

One can speculate on why the findings from the zebrafish experiments were not completely replicable in human HepG2 cells. It might be that since HepG2 cells are a cancer line, the results could be more alike if using primary human hepatocyte cells. Also, it can be argued that the *in vivo* zebrafish experiments target the whole liver, with all the different cells that constitute the organ. In contrast, *in vitro* experiments are, by definition, a simplification of the organ's complexity.

Zebrafish has been proposed as a suitable model for studying human liver development and disease, having at 5dpf an already developed liver comprised of well-differentiated hepatocytes networking with biliary channels, contiguous via extrahepatic biliary ducts with the gallbladder and intestine. Although the molecular determinants of development and disease are well conserved, implying a high degree of recapitulation of the human condition, there are still differences in the morphogenesis and anatomy. These differences, such as the tubular architecture of

the zebrafish liver (opposed to the lobular one in humans) might be associated with differences in physiology (Wilkins & Pack, 2013).

Lastly, despite the conserved residues in pcsk9 catalytic domain in vertebrates, the extend of overall conservation between zebrafish and humans remains a factor to consider, when comparing functional experiments between species (Cameron et al, 2008).

6.4 The anti-apoptotic role of PCSK9 in ovarian cancer

To date, very little is known about the role of PCSK9, a cholesterol-regulating enzyme, in OC. An emerging hallmark in OC, common to several other malignancies, is dysregulated lipid metabolism. The altered cellular metabolism plays a key role in OC tumorigenesis and progression (Pavlova & Thompson, 2016). About 80% of patients suffering from serous ovarian carcinoma present omental metastasis and the development of abdominal ascites (Adam & Adam, 2004; Nieman et al., 2011).

Thus, the main aim of this study was to elucidate the expression and role of PCSK9 in OC cell survival and its downstream signaling. Altogether, we investigated the cytotoxic efficacy of a small library of metabolic (n=11) and mTOR (n=10) inhibitors using OC cell lines (n=8) and *ex vivo* PDCs (n=5) to identify clinically relevant drug vulnerabilities.

OC cell line models as well as PDCs were chosen as representative models of HGSOC (n=9) and LGSOC (n=2). Cell lines included paired lines according to the pre- and post- development of cisplatin resistance. An ovarian endometroid adenocarcinoma was also included (I.e., A2780 and its sister line, cisplatin-resistant). HeLa was used as an internal control, as it is a cervical carcinoma.

We reported for the first time that OC cell lines and patient derived cells express and secrete PCSK9, suggesting paracrine modulation. Not all PCSK9 expressing tissues secrete PCSK9, like for example the recently reported mature differentiated intestinal cells (François et al., 2021).

The OVCAR3/OVCAR3cis cell line pair, representative of the HGSOC subtype, showed a different expression level of mature PCSK9 than the other cells. The resistant cell line has less mature PCSK9 than the parental line. This difference was not observed in the endometroid adenocarcinoma pair (A2780/A2780cis). The difference between both sister cells might be due to their different tissue origin and

thus, type of EOC. These differences should be screened for further in different cell lines to better understand how resistance is acquired.

Another interesting finding, not reported in the original publication III, was the exploration of PCSK9 levels in ascites, a hallmark of OC, correlating with an advanced disease and poor prognosis. Although many studies have analyzed and mined the proteome of ascites (Ahmed et al., 2016; Gortzak-Uzan et al., 2008; Kuk et al., 2009; Shender et al., 2014), rich in cholesterol (Penet et al., 2018), PCSK9 was not explored before. In our research, in 18 ascites samples, the PCSK9 levels ranged from 14-79ng/ml, 56ng/ml being the average value. When comparing with other tissues, under physiological conditions, human plasma has ~200ng/ml (Boyd et al., 2016), and cerebrospinal fluid has ten times less PCSK9 than ascites, ~5ng/ml (Chen et al., 2014). Another study explored the PCSK9 levels in the blood of parturition women against non-pregnant ones. Pregnant women have a significant increase (1.7 times) of circulating PCSK9 compared no non-pregnant women (493.1ng/mL and 289.7 ng/mL, respectively), as well as to newborns (493.1ng/mL and 278.2 ng/mL, respectively) (Peticca et al., 2013). These results could suggest that, since ascites fluid is a lipid-rich environment, keeping PCSK9 at low levels of might be beneficial for the growth of the cancer cells and cancer progression. More research is warranted to better understand this complex environment, considering FURIN as well, since it is known to be highly expressed in the omentum (Chen et al., 2020).

Also, we observed that silencing PCSK9 impaired OC cell survival and proliferation mediated by the activation of intracellular AKT/ERK/MEK signaling (at least, partially). In contrast, when overexpressing PCSK9, a robust AKT phosphorylation was induced along with increased expression of ERK1/2 and MEK1/2, suggesting a pro-survival role for PCSK9.

It has been reported that in hepatocellular carcinoma, PCSK9 promotes tumor growth by inhibiting tumor cell apoptosis (He et al., 2021; Zhang et al., 2021), whereas in gastric cancers, PCSK9 favors metastasis and suppresses apoptosis via the MAPK signaling pathway (Xu et al., 2021). In neuronal cells, it has been reported that PCSK9 contributes to apoptosis via Caspase-3 and when overexpressed, PCSK9 inhibited apoptosis (Bingham et al., 2006). In lung cancer A549 cells, it has been shown that PCSK9 has also an anti-apoptotic effect (Xu et al., 2017). This outpour of data suggested that when silencing PCSK9 the relative proliferation of malignant cells is suppressed, which is in line with our results on OC cells.

Interestingly, it was reported in 2009 that annexin A11 was downregulated in OC cisplatin-resistant cells (compared with their parental cells), and that this plays an

important role in cell proliferation (Song et al., 2009). When suppressing A11, *PCSK9* was one of the genes that was downregulated.

Moreover, multicellular organisms maintain tissue homeostasis via regulating cell death. One of the better characterized processes is cellular apoptosis, a tightly regulated and evolutionarily conserved cell death program. This process has two pathways, the extrinsic one (when Fas cell-surface death receptors interact with their ligands) and the intrinsic one (when BCL-2 proteins permeabilize the mitochondrial outer membrane). Both pathways lead to the activation of several caspases, a family of cysteine proteases. Apoptosis is common during early embryonic development, and its purpose is to eliminate unnecessary cells. Later during development and adulthood, apoptosis removes damaged cells and prevents the accumulation of aberrations. During infections, apoptosis eliminates infected cells (Friedrich et al., 2017). In cancer, a phenomena known as "the apoptosis paradox", has been described (Morana et al., 2022). During the development of any cancer, there is an imbalance between cell gain and cell loss, with proliferation exceeding self-termination or elimination. But high-grade cancers with a poor prognosis are generally associated with higher apoptosis (Alcaide et al., 2013; Jalalinadoushan et al., 2004; Mangili et al., 1998; Villar et al., 2001). Thus, although the evasion of apoptosis is a cancer hallmark, tumor cell populations are not able to suppress the apoptotic program continuously. And at the same time, apoptosis is also an important cellular response to cancer therapy (Cvetanovic et al., 2006).

Furthermore, it has been reported that apoptosis can be induced via TLR2 and MyD88-dependent activation (Aliprantis et al., 1999, 2000), the same receptor that triggers immune responses upon detecting bacterial LTA (Yoshimura et al., 1999). Despite all the research, the complete molecular mechanisms that drive the deregulation of apoptosis during the onset of diseases remains unclear (Singh et al., 2019). Nor do we know how to modulate the pathways in a way that could be beneficial for the patients (Carneiro & El-Deiry, 2020).

Targeting PCSK9 with its specific inhibitor had an impact on OC cell viability, and this was further investigated by evaluating the cytotoxic effects of 21 compounds involved in lipid-metabolism over OC cells. Among them, the second generation mTOR inhibitors (tyrosine kinase inhibitors) were the most efficient. Drug testing demonstrated a metabolic heterogeneity related to OC subtypes.

Activation of the PI3K/mTOR pathway correlates with a resistance to chemotherapy in OC2 (Brasseur et al., 2017; Foster et al., 2010). The PI3K pathway is one of the most deregulated signaling pathways in many tumors, including OC, contributing to increased cell survival and chemoresistance, being another interesting

target for treatment (Huang et al., 2020). AKT and mTOR phosphorylation has been detected in OC and targeting them has been shown to disrupt the growth of OC tumors (Altomare et al., 2004). The effects of mTOR inhibitors in human OC was investigated already in the early 2000s. Its complex biology demonstrated that the need for combination treatment strategies.

Thus, dysregulation of the PI3K/AKT/mTOR signaling pathway is very frequent in human cancers, including OC. The aberrant activation has been reported mainly through the various genomic alterations associated with *PTEN, AKT, PIK3CA, PIK3R1,mTOR, TSC1 and TSC2* (Dobbin & Landen, 2013; Gasparri et al., 2017).

mTOR regulates several cellular processes such as lipid synthesis and metabolism, cell proliferation, autophagy, and apoptosis by participating in multiple signaling pathways. It is a component of the phosphatidylinositol 3-kinase (PI3K) cell survival pathway, which monitors the availability of nutrients, mitogenic signals and oxygen levels. mTOR is activated by different molecules such as insulin or growth factors, and it is impaired by nutrient deficiency, for example. Thus, mTOR plays an important role in cell growth and proliferation, immune cell differentiation and is subsequently relevant for tumor metabolism.

The metabolism of cancer cells is different compared to non-malignant cells, including an altered central carbon metabolism, and pathways that regulate lipid metabolism. HGSOC patients have profound alterations in lipid metabolism, with decreased levels of plasma HDL-cholesterol (Braicu et al., 2017). OC patients are reported to be at an increased risk of developing ischemic stroke (Kuan et al., 2014). PCSK9 is a key protein in the regulation of lipid metabolism, presenting an abnormal pattern of expression in many cancers. Thus, the cytotoxic effects we saw when testing anti-metabolic drugs in cancer cell lines, could contribute to the better understanding of metabolic alterations in cancer.

Concordantly, there are OC subtype-specific efficacies due to a different metabolic pathway in HGSOC, compared to LGSOC. It would be interesting to further explore the additive cytotoxicity activity of AVN944 when combined with cisplatin treatment (independently of HGSOC/LGOSC subtype), since this could have clinical relevance. Published evidence endorsed AVN944 as a suitable drug for inhibiting the growth of human prostate cancer cells by inducing cell cycle arrest and apoptosis (Floryk & Thompson, 2008).

The second generation of mTOR inhibitors produce higher effects when compared with other rapalogs. According to our results, special attention should be

given to AZD8055, Vistusertib, Dactolisib and Sapanisertib. Several studies evidenced the importance of multitargeted strategies against ovarian cancer.

It has been reported that AZD8055, responsible for mTORC1/2 inhibition, strengthens the efficiency of Trametinib (a MEK inhibitor) (Pétigny-Lechartier et al., 2017). Even cell lines that are unresponsive to conventional platinum-based chemotherapy (e.g., advanced-stage ovarian clear cell carcinoma) are especially sensitive to AZD8055 (Caumanns et al., 2018).

Vistusertib (also known as AZD2014, a dual mTORC1/2 inhibitor) treatment after cisplatin chemotherapy delayed the recurrence of EOC (Pi et al., 2021). A recent clinical trial proposed the use of Vistusertib in combination with Paclitaxel in HGSOC patients (Basu et al., 2018).

The enhanced effects of Dactolisib (aka, BEZ235) combined with ERK inhibitors both in monolayer and three-dimensional OC cell models were recently reported (Dunn et al., 2022).

Sapanisertib (aka, TAK228) in combination with Paclitaxel is currently being evaluated for OC treatment in a phase II trial (NCT03648489). More research is needed to improve co-treatments employing Paclitaxel and mTOR second generation inhibitors.

These findings, together with the extensive reviewing of the therapeutic relevance of mTORi in OC support further research (Boussios et al., 2019; Ediriweera et al., 2019). Specially interesting might be to focus the research on the putative connections between PCSK9 and the effects produced by the employed drugs, to better understand the metabolic alterations of OC cells, and how to treat them.

6.5 Targeting PCSK9 and lipid-metabolism related genes in infectious diseases and cancer

PCSK9 expression is linked to cholesterol metabolism via LDLR (Maxwell et al., 2005), bacterial lipid clearance (Grin et al., 2018; Shimada et al., 2020), innate immunity and apoptosis via TLR4 (Scalise et al., 2021; Wu et al., 2022), and adaptive immunity via MHC-I independently of LDLR (Liu et al., 2020). In addition to infections and inflammation, LDLR degradation relates to the anti-tumor activity of CD8-T-cells, by reducing the amount of LDLR-T-cell receptor (TRC) complexes on the cell surface (Yuan et al., 2021). Also, PCSK9 is linked to the detection and

uptake of Gram positive lipids and to apoptosis via the activation of TLR2 (Aliprantis et al., 1999, 2000; Malley et al., 2003; Yoshimura et al., 1999).

Many genes related to lipid-metabolism are altered in several bacterial infections and cancer, and dysregulated cholesterol homeostasis plays an important role in cancer (Hsu & Sabatini, 2008) and infections (Barlage et al., 2001; Lee et al., 2015). Cancer cells have a higher demand for energy to endorse their high growth rates (Mayengbam et al., 2021). Much evidence points to an upregulation of LDLR levels in several tumors, and low circulating cholesterol levels (Cruz et al., 2013; Korneva et al., 2021).

It is estimated that three quarters of the total present cholesterol in the human body are synthesized *de novo*, and the rest is obtained from the diet. Chemically cholesterol is a steroid molecule, essential to animal life, since it is a principal component of structures and precursor to many biomolecules, such as cell membranes, hormones (as estradiol or testosterone), vitamins (e.g., D) or biliary acids (cholic acid).

Several factors such as the intracellular LDL-c levels regulate *PCSK9* transcription (Krysa et al., 2017), although certain studies suggested that this correlation might be due to a sex dependency in normolipidic humans (Mayne et al., 2007).

Sterol regulatory-element binding proteins (SREBPs) are transcription factors that regulate the expression of several genes involved in lipid synthesis (Shimano & Sato, 2017). In particular, SREBP2 regulates genes such as *HMGCR, FDFT1, SQLE, LDLR* and *PCSK9* (Dubuc et al., 2004; Eberlé et al., 2004; Lebeau et al., 2022). In turn, SREBP2 activity is regulated by intracellular cholesterol levels (Eberlé et al., 2004), and the PI3K/AKT/mTOR signaling pathway (Düvel et al., 2010). SREBP2 remains inactive in the ER until intracellular cholesterol depletion occurs, which is when it translocates to the GA to become active and continues to the nucleus, where it binds other regulatory factors at the promotor regions of the genes (Eberlé et al., 2004). SREBP2 is upregulated in OC and contributes to cisplatin resistance via the upregulation of cholesterol synthesis (Zheng et al., 2018). Thus, may be of interest to target SREBP2 since might increase drug sensitivity and therefore contribute to reduce OC recurrence.

The use of PCSK9 as an early biomarker for different types of cancers (e.g., liver, gut, breast or pancreas) and infectious diseases, have been investigated (Bhattacharya et al., 2021), with inconclusive results. In this regard, our findings pointed out that in the early phase of bacteremia, when patients are in the emergency room, lower plasma PCSK9 levels correlate with fatal outcome and therefore predict mortality.

Independently of the idiosyncrasy of a given disease, it could be that PCSK9 should be investigated as a late biomarker instead. For example, a randomized controlled trial demonstrated that circulating PCSK9 concentrations were induced after severe trauma in patients admitted into the ICU, and that PCSK9 levels turned out to be a suitable biomarker for the severity of the illness (prognostic marker) on day 8 instead of day 0 (Le Bras et al., 2013).

In OC, another pro-protein convertase enzyme, exerting a modulation over PCSK9, has already been proposed as a prognostic marker for tumor progression. FURIN expression is increased and predicts a lower survival (Page et al., 2007). Recently, a study underscored the importance of FURIN in this disease, since it was reported that activates the IGF1R/STAT3 signaling axis in OC cells, promoting cell progression and metastasis (Chen et al., 2020). Thus, targeting the expression of FURIN reduced tumor growth *in vivo*. PCSK9 is cleaved by FURIN, and it would be interesting to co-study them further to better understand the OC landscape.

Regarding treatment options, complementary to antibodies used against PCSK9, it has been proposed that cancer cells could be starved using PCSK9i in drug-induced hypocholesterolemia (LDL <25 mg/dL) (Gangloff et al., 2017). In fact, PCSK9 inhibition could attenuate the progression of certain cancers (e.g., breast, glioma, colon, liver, prostate and lung adenocarcinoma), promoting cellular apoptosis (Sun et al., 2022). One interesting question would be to evaluate how PCSK9 inhibition would matter in tissues where *de novo* cholesterol synthesis is relatively high.

Moreover, although both PCSK9 loss and inhibition were suggested as promising strategies for treating infectious diseases (Dwivedi et al., 2016; Walley et al., 2014), some considerations arise regarding age-dependent pleiotropic effects of PCSK9 on certain receptors or in the context of inflammation (Cesaro et al., 2020). For instance, it was reported that PCSK9i may be beneficial for septic adult patients, but not for young children. Also, LOF variants were associated with decreased survival, both in young patients and juvenile mice (Atreya et al., 2020). It would be interesting to further address the question if PCSK9 polymorphisms provide any advantage or, disadvantage regarding cancer. Two human studies evaluated this matter but they were not conclusive in finding any association between heterozygote PCSK9 LOF with higher cancer occurrence (Benn et al., 2011; Folsom et al., 2007).

Furthermore, a recent study explored the plasma PCSK9 levels of 73 children (Vlachopoulos et al., 2019), and the average value (184.4ng/ml, with a range of 133.8–235.5ng/ml) was similar to the one for healthy adults reported by Boyd and colleagues. Thus, this parameter does not help explain why PCSK9i are not beneficial

for septic young patients. Other factors may be involved, such as hormones or certain tissues. For example, a recent murine *in vivo* study focused on the role of brown adipose tissue, stating that brown fat activation enhances the therapeutic effects of PCSK9 inhibition (alirocumab) in dyslipidemia and atherogenic CVD (Zhou et al., 2021). As we discussed before, it has been observed that obese patients have lower mortality due to sepsis (Shimada et al., 2020), thus, might be interesting to further investigate the participation of different adipose depots.

However, it has been reported that before surgery, it is beneficial to neutralize circulating PCSK9 to increase LDLR levels before the onset of sepsis. After surgery, circulating levels of PCSK9 and lipids experience a drastic lowering (Druce et al., 2018). Thus, in the light of the available evidence, the advantage of using inhibitors cannot be denied completely.

More research is warranted to elucidate, if PCSK9 could serve as a biomarker for improved diagnostics, better prognostic estimation and predicted response to a given treatment. As well as if the use of PCSK9i would be beneficial for infectious and/or cancer patients, tailored to their medical records and genetic backgrounds. Ongoing clinical trials are expected to generate new data to better decide on this matter (NCT03634293, NCT03869073, NCT04937413, NCT05128539, NCT04862260).

7 CONCLUSIONS

The aim of this doctoral research was to contribute to the better understanding of PCSK9 participation in diseases commonly related to lipid metabolism, such as pneumococcal infections and ovarian cancer. Up to date, the role of PCSK9 in bacterial infections has been explored with apparent contradictory results, whereas in ovarian cancer has been very little investigated.

Some of our initial hypotheses were confirmed, however further research is granted to clarify the participation of PCSK9 in that context, as well as to determine the best strategies to implement inhibitors or antibodies against PCSK9 in the clinic.

CRISPR/Cas9 is a precise gene-editing methodology for inducing mutations at target loci, minimizing deleterious off-target effects in zebrafish embryos.

In zebrafish, *pcsk9* is dispensable for correct neurogenesis during the early developmental stages, and its protein is dispensable for a protective host immune response against *Streptococcus pneumoniae* challenge. Noteworthy, the protein has a conserved immunoregulatory function on acute-phase reactant protein (APR) production by the liver. In Pcsk9-deficient zebrafish, upon a *Streptococcus pneumoniae* infection, the innate immune related genes are downregulated, whereas lipid-metabolism related genes are upregulated.

Both in humans and zebrafish, can be concluded that PCSK9 is upregulated upon systemic infections (higher in *Streptococcus pneumoniae* bacteraemia), and it resembles an acute-phase reactant *in vivo*.

Investigations on infectious' disease patients lead to conclude that PCSK9 expression correlates positively with CRP. Also, having lower upregulated levels of plasma PCSK9 correlates with a worse prognosis.

PCSK9 is secreted by human ovarian cancer cells (established cell lines and patient-derived cancer cell cultures), and it is detected at low levels in the patients' ascites fluids. When silencing PCSK9 (with siRNA or PCSK9-specific inhibitor PF-06446846), ovarian cancer cell survival is impaired suggesting that PCSK9 may play an anti-apoptotic role, via activation (at least partially) of intracellular AKT/ERK/MEK signalling. Also, OC subtypes have marked metabolic differences in their response to anti-metabolic and mTOR inhibitors that could be exploited in clinical practice.

8 ACKNOWLEDGEMENTS

Part of the research used patient samples. A special mention to their altruistic contributions, which bestow biomedical research with purpose, and sense of direction. Another part used zebrafishes, a living organism not a mere tool. Until science is not able to reproduce precise and more ethical alternatives, *paenitemus*.

Foremost, I want to express my deepest gratitude to my supervisors. First, Marko Pesu (MD, PhD) is warmly thanked for granting me the opportunity of joining his research group and for introducing me to work with such an interesting family of proteins. Thank you for your analytical insights, scientific discussions, and valuable time. Extended thanks to the Immunoregulation group members and office co-workers for all the driving force, feedback, and time: Markus Ojanen (PhD); Zsuzsanna Ortutay (PhD); Zuzet Martínez Córdova (PhD); Johanna Laakkonen (PhD Candidate); Giacomo Mantegazza (PhD Candidate); Fernanda Muñoz Caro (MSc); Noora Ranta (MD, PhD); Atte Valli (MD, PhD Candidate), and Pia Isomäki (MD, PhD, Docent). We have good times to remember, like when few of us did attend at 17th IUIS International Congress of Immunology in Beijing, China.

Second, my most sincere gratitude to Daniela Ungureanu (PhD, Associate Professor) for her scientific support, discussions, and her driven sense towards research. Words cannot stress enough; thanks for guiding my steps into the lab and occasionally into the woods. In

9 REFERENCES

(1). Abbas, M. B. A., Sarvenaz, S. R., Gotto, A. M., Pirro, M., Banach, M., Awan, Z., Barreto, G. E., & Sahebkar, A. (2019). PCSK9 and inflammation: a review of experimental and clinical evidence. *European Heart Journal. Cardiovascular Pharmacotherapy*, *5*(4), 237–245.

(2). Abbenante, G., & Fairlie, D. (2006). Protease Inhibitors in the Clinic. *Medicinal Chemistry*, *1*(1), 71–104. https://doi.org/10.2174/1573406053402569

(3). Abegaz, S. B. (2021). Human ABO Blood Groups and Their Associations with Different Diseases. *BioMed Research International*, *2021*. https://doi.org/10.1155/2021/6629060

(4). Abifadel, M., Varret, M., Rabès, J. P., Allard, D., Ouguerram, K., Devillers, M., Cruaud, C., Benjannet, S., Wickham, L., Erlich, D., Derré, A., Villéger, L., Farnier, M., Beucler, I., Bruckert, E., Chambaz, J., Chanu, B., Lecerf, J. M., Luc, G., … Boileau, C. (2003). Mutations in PCSK9 cause autosomal dominant hypercholesterolemia. *Nature Genetics*, *34*(2), 154–156. https://doi.org/10.1038/ng1161

(5). Adam, R. A., & Adam, Y. G. (2004). Malignant ascites: past, present, and future. *Journal of the American College of Surgeons*, *198*(6), 999–1011.

(6). Adli, M. (2018). The CRISPR tool kit for genome editing and beyond. *Nature Communications*, *9*(1). https://doi.org/10.1038/S41467-018-04252-2

(7). Ahmed, N., Greening, D., Samardzija, C., Escalona, R. M., Chen, M., Findlay, J. K., & Kannourakis, G. (2016). Unique proteome signature of post-chemotherapy ovarian cancer ascites-derived tumor cells. *Scientific Reports*, *6*. https://doi.org/10.1038/SREP30061

(8). Albiger, B., Dahlberg, S., Sandgren, A., Wartha, F., Beiter, K., Katsuragi, H., Akira, S., Normark, S., & Henriques-Normark, B. (2007). Toll-like receptor 9 acts at an early stage in host defence against pneumococcal infection. *Cellular Microbiology*, *9*(3), 633–644.

(9). Ali, M. Q., Kohler, T. P., Schulig, L., Burchhardt, G., & Hammerschmidt, S. (2021). Pneumococcal Extracellular Serine Proteases: Molecular Analysis and Impact on Colonization and Disease. *Frontiers in Cellular and Infection Microbiology*, *11*(November), 1–19.

(10). Aliprantis, A. O., Yang, R. B., Mark, M. R., Suggett, S., Devaux, B., Radolf, J. D., Klimpel, G. R., Godowski, P., & Zychlinsky, A. (1999). Cell activation and apoptosis by bacterial lipoproteins through toll-like receptor-2. *Science (New York, N.Y.)*, *285*(5428), 736–739.

(11). Almeida, C. R., Ferreira, B. H., & Duarte, I. F. (2021). Targeting PCSK9: a promising adjuvant strategy in cancer immunotherapy. *Signal Transduction and Targeted Therapy*, *6*(1).

(12). Altomare, D. A., Hui, Q. W., Skele, K. L., De Rienzo, A., Klein-Szanto, A. J., Godwin, A. K., & Testa, J. R. (2004). AKT and mTOR phosphorylation is frequently detected in ovarian cancer and can be targeted to disrupt ovarian tumor cell growth. *Oncogene*, *23*(34), 5853–5857. https://doi.org/10.1038/SJ.ONC.1207721

(13). Altschul, S. F., Madden, T. L., Schäffer, A. A., Zhang, J., Zhang, Z., Miller, W., & Lipman, D. J. (1997). Gapped BLAST and PSI-BLAST: a new generation of protein database search programs. *Oxford University Press*, *25*(17), 3389–3402.

(14). Amé, J. C., Spenlehauer, C., & De Murcia, G. (2004). The PARP superfamily. *BioEssays*, *26*(8), 882–893. https://doi.org/10.1002/bies.20085

(15). Arida, A., Legaki, A.I., Kravvariti, E., Protogerou, A., Sfikakis, P.P., & Chatzigeorgiou, A. (2021). PCSK9/LDLR System and Rheumatoid Arthritis-Related Atherosclerosis. *Frontiers in Cardiovascular Medicine, 8*:738764.

(16). Artenstein, A. W., & Opal, S. M. (2011). Proprotein convertases in health and disease. *New England Journal of Medicine*, *365*(26), 2507–2518. https://doi.org/10.1056/NEJMra1106700

(17). Artimo, P., Jonnalagedda, M., Arnold, K., Baratin, D., Csardi, G., De Castro, E., Duvaud, S., Flegel, V., Fortier, A., Gasteiger, E., Grosdidier, A., Hernandez, C., Ioannidis, V., Kuznetsov, D., Liechti, R., Moretti, S., Mostaguir, K., Redaschi, N., Rossier, G., … Stockinger, H. (2012). ExPASy: SIB bioinformatics resource portal. *Nucleic Acids Research*, *40*(W1), 597–603. https://doi.org/10.1093/nar/gks400

(18). Ashraf, Y., Duval, S., Sachan, V., Essalmani, R., Susan-Resiga, D., Roubtsova, A., Hamelin, J., Gerhardy, S., Kirchhofer, D., Tagliabracci, V. S., Prat, A., Kiss, R. S., & Seidah, N. G. (2020). Proprotein convertase 7 (PCSK7) reduces apoA-V levels. *FEBS Journal*, *287*(16), 3565–3578. https://doi.org/10.1111/febs.15212

(19). Atreya, M. R., Whitacre, B. E., Cvijanovich, N. Z., Bigham, M. T., Thomas, N. J., Schwarz, A. J., Weiss, S. L., Fitzgerald, J. C., Allen, G. L., Lutfi, R., Nowak, J. E., Quasney, M. W., Shah, A. S., & Wong, H. R. (2020). Proprotein Convertase Subtilisin/Kexin Type 9 Loss-of-Function Is Detrimental to the Juvenile Host With Septic Shock. *Critical Care Medicine*, *48*(10), 1513–1520. https://doi.org/10.1097/CCM.0000000000004487

(20). Awan, Z., Baass, A., & Genest, J. (2014). Proprotein convertase subtilisin/kexin type 9 (PCSK9): Lessons learned from patients with hypercholesterolemia. *Clinical Chemistry*, *60*(11), 1380–1389. https://doi.org/10.1373/clinchem.2014.225946

(21). Azzam, K. M., & Fessler, M. B. (2012). Crosstalk between reverse cholesterol transport and innate immunity. *Trends in Endocrinology and Metabolism: TEM*, *23*(4), 169–178.

(22). Badimon, L., Luquero, A., Crespo, J., Peña, E., & Borrell-Pages, M. (2021). PCSK9 and LRP5 in macrophage lipid internalization and inflammation. *Cardiovascular Research*, *117*(9), 2054–2068. https://doi.org/10.1093/cvr/cvaa254

(23). Barlage, S., Fröhlich, D., Böttcher, A., Jauhiainen, M., Müller, H. P., Noetzel, F., Rothe, G., Schütt, C., Linke, R. P., Lackner, K. J., Ehnholm, C., & Schmitz, G. (2001). ApoE-containing high density lipoproteins and phospholipid transfer protein activity increase in patients with a systemic inflammatory response. *Journal of Lipid Research*, *42*(2), 281–290.

(24). Barnett, K. C., & Kagan, J. C. (2020). Lipids that directly regulate innate immune signal transduction. *Innate Immunity*, *26*(1), 4–14. https://doi.org/10.1177/1753425919852695

(25). Bassi, D. E., Fu, J., De Cicco, R. L., & Klein-Szanto, A. J. P. (2005). Proprotein convertases: "Master switches" in the regulation of tumor growth and progression. *Molecular Carcinogenesis*, *44*(3), 151–161. https://doi.org/10.1002/mc.20134

(26). Bassi, D. E., Mahloogi, H., Al-Saleem, L., De Cicco, R. L., Ridge, J. A., & Klein-Szanto, A. J. P. (2001). Elevated furin expression in aggressive human head and neck tumors and tumor cell lines. *Molecular Carcinogenesis*, *31*(4), 224–232. https://doi.org/10.1002/mc.1057

(27). Benjannet, Suzanne, Rhainds, D., Essalmani, R., Mayne, J., Wickham, L., Jin, W., Asselin, M.-C. C., Hamelin, J. E., Varret, M., Allard, D., Lanie Trillard, M., Abifadel, M., Tebon, A., Attie, A. D., Rader, D. J., Boileau, C., Brissette, L., Chré, M., Prat, A., … Seidah, N. G. (2004). NARC-1/PCSK9 and its natural mutants: Zymogen cleavage and effects on the low density lipoprotein (LDL) receptor and LDL cholesterol. *Journal of Biological Chemistry*, *279*(47), 48865–48875. https://doi.org/10.1074/jbc.M409699200

(28). Benjannet, Suzanne, Rhainds, D., Hamelin, J., Nassoury, N., & Seidah, N. G. (2006). The proprotein convertase (PC) PCSK9 is inactivated by furin and/or PC5/6A: Functional consequences of natural mutations and post-translational modifications. *Journal of Biological Chemistry*, *281*(41), 30561–30572. https://doi.org/10.1074/jbc.M606495200

(29). Benn, M., Tybjærg-Hansen, A., Stender, S., Frikke-Schmidt, R., & Nordestgaard, B. G. (2011). Low-density lipoprotein cholesterol and the risk of cancer: A mendelian randomization study. *Journal of the National Cancer Institute*, *103*(6), 508–519.

(30). Bennett, D. L., Bailyes, E. M., Nielsen, E., Guest, P. C., Rutherford, N. G., Arden, S. D., &

Hutton, J. C. (1992). Identification of the type 2 proinsulin processing endopeptidase as PC2, a member of the eukaryote subtilisin family. *Journal of Biological Chemistry*, *267*(21), 15229–15236. https://doi.org/10.1016/s0021-9258(18)42170-9

(31). Berger, J. M., Valdes, A. L., Gromada, J., Anderson, N., & Horton, J. D. (2017). Inhibition of PCSK9 does not improve lipopolysaccharide-induced mortality in mice. *Journal of Lipid Research*, *58*(8), 1661–1669. https://doi.org/10.1194/JLR.M076844

(32). Bhat, M., Skill, N., Marcus, V., Deschenes, M., Tan, X., Bouteaud, J., Negi, S., Awan, Z., Aikin, R., Kwan, J., Amre, R., Tabaries, S., Hassanain, M., Seidah, N. G., Maluccio, M., Siegel, P., & Metrakos, P. (2015). Decreased PCSK9 expression in human hepatocellular carcinoma. *BMC Gastroenterology*, *15*(1). https://doi.org/10.1186/S12876-015-0371-6

(33). Bhattacharya, A., Chowdhury, A., Chaudhury, K., & Shukla, P. C. (2021). Proprotein convertase subtilisin/kexin type 9 (PCSK9): A potential multifaceted player in cancer. *Biochimica et Biophysica Acta. Reviews on Cancer*, *1876*(1), 188581.

(34). Bingham, B., Shen, R., Kotnis, S., Lo, C. F., Ozenberger, B. A., Ghosh, N., Kennedy, J. D., Jacobsen, J. S., Grenier, J. M., DiStefano, P. S., Chiang, L. W., & Wood, A. (2006). Proapoptotic effects of NARC 1, the gene encoding a novel serine proteinase. *Cytometry. Part A : The Journal of the International Society for Analytical Cytology*,*69*(11),1123–1131.

(35). Boyd, J. H., Fjell, C. D., Russell, J. A., Sirounis, D., Cirstea, M. S., & Walley, K. R. (2016). Increased Plasma PCSK9 Levels Are Associated with Reduced Endotoxin Clearance and the Development of Acute Organ Failures during Sepsis. *Journal of Innate Immunity*, *8*(2), 211–220. https://doi.org/10.1159/000442976

(36). Braicu, E. I., Darb-Esfahani, S., Schmitt, W. D., Koistinen, K. M., Heiskanen, L., Pöhö, P., Budczies, J., Kuhberg, M., Dietel, M., Frezza, C., Denkert, C., Sehouli, J., & Hilvo, M. (2017). High-grade ovarian serous carcinoma patients exhibit profound alterations in lipid metabolism. *Oncotarget*, *8*(61), 102912–102922. https://doi.org/10.18632/oncotarget.22076

(37). Brasseur, K., Gévry, N., & Asselin, E. (2017). Chemoresistance and targeted therapies in ovarian and endometrial cancers. *Oncotarget*, *8*(3), 4008–4042.

(38). Browning, J. D., & Horton, J. D. (2010). Fasting reduces plasma proprotein convertase, subtilisin/kexin type 9 and cholesterol biosynthesis in humans. *Journal of Lipid Research*, *51*(11), 3359–3363. https://doi.org/10.1194/jlr.P009860

(39). Camera, M., Rossetti, L., Barbieri, S. S., Zanotti, I., Canciani, B., Trabattoni, D., Ruscica, M., Tremoli, E., & Ferri, N. (2018). PCSK9 as a Positive Modulator of Platelet Activation. *Journal of the American College of Cardiology*, *71*(8), 952–954.

(40). Cameron, J., Holla, Ø. L., Berge, K. E., Kulseth, M. A., Ranheim, T., Leren, T. P., & Laerdahl, J. K. (2008). Investigations on the evolutionary conservation of PCSK9 reveal a functionally important protrusion. *The FEBS Journal*, *275*(16), 4121–4133.

(41). Cariou, B., Le May, C., & Costet, P. (2011). Clinical aspects of PCSK9. *Atherosclerosis*, *216*(2), 258–265. //doi.org/10.1016/j.atherosclerosis.2011.04.018

(42). Cera, E. Di. (2009). Serine Proteases. *International Union of Biochemistry and Molecular Biology Life*, *61*(5), 510–515. https://doi.org/10.1002/iub.186.Serine

(43). Cesaro, A., Bianconi, V., Gragnano, F., Moscarella, E., Fimiani, F., Monda, E., Scudiero, O., Limongelli, G., Pirro, M., & Calabrò, P. (2020). Beyond cholesterol metabolism: The pleiotropic effects of proprotein convertase subtilisin/kexin type 9 (PCSK9). Genetics, mutations, expression, and perspective for long-term inhibition. *BioFactors*, *46*(3), 367–380.

(44). Chaplin, D. D. (2010). Overview of the immune response. *The Journal of Allergy and Clinical Immunology*, *125*(2 Suppl 2). https://doi.org/10.1016/J.JACI.2009.12.980

(45). Chen, Y. Q., Troutt, J. S., & Konrad, R. J. (2014). PCSK9 is present in human cerebrospinal fluid and is maintained at remarkably constant concentrations throughout the course of the day. *Lipids*, *49*(5), 445–455. https://doi.org/10.1007/s11745-014-3895-6

(46). Cho, S. W., Kim, S., Kim, J. M., & Kim, J. S. (2013). Targeted genome engineering in

human cells with the Cas9 RNA-guided endonuclease. *Nature Biotechnology*, *31*(3), 230–232.

(47). Cho, S. W., Kim, S., Kim, Y., Kweon, J., Kim, H. S., Bae, S., & Kim, J. S. (2014). Analysis of off-target effects of CRISPR/Cas-derived RNA-guided endonucleases and nickases. *Genome Research*, *24*(1), 132–141. https://doi.org/10.1101/GR.162339.113

(48). Chrétien, M., Benjannet, S., Lazure, C., & Seidah, N. G. (1983). Biosynthesis of hormonal and neural peptides. *Transactions of the American Clinical and Climatological Association*, *95*, 19–25.

(49). Christie, E. L., & Bowtell, D. D. L. (2017). Acquired chemotherapy resistance in ovarian cancer. *Annals of Oncology : Official Journal of the European Society for Medical Oncology*, *28*(suppl_8), viii13–viii15. https://doi.org/10.1093/ANNONC/MDX446

(50). Ciesielska, A., Matyjek, M., & Kwiatkowska, K. (2021). TLR4 and CD14 trafficking and its influence on LPS-induced pro-inflammatory signaling. *Cellular and Molecular Life Sciences : CMLS*, *78*(4), 1233–1261. https://doi.org/10.1007/S00018-020-03656-Y

(51). Clark, R., Krishnan, V., Schoof, M., Rodriguez, I., Theriault, B., Chekmareva, M., & Rinker-Schaeffer, C. (2013). Milky spots promote ovarian cancer metastatic colonization of peritoneal adipose in experimental models. *The American Journal of Pathology*, *83*(2), 576–591.

(52). Cornel, A. M., Mimpen, I. L., & Nierkens, S. (2020). MHC Class I Downregulation in Cancer: Underlying Mechanisms and Potential Targets for Cancer Immunotherapy. *Cancers*, *12*(7), 1–33. https://doi.org/10.3390/CANCERS12071760

(53). Costet, P., Cariou, B., Lambert, G., Lalanne, F., Lardeux, B., Jarnoux, A. L., Grefhorst, A., Staels, B., & Krempf, M. (2006). Hepatic PCSK9 expression is regulated by nutritional status via insulin and sterol regulatory element-binding protein 1c. *Journal of Biological Chemistry*, *281*(10), 6211–6218. https://doi.org/10.1074/jbc.M508582200

(54). Creemers, J. W. M., & Khatib, A. M. (2008). Knock-out mouse models of proprotein convertases: Unique functions or redundancy? *Frontiers in Bioscience*, *13*(13), 4960–4971.

(55). Creemers, J. W. M., Roebroek, A. J. M., & Van de Ven, W. J. M. (1992). Expression in human lung tumor cells of the proprotein processing enzyme PC1/PC3 Cloning and primary sequence of a 5 kb cDNA. *FEBS Letters*, *300*(1), 82–88.

(56). Crunkhorn, S. (2021). Blocking PCSK9 enhances immune checkpoint therapy. *Nature Reviews. Drug Discovery*, *20*(1), 20. https://doi.org/10.1038/D41573-020-00208-8

(57). Cruz, P. M. R., Mo, H., McConathy, W. J., Sabnis, N., & Lacko, A. G. (2013). The role of cholesterol metabolism and cholesterol transport in carcinogenesis: a review of scientific findings, relevant to future cancer therapeutics. *Frontiers in Pharmacology*, *4*.

(58). Cunningham, D., Danley, D. E., Geoghegan, K. F., Griffor, M. C., Hawkins, J. L., Subashi, T. A., Varghese, A. H., Ammirati, M. J., Culp, J. S., Hoth, L. R., Mansour, M. N., McGrath, K. M., Seddon, A. P., Shenolikar, S., Stutzman-Engwall, K. J., Warren, L. C., Xia, D., & Qiu, X. (2007). Structural and biophysical studies of PCSK9 and its mutants linked to familial hypercholesterolemia. *Nature Structural and Molecular Biology*, *14*(5), 413–419.

(59). Cyranoski, D. (2016). Chinese scientists to pioneer first human CRISPR trial. *Nature*, *535*(7613), 476–477. https://doi.org/10.1038/NATURE.2016.20302

(60). D'Anjou, F., Routhier, S., Perreault, J. P., Latil, A., Bonnel, D., Fournier, I., Salzet, M., & Day, R. (2011). Molecular validation of pace4 as a target in prostate cancer. *Translational Oncology*, *4*(3), 157–172. https://doi.org/10.1593/tlo.10295

(61). Dahril, A., Keumala, V., & Mustafa, A.(2019). Human spermatozoa anti-proprotein convertase subtilisin/kexin type 4 synthesis using New Zealand rabbit for novel immunocontraception in males. *Investigative and Clinical Urology*, *60*(4):303-311.

(62). Danilova, N., Bussmann, J., Jekosch, K., & Steiner, L. A. (2005). The immunoglobulin heavy-chain locus in zebrafish: identification and expression of a previously unknown isotype, immunoglobulin Z. *Nature Immunology*, *6*(3), 295–302.

(63). Davignin, J., & Dubuc, G. (2009). Statins and ezetimibe modulate plasma proprotein convertase subtilisin kexin-9 (PCSK9) levels. *Transactions of the American Clinical and*

Climatological Association, *120*, 163–173.

(64). de Zoeten, E.F., Lee, I., Wang, L., Chen, C., Ge, G., Wells, A.D., Hancock, W.W., & Ozkaynak, E. (2009). Foxp3 processing by proprotein convertases and control of regulatory T cell function. *Journal of Biological Chemistry, 284*(9):5709-16.

(65). Decroly, E., Benjannet, S., Savaria, D., & Seidah, N.G. (1997). Comparative functional role of PC7 and furin in the processing of the HIV envelope glycoprotein gp160. *FEBS Letters, 405*(1):68-72. https://doi.org/10.1016/s0014-5793(97)00156-7.

(66). Demers, A., Samami, S., Lauzier, B., Des Rosiers, C., Tudor Ngo Sock, E., Ong, H., & Mayer, G. (2015). PCSK9 induces CD36 degradation and affects long-chain fatty acid uptake and triglyceride metabolism in adipocytes and in mouse liver. *Arterioscler Thromb Vasc Biol.*, *35*, 2517–2525. https://doi.org/DOI: 10.1161/ATVBAHA.115.306032

(67). Denis, M., Marcinkiewicz, J., Zaid, A., Gauthier, D., Poirier, S., Lazure, C., Seidah, N. G., & Prat, A. (2012). Gene inactivation of proprotein convertase subtilisin/kexin type 9 reduces atherosclerosis in mice. *Circulation*, *125*(7), 894–901.

(68). Dewpura, T., Raymond, A., Hamelin, J., Seidah, N. G., Mbikay, M., Chrétien, M., & Mayne, J. (2008). PCSK9 is phosphorylated by a Golgi casein kinase-like kinase ex vivo and circulates as a phosphoprotein in humans. *FEBS Journal*, *275*(13), 3480–3493. https://doi.org/10.1111/j.1742-4658.2008.06495.x

(69). Dobbin, Z. C., & Landen, C. N. (2013). The importance of the PI3K/AKT/MTOR pathway in the progression of ovarian cancer. *International Journal of Molecular Sciences*, *14*(4), 8213–8227. https://doi.org/10.3390/IJMS14048213

(70). Dobin, A., Davis, C. A., Schlesinger, F., Drenkow, J., Zaleski, C., Jha, S., Batut, P., Chaisson, M., & Gingeras, T. R. (2013). STAR: Ultrafast universal RNA-seq aligner. *Bioinformatics*, *29*(1), 15–21. https://doi.org/10.1093/bioinformatics/bts635

(71). Dong, B., Wu, M., Li, H., Kraemer, F. B., Adeli, K., Seidah, N. G., Park, S. W., & Liu, J. (2010). Strong induction of PCSK9 gene expression through HNF1α and SREBP2: Mechanism for the resistance to LDL-cholesterol lowering effect of statins in dyslipidemic hamsters. *Journal of Lipid Research*, *51*(6), 1486–1495. https://doi.org/10.1194/jlr.M003566

(72). Dos Santos, C., & Marshall, J. C. (2014). Bridging lipid metabolism and innate host defense. *Science Translational Medicine*, *6*(258), 258fs41.

(73). Doubeni, C. A., Doubeni, A. R., & Myers, A. E. (2016). Diagnosis and Management of Ovarian Cancer. *American Family Physician*, *93*(11), 937–944.

(74). Druce, I., Abujrad, H., Chaker, S., Meggison, H., Hill, A., Raymond, A., Mayne, J., & Ooi, T. C. (2018). Circulating PCSK9 is lowered acutely following surgery. *Journal of Clinical Laboratory Analysis*, *32*(4). https://doi.org/10.1002/JCLA.22358

(75). Dubois, C. M., Blanchette, F., Laprise, M.-H., Leduc, R., Grondin, F., & Seidah, and N. G. (2001). Evidence that Furin Is an Authentic Transforming Growth Factor-β1-Converting Enzyme. *American Journal of Pathology*, *158*(1), 305–316.

(76). Dubuc, G., Chamberland, A., Wassef, H., Davignon, J., Seidah, N. G., Bernier, L., & Prat, A. (2004). Statins upregulate PCSK9, the gene encoding the proprotein convertase neural apoptosis-regulated convertase-1 implicated in familial hypercholesterolemia. *Arteriosclerosis, Thrombosis, and Vascular Biology*, *24*(8), 1454–1459.

(77). Dubuc, G., Tremblay, M., Paré, G., Jacques, H., Hamelin, J., Benjannet, S., Boulet, L., Genest, J., Bernier, L., Seidah, N. G., & Davignon, J. (2010). A new method for measurement of total plasma PCSK9: clinical applications. *Journal of Lipid Research*, *51*(1), 140–149. https://doi.org/10.1194/JLR.M900273-JLR200

(78). Duckert, P., Brunak, S., & Blom, N. (2004). Prediction of proprotein convertase cleavage sites. *Protein Engineering, Design and Selection*, *17*(1), 107–112.

(79). Duhamel, M., Rodet, F., Delhem, N., Vanden Abeele, F., Kobeissy, F., Nataf, S., Pays, L., Desjardins, R., Gagnon, H., Wisztorski, M., Fournier, I., Day, R., & Salzet, M. (2015).

Molecular Consequences of Proprotein Convertase 1/3 (PC1/3) Inhibition in Macrophages for Application to Cancer Immunotherapy: A Proteomic Study. *Molecular & Cellular Proteomics : MCP*, *14*(11), 2857–2877. https://doi.org/10.1074/MCP.M115.052480

(80). Duhamel, M., Rodet, F., Murgoci, A.N., Desjardins, R., Gagnon, H., Wisztorski, M., Fournier, I., Day, R., & Salzet, M. (2016). The proprotein convertase PC1/3 regulates TLR9 trafficking and the associated signaling pathways. *Scientific Reports, 18* (6):19360.

(81). Dunn, E., Chitcholtan, K., Sykes, P., & Garrill, A. (2022). The Anti-Proliferative Effect of PI3K/mTOR and ERK Inhibition in Monolayer and Three-Dimensional Ovarian Cancer Cell Models. *Cancers*, *14*(2). https://doi.org/10.3390/CANCERS14020395

(82). Durinck, S., Spellman, P. T., Birney, E., & Huber, W. (2009). Mapping Identifiers for the Integration of Genomic Datasets with the R/Bioconductor package biomaRt. *Bone*, *4*(8), 1184–1191. https://doi.org/10.1038/nprot.2009.97

(83). Düvel, K., Yecies, J. L., Menon, S., Raman, P., Lipovsky, A. I., Souza, A. L., Triantafellow, E., Ma, Q., Gorski, R., Cleaver, S., Vander Heiden, M. G., MacKeigan, J. P., Finan, P. M., Clish, C. B., Murphy, L. O., & Manning, B. D. (2010). Activation of a metabolic gene regulatory network downstream of mTOR complex 1. *Molecular Cell*, *39*(2), 171–183.

(84). Dwivedi, D. J., Grin, P. M., Khan, M., Prat, A., Zhou, J., Fox-Robichaud, A. E., Seidah, N. G., & Liaw, P. C. (2016). Differential Expression of PCSK9 Modulates Infection, Inflammation, and Coagulation in a Murine Model of Sepsis. *Shock (Augusta, Ga.)*, *46*(6), 672–680. https://doi.org/10.1097/SHK.0000000000000682

(85). Eberlé, D., Hegarty, B., Bossard, P., Ferré, P., & Foufelle, F. (2004). SREBP transcription factors: master regulators of lipid homeostasis. *Biochimie*, *86*(11), 839–848.

(86). Eden, E., Lipson, D., Yogev, S., & Yakhini, Z. (2007). Discovering motifs in ranked lists of DNA sequences. *PLoS Computational Biology*, *3*(3), 0508–0522. https://doi.org/10.1371/journal.pcbi.0030039

(87). Eden, E., Navon, R., Steinfeld, I., Lipson, D., & Yakhini, Z. (2009). GOrilla: A tool for discovery and visualization of enriched GO terms in ranked gene lists. *BMC Bioinformatics*, *10*, 1–7. https://doi.org/10.1186/1471-2105-10-48

(88). Ediriweera, M. K., Tennekoon, K. H., & Samarakoon, S. R. (2019). Role of the PI3K/AKT/mTOR signaling pathway in ovarian cancer: Biological and therapeutic significance. *Seminars in Cancer Biology*, *59*, 147–160. https://doi.org/10.1016/J.SEMCANCER.2019.05.012

(89). Endo, A. (2010). A historical perspective on the discovery of statins. *Proceedings of the Japan Academy Series B: Physical and Biological Sciences*, *86*(5), 484–493.

(90). Essalmani, R., Susan-Resiga, D., Chamberland, A., Abifadel, M., Creemers, J. W., Boileau, C., Seidah, N. G., & Prat, A. (2011). In vivo evidence that furin from hepatocytes inactivates PCSK9. *Journal of Biological Chemistry*, *286*(6), 4257–4263.

(91). Feingold, K. R., Moser, A. H., Shigenaga, J. K., Patzek, S. M., & Grunfeld, C. (2008). Inflammation stimulates the expression of PCSK9. *Biochemical and Biophysical Research Communications*, *374*(2), 341–344. https://doi.org/10.1016/J.BBRC.2008.07.023

(92). Ferri, N., Tibolla, G., Pirillo, A., Cipollone, F., Mezzetti, A., Pacia, S., Corsini, A., & Catapano, A. L. (2012). Proprotein convertase subtilisin kexin type 9 (PCSK9) secreted by cultured smooth muscle cells reduces macrophages LDLR levels. *Atherosclerosis*, *220*(2), 381–386. https://doi.org/10.1016/J.ATHEROSCLEROSIS.2011.11.026

(93). Folsom, A. R., Peacock, J. M., & Boerwinkle, E. (2007). Sequence variation in proprotein convertase subtilisin/kexin type 9 serine protease gene, low LDL cholesterol, and cancer incidence. *Cancer Epidemiology Biomarkers and Prevention*, *16*(11), 2455–2458.

(94). Ford, C. E., Werner, B., Hacker, N. F., & Warton, K. (2020). The untapped potential of ascites in ovarian cancer research and treatment. *British Journal of Cancer*, *123*(1), 9–16.

(95). Foster, H., Coley, H. M., Goumenou, A., Pados, G., Harvey, A., & Karteris, E. (2010).

Differential expression of mTOR signalling components in drug resistance in ovarian cancer. *Anticancer Research*, *30*(9), 3529–3534.

(96). François, M., Thédrez, A., Garçon, D., Ayer, A., Sotin, T., Dijk, W., Blanchard, C., Chadeuf, G., Arnaud, L., Croyal, M., van Landeghem, L., Touvron, M., Prieur, X., Roubtsova, A., Seidah, N., Prat, A., Cariou, B., & Le May, C. (2021). PCSK9 is not secreted from mature differentiated intestinal cells. *Journal of Lipid Research*, *62*.

(97). Gangloff, A., Calon, F., & Seidah, N. G. (2017). Can iPCSK9-induced hypocholesterolemia starve cancer cells? *Journal of Clinical Lipidology*, *11*(3), 600–601.

(98). Gao, Y., Qiu, Y., Wu, J., Diao, W., Zhang, H., Wang, S., Du, Z., Dong, J., Zhang, M., & Jiang, L. (2018). Acute-Phase Plasma PCSK9 Levels and Recurrent Cardiovascular Events in a Chinese Acute Myocardial Infarction Cohort. *Cardiology*, *141*(2), 88–97.

(99). Gaona-Luviano, P., Adriana, L., Medina-Gaona, & Magaña-Pérez, K. (2020). Epidemiology of ovarian cancer. *Chinese Clinical Oncology*, *9*(4).

(100). Gasparri, M. L., Bardhi, E., Ruscito, I., Papadia, A., Farooqi, A. A., Marchetti, C., Bogani, G., Ceccacci, I., Mueller, M. D., & Benedetti Panici, P. (2017). PI3K/AKT/mTOR Pathway in Ovarian Cancer Treatment: Are We on the Right Track? *Geburtshilfe Und Frauenheilkunde*, *77*(10), 1095–1103. https://doi.org/10.1055/S-0043-118907

(101). Gortzak-Uzan, L., Ignatchenko, A., Evangelou, A. I., Agochiya, M., Brown, K. A., St.Onge, P., Kireeva, I., Schmitt-Ulms, G., Brown, T. J., Murphy, J., Rosen, B., Shaw, P., Jurisica, I., & Kislinger, T. (2008). A proteome resource of ovarian cancer ascites: integrated proteomic and bioinformatic analyses to identify putative biomarkers. *Journal of Proteome Research*, *7*(1), 339–351. https://doi.org/10.1021/PR0703223

(102). Gil-Torregrosa, B.C., Castaño, A.R., López, D., & Del Val, M. (2000). Generation of MHC class I peptide antigens by protein processing in the secretory route by furin. *Traffic, 1*(8):641-51. https://doi.org/10.1034/j.1600-0854.2000.010808.x.

(103). Grin, P. M., Dwivedi, D. J., Chathely, K. M., Trigatti, B. L., Prat, A., Seidah, N. G., Liaw, P. C., & Fox-Robichaud, A. E. (2018). Low-density lipoprotein (LDL)-dependent uptake of Gram-positive lipoteichoic acid and Gram-negative lipopolysaccharide occurs through LDL receptor. *Scientific Reports*, *8*(1). https://doi.org/10.1038/S41598-018-28777-0

(104). Guillemot, J., Canuel, M., Essalmani, R., Prat, A., & Seidah, N.G. (2013). Implication of the proprotein convertases in iron homeostasis: proprotein convertase 7 sheds human transferrin receptor 1 and furin activates hepcidin. *Hepatology, 57*(6):2514-24.

(105). Gu, H. M., Adijiang, A., Mah, M., & Zhang, D. W. (2013). Characterization of the role of EGF-A of low density lipoprotein receptor in PCSK9 binding. *Journal of Lipid Research*, *54*(12), 3345–3357. https://doi.org/10.1194/jlr.M041129

(106). Han, B., Eacho, P. I., Knierman, M. D., Troutt, J. S., Konrad, R. J., Yu, X., & Schroeder, K. M. (2014). Isolation and characterization of the circulating truncated form of PCSK9. *Journal of Lipid Research*, *55*(7), 1505–1514. https://doi.org/10.1194/JLR.M049346

(107). Hanahan, D. (2000). The Hallmarks of Cancer. *Cell*, *100*, 57–70.

(108). Hanahan, D., & Weinberg, R. A. (2011). Hallmarks of cancer: The next generation. *Cell*, *144*(5), 646–674. https://doi.org/10.1016/j.cell.2011.02.013

(109). He, M., Hu, J., Fang, T., Tang, W., Lv, B., Yang, B., & Xia, J. (2021). Protein convertase subtilisin/Kexin type 9 inhibits hepatocellular carcinoma growth by interacting with GSTP1 and suppressing the JNK signaling pathway. *Cancer Biology & Medicine*, *19*(1), 90–103. https://doi.org/10.20892/J.ISSN.2095-3941.2020.0313

(110). Hedstrom, L. (2002). Serine protease mechanism and specificity. *Chemical Reviews*, *102*(12), 4501–4523. https://doi.org/10.1021/cr000033x

(111). Henriques-Normark, B., & Normark, S. (2010). Commensal pathogens, with a focus on Streptococcus pneumoniae, and interactions with the human host. *Experimental Cell Research*, *316*(8), 1408–1414. https://doi.org/10.1016/j.yexcr.2010.03.003

(112).   Hipp, M. M., Shepherd, D., Gileadi, U., Aichinger, M. C., Kessler, B. M., Edelmann, M. J., Essalmani, R., Seidah, N. G., Reisesousa, C., & Cerundolo, V. (2013). Processing of human toll-like receptor 7 by furin-like proprotein convertases is required for its accumulation and activity in endosomes. *Immunity*, *39*(4), 711–721.

(113).   Hoebe, K., Georgel, P., Rutschmann, S., Du, X, Mudd, S., Crozat, K., Sovath, S., Shamel, L., Hartung, T., Zähringer, U., & Beutler, B. (2005). CD36 is a sensor of diacylglycerides. *Nature*, *433*(7025), 523–527. https://doi.org/10.1038/NATURE03253

(114).   Horimoto, T., Nakayama, K., Smeekens, S.P., Kawaoka, Y. (1994). Proprotein-processing endoproteases PC6 and furin both activate hemagglutinin of virulent avian influenza viruses. *Journal of Virology, 68*(9):6074-8.

(115).   Holla, Ø. L., Cameron, J., Tveten, K., Strøm, T. B., Berge, K. E., Laerdahl, J. K., & Leren, T. P. (2011). Role of the C-terminal domain of PCSK9 in degradation of the LDL receptors. *Journal of Lipid Research*, *52*(10), 1787. https://doi.org/10.1194/JLR.M018093

(116).   Horton, J. D., Shah, N. A., Warrington, J. A., Anderson, N. N., Park, S. W., Brown, M. S., & Goldstein, J. L. (2003). Combined analysis of oligonucleotide microarray data from transgenic and knockout mice identifies direct SREBP target genes. *Proceedings of the National Academy of Sciences of the United States of America*, *100*(21), 12027–12032.

(117).   Howe, K., Clark, M. D., Torroja, C. F., Torrance, J., Berthelot, C., Muffato, M., Collins, J. E., Humphray, S., McLaren, K., Matthews, L., McLaren, S., Sealy, I., Caccamo, M., Churcher, C., Scott, C., Barrett, J. C., Koch, R., Rauch, G. J., White, S., … Stemple, D. L. (2013). The zebrafish reference genome sequence and its relationship to the human genome. *Nature*, *496*(7446), 498–503. https://doi.org/10.1038/NATURE12111

(118).   Hruscha, A., & Schmid, B. (2015). Generation of zebrafish models by CRISPR /Cas9 genome editing. *Methods in Molecular Biology (Clifton, N.J.)*, *1254*, 341–350.

(119).   Huttunen, R., Syrjänen, J., Aittoniemi, J., Oja, S. S., Raitala, A., Laine, J., Pertovaara, M., Vuento, R., Huhtala, H., & Hurme, M. (2010). High activity of indoleamine 2,3 dioxygenase enzyme predicts disease severity and case fatality in bacteremic patients. *Shock*, *33*(2), 149–154. https://doi.org/10.1097/SHK.0b013e3181ad3195

(120).   Innocenti, F., Gori, A. M., Giusti, B., Tozzi, C., Donnini, C., Meo, F., Giacomelli, I., Ralli, M. L., Sereni, A., Sticchi, E., Tassinari, I., Marcucci, R., & Pini, R. (2021). Plasma PCSK9 levels and sepsis severity: an early assessment in the emergency department. *Clinical and Experimental Medicine*, *21*(1), 101–107. https://doi.org/10.1007/S10238-020-00658-9

(121).   Ito, H., Nozaki, K., Sakimura, K., Abe, M., Yamawaki, S., & Aizawa, H. (2021). Activation of proprotein convertase in the mouse habenula causes depressive-like behaviors through remodeling of extracellular matrix. *Neuropsychopharmacology,46*(2):442-454.

(122).   Jablonski, N. G., & Chaplin, G. (2000). The evolution of human skin coloration. *Journal of Human Evolution*, *39*(1), 57–106. https://doi.org/10.1006/JHEV.2000.0403

(123).   Jang, H. D., Lee, S. E., Yang, J., Lee, H. C., Shin, D., Lee, H., Lee, J., Jin, S., Kim, S., Lee, S. J., You, J., Park, H. W., Nam, K. Y., Lee, S. H., Park, S. W., Kim, J. S., Kim, S. Y., Kwon, Y. W., Kwak, S. H., & Kim, H. S. (2020). Cyclase-associated protein 1 is a binding partner of proprotein convertase subtilisin/kexin type-9 and is required for the degradation of low-density lipoprotein receptors by proprotein convertase subtilisin/kexin type-9. *European Heart Journal*, *41*(2), 239–252. https://doi.org/10.1093/eurheartj/ehz566

(124).   Jim, K. K., Engelen-Lee, J. Y., van der Sar, A. M., Bitter, W., Brouwer, M. C., van der Ende, A., Veening, J. W., van de Beek, D., & Vandenbroucke-Grauls, C. M. J. E. (2016). Infection of zebrafish embryos with live fluorescent Streptococcus pneumoniae as a real-time pneumococcal meningitis model. *Journal of Neuroinflammation*, *13*(1).

(125).   Kadioglu, A., Weiser, J. N., Paton, J. C., & Andrew, P. W. (2008). The role of Streptococcus pneumoniae virulence factors in host respiratory colonization and disease. *Nature Reviews. Microbiology*, *6*(4), 288–301. https://doi.org/10.1038/NRMICRO1871

(126).   Kanehisa, M., Goto, S., Furumichi, M., Tanabe, M., & Hirakawa, M. (2009). KEGG for representation and analysis of molecular networks involving diseases and drugs. *Nucleic Acids Research*, *38*(SUPPL.1), 355–360. https://doi.org/10.1093/nar/gkp896

(127).   Kawai, T., & Akira, S. (2010). The role of pattern-recognition receptors in innate immunity: update on Toll-like receptors. *Nature Immunology*, *11*(5), 373–384.

(128).   Keij, F. M., Koch, B. E. V., Lozano Vigario, F., Simons, S. H. P., van Hasselt, J. G. C., Taal, H. R., Knibbe, C. A. J., Spaink, H. P., Reiss, I. K. M., & Krekels, E. H. J. (2021). Zebrafish larvae as experimental model to expedite the search for new biomarkers and treatments for neonatal sepsis. *Journal of Clinical and Translational Science*, *5*(1).

(129).   Khatib, A. M., Siegfried, G., Chrétien, M., Metrakos, P., & Seidah, N. G. (2002). Proprotein convertases in tumor progression and malignancy: Novel targets in cancer therapy. *American Journal of Pathology*, *160*(6), 1921–1935.

(130).   Koppe, U., Suttorp, N., & Opitz, B. (2012). Recognition of Streptococcus pneumoniae by the innate immune system. *Cellular Microbiology*, *14*(4), 460–466.

(131).   Korneva, V., Kuznetsova, T., & Julius, U. (2021). The State of the Problem of Achieving Extremely Low LDL Levels. *Current Pharmaceutical Design*, *27*(37).

(132).   Köster, J., & Rahmann, S. (2012). Snakemake-a scalable bioinformatics workflow engine. *Bioinformatics*, *28*(19), 2520–2522. https://doi.org/10.1093/bioinformatics/bts480

(133).   Kuyama, N., Kataoka, Y., Takegami, M., Nishimura, K., Harada-Shiba, M., Hori, M., Ogura, M., Otsuka, F., Asaumi, Y., Noguchi, T., Tsujita, K., & Yasuda, S. (2021). Circulating Mature PCSK9 Level Predicts Diminished Response to Statin Therapy. *Journal of the American Heart Association*, *10*(11). https://doi.org/10.1161/JAHA.120.019525

(134).   Kwok, S. C. M., Chakraborty, D., Soares, M. J., & Dai, G. (2013). Relative expression of proprotein convertases in rat ovaries during pregnancy. *Journal of Ovarian Research*, *6*(1).

(135).   Kysenius, K., Muggalla, P., Mätlik, K., Arumäe, U., & Huttunen, H. J. (2012). PCSK9 regulates neuronal apoptosis by adjusting ApoER2 levels and signaling. *Cellular and Molecular Life Sciences : CMLS*, *69*(11), 1903–1916.

(136).   Labonté, P., Begley, S., Guévin, C., Asselin, M.C., Nassoury, N., Mayer, G., Prat, A., & Seidah, N.G. (2009). PCSK9 impedes hepatitis C virus infection in vitro and modulates liver CD81 expression. *Hepatology, 50*(1):17-24. https://doi.org/10.1002/hep.22911.

(137).   Labun, K., Montague, T. G., Gagnon, J. A., Thyme, S. B., & Valen, E. (2016). CHOPCHOP v2: a web tool for the next generation of CRISPR genome engineering. *Nucleic Acids Research*, *44*(W1), W272–W276. https://doi.org/10.1093/NAR/GKW398

(138).   Lakoski, S. G., Lagace, T. A., Cohen, J. C., Horton, J. D., & Hobbs, H. H. (2009). Genetic and metabolic determinants of plasma PCSK9 levels. *Journal of Clinical Endocrinology and Metabolism*, *94*(7), 2537–2543. https://doi.org/10.1210/jc.2009-0141

(139).   Lansac, G., Dong, W., Dubois, C. M., BenLarbi, N., Afonso, C., Fournier, I., Salzet, M., & Day, R. (2006). Lipopolysaccharide mediated regulation of neuroendocrine associated proprotein convertases and neuropeptide precursor processing in the rat spleen. *Journal of Neuroimmunology*, *171*(1–2), 57–71.

(140).   Le Bras, M., Roquilly, A., Deckert, V., Langhi, C., Feuillet, F., Sébille, V., Mahé, P. J., Bach, K., Masson, D., Lagrost, L., Costet, P., Asehnoune, K., & Cariou, B. (2013). Plasma PCSK9 is a late biomarker of severity in patients with severe trauma injury. *The Journal of Clinical Endocrinology and Metabolism*, *98*(4). https://doi.org/10.1210/JC.2012-4236

(141).   Le, Q. T., Blanchet, M., Seidah, N. G., & Labonté, P. (2015). Plasma membrane tetraspanin CD81 complexes with proprotein convertase subtilisin/kexin type 9 (PCSK9) and low density lipoprotein receptor (LDLR), and Its levels are reduced by PCSK9. *Journal of Biological Chemistry*, *290*(38), 23385–23400. https://doi.org/10.1074/jbc.M115.642991

(142).   Lebeau, P. F., Byun, J. H., Platko, K., Saliba, P., Sguazzin, M., MacDonald, M. E., Paré, G., Steinberg, G. R., Janssen, L. J., Igdoura, S. A., Tarnopolsky, M. A., Wayne Chen,

S. R., Seidah, N. G., Magolan, J., & Austin, R. C. (2022). Caffeine blocks SREBP2-induced hepatic PCSK9 expression to enhance LDLR-mediated cholesterol clearance. *Nature Communications*, *13*(1). https://doi.org/10.1038/s41467-022-28240-9

(143). Lee, S. H., Park, M. S., Park, B. H., Jung, W. J., Lee, I. S., Kim, S. Y., Kim, E. Y., Jung, J. Y., Kang, Y. A., Kim, Y. S., Kim, S. K., Chang, J., & Chung, K. S. (2015). Prognostic Implications of Serum Lipid Metabolism over Time during Sepsis. *BioMed Research International*, *2015*. https://doi.org/10.1155/2015/789298

(144). Lee, W. J., Ko, S. Y., Mohamed, M. S., Kenny, H. A., Lengyel, E., & Naora, H. (2019). Neutrophils facilitate ovarian cancer premetastatic niche formation in the omentum. *The Journal of Experimental Medicine*, *216*(1), 176–194. https://doi.org/10.1084/JEM.20181170

(145). Lei, L., Li, X., Yuan, Y. J., Chen, Z. L., He, J. H., Wu, J. H., & Cai, X. S. (2020). Inhibition of proprotein convertase subtilisin/kexin type 9 attenuates 2,4,6-trinitrobenzenesulfonic acid-induced colitis via repressing toll-like receptor 4/nuclear factor-kappa B. *Kaohsiung Journal of Medical Sciences*, *36*(9), 705–711.

(146). Leonhardt, R.M., Fiegl, D., Rufer, E., Karger, A., Bettin, B., & Knittler, M.R. (2010). Post-endoplasmic reticulum rescue of unstable MHC class I requires proprotein convertase PC7. *Journal of Immunology,184*(6):2985-98. https://doi.org/10.4049/jimmunol.0900308.

(147). Lepor, N. E., & Kereiakes, D. J. (2015). The PCSK9 Inhibitors: A Novel Therapeutic Target Enters Clinical Practice. *American Health & Drug Benefits*, *8*(9), 483–489.

(148). Leung, A. K. K., Genga, K. R., Topchiy, E., Cirstea, M., Shimada, T., Fjell, C., Russell, J. A., Boyd, J. H., & Walley, K. R. (2019). Reduced Proprotein convertase subtilisin/kexin 9 (PCSK9) function increases lipoteichoic acid clearance and improves outcomes in Gram positive septic shock patients. *Scientific Reports*, *9*(1).

(149). Levy, E., Ouadda, A. B. D., Spahis, S., Sane, A. T., Garofalo, C., Grenier, émilie, Emonnot, L., Yara, S., Couture, P., Beaulieu, J. F., Ménard, D., Seidah, N. G., & Elchebly, M. (2013). PCSK9 plays a significant role in cholesterol homeostasis and lipid transport in intestinal epithelial cells. *Atherosclerosis*, *227*(2), 297–306.

(150). Levy, S., Todd, S. C., & Maecker, H. T. (1998). CD81 (TAPA-1): a molecule involved in signal transduction and cell adhesion in the immune system. In *Annu. Rev. Immunol,*16.

(151). Lipari, M. T., Li, W., Moran, P., Kong-beltran, M., Sai, T., Lai, J., Lin, S. J., Kolumam, G., Zavala-solorio, J., Izrael-Tomasevic, A., Arnott, D., Wang, J., Peterson, A. S., & Kirchhofer, D. (2012). Furin-cleaved proprotein convertase subtilisin/kexin type 9 (PCSK9) is active and modulates low density lipoprotein receptor and serum cholesterol levels. *Journal of Biological Chemistry*, *287*(52), 43482–43491.

(152). Liu, A., Rahman, M., Hafström, I., Ajeganova, S., & Frostegård, J. (2020). Proprotein convertase subtilisin kexin 9 is associated with disease activity and is implicated in immune activation in systemic lupus erythematosus. *Lupus,29*(8):825-835.

(153). Liu, Xinjian, Bao, X., Hu, M., Chang, H., Jiao, M., Cheng, J., Xie, L., Huang, Q., Li, F., & Li, C. Y. (2020). Inhibition of PCSK9 potentiates immune checkpoint therapy for cancer. *Nature*, *588*(7839), 693–698. https://doi.org/10.1038/s41586-020-2911-7

(154). Lohoff, F. W., Sorcher, J. L., Rosen, A. D., Mauro, K. L., Fanelli, R. R., Momenan, R., Hodgkinson, C. A., Vendruscolo, L. F., Koob, G. F., Schwandt, M., George, D. T., Jones, I. S., Holmes, A., Zhou, Z., Xu, M., Gao, B., Sun, H., Phillips, M. J., Muench, C., & Kaminsky, Z. A. (2018). Methylomic profiling and replication implicates deregulation of PCSK9 in alcohol use disorder. *23*(9), 1–11. https://doi.org/doi:10.1038/mp.2017.168

(155). Longuespée, R., Couture, F., Levesque, C., Kwiatkowska, A., Desjardins, R., Gagnon, S., Vergara, D., Maffia, M., Fournier, I., Salzet, M., & Day, R. (2014). Implications of Proprotein Convertases in Ovarian Cancer Cell Proliferation and Tumor Progression: Insights for PACE4 as a Therapeutic Target. *Translational Oncology*, *7*(3), 410–419.

(156). López-Otín, C., & Overall, C. M. (2002). Protease degradomics: A new challenge for

proteomics. *Nature Reviews Molecular Cell Biology*, *3*(7), 509–519.

(157).   Love, M. I., Huber, W., & Anders, S. (2014). Moderated estimation of fold change and dispersion for RNA-seq data with DESeq2. *Genome Biology*, *15*(12), 1–21.

(158).   Maarouf, N., Chen, Y. X., Shi, C., Deng, J., Diao, C., Rosin, M., Shrivastava, V., Batulan, Z., Liu, J., & O'Brien, E. R. (2020). Unlike estrogens that increase PCSK9 levels post-menopause HSP27 vaccination lowers cholesterol levels and atherogenesis due to divergent effects on PCSK9 and LDLR. *Pharmacological Research*, *161*.

(159).   Malley, R., Henneke, P., Morse, S. C., Cieslewicz, M. J., Lipsitch, M., Thompson, C. M., Kurt-jones, E., Paton, J. C., Wessels, M. R., & Golenbock, D. T. (2003). Recognition of pneumolysin by Toll-like receptor 4 confers resistance to pneumococcal infection. *100*(4), 1966–1971. https://doi.org/10.1073/pnas.0435928100

(160).   Mantovani, A., Allavena, P., Sica, A., & Balkwill, F. (2008). Cancer-related inflammation. *Nature*, *454*(7203), 436–444. https://doi.org/10.1038/NATURE07205

(161).   Marianes, A. E., & Zimmerman, A. M. (2011). Targets of somatic hypermutation within immunoglobulin light chain genes in zebrafish. *Immunology*, *132*(2), 240–255.

(162).   Marquart, M. E. (2021). Pathogenicity and virulence of Streptococcus pneumoniae: Cutting to the chase on proteases. *Virulence*, *12*(1), 766–787.

(163).   Marschner, K., Kollmann, K., Schweizer, M., Braulke, T., & Pohl, S. (2011). A key enzyme in the biogenesis of lysosomes is a protease that regulates cholesterol metabolism. *Science*, *333*(6038), 87–90. https://doi.org/10.1126/science.1205677

(164).   Maxwell, K. N., & Breslow, J. L. (2004). Adenoviral-mediated expression of Pcsk9 in mice results in a low-density lipoprotein receptor knockout phenotype. *Proceedings of the National Academy of Sciences of the United States of America*, *101*(18), 7100–7105.

(165).   Maxwell, K. N., Fisher, E. A., & Breslow, J. L. (2005). Overexpression of PCSK9 accelerates the degradation of the LDLR in a post-endoplasmic reticulum compartment. *Proceedings of the National Academy of Sciences of the United States of America*, *102*(6), 2069–2074.

(166).   Maxwell, K. N., Soccio, R. E., Duncan, E. M., Sehayek, E., & Breslow, J. L. (2003). Novel putative SREBP and LXR target genes identified by microarray analysis in liver of cholesterol-fed mice. *Journal of Lipid Research*, *44*(11), 2109–2119.

(167).   Mayengbam, S. S., Singh, A., Pillai, A. D., & Bhat, M. K. (2021). Influence of cholesterol on cancer progression and therapy. *Translational Oncology*, *14*(6).

(168).   Mayne, J., Dewpura, T., Raymond, A., Cousins, M., Chaplin, A., Lahey, K. A., LaHaye, S. A., Mbikay, M., Ooi, T. C., & Chrétien, M. (2008). Plasma PCSK9 levels are significantly modified by statins and fibrates in humans. *Lipids in Health and Disease*, *7*.

(169).   Mayne, J., Raymond, A., Chaplin, A., Cousins, M., Kaefer, N., Gyamera-Acheampong, C., Seidah, N. G., Mbikay, M., Chrétien, M., & Ooi, T. C. (2007). Plasma PCSK9 levels correlate with cholesterol in men but not in women. *Biochemical and Biophysical Research Communications*, *361*(2), 451–456. https://doi.org/10.1016/J.BBRC.2007.07.029

(170).   Mbikay, M., Chretien, M., & Seidah, N. G. (2001). Neuroendocrine secretory protein 7B2: structure, expression and functions. *Biochemical Journal*, *282*(37), 27402–27413.

(171).   Mbikay, M., Seidah, N. G., & Chretien, M. (1993). From Proopiomelanocortin to Cancer: Possible Role of Convertases in Neoplasia. *Annals of the New York Academy of Sciences*, *680*(1), 13–19. https://doi.org/10.1111/j.1749-6632.1993.tb19671.x

(172).   Mbikay, M., Sirois, F., Yao, J., Seidah, N. G., & Chrétien, M. (1997). Comparative analysis of expression of the proprotein convertases furin, PACE4, PC1 and PC2 in human lung tumours. *British Journal of Cancer*, *75*(10), 1509–1514.

(173).   Mbikay, Majambu;, Tadros, H., Ishida, N., Lerner, C. P. ., De Lamirande, E., Chen, A., El-Alfy, M., Clermont, Y., Seidah, N. G. ., Chrétien, M., Gagnon, C. and, & Simpson, E. M. (1997). Impaired fertility in mice deficient for the testicular germ-cell protease PC4. *Proceedings of the National Academy of Sciences of the United States of America*, *94*(13), 6842–6846.

(174).   Mbikay, Majambu, Sirois, F., Mayne, J., Wang, G. S., Chen, A., Dewpura, T., Prat, A., Seidah, N. G., Chretien, M., & Scott, F. W. (2010). PCSK9-deficient mice exhibit impaired glucose tolerance and pancreatic islet abnormalities. *FEBS Letters*, *584*(4), 701–706.

(175).   Medina, F., Ramos, M., Iborra, S., de León, P., Rodríguez-Castro, M., & Del Val, M. (2009). Furin-processed antigens targeted to the secretory route elicit functional TAP1-/-CD8+ T lymphocytes in vivo. *Journal of Immunology, 183*(7):4639-47.

(176).   Meeker, N. D., & Trede, N. S. (2008). Immunology and zebrafish: spawning new models of human disease. *Developmental and Comparative Immunology*, *32*(7), 745–757.

(177).   Mefford, M. T., Rosenson, R. S., Cushman, M., Farkouh, M. E., McClure, L. A., Wadley, V. G., Irvin, M. R., Bittner, V., Safford, M. M., Somaratne, R., Monda, K. L., Muntner, P., & Levitan, E. B. (2018). PCSK9 Variants, Low-Density Lipoprotein Cholesterol, and Neurocognitive Impairment: Reasons for Geographic and Racial Differences in Stroke Study (REGARDS). *Circulation*, *137*(12), 1260–1269.

(178).   Mikaeeli, S., Susan-Resiga, D., Girard, E., Ben Djoudi Ouadda, A., Day, R., Prost, S., & Seidah, N. G. (2020). Functional analysis of natural PCSK9 mutants in modern and archaic humans. *FEBS Journal*, *287*(3), 515–528. https://doi.org/10.1111/febs.15036

(179).   Miller, J. C., Holmes, M. C., Wang, J., Guschin, D. Y., Lee, Y. L., Rupniewski, I., Beausejour, C. M., Waite, A. J., Wang, N. S., Kim, K. A., Gregory, P. D., Pabo, C. O., & Rebar, E. J. (2007). An improved zinc-finger nuclease architecture for highly specific genome editing. *Nature Biotechnology*, *25*(7), 778–785. https://doi.org/10.1038/NBT1319

(180).   Miller, J. C., Tan, S., Qiao, G., Barlow, K. A., Wang, J., Xia, D. F., Meng, X., Paschon, D. E., Leung, E., Hinkley, S. J., Dulay, G. P., Hua, K. L., Ankoudinova, I., Cost, G. J., Urnov, F. D., Zhang, H. S., Holmes, M. C., Zhang, L., Gregory, P. D., & Rebar, E. J. (2011). A TALE nuclease architecture for efficient genome editing. *Nature Biotechnology*, *29*(2), 143–150. https://doi.org/10.1038/NBT.1755

(181).   Mitchell, K. A., Moore, J. X., Rosenson, R. S., Irvin, R., Guirgis, F. W., Shapiro, N., Safford, M., & Wang, H. E. (2019). PCSK9 loss-of-function variants and risk of infection and sepsis in the Reasons for Geographic and Racial Differences in Stroke (REGARDS) cohort. *PloS One*, *14*(2). https://doi.org/10.1371/JOURNAL.PONE.0210808

(182).   Mondal, K., Chakraborty, P., & Kabir, S. N. (2018). Hyperhomocysteinemia and hyperandrogenemia share PCSK9-LDLR pathway to disrupt lipid homeostasis in PCOS. *Biochemical and Biophysical Research Communications*, *503*(1), 8–13.

(183).   Munir, R., Usman, H., Hasnain, S., Smans, K., Kalbacher, H., & Zaidi, N. (2014). Atypical plasma lipid profile in cancer patients: cause or consequence? *Biochimie*, *102*(1), 9–18.

(184).   Musunuru, K., Chadwick, A. C., Mizoguchi, T., Garcia, S. P., DeNizio, J. E., Reiss, C. W., Wang, K., Iyer, S., Dutta, C., Clendaniel, V., Amaonye, M., Beach, A., Berth, K., Biswas, S., Braun, M. C., Chen, H. M., Colace, T. V., Ganey, J. D., Gangopadhyay, S. A., … Kathiresan, S. (2021). In vivo CRISPR base editing of PCSK9 durably lowers cholesterol in primates. *Nature*, *593*(7859), 429–434.

(185).   Nakagawa, T., Murakami, K., & Nakayama, K. (1993). Identification of an isoform with an extremely large Cys-rich region of PC6, a Kex2-like processing endoprotease. *FEBS Letters*, *327*(2), 165–171. https://doi.org/10.1016/0014-5793(93)80163-O

(186).   Napolitano, L. M. (2018). Sepsis 2018: Definitions and Guideline Changes. *Surgical Infections*, *19*(2), 117–125. https://doi.org/10.1089/SUR.2017.278

(187).   Narayanan, V. (1997). Apoptosis in development and disease of the nervous system: 1. Naturally occurring cell death in the developing nervous system. *Pediatric Neurology*, *16*(1), 9–13. https://doi.org/10.1016/S0887-8994(96)00257-3

(188).   Nasevicius, A., & Ekker, S. C. (2000). Effective targeted gene "knockdown" in zebrafish. *Nature Genetics*, *26*(2), 216–220. https://doi.org/10.1038/79951

(189).   Nassoury, N., Blasiole, D. A., Tebon Oler, A., Benjannet, S., Hamelin, J., Poupon, V.,

McPherson, P. S., Attie, A. D., Prat, A., & Seidah, N. G. (2007). The cellular trafficking of the secretory proprotein convertase PCSK9 and its dependence on the LDLR. *Traffic*, *8*(6), 718–732. https://doi.org/10.1111/j.1600-0854.2007.00562.x

(190).   Naureckiene, S., Ma, L., Sreekumar, K., Purandare, U., Lo, C. F., Huang, Y., Chiang, L. W., Grenier, J. M., Ozenberger, B. A., Jacobsen, J. S., Kennedy, J. D., DiStefano, P. S., Wood, A., & Bingham, B. (2003). Functional characterization of Narc 1, a novel proteinase related to proteinase K. *Archives of Biochemistry and Biophysics*, *420*(1), 55–67.

(191).   Neely, M. N., Pfeifer, J. D., & Caparon, M. (2002). Streptococcus-zebrafish model of bacterial pathogenesis. *Infection and Immunity*, *70*(7), 3904–3914.

(192).   Nehring, S. M., Goyal, A., & Patel, B. C. (2021). *C Reactive Protein*. Treasure Island (FL): StatPearls Publishing.

(193).   Neurath, H., & Walsh, K. A. (1976). Role of proteolytic enzymes in biological regulation (A review). *Proceedings of the National Academy of Sciences of the United States of America*, *73*(11), 3825–3832. https://doi.org/10.1073/pnas.73.11.3825

(194).   Norata, G. D., Tavori, H., Pirillo, A., Fazio, S., & Catapano, A. L. (2016). Biology of proprotein convertase subtilisin kexin 9: Beyond low-density lipoprotein cholesterol lowering. *Cardiovascular Research*, *112*(1), 429–442. https://doi.org/10.1093/cvr/cvw194

(195).   O'Brien, K. L., Wolfson, L. J., Watt, J. P., Henkle, E., Deloria-Knoll, M., McCall, N., Lee, E., Mulholland, K., Levine, O. S., & Cherian, T. (2009). Burden of disease caused by Streptococcus pneumoniae in children younger than 5 years: global estimates. *Lancet (London, England)*, *374*(9693), 893–902. https://doi.org/10.1016/S0140-6736(09)61204-6

(196).   O'Shea, A. S. (2022). Clinical Staging of Ovarian Cancer. *Methods in Molecular Biology (Clifton, N.J.)*, *2424*, 3–10. https://doi.org/10.1007/978-1-0716-1956-8_1

(197).   Ojanen, M. J. T., Uusi-Mäkelä, M. I. E., Harjula, S. K. E., Saralahti, A. K., Oksanen, K. E., Kähkönen, N., Määttä, J. A. E., Hytönen, V. P., Pesu, M., & Rämet, M. (2019). Intelectin 3 is dispensable for resistance against a mycobacterial infection in zebrafish (Danio rerio). *Scientific Reports*, *9*(1), 1–17. https://doi.org/10.1038/s41598-018-37678-1

(198).   Oleaga, C., Hay, J., Gurcan, E., David, L. L., Mueller, P. A., Tavori, H., Shapiro, M. D., Pamir, N., & Fazio, S. (2021). Insights into the kinetics and dynamics of the furin-cleaved form of PCSK9. *Journal of Lipid Research*, *62*(15), 100003.

(199).   Ong, J. S., Cuellar-Partida, G., Lu, Y., Fasching, P. A., Hein, A., Burghaus, S., Beckmann, M. W., Lambrechts, D., Van Nieuwenhuysen, E., Vergote, I., Vanderstichele, A., Doherty, J. A., Rossing, M. A., Chang-Claude, J., Eilber, U., Rudolph, A., Wang-Gohrke, S., Goodman, M. T., Bogdanova, N., … MacGregor, S. (2016). Association of vitamin D levels and risk of ovarian cancer: a Mendelian randomization study. *International Journal of Epidemiology*, *45*(5), 1619–1630. https://doi.org/10.1093/IJE/DYW207

(200).   Ortega, M., Almela, M., Martinez, J. A., Marco, F., Soriano, A., López, J., Sánchez, M., Muñoz, A., & Mensa, J. (2007). Epidemiology and outcome of primary community-acquired bacteremia in adult patients. *European Journal of Clinical Microbiology & Infectious Diseases : Official Publication of the European Society of Clinical Microbiology*, *26*(7), 453–457.

(201).   Ortutay, Z., Grönholm, A., Laitinen, M., Keresztes-Andrei, M., Hermelo, I., & Pesu, M. (2021). Identification of Novel Genetic Regulatory Region for Proprotein Convertase FURIN and Interferon Gamma in T Cells. *Frontiers in Immunology, 12*:630389.

(202).   Page, R. E., Klein-Szanto, A. J. P., Litwin, S., Nicolas, E., Al-Jumaily, R., Alexander, P., Godwin, A. K., Ross, E. A., Schilder, R. J., & Bassi, D. E. (2007). Increased expression of the pro-protein convertase furin predicts decreased survival in ovarian cancer. *Cellular Oncology*, *29*(4), 289–299. https://doi.org/10.1155/2007/930321

(203).   Paik, D. Y., Janzen, D. M., Schafenacker, A. M., Velasco, V. S., Shung, M. S., Cheng, D., Huang, J., Witte, O. N., & Memarzadeh, S. (2012). Stem-like epithelial cells are concentrated in the distal end of the fallopian tube: a site for injury and serous cancer

initiation. *Stem Cells (Dayton, Ohio)*, *30*(11), 2487–2497.

(204).   Pasquato, A., Pullikotil, P., Asselin, M. C., Vacatello, M., Paolillo, L., Ghezzo, F., Basso, F., Di Bello, C., Dettin, M., & Seidah, N. G. (2006). The proprotein convertase SKI-1/S1P: In vitro analysis of Lassa virus glycoprotein-derived substrates and ex vivo validation of irreversible peptide inhibitors. *Journal of Biological Chemistry*, *281*(33), 23471–23481. https://doi.org/10.1074/jbc.M513675200

(205).   Pavlova, N. N., & Thompson, C. B. (2016). The Emerging Hallmarks of Cancer Metabolism. *Cell Metabolism*, *23*(1), 27–47. https://doi.org/10.1016/J.CMET.2015.12.006

(206).   Pei, D., & Weiss, S. J. (1995). Furin-dependent intracellular activation of the human stromelysin-3 zymogen. In *Nature* (Vol. 375, Issue 6528, pp. 244–247).

(207).   Penet, M. F., Krishnamachary, B., Wildes, F. B., Mironchik, Y., Hung, C. F., Wu, T. C., & Bhujwalla, Z. M. (2018). Ascites Volumes and the Ovarian Cancer Microenvironment. *Frontiers in Oncology*, *8*(DEC).

(208).   Penninkilampi, R., & Eslick, G. D. (2018). Perineal Talc Use and Ovarian Cancer: A Systematic Review and Meta-Analysis. *Epidemiology (Cambridge, Mass.)*, *29*(1), 41–49.

(209).   Persson, L., Cao, G., Ståhle, L., Sjöberg, B. G., Troutt, J. S., Konrad, R. J., Gälman, C., Wallén, H., Eriksson, M., Hafström, I., Lind, S., Dahlin, M., Åmark, P., Angelin, B., & Rudling, M. (2010). Circulating proprotein convertase subtilisin kexin type 9 has a diurnal rhythm synchronous with cholesterol synthesis and is reduced by fasting in humans. *Arteriosclerosis, Thrombosis, and Vascular Biology*, *30*(12), 2666–2672.

(210).   Pesu, M., Muul, L., Kanno, Y., & O'Shea, J. J. (2006). Proprotein convertase furin is preferentially expressed in T helper 1 cells and regulates interferon gamma. *Blood*, *108*(3), 983–985. https://doi.org/10.1182/blood-2005-09-3824

(211).   Pesu, M., Watford, W. T., Wei, L., Xu, L., Fuss, I., Strober, W., Andersson, J., Shevach, E. M., Quezado, M., Bouladoux, N., Roebroek, A., Belkaid, Y., Creemers, J., & O'Shea, J. J. (2008). T-cell-expressed proprotein convertase furin is essential for maintenance of peripheral immune tolerance. *Nature*, *455*(7210), 246–250.

(212).   Petersen-Uribe, Á., Kremser, M., Rohlfing, A. K., Castor, T., Kolb, K., Dicenta, V., Emschermann, F., Li, B., Borst, O., Rath, D., Müller, K. A. L., & Gawaz, M. P. (2021). Platelet-Derived PCSK9 Is Associated with LDL Metabolism and Modulates Atherothrombotic Mechanisms in Coronary Artery Disease. *International Journal of Molecular Sciences*, *22*(20). https://doi.org/10.3390/IJMS222011179

(213).   Peticca, P., Raymond, A., Gruslin, A., Cousins, M., Adetola, E., Abujrad, H., Mayne, J., & Ooi, T. C. (2013). Human Serum PCSK9 Is Elevated at Parturition in Comparison to Nonpregnant Subjects While Serum PCSK9 from Umbilical Cord Blood is Lower Compared to Maternal Blood. *ISRN Endocrinology*, *2013*, 1–8.

(214).   Pétigny-Lechartier, C., Duboc, C., Jebahi, A., Louis, M. H., Abeilard, E., Denoyelle, C., Gauduchon, P., Poulain, L., & Villedieu, M. (2017). The mTORC1/2 Inhibitor AZD8055 Strengthens the Efficiency of the MEK Inhibitor Trametinib to Reduce the Mcl-1/[Bim and Puma] ratio and to Sensitize Ovarian Carcinoma Cells to ABT-737. *Molecular Cancer Therapeutics*, *16*(1), 102–115.

(215).   Phelps, H. A., Runft, D. L., & Neely, M. N. (2009). Adult zebrafish model of streptococcal infection. *Current Protocols in Microbiology*, *Chapter 9*(SUPPL. 13).

(216).   Piao, M.X., Bai, J.W., Zhang, P.F., & Zhang, Y.Z. (2015). PCSK9 regulates apoptosis in human neuroglioma u251 cells via mitochondrial signaling pathways. *International Journal of Clinical and Experimental Pathology, 8*(3):2787-94.

(217).   Piper, D. E., Jackson, S., Liu, Q., Romanow, W. G., Shetterly, S., Thibault, S. T., Shan, B., & Walker, N. P. C. (2007). The Crystal Structure of PCSK9: A Regulator of Plasma LDL-Cholesterol. *Structure*, *15*(5), 545–552. https://doi.org/10.1016/j.str.2007.04.004

(218).   Poirier, S., Mayer, G., Benjannet, S., Bergeron, E., Marcinkiewicz, J., Nassoury, N.,

Mayer, H., Nimpf, J., Prat, A., & Seidah, N. G. (2008). The proprotein convertase PCSK9 induces the degradation of low density lipoprotein receptor (LDLR) and its closest family members VLDLR and ApoER2. *The Journal of Biological Chemistry*, *283*(4), 2363–2372.

(219).   Poirier, S., Prat, A., Marcinkiewicz, E., Paquin, J., Chitramuthu, B. P., Baranowski, D., Cadieux, B., Bennett, H. P. J., & Seidah, N. G. (2006). Implication of the proprotein convertase NARC-1/PCSK9 in the development of the nervous system. *Journal of Neurochemistry*, *98*(3), 838–850. https://doi.org/10.1111/j.1471-4159.2006.03928.x

(220).   Polgár, L. (2013). Catalytic mechanisms of serine and threonine peptidases. *Handbook of Proteolytic Enzymes*, *3*, 2524–2534. https://doi.org/10.1016/B978-0-12-382219-2.00560-3

(221).   Popkin, D.L., Teijaro, J.R., Sullivan, B.M., Urata, S., Rutschmann, S., de la Torre, J.C,, Kunz, S., Beutler, B., & Oldstone, M. (2011). Hypomorphic mutation in the site-1 protease Mbtps1 endows resistance to persistent viral infection in a cell-specific manner. *Cell Host Microbe, 9* (3):212-222.

(222).   Prat, J. (2012). Ovarian carcinomas: five distinct diseases with different origins, genetic alterations, and clinicopathological features. *Virchows Archiv : An International Journal of Pathology*, *460*(3), 237–249. https://doi.org/10.1007/S00428-012-1203-5

(223).   Pruitt, K. D., Tatusova, T., & Maglott, D. R. (2007). NCBI reference sequences (RefSeq): A curated non-redundant sequence database of genomes, transcripts and proteins. *Nucleic Acids Research*, *35*(SUPPL. 1), 61–65. https://doi.org/10.1093/nar/gkl842

(224).   Puente, X. S., Sánchez, L. M., Overall, C. M., & López-Otín, C. (2003). Human and mouse proteases: A comparative genomic approach. *Nature Reviews Genetics*, *4*(7), 544–558.

(225).   Pullikotil, P., Benjannet, S., Mayne, J., & Seidah, N. G. (2007). The proprotein convertase SKI-1/S1P: Alternate translation and subcellular localization. *Journal of Biological Chemistry*, *282*(37), 27402–27413. https://doi.org/10.1074/jbc.M703200200

(226).   Puls, L. E., Duniho, T., Hunter IV, J. E., Kryscio, R., Blackhurst, D., & Gallion, H. (1996). The prognostic implication of ascites in advanced-stage ovarian cancer. *Gynecologic Oncology*, *61*(1), 109–112. https://doi.org/10.1006/GYNO.1996.0106

(227).   Ramin-Mangata, S., Thedrez, A., Nativel, B., Diotel, N., Blanchard, V., Wargny, M., Aguesse, A., Billon-Crossouard, S., Vindis, C., Le May, C., Hulin, P., Armanet, M., Gmyr, V., Pattou, F., Croyal, M., Meilhac, O., Nobécourt, E., Cariou, B., & Lambert, G. (2021). Effects of proprotein convertase subtilisin kexin type 9 modulation in human pancreatic beta cells function. *Atherosclerosis*, *326*, 47–55.

(228).   Ran, F. A., Hsu, P. D., Wright, J., Agarwala, V., Scott, D. A., & Zhang, F. (2013). Genome engineering using the CRISPR-Cas9 system. *Nature Protocols*, *8*(11), 2281–2308.

(229).   Rannikko, J., Syrjänen, J., Seiskari, T., Aittoniemi, J., & Huttunen, R. (2017). Sepsis-related mortality in 497 cases with blood culture-positive sepsis in an emergency department. *International Journal of Infectious Diseases : IJID : Official Publication of the International Society for Infectious Diseases*, *58*, 52–57. https://doi.org/10.1016/J.IJID.2017.03.005

(230).   Rashid, S., Curtis, D. E., Garuti, R., Anderson, N. H., Bashmakov, Y., Ho, Y. K., Hammer, R. E., Moon, Y. A., & Horton, J. D. (2005). Decreased plasma cholesterol and hypersensitivity to statins in mice lacking Pcsk9. *Proceedings of the National Academy of Sciences of the United States of America*, *102*(15), 5374–5379.

(231).   Rawlings, N. D., & Barrett, A. J. (1994). Families of serine peptidases. In *Methods in Enzymology* (Vol. 244, Issue C). https://doi.org/10.1016/0076-6879(94)44004-2

(232).   Rawlings, N. D., & Barrett, A. J. (2013). Introduction: Serine Peptidases and Their Clans. In *Handbook of Proteolytic Enzymes,3*.

(233).   Refaie, S., Gagnon, S., Gagnon, H., Desjardins, R., D'Anjou, F., D'Orléans-Juste, P., Zhu, X., Steiner, D. F., Seidah, N. G., Lazure, C., Salzet, M., & Day, R. (2012). Disruption of proprotein convertase 1/3 (PC1/3) expression in mice causes innate immune defects and uncontrolled cytokine secretion. *Journal of Biological Chemistry*, *287*(18), 14703–14717.

(234).   Remacle, A. G., Shiryaev, S. A., Oh, E. S., Cieplak, P., Srinivasan, A., Wei, G., Liddington, R. C., Ratnikov, B. I., Parent, A., Desjardins, R., Day, R., Smith, J. W., Lebl, M., & Strongin, A. Y. (2008). Substrate cleavage analysis of furin and related proprotein convertases: A comparative study. *Journal of Biological Chemistry*, *283*(30), 20897–20906.

(235).   Rodet, F., Capuz, A., Ozcan, B.A., Le Beillan, R., Raffo-Romero, A., Kobeissy, F., Duhamel, M. & Salzet M. (2019). PC1/3 KD Macrophages Exhibit Resistance to the Inhibitory Effect of IL-10 and a Higher TLR4 Activation Rate, Leading to an Anti-Tumoral Phenotype. Cells, 8(12):1490. https://doi.org/10.3390/cells8121490.

(236).   Rojas, V., Hirshfield, K. M., Ganesan, S., & Rodriguez-Rodriguez, L. (2016). Molecular Characterization of Epithelial Ovarian Cancer: Implications for Diagnosis and Treatment. *International Journal of Molecular Sciences*, *17*(12).

(237).   Rose, M., Duhamel, M., Rodet, F., & Salzet, M. (2021). The Role of Proprotein Convertases in the Regulation of the Function of Immune Cells in the Oncoimmune Response. *Frontiers in Immunology*, *12*(April), 1–10.

(238).   Roubtsova, A., Munkonda, M. N., Awan, Z., Marcinkiewicz, J., Chamberland, A., Lazure, C., Cianflone, K., Seidah, N. G., & Prat, A. (2011). Circulating proprotein convertase subtilisin/kexin 9 (PCSK9) regulates VLDLR protein and triglyceride accumulation in visceral adipose tissue. *Arteriosclerosis, Thrombosis, and Vascular Biology*, *31*(4), 785–791. https://doi.org/10.1161/ATVBAHA.110.220988

(239).   Rounioja, S., Saralahti, A., Rantala, L., Parikka, M., Henriques-Normark, B., Silvennoinen, O., & Rämet, M. (2012). Defense of zebrafish embryos against Streptococcus pneumoniae infection is dependent on the phagocytic activity of leukocytes. *Developmental and Comparative Immunology*, *36*(2), 342–348.

(240).   Ruscica, M., Ricci, C., Macchi, C., Magni, P., Cristofani, R., Liu, J., Corsini, A., & Ferri, N. (2016). Suppressor of Cytokine Signaling-3 (SOCS-3) Induces Proprotein Convertase Subtilisin Kexin Type 9 (PCSK9) Expression in Hepatic HepG2 Cell Line. *The Journal of Biological Chemistry*, *291*(7), 3508–3519. https://doi.org/10.1074/JBC.M115.664706

(241).   Saralahti, A., Piippo, H., Parikka, M., Henriques-Normark, B., Rämet, M., & Rounioja, S. (2014). Adult zebrafish model for pneumococcal pathogenesis. *Developmental and Comparative Immunology*, *42*(2), 345–353. https://doi.org/10.1016/j.dci.2013.09.009

(242).   Savva, A., & Roger, T. (2013). Targeting toll-like receptors: promising therapeutic strategies for the management of sepsis-associated pathology and infectious diseases. *Frontiers in Immunology*, *4*(NOV). https://doi.org/10.3389/FIMMU.2013.00387

(243).   Sawamura, T. (2009). New idol for cholesterol reduction? *Clinical Chemistry*, *55*(12), 2082–2084. https://doi.org/10.1373/clinchem.2009.134023

(244).   Scalise, V., Sanguinetti, C., Neri, T., Cianchetti, S., Lai, M., Carnicelli, V., Celi, A., & Pedrinelli, R. (2021). Pcsk9 induces tissue factor expression by activation of tlr4/nfkb signaling. *International Journal of Molecular Sciences*, *22*(23).

(245).   Scamuffa, N., Calvo, F., Chrétien, M., Seidah, N. G., & Khatib, A. M. (2006). Proprotein convertases: lessons from knockouts. *The FASEB Journal*, *20*(12), 1954–1963.

(246).   Schlegel, V., Treuner-Kaueroff, T., Seehofer, D., Berg, T., Becker, S., Ceglarek, U., Thiery, J., & Kaiser, T. (2017). Low PCSK9 levels are correlated with mortality in patients with end-stage liver disease. *PloS One*, *12*(7).

(247).   Schmitz, G., & Orsó, E. (2002). CD14 signalling in lipid rafts: new ligands and co-receptors. *Current Opinion in Lipidology*, *13*(5), 513–521.

(248).   Schröder, N. W. J., Morath, S., Alexander, C., Hamann, L., Hartung, T., Zähringer, U., Göbel, U. B., Weber, J. R., & Schumann, R. R. (2003). Lipoteichoic acid (LTA) of Streptococcus pneumoniae and Staphylococcus aureus activates immune cells via Toll-like receptor (TLR)-2, lipopolysaccharide-binding protein (LBP), and CD14, whereas TLR-4 and MD-2 are not involved. *The Journal of Biological Chemistry*, *278*(18), 15587–15594.

(249).   Scotti, E., Calamai, M., Goulbourne, C. N., Zhang, L., Hong, C., Lin, R. R., Choi, J., Pilch, P. F., Fong, L. G., Zou, P., Ting, A. Y., Pavone, F. S., Young, S. G., & Tontonoz, P. (2013). IDOL Stimulates Clathrin-Independent Endocytosis and Multivesicular Body-Mediated Lysosomal Degradation of the Low-Density Lipoprotein Receptor. *Molecular and Cellular Biology*, *33*(8), 1503–1514. https://doi.org/10.1128/mcb.01716-12

(250).   Seidah, N. (2011). The Proprotein Convertases, 20 Years Later. *Methods in Molecular Biology*, *768*, 23–57. https://doi.org/10.1007/978-1-61779-204-5_3

(251).   Seidah, N. G., Hamelin, J., Mamarbachi, M., Dong, W., Tadros, H., Mbikay, M., Chretien, M., & Day, R. (1996). cDNA structure, tissue distribution, and chromosomal localization of rat PC7, a novel mammalian proprotein convertase closest to yeast kexin-like proteinases. *Proceedings of the National Academy of Sciences of the United States of America*, *93*(8), 3388–3393. https://doi.org/10.1073/pnas.93.8.3388

(252).   Seidah, N. G., Mowla, S. J., Hamelin, J., Mamarbachi, A. M., Benjannet, S., Touré, B. B., Basak, A., Munzer, J. S., Marcinkiewicz, J., Zhong, M., Barale, J. C., Lazure, C., Murphy, R. A., Chrétien, M., & Marcinkiewicz, M. (1999). Mammalian subtilisin/kexin isozyme SKI-1: A widely expressed proprotein convertase with a unique cleavage specificity and cellular localization. *Proceedings of the National Academy of Sciences of the United States of America*, *96*(4), 1321–1326. https://doi.org/10.1073/pnas.96.4.1321

(253).   Seidah, N. G. N. ., & Prat, A. (2021). The multifaceted biology of PCSK9. *Endocrine Reviews*, *XX*(Xx), 1–28. https://doi.org/10.1210/endrev/bnab035

(254).   Seidah, Nabil G;, & Chretien, M. (1999). Interactive report Proprotein and prohormone convertases : a family of subtilases generating diverse bioactive polypeptides 1. *Brain Research*, *848*(1–2), 45–62.

(255).   Seidah, Nabil G. (2015). The PCSK9 revolution and the potential of PCSK9-based therapies to reduce LDL-cholesterol. *Global Cardiology Science and Practice*, *2015*(5), 59. https://doi.org/10.21542/gcsp.2017.2

(256).   Seidah, Nabil G. (2021). The PCSK9 discovery, an inactive protease with varied functions in hypercholesterolemia, viral infections, and cancer. *Journal of Lipid Research*, *62*, 100130. https://doi.org/10.1016/j.jlr.2021.100130

(257).   Seidah, Nabil G., Abifadel, M., Prost, S., Boileau, C., & Prat, A. (2017). The proprotein convertases in hypercholesterolemia and cardiovascular diseases: Emphasis on proprotein convertase subtilisin/Kexin 9. *Pharmacological Reviews*, *69*(1), 33–52.

(258).   Seidah, Nabil G., Benjannet, S., Wickham, L., Marcinkiewicz, J., Bélanger Jasmin, S., Stifani, S., Basak, A., Prat, A., & Chrétien, M. (2003). The secretory proprotein convertase neural apoptosis-regulated convertase 1 (NARC-1): Liver regeneration and neuronal differentiation. *Proceedings of the National Academy of Sciences of the United States of America*, *100*(3), 928–933. https://doi.org/10.1073/pnas.0335507100

(259).   Seidah, Nabil G., Chrétien, M., & Mbikay, M. (2018). The ever-expanding saga of the proprotein convertases and their roles in body homeostasis: Emphasis on novel proprotein convertase subtilisin kexin number 9 functions and regulation. *Current Opinion in Lipidology*, *29*(2), 144–150. https://doi.org/10.1097/MOL.0000000000000484

(260).   Seidah, Nabil G., Day, R., Hamelin, J., Gaspar, A., Collard, M. W., & Chrétien, M. (1992). Testicular expression of PC4 in the rat: Molecular diversity of a novel germ cell-specific Kex2/subtilisin-like proprotein convertase. *Molecular Endocrinology*, *6*(10), 1559–1570. https://doi.org/10.1210/mend.6.10.1448111

(261).   Seidah, Nabil G., Khatib, A. M., & Prat, A. (2006). The proprotein convertases and their implication in sterol and/or lipid metabolism. *Biological Chemistry*, *387*(7), 871–877.

(262).   Seidah, Nabil G., Mayer, G., Zaid, A., Rousselet, E., Nassoury, N., Poirier, S., Essalmani, R., & Prat, A. (2008). The activation and physiological functions of the proprotein convertases. *International Journal of Biochemistry and Cell Biology*, *40*(6–7), 1111–

1125. https://doi.org/10.1016/j.biocel.2008.01.030

(263). Seidah, Nabil G., Pasquato, A., & Andréo, U. (2021). How do enveloped viruses exploit the secretory proprotein convertases to regulate infectivity and spread? *Viruses*, *13*(7), 1–24. https://doi.org/10.3390/v13071229

(264). Seidah, Nabil G., & Prat, A. (2012). The biology and therapeutic targeting of the proprotein convertases. *Nature Reviews Drug Discovery*, *11*(5), 367–383.

(265). Seidah, Nabil G., Prat, A., Pirillo, A., Catapano, A. L., & Norata, G. D. (2019). Novel strategies to target proprotein convertase subtilisin kexin 9: Beyond monoclonal antibodies. *Cardiovascular Research*, *115*(3), 510–518. https://doi.org/10.1093/cvr/cvz003

(266). Seidah, Nabil G., Sadr, M. S., Chrétien, M., & Mbikay, M. (2013). The multifaceted proprotein convertases: Their unique, redundant, complementary, and opposite functions. *Journal of Biological Chemistry*, *288*(30), 21473–21481.

(267). Sharotri, V., Collier, D. M., Olson, D. R., Zhou, R., & Snyder, P. M. (2012). Regulation of epithelial sodium channel trafficking by proprotein convertase subtilisin/kexin type 9 (PCSK9). *The Journal of Biological Chemistry*, *287*(23), 19266–19274.

(268). Shen, X., Li, Q. L., Brent, G. A., & Friedman, T. C. (2004). Thyroid hormone regulation of prohormone convertase 1 (PC1): Regional expression in rat brain and in vitro characterization of negative thyroid hormone response elements. *Journal of Molecular Endocrinology*, *33*(1), 21–33. https://doi.org/10.1677/jme.0.0330021

(269). Shimada, T., Topchiy, E., Leung, A. K. K., Kong, H. J. J., Genga, K. R., Boyd, J. H., Russell, J. A., Oda, S., Nakada, T. A., Hirasawa, H., & Walley, K. R. (2020). Very Low Density Lipoprotein Receptor Sequesters Lipopolysaccharide Into Adipose Tissue During Sepsis. *Critical Care Medicine*, *48*(1), 41–48.

(270). Shimano, H., & Sato, R. (2017). SREBP-regulated lipid metabolism: convergent physiology - divergent pathophysiology. *Nature Reviews. Endocrinology*, *13*(12), 710–730.

(271). Siegfried, G., Descarpentrie, J., Evrard, S., & Khatib, A. M. (2020). Proprotein convertases: Key players in inflammation-related malignancies and metastasis. *Cancer Letters*, *473*(January), 50–61. https://doi.org/10.1016/j.canlet.2019.12.027

(272). Siezen, R. J., & Leunissen, J. A. M. (1997). Subtilases: The superfamily of subtilisin-like serine proteases. *Protein Science*, *6*(3), 501–523. https://doi.org/10.1002/pro.5560060301

(273). Singer, M., Deutschman, C. S., Seymour, C. W., Shankar-Hari, M., Annane, D., Bauer, M., Bellomo, R., Bernard, G. R., Chiche, J. D., Coopersmith, C. M., Hotchkiss, R. S., Levy, M. M., Marshall, J. C., Martin, G. S., Opal, S. M., Rubenfeld, G. D., van der Poll, T., Vincent, J. L., & Angus, D. C. (2016). The Third International Consensus Definitions for Sepsis and Septic Shock (Sepsis-3). *JAMA - Journal of the American Medical Association*, *315*(8), 801–810. https://doi.org/doi:10.1001/jama.2016.0287

(274). Smeekens, S. P., & Steiner, D. F. (1990). Identification of a human insulinoma cDNA encoding a novel mammalian protein structurally related to the yeast dibasic processing protease Kex2. *Journal of Biological Chemistry*, *265*(6), 2997–3000.

(275). Sproston, N.R. & Ashworth, J.J. (2018). Role of C-Reactive Protein at Sites of Inflammation and Infection. *Frontiers in Immunology, 9:*754.

(276). Stancu, C., & Sima, A. (2001). Statins: mechanism of action and effects. *Journal of Cellullar and Molecular Medicine*, *5*(4), 378–387.

(277). Subramanian, K., Henriques-Normark, B., & Normark, S. (2019). Emerging concepts in the pathogenesis of the Streptococcus pneumoniae: From nasopharyngeal colonizer to intracellular pathogen. *Cellular Microbiology*, *21*(11). https://doi.org/10.1111/CMI.13077

(278). Sullivan, C., & Kim, C. H. (2008). Zebrafish as a model for infectious disease and immune function. *Fish & Shellfish Immunology*, *25*(4), 341–350.

(279). Summerton, J., & Weller, D. (1997). Morpholino antisense oligomers: design, preparation, and properties. *Antisense & Nucleic Acid Drug Development*, *7*(3), 187–195.

(280).   Sun, H., Meng, W., Zhu, J., & Wang, L. (2022). Antitumor activity and molecular mechanism of proprotein convertase subtilisin/kexin type 9 (PCSK9) inhibition. *Naunyn-Schmiedeberg's Archives of Pharmacology*. https://doi.org/10.1007/S00210-022-02200-Y

(281).   Szumska, D., Cioroch, M., Keeling, A., Prat, A., Seidah, N. G., & Bhattacharya, S. (2017). Pcsk5 is required in the early cranio-cardiac mesoderm for heart development. *BMC Developmental Biology*, *17*(1), 1–10. https://doi.org/10.1186/s12861-017-0148-y

(282).   Tang, Z. H., Peng, J., Ren, Z., Yang, J., Li, T. T., Li, T. H., Wang, Z., Wei, D. H., Liu, L. S., Zheng, X. L., & Jiang, Z. S. (2017a). New role of PCSK9 in atherosclerotic inflammation promotion involving the TLR4/NF-ϰB pathway. *Atherosclerosis*, *262*, 113–122. https://doi.org/10.1016/J.ATHEROSCLEROSIS.2017.04.023

(283).   Tao, R., Xiong, X., DePinho, R. A., Deng, C. X., & Dong, X. C. (2013). FoxO3 transcription factor and Sirt6 deacetylase regulate low density lipoprotein (LDL)-cholesterol homeostasis via control of the proprotein convertase subtilisin/kexin type 9 (Pcsk9) gene expression. *Journal of Biological Chemistry*, *288*(41), 29252–29259.

(284).   Thomas, G. (2002). Furin at the cutting edge: from protein traffic to embryogenesis and disease. *Nat Rev Mol Cell Biol*, *3*(10), 753–766.

(285).   Trede, N. S., Langenau, D. M., Traver, D., Look, A. T., & Zon, L. I. (2004). The use of zebrafish to understand immunity. *Immunity*, *20*(4), 367–379.

(286).   Trinder, M., Boyd, J. H., & Brunham, L. R. (2019). Molecular regulation of plasma lipid levels during systemic inflammation and sepsis. *Current Opinion in Lipidology*, *30*(2), 108–116. https://doi.org/10.1097/MOL.0000000000000577

(287).   Turpeinen, H., Kukkurainen, S., Pulkkinen, K., Kauppila, T., Ojala, K., Hytönen, V. P., & Pesu, M. (2011). Identification of proprotein convertase substrates using genome-wide expression correlation analysis. *BMC Genomics*, *12*(1), 618.

(288).   Uusi-Mäkelä, M. I. E., Barker, H. R., Bäuerlein, C. A., Häkkinen, T., Nykter, M., & Rämet, M. (2018). Chromatin accessibility is associated with CRISPR-Cas9 efficiency in the zebrafish (Danio rerio). *PLoS ONE*, *13*(4), 1–15.

(289).   Uusitalo-Seppälä, R., Huttunen, R., Aittoniemi, J., Koskinen, P., Leino, A., Vahlberg, T., & Rintala, E. M. (2013). Pentraxin 3 (PTX3) is associated with severe sepsis and fatal disease in emergency room patients with suspected infection: a prospective cohort study. *PloS One*, *8*(1). https://doi.org/10.1371/JOURNAL.PONE.0053661

(290).   van Asch, B., & Teixeira da Costa, L. F. (2021). Patterns and tempo of PCSK9 pseudogenizations suggest an ancient divergence in mammalian cholesterol homeostasis mechanisms. *Genetica*, *149*(1), 1–19. https://doi.org/10.1007/s10709-021-00113-x

(291).   Vecchié, A., Bonaventura, A., Meessen, J., Novelli, D., Minetti, S., Elia, E., Ferrara, D., Ansaldo, A. M., Scaravilli, V., Villa, S., Ferla, L., Caironi, P., Latini, R., Carbone, F., Montecucco, F., Bruzzone, P., Pagan, F., Russo, R., Confalonieri, A., … Zagara, G. (2021). PCSK9 is associated with mortality in patients with septic shock: data from the ALBIOS study. *Journal of Internal Medicine*, *289*(2), 179–192. https://doi.org/10.1111/JOIM.13150

(292).   Vlachopoulos, C., Kosteria, I., Sakka, S., Gkourogianni, A., Terentes-Printzios, D., Koutagiar, I., Skoumas, I., Miliou, A., Papassotiriou, I., Gardikioti, V., Loutradis, D., Chrousos, G., Kanaka-Gantenbein, C., & Tousoulis, D. (2019). PCSK9 and Lp(a) levels of children born after assisted reproduction technologies. *Journal of Assisted Reproduction and Genetics*, *36*(6), 1091–1099. https://doi.org/10.1007/S10815-019-01474-1

(293).   Walker, M. B., Miller, C. T., Coffin Talbot, J., Stock, D. W., & Kimmel, C. B. (2006). Zebrafish furin mutants reveal intricacies in regulating Endothelin1 signaling in craniofacial patterning. *Developmental Biology*, *295*(1), 194–205.

(294).   Walley, K. R., Francis, G. A., Opal, S. M., Stein, E. A., Russell, J. A., & Boyd, J. H. (2015). The central role of proprotein convertase subtilisin/kexin type 9 in septic pathogen lipid transport and clearance. *American Journal of Respiratory and Critical Care Medicine*, *192*(11),

1275–1286. https://doi.org/10.1164/rccm.201505-0876CI

(295).   Walley, K. R., Thain, K. R., Russell, J. A., Reilly, M. P., Meyer, N. J., Ferguson, J. F., Christie, J. D., Nakada, T. A., Fjell, C. D., Thair, S. A., Cirstea, M. S., & Boyd, J. H. (2014). PCSK9 is a critical regulator of the innate immune response and septic shock outcome. *Science Translational Medicine*, *6*(258), 258ra143.

(296).   Walsh, C. T., Garneau-Tsodikova, S., & Gatto, G. J. (2005). Protein posttranslational modifications: The chemistry of proteome diversifications. *Angewandte Chemie - International Edition*, *44*(45), 7342–7372. https://doi.org/10.1002/anie.200501023

(297).   Wang, M., Zhao, D., Xu, L., Guo, W., Nie, L., Lei, Y., Long, Y., Liu, M., Wang, Y., Zhang, X., Zhang, L., Li, H., Zhang, J., Yuan, D., & Yue, L. (2019). Role of PCSK9 in lipid metabolic disorders and ovarian dysfunction in polycystic ovary syndrome. *Metabolism: Clinical and Experimental*, *94*, 47–58. https://doi.org/10.1016/j.metabol.2019.02.002

(298).   Wang, X., Chen, X., Zhang, X., Su, C., Yang, M., He, W., Du, Y., Si, S., Wang, L., & Hong, B. (2020). A small-molecule inhibitor of PCSK9 transcription ameliorates atherosclerosis through the modulation of FoxO1/3 and HNF1α. *EBioMedicine*, *52*.

(299).   Wang, Y., Huang, Y., Hobbs, H. H., & Cohen, J. C. (2012). Molecular characterization of proprotein convertase subtilisin/kexin type 9-mediated degradation of the LDLR. *Journal of Lipid Research*, *53*(9), 1932–1943. https://doi.org/10.1194/JLR.M028563

(300).   Ward, O. P. (2011). *Proteases* (Elsevier (Ed.); Issue January).

(301).   Wrighting, D. M., & Andrews, N. C. (2006). Interleukin-6 induces hepcidin expression through STAT3. *Blood*, *108*(9), 3204–3209.

(302).   Wu, N.-Q., Shi, H.-W., & Li, J.-J. (2022). Proprotein Convertase Subtilisin/Kexin Type 9 and Inflammation: An Updated Review. *Frontiers in Cardiovascular Medicine*, *9*.

(303).   Xavier, L. B., Sóter, M. O., Sales, M. F., Oliveira, D. K., Reis, H. J., Candido, A. L., Reis, F. M., Silva, I. O., Gomes, K. B., & Ferreira, C. N. (2018). Evaluation of PCSK9 levels and its genetic polymorphisms in women with polycystic ovary syndrome. *Gene*, *644*, 129–136.

(304).   Xu, B., Li, S., Fang, Y., Zou, Y., Song, D., Zhang, S., & Cai, Y. (2021). Proprotein Convertase Subtilisin/Kexin Type 9 Promotes Gastric Cancer Metastasis and Suppresses Apoptosis by Facilitating MAPK Signaling Pathway Through HSP70 Up-Regulation. *Frontiers in Oncology*, *10*. https://doi.org/10.3389/FONC.2020.609663

(305).   Xu, X., Cui, Y., Cao, L., Zhang, Y., Yin, Y., & Hu, X. (2017). PCSK9 regulates apoptosis in human lung adenocarcinoma A549 cells via endoplasmic reticulum stress and mitochondrial signaling pathways. *Experimental and Therapeutic Medicine*, *13*(5), 1993–1999.

(306).   Yadav, B., Pemovska, T., Szwajda, A., Kulesskiy, E., Kontro, M., Karjalainen, R., Majumder, M. M., Malani, D., Murumägi, A., Knowles, J., Porkka, K., Heckman, C., Kallioniemi, O., Wennerberg, K., & Aittokallio, T. (2014). Quantitative scoring of differential drug sensitivity for individually optimized anticancer therapies. *Scientific Reports*, *4*, 1–10. https://doi.org/10.1038/srep05193

(307).   Yip, B. H. (2020). Recent Advances in CRISPR/Cas9 Delivery Strategies. *Biomolecules*, *10*(6). https://doi.org/10.3390/BIOM10060839

(308).   Yuan, J., Cai, T., Zheng, X., Ren, Y., Qi, J., Lu, X., Chen, H., Lin, H., Chen, Z., Liu, M., He, S., Chen, Q., Feng, S., Wu, Y., Zhang, Z., Ding, Y., & Yang, W. (2021). Potentiating CD8+ T cell antitumor activity by inhibiting PCSK9 to promote LDLR-mediated TCR recycling and signaling. *Protein and Cell*, *12*(4), 240–260.

(309).   Yuan, Y., Wu, W., Sun, S., Zhang, Y., & Chen, Z. (2020). PCSK9: A Potential Therapeutic Target for Sepsis. *Journal of Immunology Research*, *2020*.

(310).   Zelcer, N., Hong, C., Boyadjian, R., & Tontonoz, P. (2009). LXR Regulates Cholesterol Uptake through Idol-dependent Ubiquitination of the LDL Receptor. *Science*, *325*(5936), 100–104. https://doi.org/DOI: 10.1126/science.1168974

(311).   Zhang, D. W., Garuti, R., Tang, W. J., Cohen, J. C., & Hobbs, H. H. (2008). Structural requirements for PCSK9-mediated degradation of the low-density lipoprotein receptor. *Proceedings of the National Academy of Sciences of the United States of America*, *105*(35), 13045–13050. https://doi.org/10.1073/pnas.0806312105

(312).   Zhang, S. Z., Zhu, X. D., Feng, L. H., Li, X. L., Liu, X. F., Sun, H. C., & Tang, Z. Y. (2021). PCSK9 promotes tumor growth by inhibiting tumor cell apoptosis in hepatocellular carcinoma. *Experimental Hematology & Oncology*, *10*(1).

(313).   Zheng, L., Li, L., Lu, Y., Jiang, F., & Yang, X. A. (2018). SREBP2 contributes to cisplatin resistance in ovarian cancer cells. *Experimental Biology and Medicine (Maywood, N.J.)*, *243*(7), 655–662. https://doi.org/10.1177/1535370218760283

(314).   Zhou, E., Li, Z., Nakashima, H., Choukoud, A., Kooijman, S., Berbée, J. F. P., Rensen, P. C. N., & Wang, Y. (2021). Beneficial effects of brown fat activation on top of PCSK9 inhibition with alirocumab on dyslipidemia and atherosclerosis development in APOE*3-Leiden.CETP mice. *Pharmacological Research*, *167*.

10 ORIGINAL PUBLICATIONS

PUBLICATION
I

Reduced plasma PCSK9 response in patients with bacteraemia is associated with mortality

Juha Rannikko, <u>Dafne Jacome Sanz</u>, Zsuzsanna Ortutay, Tapio Seiskari, Janne Aittoniemi, Reetta Huttunen, Jaana Syrjänen and Marko Pesu

Reduced plasma PCSK9 response in patients with bacteraemia is associated with mortality

■ J. Rannikko[1,2] (iD), D. Jacome Sanz[2], Z. Ortutay[2], T. Seiskari[3], J. Aittoniemi[3], R. Huttunen[1], J. Syrjänen[1] & M. Pesu[2,4] (iD)

From the [1]Department of Internal Medicine, Tampere University Hospital; [2]Faculty of Medicine and Health Technology, Tampere University, ; [3]Department of Clinical Microbiology, Fimlab Laboratories Ltd, ; and [4]Department of Dermatology, Tampere University Hospital, Tampere, Finland

Abstract. Rannikko J, Jacome Sanz D, Ortutay Z, Seiskari T, Aittoniemi J, Huttunen R, Syrjänen J, Pesu M (Tampere University Hospital; Tampere University; Fimlab Laboratories Ltd; Tampere, Finland). Reduced plasma PCSK9 response in patients with bacteraemia is associated with mortality. *J Intern Med* 2019; **286**: 553–561.

Background. The proprotein convertase subtilisin/kexin type 9 (PCSK9) enzyme controls blood cholesterol levels by downregulating the expression of the low-density lipoprotein receptor (LDLR). Pathogenic lipids (e.g. lipopolysaccharide) are removed from the circulation by an LDLR/PCSK9-dependent mechanism; thus, it has been suggested that PCSK9 inhibitors may be beneficial in the treatment of infections. We measured plasma PCSK9 levels in patients with culture-positive bacteraemia and explored pathogen-dependent and infection site-dependent effects as well as correlations between patient characteristics and outcome.

Methods. Proprotein convertase subtilisin/kexin type 9 in the plasma was measured with an enzyme-linked immunosorbent assay from 481 patients with blood culture-positive infection on days 0 to 4 after admission to the emergency department. Patient outcome and clinical and laboratory data were gathered retrospectively from patient records.

Results. The plasma PCSK9 level was elevated equally in patients with Gram-positive or Gram-negative bacterial infections; particularly high levels were seen in patients with a lower respiratory tract infection and *Streptococcus pneumoniae* bacteraemia. PCSK9 levels showed a significant positive correlation with C-reactive protein (CRP) level. Bacteraemia patients with liver disease or a history of alcohol abuse had significantly lower levels of plasma PCSK9. Reduced PCSK9 plasma responses in patients were significantly associated with mortality at days 7, 28 and 90.

Conclusion. Proprotein convertase subtilisin/kexin type 9 is upregulated in blood culture-positive infections. Plasma PCSK9 resembles acute-phase proteins; its expression is induced during an infection, reduced in liver disease and correlates positively with CRP level. We have shown that PCSK9 levels are lower in patients with a fatal prognosis.

Keywords: bacteraemia, CRP, PCSK9, sepsis.

Introduction

The proprotein convertase subtilisin/kexin enzyme 9 (PCSK9) is a serine protease that is preferentially expressed in the liver and known to possess autoproteolytic activity [1–3]. The mature PCSK9 protein serves as a chaperone for cell-surface receptors and escorts them to intracellular endosome/lysosome degradation compartments. The key function of PCSK9 is to upregulate the levels of circulating low-density lipoprotein (LDL) by reducing the expression of the LDL receptor (LDLR) and reducing the clearance of hepatic lipids.

Patients with a *PCSK9* loss-of-function genotype are healthy and show exceptionally low levels of LDL and a low incidence of coronary heart disease, which validates PCSK9 as a biological target for drug development [4]. The first two PCSK9-targeting monoclonal antibodies, alirocumab and evolocumab, are now being used to treat patients with statin-resistant hypercholesterolaemia to reduce the risk of cardiovascular events [5,6].

In addition to its fundamental role in cholesterol metabolism, PCSK9 regulates host defence responses. The expression and secretion of PCSK9

are upregulated by inflammatory stimuli via the induction of mitochondrial reactive oxygen species and the NF-κB signalling pathway [7,8]. Elevated PCSK9 levels have been shown to promote pro-inflammatory and inhibit anti-inflammatory cytokines [9]. In patients with sepsis, pathogenic lipids such as lipopolysaccharide (LPS; Gram-negative bacteria), lipoteichoic acid (LTA; Gram-positive bacteria) and phospholipomannan (fungal organisms) bind to the pattern recognition receptors of the host and ultimately trigger an uncontrolled systemic inflammatory response. These lipids are carried in the circulation within lipoprotein particles and removed through binding to LDLR and the very low-density lipoprotein receptor to become detoxified by the liver [10]. Thus, the upregulation of LDLR expression in the liver by inhibiting PCSK9 has recently emerged as a potential strategy to reduce exacerbated inflammation in patients with sepsis [11,12]. The first clinical Phase II/III trials were started in January 2019 (clinicaltrials.gov: NCT03634293 and NCT03869073).

Boyd and colleagues investigated plasma PCSK9 levels in patients admitted to the emergency department (ED) with suspected sepsis [13]. The authors found that PCSK9 was markedly increased in patients compared to reference values from healthy individuals and that there was a positive correlation between high PCSK9 levels and cardiovascular and respiratory failure. Two other studies have explored the circulating PCSK9 levels in critically ill patients who were admitted to the intensive care unit (ICU) [14,15]. The results showed that plasma concentrations were similarly elevated in patients with and without sepsis and were higher than normal in ICU patients with severe trauma injury, which suggests that plasma PCSK9 is also upregulated by noninfectious stress to the body.

In this study, we determined plasma PCSK9 levels during the first 4 days of hospitalization in 481 patients who had blood culture-positive bacteraemia when admitted to the ED. Specifically, we explored the pathogen-dependent and infection site-dependent effects on plasma PCSK9 and correlation with patient characteristics and outcome. Our results demonstrate that a reduced PCSK9 plasma response to an infection is significantly associated with a fatal prognosis.

Materials and methods

Bacteraemia patient cohort

Tampere University Hospital is a tertiary hospital with a catchment population of approximately 524 700 inhabitants in Pirkanmaa County, Finland. All patients with blood culture-positive infection who were admitted to the hospital ED between 1 March 2012 and 28 February 2014 were included in the study cohort (contaminants were excluded). The day 0 EDTA blood sample was obtained within 24 h after the patient was admitted to the ED. Follow-up samples were collected from patients alongside treatment-based routine laboratory testing. Blood was collected in BacT/Alert Aerobic (FA Plus) and Anaerobic (FN Plus) blood culture bottles and placed in an automated microbial detection system (BacT/Alert 3D; bioMérieux, Marcy l'Etoile, France). Clinical data were collected retrospectively from patient records. Diagnoses of severe sepsis and septic shock were made according to Sepsis-2 consensus definitions [16]. The qSOFA score was calculated based on Sepsis-3 definitions [17]. The Pitt Bacteraemia Score was calculated as reported by Korvick *et al.* [18]. The site of infection was determined retrospectively. A more detailed description of the patient cohort is available in our previous publications [19,20]. In addition, we used 17 plasma samples from a separate patient cohort as healthy controls. These control samples were collected 1 year after recovery from bacteremia [21]. The median PCSK9 level in the control samples was 188 ng mL^{-1} [interquartile range (IQR) 139–264], which is in line with the result of a meta-analysis of the level of PCSK9 in healthy individuals [13].

The present study was approved by the Ethics Committee of Tampere University Hospital, Finland (permit # R11099). The requirement for informed consent was waived as no additional blood sampling was needed and routine patient care was not modified.

Plasma PCSK9 level measurement

Plasma PCSK9 was quantitated from plasma samples using a commercially available enzyme-linked immunosorbent assay (ELISA; DPC900; R&D Systems, Minneapolis, MN, USA) and the manufacturer's recommended protocol. To validate the reproducibility of the PCSK9 ELISA, some of the samples were measured as duplicates on the same

or separate plates. The intra-array and inter-array variations of the samples were on average 3.5% of the defined final concentration.

Statistical analyses

SPSS version 22.0 software (IBM Corp., Armonk, NY, USA) and R (version 3.4.4.; https://www.r-project.org) were used for statistical analyses. Nonparametric data were analysed using the Mann–Whitney *U*-test. The Pearson's product-moment coefficient was used to test correlation. A *P*-value of <0.05 was considered significant.

Results

PCSK9 levels are equally upregulated in Gram-positive and Gram-negative bacterial infections and show a positive correlation with CRP level

During the study period, a total of 800 consecutive blood culture-positive cases were admitted to the ED [19]. After excluding contaminants ($n = 136$) and disregarding missed samples due to technical reasons, we collected the day 0 plasma samples from 481 blood culture-positive cases. As 10 patients were admitted twice and 1 patient three times, the number of individual patients in the cohort was 469. Follow-up blood samples were collected from patients alongside treatment-based routine laboratory testing within the first 4 days of hospitalization. The numbers of samples declined during follow-up, for example because patients were discharged or died. The final numbers of samples were 481, 446, 389, 300 and 137 on days 0, 1, 2, 3 and 4, respectively.

The median level of day 0 plasma PCSK9 in patients (376 ng mL^{-1}, IQR 293–483) was significantly higher than in the control group (188 ng mL^{-1}, IQR 139–264, $P = 0.001$). The PCSK9 level was elevated to the same degree in cases of Gram-positive (381 ng mL^{-1} IQR 292–493, $P < 0.001$) and Gram-negative (median level 380 ng mL^{-1}, IQR 306–465, $P < 0.001$) bacterial infection and remained at equally high levels throughout the sampling period (Fig. 1). We evaluated the correlation between plasma PCSK9 and infection-associated markers. Using Pearson's product-moment analysis, we could not observe a significant correlation between PCSK9 plasma levels and body temperature, leucocyte numbers or cell-free DNA (data not shown). By contrast, there was a significant positive correlation between the PCSK9 and CRP levels in plasma samples from

the first 4 days of hospitalization (day 0, $r = 0.324$, $P < 0.001$; day 1, $r = 0.270$, $P < 0.001$; day 2, $r = 0.251$, $P < 0.001$; day 3, $r = 0.256$, $P < 0.001$; day 4, $r = 0.214$, $P < 0.001$; Fig. 2 and Fig. S1).

The plasma PCSK9 levels are highest in patients with a lower respiratory tract infection and pneumococcal bacteraemia

The plasma PCSK9 levels in relation to different causative organisms are shown in Table 1 (day 0) and in Fig. S2 (days 1–4). When the microbes or microbe groups accounting for less than five samples were excluded, only patients with a *Streptococcus pneumoniae* infection showed significantly higher levels of PCSK9 compared to other cases on day 0 (476 ng mL^{-1}, IQR 319–561, $P = 0.003$). The lowest levels of PCSK9 were seen in patients with polymicrobial bacteraemia (311 mg mL^{-1}, IQR 235–501), but this difference was not statistically significant. When patients were grouped based on the site of infection, the lowest PCSK9 levels were found in individuals suffering from an unknown or unclassifiable infection (352 ng mL^{-1}, IQR 262–474, $P = 0.039$; Table 2). Patients with a lower respiratory tract infection had particularly high
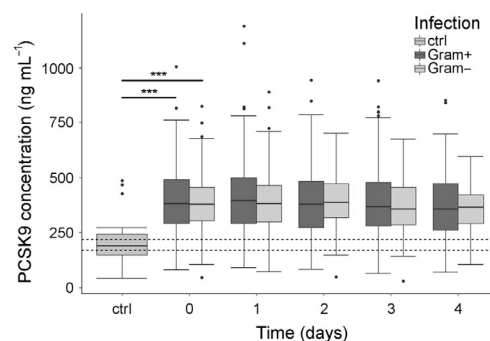

Fig. 1 *PCSK9 plasma levels of bacteraemia patients. PCSK9 concentration of 481 bacteraemia patients and 17 controls were measured using ELISA. Box plot representation of the PCSK9 plasma levels in patients with Gram-positive or Gram-negative infection and in controls on days 0–4. The box represents the interquartile range (25th–75th percentiles) and the whiskers represent the 10th–90th percentiles. Dashed lines mark the reported normal plasma PCSK9 range (170–220 ng mL^{-1}) [13]. PCSK9 levels of both Gram-positive and Gram-negative groups were compared to a control group (ctrl) and both were significantly elevated (***P < 0.001, Welch's two sample t-tests).*
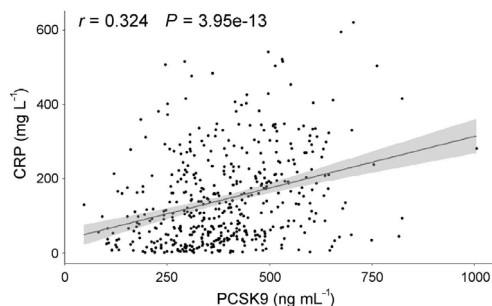
Fig. 2 *Correlation between plasma PCSK9 and CRP levels in bacteraemia patients. PCSK9 and CRP levels were measured in samples from bacteraemia patients on the day of admission to the emergency department. Plasma PCSK9 levels are plotted against CRP levels, and the correlation was calculated using Pearson's product-moment correlation coefficient (r). The grey area shows the 95% confidence interval.*

plasma PCSK9 levels (472 ng mL^{-1}, IQR 315–557, $P = 0.007$), which is in accordance with the findings from microbe type as *S. pneumoniae* is the major pneumonia-causing pathogen.

Association between plasma PCSK9 levels and characteristics of bacteraemia patients, underlying conditions and severity of bacteraemia

Table 3 shows the plasma PCSK9 levels on day 0 stratified by various patient characteristics, underlying conditions and the severity of bacteraemia. The PCSK9 level was significantly lower in male patients ($P = 0.001$), in patients with liver disease ($P < 0.001$) and in those who abused alcohol ($P < 0.001$). By contrast, there was no significant association between PCSK9 and age, cardiovascular disease, diabetes, kidney disease, solid tumours, haematological malignancies or use of oral corticosteroids. On the day of admission, 116 cases (24%) were using statins. Simvastatin (63%) and atorvastatin (28%) were the most commonly used statins with an average dose of 25 mg and 22 mg, respectively. Patients using statins had significantly higher plasma PCSK9 levels (no statin use, 363 ng mL^{-1}, IQR 283–468; statin use, 413 ng mL^{-1}, IQR 335–532, $P < 0.001$).

In our patient cohort, we found that critically ill patients needing vasopressor treatment had significantly lower plasma PCSK9 levels on day 0 (vasopressor treatment, 316 ng mL^{-1}, IQR 256–

Table 1 *Causative organisms and the median level of PCSK9 on the day of admission to the emergency department*

Organisms	n (%)	Median (IQR) plasma PCSK9 level, ng mL^{-1}
Gram-positive	213 (44)	381 (292–493)[a]
Staphylococcus aureus	71 (15)	358 (293–479)
Coagulase-negative Staphlococci	11 (2)	421 (278–484)
Streptococcus pneumoniae	46 (10)	476 (319–561)
β-haemolytic streptococci	43 (9)	382 (288–498)
Viridans streptococci	21 (4)	353 (287–470)
Enterococci	17 (4)	333 (267–414)
Other Gram-positive	4 (1)	618 (327–958)
Gram-negative	222 (46)	380 (306–465)[b]
Escherichia coli	156 (32)	388 (306–442)
Klebsiella species	23 (5)	392 (340–520)
Pseudomonas aeruginosa	18 (4)	345 (292–416)
Other Gram-negative	25 (5)	315 (226–494)
Others	46 (10)	339 (261–488)[c]
Anaerobes	15 (3)	374 (318–464)
Fungi	1 (0.2)	275 (275–275)
Polymicrobial	30 (6)	311 (235–501)
All	481 (100)	376 (293–483)

Day 7 case fatality rates: [a]5.6%; [b]9.5%; [c]23.9%.

438; no vasopressor treatment, 379 ng mL^{-1}, IQR 298–486, $P = 0.026$). There was also a nearly significant trend towards lower PCSK9 levels in patients who required ICU care (ICU patients, 343 ng mL^{-1}, IQR 256–431; non-ICU patients, 379 ng mL^{-1}, IQR 297–486, $P = 0.05$). The severity of bacteraemia according to qSOFA score ≥2, Pitt Bacteraemia Score ≥4, severe sepsis (Sepsis-2 definition) or septic shock (Sepsis-2 definition) was not significantly associated with PCSK9 levels ($P = 0.564, 0.323, 0.120$ and 0.110, respectively).

Lower plasma PCSK9 levels in patients with bacteraemia are associated with mortality

In our cohort, the day 7 case fatality rate was 9%. On day 0, the median level of circulating PCSK9

Table 2 *Site of infection, number of patients who had died by day 7 and the median level of PCSK9 on the day of admission to the emergency department*

Site of infection	n (%)	Died n (%)	Median (IQR) plasma PCSK9 level, ng mL^{-1}
Unknown/unclassifiable	116 (24)	18 (16)	352 (262–474)
Urinary tract	134 (28)	9 (7)	388 (303–468)
Intra-abdominal	83 (17)	12 (15)	365 (291–443)
Skin, soft tissue and bones	65 (14)	2 (3)	377 (306–527)
Lower respiratory tract	48 (10)	4 (8)	472 (315–557)
Surgical site or foreign body	36 (7)	0 (0)	367 (287–474)
Others	19 (4)	1 (5)	374 (310–447)

There were 29 cases with two different infection sites.

was 306 ng mL^{-1} (IQR 247–454) in patients who died by day 7 and 381 ng mL^{-1} (IQR 298–486) in patients who survived beyond the first week ($P = 0.022$, Table 4). Patients who had died by day 28 had also significantly (approximately 20%) lower PCSK9 plasma levels on days 0, 1 and 2 than survivors. The occurrence of true infection-associated deaths is lower than the occurrence of death related to underlying disease beyond the first month after diagnosis of bacteraemia. Nevertheless, lower PCSK9 levels on day 0 also showed a significant association with 90-day mortality (death by day 90, 320 ng mL^{-1}, IQR 249–442; survival on day 90, 388 ng mL^{-1}, IQR 307–489, $P = 0.001$).

Finally, we investigated whether the association between PCSK9 levels and death was dependent on patient characteristics or underlying conditions that affect PCSK9 levels. In male patients, low PCSK9 levels remained significantly associated with day 7 mortality ($P = 0.023$). Patients who did not receive statin medication also showed a significant association between PCSK9 levels on day 0 and mortality (death by day 7, 291 ng mL^{-1}, IQR 214–438; survival on day 7, 373 ng mL^{-1}, IQR 292–473, $P = 0.007$). Furthermore, there were 49 cases with liver disease and a high day 7 and day 28 fatality rate (20% and 31%, respectively) and a low median level of PCSK9 on day 0 (284 ng mL^{-1}, IQR 176–352). In patients without liver disease, the association between low PCSK9 and death by day 7 or 28 was not statistically significant ($P = 0.336$ and 0.059, respectively), indicating that the association between PCSK9 and mortality is partly dependent on liver disease.

Discussion

To our knowledge, this is the first study in which the level of plasma PCSK9 in cases with blood culture-positive infection was evaluated in a large ED patient cohort. Our results demonstrate that plasma PCSK9 levels are upregulated in bacteraemia patients irrespective of the type of causative organism or infection focus. Particularly high PCSK9 levels were seen in patients with *S. pneumoniae* infection and lower respiratory tract infections. PCSK9 levels showed a highly significant positive correlation with plasma CRP, and patients with liver disease released less PCSK9 into the plasma. Of note, our findings imply that plasma PCSK9 resembles the liver-derived acute-phase reactants [22], and a lowered PCSK9 response is significantly associated with a fatal prognosis.

Proprotein convertase subtilisin/kexin enzyme 9 levels are elevated by an inflammatory response [23] and in critically ill ICU patients [14,15], but how PCSK9 levels vary in different types of bacterial infections has not previously been explored. Our bacteraemia cases had a median day 0 PCSK9 level of 376 ng mL^{-1}, which is approximately double the value reported in a meta-analysis of 15 cholesterol studies (final pooled 95% confidence interval 170–220 ng mL^{-1} [13]). It is notable that the patients in our small control group, who had recovered from bacteraemia, had normal levels of plasma PCSK9, which indicates that the elevation of PCSK9 induced by the infection does not persist. We could not detect any differences in the levels of plasma PCSK9 between patients with Gram-negative or Gram-positive infections. This is in accordance with findings that the major lipoproteins of

Table 3 *Plasma PCSK9 levels on the day of admission to the emergency department stratified by patient characteristics, underlying conditions and severity of bacteraemia*

Factor	n (%)	Median (IQR) plasma PCSK9 level on day of admission, ng mL^{-1}		
		Factor present	Factor absent	*P*-value
Male	253 (53)	356 (273–472)	405 (310–492)	0.001
Age over 60 years	333 (69)	381 (298–486)	368 (275–478)	0.223
Age over 80 years	107 (22)	379 (304–477)	376 (289–485)	0.804
Cardiovascular disease	155 (32)	388 (299–479)	371 (291–484)	0.868
Diabetes any type	137 (29)	375 (295–468)	379 (292–487)	0.591
Chronic kidney disease[a]	66 (14)	364 (297–440)	379 (292–487)	0.152
Liver disease	49 (10)	284 (176–352)	389 (305–488)	<0.001
Alcohol abuse[b]	49 (10)	264 (190–388)	388 (306–489)	<0.001
Solid tumour with metastasis	55 (11)	399 (291–484)	375 (293–482)	0.783
Haematological malignancy	45 (9)	382 (308–485)	376 (291–484)	0.508
Use of oral corticosteroids	92 (19)	415 (306–487)	370 (291-480)	0.125
Use of statins	116 (24)	413 (335–532)	363 (283–468)	<0.001
Severity of bacteraemia				
qSOFA score ≥ 2[c]	128 (28)	378 (263–489)	376 (299–480)	0.564
Need vasopressor	49 (10)	316 (256–438)	379 (298—486)	0.026
Need mechanical ventilation	24 (5)	309 (235–593)	377 (395–481)	0.631
Severe sepsis[d]	145 (30)	363 (266–477)	380 (301–486)	0.120
Septic shock[a]	36 (8)	347 (256–438)	378 (296–486)	0.110
Admitted from ED to ICU	44 (9)	343 (256–431)	379 (297–486)	0.050
Pitt Bacteraemia Score ≥ 4[e]	58 (12)	344 (262–493)	380 (298–482)	0.323
Death by day 7	45 (9)	306 (257–454)	381 (298–486)	0.022
Death by day 28	71 (15)	308 (242–431)	387 (299–487)	0.001
Death by day 90	101 (21)	320 (249–441)	388 (307–489)	0.001

[a]History of creatinine more than 120 µmol L^{-1}. [b]Social or medical problems of alcohol abuse in the past 12 months. [c]Data available for 458 cases. [d]According to Sepsis-2 definition. [e]Data available for 474 cases.

both Gram-negative (LPS) and Gram-positive (LTA) bacteria are removed from the circulation in an LDLR/PCSK9-dependent manner [14].

Lower respiratory tract infections, especially those caused by *S. pneumoniae*, typically result in a severe inflammatory response as confirmed by a marked rise in CRP level [24]. Similarly, high PCSK9 levels in patients with blood culture-confirmed lower respiratory tract infection and *S. pneumoniae* imply that PCSK9 levels are associated with the strength of the inflammatory response. Indeed, when we evaluated the associations between infection markers, PCSK9 showed highly significant correlations with CRP levels on

days 0–4 after admission to the ED. This is in line with a previous study demonstrating that PCSK9 and TNFα plasma levels were positively correlated in healthy adults [9]. It is intriguing that in a recent study it was found that PCSK9 levels were lowered in patients after elective abdominal aortic aneurysm repair surgery [25], which indicates that PCSK9 is not universally upregulated under stress. In our study, the majority of patients (445/481) started receiving antibiotic treatment on day 0, which could in theory increase the levels of pathogenic lipids in the circulation. However, we did not observe any significant changes in PCSK9 levels during the first 4 days of hospitalization.

Table 4 *Plasma PCSK9 levels during days 0 to 4 after admission to the emergency department in all cases and in individuals who died by or survived to days 7 and 28*

| Days after admission | Median (IQR) plasma PCSK9 level, ng mL^{-1} | | | | | | |
	All	Died by day 7	Survived to day 7	*P*-value	Died by day 28	Survived to day 28	*P*-value
Day 0	376 (293–483)	306 (247–454)	381 (298–486)	0.022	308 (242–431)	387 (299–487)	0.001
Day 1	383 (296–484)	351 (228–435)	385 (300–485)	0.062	348 (213–429)	389 (303–488)	0.003
Day 2	381 (295–478)	321 (248–429)	385 (298–482)	0.030	330 (219–446)	387 (300–490)	0.005
Day 3	360 (283–465)	348 (225–428)	364 (284–472)	0.216	355 (268–438)	360 (284–470)	0.717
Day 4	356 (274–452)	324 (189–440)	359 (274–457)	0.557	344 (242–444)	356 (275–460)	0.646
Maximum level day 0–4	455 (362–566)	360 (256–502)	457 (374–559)	<0.001	378 (256–506)	470 (376–560)	<0.001

In addition to inflammatory conditions, plasma PCSK9 levels are elevated by the use of lipid-lowering drugs, such as statins [26]. We observed a similar upregulation of plasma PCSK9 in bacteraemia patients using statins, but also identified other factors that were associated with lower plasma PCSK9 levels (male sex, liver disease and alcohol abuse). The PCSK9 protein is primarily produced by liver cells, and low serum PCSK9 levels are negatively correlated with poor liver function in patients without infection [27]. However, PCSK9 is also expressed in other organs, including the brain and small intestine [28,29]. Our finding of the association between liver disease and PCSK9 level indicates that the main source of circulating PCSK9 in bacteraemia patients is the liver.

We found that the reduced elevation of PCSK9 in the plasma of bacteraemia patients was significantly associated with mortality at days 7, 28 and 90. Higher circulating PCSK9 levels in patients with suspected sepsis have previously been shown to be associated with the development of acute organ failure, indicating that higher PCSK9 levels are found in the most critically ill patients [13]. Our results are inconsistent as patients needing mechanical ventilation or vasopressors had lower levels of PCSK9 than those who did not require intensive care. Most importantly, patients who had died by day 7, 28 or 90 also had statistically significantly reduced levels of plasma PCSK9. Of note, the 28-day mortality was higher in our cohort than in a previous study by Boyd and colleagues [13] (15% vs. 5%), which could reflect the fact that we only included culture-positive cases.

Exclusion of statin users or restricting the analyses to male patients did not abolish the association between a lowered PCSK9 response and death. By contrast, mortality was at least partly dependent on liver disease as well as related alcohol abuse. This is in line with previous findings by Schlegel and colleagues in patients without infection with end-stage liver disease [27]. The authors found that liver disease patients had lower serum PCSK9 levels (medium 106.39 ng mL^{-1}) than healthy populations and that there was a negative correlation between serum PCSK9 and markers of liver function. In our bacteraemia cohort, PCSK9 levels were upregulated by infection also in patients with liver disease, but to a lesser extent. It is thus noteworthy that even higher than normal plasma PCSK9 levels can be associated with mortality in bacteraemia patients.

Proprotein convertase subtilisin/kexin enzyme 9-blocking antibodies have been proposed to be beneficial in reducing the lipoprotein-triggered inflammation in patients with systemic infectious disease [11,12]. Our results show that higher plasma PCSK9 levels are not detrimental in bacteraemia patients. It is also important to note that in an experimental model the inhibition of PCSK9 was not found to reduce LPS-induced mortality in mice [30] and that a slight rise in the incidence of upper respiratory tract infection was observed in patients treated with a PCSK9 inhibitor (2.1% alirocumab vs. 1.1% placebo) [31,32]. Moreover, a recent study showed that a *PCSK9* loss-of-function variant was not associated with an increased risk of hospitalization due to serious infection [33]. Hence, the use of PCSK9 inhibitors in sepsis remains controversial.

Our study has several limitations that should be addressed. This was a single-centre tertiary hospital study involving only culture-positive patients. Our results should not be extrapolated to culture-negative cases with infection and should be reproduced using an independent study cohort. A few culture-positive cases were missed due to technical problems concerning sample collection/storage, but the number of these samples is low and the possible bias has been demonstrated to be insignificant [19].

In conclusion, PCSK9 remains in the limelight when novel diagnostic and treatment options for systemic infectious diseases are considered. As PCSK9 inhibitors have only recently been added to the available clinical options, our understanding of their effects in the course of severe infections remains limited. As data from PCSK9 plasma measurements accumulate, we will begin to better understand the significance of PCSK9 in health and disease.

Conflict of interest statement

None of the authors has any conflicts of interest to declare.

Funding

References

1 Seidah NG, Prat A. The biology and therapeutic targeting of the proprotein convertases. *Nat Rev Drug Discov* 2012; **11:** 367–83.

2 Seidah NG, Chretien M, Mbikay M. The ever-expanding saga of the proprotein convertases and their roles in body homeostasis: emphasis on novel proprotein convertase subtilisin kexin number 9 functions and regulation. *Curr Opin Lipidol* 2018; **29:** 144–50.

3 Turpeinen H, Ortutay Z, Pesu M. Genetics of the first seven proprotein convertase enzymes in health and disease. *Curr Genomics* 2013; **14:** 453–67.

4 Cohen JC, Boerwinkle E, Mosley TH Jr, Hobbs HH. Sequence variations in PCSK9, low LDL, and protection against coronary heart disease. *N Engl J Med* 2006; **354:** 1264–72.

5 Sabatine MS, Giugliano RP, Keech AC *et al.* Evolocumab and clinical outcomes in patients with cardiovascular disease. *N Engl J Med* 2017; **376:** 1713–22.

6 Stein EA, Mellis S, Yancopoulos GD *et al.* Effect of a monoclonal antibody to PCSK9 on LDL cholesterol. *N Engl J Med* 2012; **366:** 1108–18.

7 Ding Z, Liu S, Wang X *et al.* Cross-talk between LOX-1 and PCSK9 in vascular tissues. *Cardiovasc Res* 2015; **107:** 556–67.

8 Giunzioni I, Tavori H, Covarrubias R *et al.* Local effects of human PCSK9 on the atherosclerotic lesion. *J Pathol* 2016; **238:** 52–62.

9 Ricci C, Ruscica M, Camera M *et al.* PCSK9 induces a proinflammatory response in macrophages. *Sci Rep* 2018; **8:** 2267.

10 Walley KR, Thain KR, Russell JA *et al.* PCSK9 is a critical regulator of the innate immune response and septic shock outcome. *Sci Transl Med* 2014; **6:** 258ra143.

11 Walley KR. Role of lipoproteins and proprotein convertase subtilisin/kexin type 9 in endotoxin clearance in sepsis. *Curr Opin Crit Care* 2016; **22:** 464–9.

12 Khademi F, Momtazi-Borojeni AA, Reiner Z, Banach M, Al-Rasadi KA, Sahebkar A. PCSK9 and infection: a potentially useful or dangerous association? *J Cell Physiol* 2018; **233:** 2920–7.

13 Boyd JH, Fjell CD, Russell JA, Sirounis D, Cirstea MS, Walley KR. Increased plasma PCSK9 levels are associated with reduced endotoxin clearance and the development of acute organ failures during sepsis. *J Innate Immun* 2016; **8:** 211–20.

14 Grin PM, Dwivedi DJ, Chathely KM *et al.* Low-density lipoprotein (LDL)-dependent uptake of Gram-positive lipoteichoic acid and Gram-negative lipopolysaccharide occurs through LDL receptor. *Sci Rep* 2018; **8:** 10496.

15 Le Bras M, Roquilly A, Deckert V *et al.* Plasma PCSK9 is a late biomarker of severity in patients with severe trauma injury. *J Clin Endocrinol Metab* 2013; **98:** E732–6.

16 Levy MM, Fink MP, Marshall JC *et al.* 2001 SCCM/ESICM/ACCP/ATS/SIS international sepsis definitions conference. *Crit Care Med* 2003; **31:** 1250–6.

17 Singer M, Deutschman CS, Seymour CW *et al.* The third international consensus definitions for sepsis and septic shock (Sepsis-3). *JAMA* 2016; **315:** 801–10.

18 Korvick JA, Marsh JW, Starzl TE, Yu VL. Pseudomonas aeruginosa bacteremia in patients undergoing liver transplantation: an emerging problem. *Surgery* 1991; **109:** 62–8.

19 Rannikko J, Syrjanen J, Seiskari T, Aittoniemi J, Huttunen R. Sepsis-related mortality in 497 cases with blood culture-positive sepsis in an emergency department. *Int J Infect Dis* 2017; **58:** 52–7.

20 Rannikko J, Seiskari T, Huttunen R *et al.* Plasma cell-free DNA and qSOFA score predict 7-day mortality in 481 emergency department bacteraemia patients. *J Intern Med* 2018; **284:** 418–26.

21 Huttunen R, Syrjanen J, Aittoniemi J *et al.* High activity of indoleamine 2,3 dioxygenase enzyme predicts disease severity and case fatality in bacteremic patients. *Shock* 2010; **33:** 149–54.

22 Jain S, Gautam V, Naseem S. Acute-phase proteins: as diagnostic tool. *J Pharm Bioallied Sci* 2011; **3:** 118–27.

23 Feingold KR, Moser AH, Shigenaga JK, Patzek SM, Grunfeld C. Inflammation stimulates the expression of PCSK9. *Biochem Biophys Res Commun* 2008; **374:** 341–4.

24 Almirall J, Bolibar I, Toran P *et al.* Contribution of C-reactive protein to the diagnosis and assessment of severity of community-acquired pneumonia. *Chest* 2004; **125:** 1335–42.

25 Druce I, Abujrad H, Chaker S *et al.* Circulating PCSK9 is lowered acutely following surgery. *J Clin Lab Anal* 2018; **32:** e22358.

26 Nozue T. Lipid lowering therapy and circulating PCSK9 concentration. *J Atheroscler Thromb* 2017; **24:** 895–907.

27 Schlegel V, Treuner-Kaueroff T, Seehofer D *et al.* Low PCSK9 levels are correlated with mortality in patients with end-stage liver disease. *PLoS ONE* 2017; **12:** e0181540.

28 Mannarino MR, Sahebkar A, Bianconi V, Serban MC, Banach M, Pirro M. PCSK9 and neurocognitive function: should it be still an issue after FOURIER and EBBINGHAUS results? *J Clin Lipidol* 2018; **12:** 1123–32.

29 Levy E, Ben Djoudi Ouadda A, Spahis S *et al.* PCSK9 plays a significant role in cholesterol homeostasis and lipid transport in intestinal epithelial cells. *Atherosclerosis* 2013; **227:** 297–306.

30 Berger JM, Loza Valdes A, Gromada J, Anderson N, Horton JD. Inhibition of PCSK9 does not improve lipopolysaccharide-induced mortality in mice. *J Lipid Res* 2017; **58:** 1661–9.

31 Filippatos TD, Christopoulou EC, Elisaf MS. Pleiotropic effects of proprotein convertase subtilisin/kexin type 9 inhibitors? *Curr Opin Lipidol* 2018; **29:** 333–9.

32 Jones PH, Bays HE, Chaudhari U *et al.* Safety of alirocumab (A PCSK9 Monoclonal Antibody) from 14 randomized trials. *Am J Cardiol* 2016; **118:** 1805–11.

33 Mitchell KA, Moore JX, Rosenson RS *et al.* PCSK9 loss-of-function variants and risk of infection and sepsis in the Reasons for Geographic and Racial Differences in Stroke (REGARDS) cohort. *PLoS ONE* 2019; **14:** e0210808.

Correspondence: Juha Rannikko MD, Department of Internal Medicine, Tampere University Hospital, Box 2000, FI-33521 Tampere, Finland.
(fax: +358-3-31164333; e-mail: juha.rannikko@gmail.com)
and
Marko Pesu, MD, PhD, Tampere University, Faculty of Medicine and Health Technology, Arvo Ylpön katu 34, FI-33520 Tampere, Finland.
(e-mail: marko.pesu@tuni.fi)

Supporting Information

Additional Supporting Information may be found in the online version of this article:
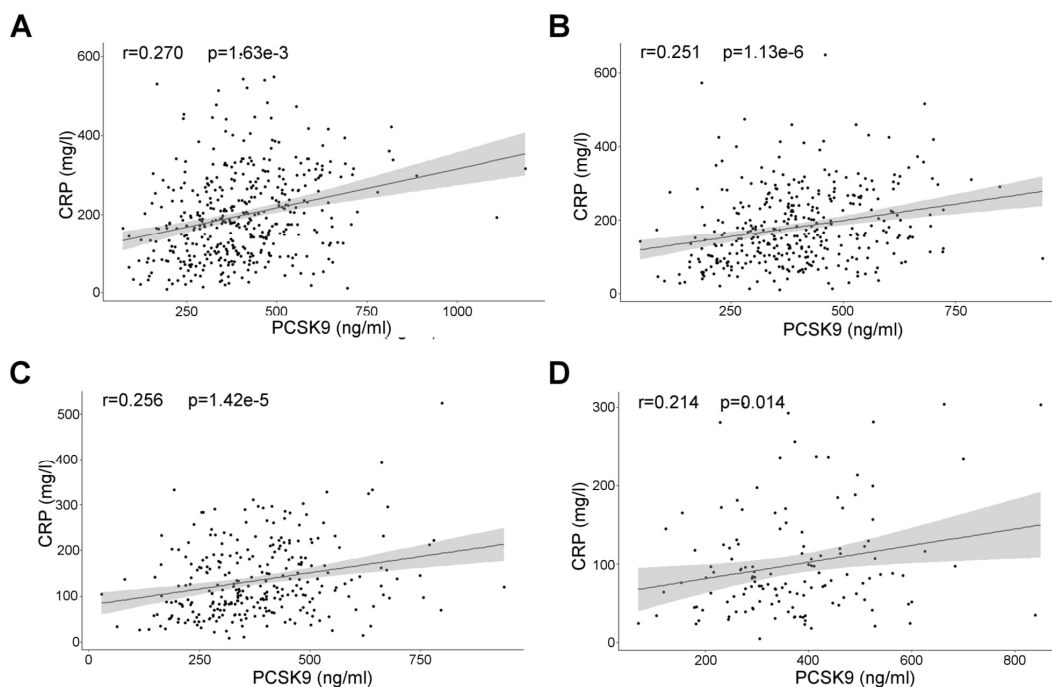
Fig. S1. CRP/PCSK9 correlation in plasma on days 1–4 after admission to the emergency department.

Fig. S2. PCSK9 plasma levels in cases with different bacterial infection aetiologies on days 1–4 after admission to the emergency department.■
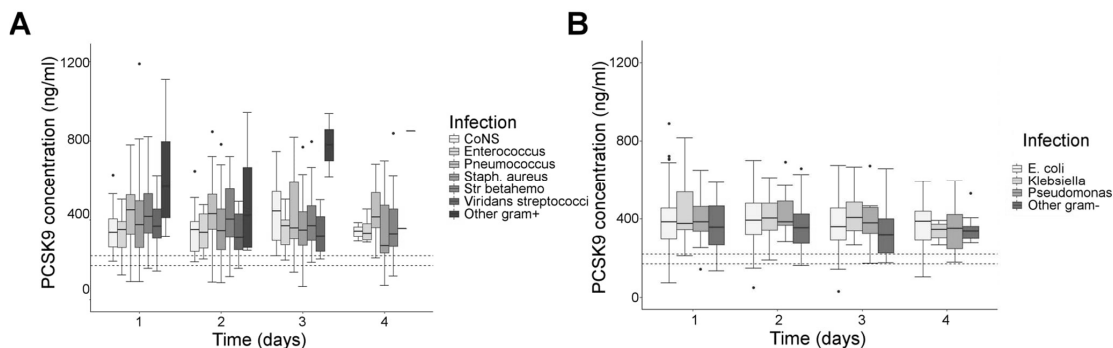
Supplementary Fig. 2 PCSK9 plasma levels in cases with different bacterial infection aetiologies on days 1–4 after admission to the emergency department. (A) Box plot representation of the PCSK9 level measured from the plasma of patients infected with Gram-positive bacteria on days 1–4. The PCSK9 concentrations in patients infected with *Staphylococcus aureus*, coagulase-negative Staphylococci (CoNS), beta-haemolytic streptococci*,* pneumococci, viridans streptococci*,* enterococci or other Gram-positive bacteria are shown separately. Dashed lines indicate the previously reported range of plasma PCSK9 levels in healthy individuals (170–220 ng/mL; [13]). (B) Plasma PCSK9 levels in patients with Gram-negative bacterial infection on days 1–4. The PCSK9 levels of patients infected with *Escherichia coli*, *Klebsiella species*, *Pseudomonas aeruginosa* or other Gram-negative bacteria are shown separately. Dashed lines indicate the previously reported range of PCSK9 plasma levels in healthy individuals.

Supplementary Fig. 1 CRP/PCSK9 correlation in plasma on days 1–4 after admission to the emergency department. CRP and PCSK9 levels were measured in samples collected on days 1–4 during hospital care. Plasma PCSK9 levels are plotted against CRP levels on day 1 (A), day 2 (B), day 3 (C) and day 4 (D). The correlation between PCSK9 and CRP was calculated using the Pearson's product-moment correlation coefficient (*r*). The grey area shows the 95% confidence interval.

PUBLICATION
II

The Proprotein Convertase Subtilisin/Kexin Type 9 (PCSK9) Regulates the Production of Acute Phase Reactants from the Liver

Dafne Jacome Sanz, Anni Saralahti, Meeri Pekkarinen, Juha Kesseli, Matti Nykter, Mika Rämet, Markus Ojanen and Marko Pesu

ORIGINAL ARTICLE

Proprotein convertase subtilisin/kexin type 9 regulates the production of acute-phase reactants from the liver

Dafne Jacome Sanz[1] | Anni K. Saralahti[2] | Meeri Pekkarinen[3] | Juha Kesseli[3] |
Matti Nykter[3] | Mika Rämet[2,4,5,6] | Markus J. T. Ojanen[1] 🄳 | Marko Pesu[1,7]

[1]Laboratory of Immunoregulation, Faculty of Medicine and Health Technology, Tampere University, Tampere, Finland

[2]Laboratory of Experimental Immunology, Faculty of Medicine and Health Technology, Tampere University, Tampere, Finland

[3]Laboratory of Computational Biology, Faculty of Medicine and Health Technology, Tampere University, Tampere, Finland

[4]Vaccine Research Center, Faculty of Medicine and Health Technology, Tampere University, Tampere, Finland

[5]PEDEGO Research Unit, Medical Research Center, University of Oulu, Oulu, Finland

[6]Department of Children and Adolescents, Oulu University Hospital, Oulu, Finland

[7]Fimlab laboratories Ltd, Tampere, Finland

Correspondence
Dr. Markus J. T. Ojanen, Faculty of Medicine and Health Technology, Tampere University, Arvo Ylpön katu 34, FI-33520 Tampere, Finland.
Email: markus.ojanen@tuni.fi

Funding information
This study was financially supported by the Academy of Finland (Grant 295814; MO/Ma.P.), the Cancer Foundation of Finland (Grant 180138; Ma.P. and 190146; MO/Ma.P.), the Paulo Foundation (MO), Tampere ImmunoExcellence—Vaccines and Immunomodulation Platform (AS, MO), the Tampere University Doctoral Programme in Medicine and Health Technology (DS), the Tampere Tuberculosis Foundation (DS, MR, MO, Ma.P.), the Competitive State Research Financing of the Expert Responsibility Area of Tampere University Hospital (Grant X50070; Ma.P.). The funding parties were not involved in study design, in the collection, analysis and interpretation of data, in the writing of the report or in the decision to submit the article for publication.

Handling Editor: Stefano Romeo

Abstract

Background & Aims: Proprotein convertase subtilisin/kexin type 9 (PCSK9) controls blood cholesterol levels by fostering the LDL receptor (LDLR) degradation in hepatocytes. Additionally, PCSK9 has been suggested to participate in immunoregulation by modulating cytokine production. We studied the immunological role of PCSK9 in *Streptococcus pneumoniae* bacteraemia in vivo and in a human hepatocyte cell line.

Methods: CRISPR/Cas9 mutagenesis was utilized to create *pcsk9* knock-out (KO) zebrafish, which were infected with *S pneumoniae* to assess the role of PCSK9 for the survival of the fish and in the transcriptomic response of the liver. The direct effects of PCSK9 on the expression of acute-phase reaction (APR) genes were studied in HepG2 cells.

Results: The *pcsk9* KO zebrafish lines (*pcsk9*[tpu-13] and *pcsk9*[tpu-2,+15]) did not show developmental defects or gross phenotypical differences. In the *S pneumoniae* infected zebrafish, the mortality of *pcsk9* KOs was similar to the controls. A liver-specific gene expression analysis revealed that a pneumococcal challenge upregulated *pcsk9*, and that the *pcsk9* deletion reduced the expression of APR genes, including *hepcidin antimicrobial peptide* (*hamp*) and *complement component 7b* (*c7b*). Accordingly, silencing *PCSK9* in vitro in HepG2 cells using small interfering RNAs (siRNAs) decreased *HAMP* expression.

Conclusions: We demonstrate that PCSK9 is not critical for zebrafish survival in a systemic pneumococcal infection. However, *PCSK9* deficiency was associated with the lower expression of APR genes in zebrafish and altered the expression of innate immunity genes in a human hepatocyte cell line. Overall, our data suggest an evolutionarily conserved function for PCSK9 in APR in the liver.

KEYWORDS

innate immunity, *Pneumococcus*, sepsis, zebrafish

1 | INTRODUCTION

Proprotein convertase subtilisin/kexins (PCSKs) are serine endoproteases that enzymatically process and convert biologically inactive proproteins into functional end-products. PCSKs are important not only in maintaining homeostasis in the body, but also in a number of pathological conditions, such as malignancies and inflammatory disorders.[1,2] In contrast to the other PCSK enzymes, PCSK9 has a fundamental non-enzymatic role in cholesterol homeostasis by targeting the LDL receptor (LDLR) for lysosomal degradation.[3,4] Consequently, loss-of-function mutations of PCSK9 are associated with decreased plasma LDL-cholesterol levels and protection against coronary heart disease (CHD),[5] whereas gain-of-function PCSK9 variants have been reported to cause hypercholesterolemia.[6] Collectively, mechanistic and genetic insights into the PCSK9-mediated regulation of hepatic clearance of blood LDL-cholesterol have paved the way for the existing anti-PCSK9 antibodies and small interfering RNAs (siRNAs) as therapeutics to prevent CHD.[7–9]

In addition to its undisputable significance in lipid metabolism, PCSK9 has recently been suggested to affect the pathogenesis of dengue virus infection[10] as well as to regulate the production of inflammatory cytokines. In fact, although tomographic analysis in patients receiving PCSK9 inhibitors has suggested that the arterial inflammation is not affected by the PCSK9 levels,[11] experimental evidence from mice argues that PCSK9 can increase the magnitude of the pro-inflammatory response in macrophages, and subsequently exacerbate foam cell formation and atherosclerosis.[12,13] Moreover, the PCSK9-controlled production of inflammatory cytokines, such as tumour necrosis factor (TNF) and interleukin 6 (IL6), leads to a dysregulated systemic inflammatory response in septic infections.[14,15] Importantly, since lipoprotein particles, particularly VLDL, LDL, and HDL, are able to bind and neutralize pathogen-associated lipids such as lipopolysaccharide (LPS) and lipoteichoic acid from the circulation,[14,16] the inhibition of PCSK9 has potentially a dual beneficial effect in treating septic patients. Accordingly, improved survival has been reported in septic patients with loss-of-function mutations in *PCSK9* as well as in situations where the levels of PCSK9 in the plasma are lowered.[14,15,17] In contrast, recent clinical data have suggested that neither loss- nor gain-of-function variants of PCSK9 are associated with morbidity,[18] and that low PCSK9 levels in bacteraemia patients are associated with increased mortality.[19–21] All in all, the contradictory clinical data necessitates additional research into the role of PCSK9 in systemic bacterial infections.

Lay summary

We deleted the proprotein convertase *pcsk9* gene in zebrafish and demonstrated that the lack of *pcsk9* does not cause developmental defects or impact the survival from pneumococcal infection. However, gene expression studies indicated that deleting PCSK9 is associated with lower production of the acute-phase response genes from the liver. Our findings unravel a novel immunoregulatory function for the proprotein convertase PCSK9 in the liver.

Key points

- Deleting pcsk9 in zebrafish using CRISPR/Cas9 mutagenesis does not cause developmental defects or morphological abnormalities.
- Pcsk9 is dispensable for zebrafish survival in a systemic S. pneumoniae infection.
- Pcsk9 KO is associated with reduced expression of acute-phase reaction genes in pneumococcus infected zebrafish.
- PCSK9 siRNA alters the expression of innate immunity genes in a human hepatocellular carcinoma cell line.

We have previously shown that a *Streptococcus pneumoniae* infection can model the pathogenesis of streptococcal bacteraemia in both zebrafish (*Danio rerio*) larvae and in adult fish.[22,23] Although the larvae can be specifically used to study the innate immunity against bacteria, the adult zebrafish model enables systemic and organ-specific studies of the immune response as a whole.[24,25] Furthermore, the zebrafish CRISPR/Cas9 mutagenesis system enables targeted modification of the fish genome to create gene knockout (KO) animals.[26] In this study, we used CRISPR/Cas9 to create two *pcsk9* KO zebrafish lines (*pcsk9*[tpu-13] and *pcsk9*[tpu-2,+15]) and determined whether *pcsk9* is critical for zebrafish survival in a systemic *S pneumoniae* infection. Additionally, we used RNA profiling in the

in vivo zebrafish pneumococcal model and in human HepG2 cells to evaluate the immunoregulatory function of PCSK9 at the molecular level in the liver.

2 | EXPERIMENTAL PROCEDURES

2.1 | Zebrafish use and ethics statement

The zebrafish maintenance and the experiments followed the Reporting of In Vivo Experiments (ARRIVE) and EU Directive (2010/63/EU) guidelines and the Finnish Act on the Protection of Animals Used for Scientific or Educational Purposes (497/2013). The experiments were approved by the Animal Experiment Board of Finland (permits: ESAVI/10079/04.10.06/2015 and ESAVI/2235/04.10.07/2015). F2-generation $pcsk9^{tpu-13}$ and $pcsk9^{tpu-2,+15}$ mutants were used in the larval infections. In the adult zebrafish experiments, 4- to 7-month-old wild type (WT) AB, F2-generation $pcsk9^{tpu-13}$ and F3-generation $pcsk9^{tpu-2,+15}$ zebrafish were used. Zebrafish larvae were maintained in E3-medium (5 mM NaCl, 0.17 mM KCl, 0.33 mM CaCl$_2$, 0.33 mM MgSO$_4$, 0.0003 g/l methylene blue) at 28.5℃ until 7 days postfertilization (dpf). Unchallenged adult fish were maintained in a conventional flow through system (Aquatic Habitats, Florida, USA) with an automated light/dark cycle (14 h/10 h) and fed once a day with Gemma Micro 500 (Skretting, Stavanger, Norway). *S pneumoniae* infected adults were kept in a separate flow through system (Aqua Schwarz GMbH, Göttingen, Germany) or conductivity- (800 μs) and pH- (7.6) adjusted water was manually changed twice a day and the tanks kept at 28.5℃ for the duration of the experiment. An identical light/dark cycle compared with the unchallenged fish was used and the fish were fed once a day with Gemma Micro 500 (Skretting). Adult zebrafish infected with pneumococcus were monitored at least two times a day to follow the humane endpoint criteria as defined in the permit for animal experiments.

2.2 | Zebrafish genotyping

Both $pcsk9^{tpu-13}$ and $pcsk9^{tpu-2,+15}$ mutant zebrafish lines were genotyped using Sanger sequencing and the following primers; F: 5´-AGTAAAGTTGCCCCATGTGG-3´ and R: 5´-TAAGTGCAAAGAGTGTGATTTGG-3´. CRISPR/Cas9 mutagenesis efficiency was estimated with the following formula: % mutagenesis = $100 \times [1 - (1 - \text{fraction of cleavage})^{1/2}]$ [27] and the effects of the indel mutations on the protein sequence using the Translate tool (Expasy; SIB, Swiss Institute of Bioinformatics, https://web.expasy.org/translate/).[28]

2.3 | CRISPR/Cas9 mutagenesis

Nonsense *pcsk9* mutation carrying zebrafish lines ($pcsk9^{tpu-13}$ and $pcsk9^{tpu-2,+15}$) were created as previously described with slight adjustments.[26,29] Susceptible guide RNA (gRNA) target sites were identified using CHOPCHOP v2 (https://chopchop.cbu.uib.no/),[30] and 170 ng of *pcsk9* exon 3 gRNA together with 300 pg of in-house produced Cas9 protein (Protein Service core facility, Tampere University) (Supplementary Methods) was used for mutagenesis. The Cas9 expression plasmid 1xNLS-pMJ915v2 was a gift from Jennifer Doudna (Addgene plasmid #88915; http://n2t.net/addgene:88915).[31]

2.4 | Experimental *S pneumoniae* infections

The pneumococcal (*S pneumoniae* serotype 4, T4, sequence type 205) culture and infections followed previously established protocols.[22,23] In brief, 2-day-old zebrafish were anesthetized with 0.02% 3-aminobenzoic acid ethyl ester (Sigma-Aldrich, Missouri, USA) and 2 nl of bacteria were suspended in 0.2 M potassium chloride (KCl) with 7 mg/ml of tetramethylrhodamine dextran (Thermo Fisher Scientific, Massachusetts, USA) and microinjected into the blood circulation valley. The survival of the larvae was monitored twice a day during the first 50 hours post infection (hpi) and subsequently once a day until 5 days post infection (dpi). Adult zebrafish were similarly anesthetized, and then injected with 5 μl of *S pneumoniae* in a suspension of 10 mM phosphate-buffered saline (PBS) and 0.3 mg/ml phenol red (Sigma-Aldrich) into the abdominal cavity using a 30-gauge Omnican 100 insulin needle (Braun, Melsungen, Germany). Colony forming units (CFU) of viable *S pneumoniae* were counted after culturing inoculates of bacteria on 5% lamb blood agar plates overnight at 37℃ with 5% CO$_2$. To create randomized and blinded experimental set up for the survival experiments, both fish lines were infected prior genotyping as larvae, whereas the $pcsk9^{tpu-2,+15}$ fish line was infected prior genotyping in the adult fish experiments. Thirteen samples were excluded from the larvae survival analysis and four samples from the adult zebrafish experiments because of failed genotyping. Acclimatization periods were not used prior infections.

2.5 | RNA isolation and quantitative PCR

Adult zebrafish tissues or HepG2 cells were homogenized and the removal of genomic DNA (gDNA) and RNA isolation were performed according to the manufacturer's instructions using the RNeasy Mini Kit or RNeasy Plus Mini Kit (Qiagen, Hilden, Germany). Reverse transcriptions were done using the iScript cDNA synthesis kit (Bio-Rad Laboratories, California, USA), and the relative gene expression of the target genes were determined with quantitative PCR (qPCR) using the PowerUp SYBR master mix (Thermo Fisher Scientific) and either the CFX96 (Bio-Rad Laboratories) or the QuantStudio 12K Flex (Applied Biosystems, California, USA) detection systems. CFX Manager software (v.3.1; Bio-Rad Laboratories) and QuantStudio 12K Flex Software (v.1.2.2; Applied Biosystems) was used for data analysis. The target gene expression was normalized to either the *eukaryotic translation elongation factor 1 alpha 1, like 1* (*eef1a1l1* or *ef1a*, zebrafish

data) expression [32] or to *glyceraldehyde 3-phosphate dehydrogenase* (*GAPDH*, HepG2 data) using the $2^{(-\Delta Ct)}$ method. PCR contamination as well as the specificity of the qPCR products were monitored using non-template (H_2O) as well as no-reverse transcriptase controls and performing a melt curve analysis and 1.5% agarose TAE gel electrophoresis. qPCR primer sequences are depicted in Table S1.

2.6 | RNA sequencing

The RNA quality was controlled with the Fragment Analyzer system (Advanced Analytical, Inc, Ankeny, USA) and the Standard Sensitivity RNA Analysis Kit (15 nt) (Advanced Analytical). RNA sequencing was done by Novogene Co. (Hong Kong, Special Administrative Region of the People's Republic of China) and the data were provided in a FASTQ format. Detailed description of the differential gene expression analysis is found in the Supplementary Methods.

2.7 | Cell culture and transfections

The human HCC cell line HepG2 was cultured in RPMI 1640 (Lonza, Basel, Switzerland) supplemented with 10% fetal bovine serum, 2 mM L-glutamine and 6 mM of both penicillin and streptomycin at 37℃ and 5% CO_2. ON-TARGETplus Non-targeting Control Pool (Dharmacon, Colorado, USA) or ON-TARGETplus Human PCSK9 small interfering RNA (siRNA)—SMART pool (GE Dharmacon) was transfected at a final concentration of 6 nM using Transfection Reagent 4 (GE Dharmacon).

2.8 | Statistical analysis

Sample sizes are based on our previous calculations and experimental observations.[23,33] Statistical analyses were performed with the Prism program (v. 5.02, GraphPad Software, Inc, California, USA). In zebrafish survival experiments a log-rank (Mantel-Cox) test was used to compare differences between the experimental groups, whereas a nonparametric two-tailed Mann-Whitney was used to analyse the zebrafish qPCR data. A 2-tailed *t* test was used in the analysis of HepG2 qPCR results. Statistics of the RNA sequencing have been described in the Supplementary Methods. *P*-values (or the adjusted *P*-value in RNA sequencing data) less than .05 was considered statistically significant.

3 | RESULTS

3.1 | Nonsense *pcsk9*[tpu-13/tpu-13] and *pcsk9*[tpu-2,+15/tpu-2,+15] mutant zebrafish have diminished *pcsk9* expression and are morphologically comparable with WT fish

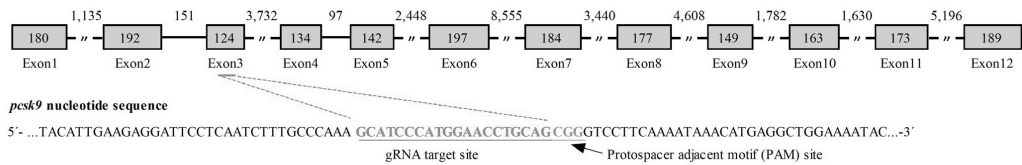The engineered type II CRISPR/Cas system known as CRISPR/Cas9 is an efficient tool for reverse genetics,[27,34] and it has been widely used in both cell and animal models of human diseases. Here, we used CRISPR/Cas9 mutagenesis to disrupt the open reading frame of zebrafish *pcsk9* (ENSDARG00000074185), and subsequently to create *pcsk9* KO zebrafish lines. By using a functional gRNA that targeted the third exon of *pcsk9*, we could induce parental (F0-generation) insertion/deletion (indel) mutations at the target site with an average efficiency of 40% (Figure 1A and 1B). Sequencing the mutated loci in the outcrossed F1-progeny [F0-generation × WT (Tüpfel long fin) zebrafish] revealed 2 germ-line transmitted nonsense *pcsk9* mutations; one with a loss of 13 bp (AACCTGCAGCGGG) and another with a loss of 2 bp (TG) and gain of 15 bp (AGCATCCATGCGAAC) leading to disrupted reading frames after 147 and 148 amino acids (aa) and to predicted premature stop-codons at the beginning of the core-protein regions at 173 aa and 159 aa respectively (Figure 1C). The *pcsk9* KO lines were concomitantly named *pcsk9*[tpu-13] (loss of 13 bp mutation) and *pcsk9*[tpu-2,+15] (loss of 2 bp and gain of 15 bp mutation).

Our previous work has demonstrated that CRISPR/Cas9-mediated indel mutations not only affect the protein translation, causing inability to produce intact protein, but can also lead to changes in the transcription of the target gene.[26] In line with this, qPCR quantification of *pcsk9* expression in adult steady-state zebrafish revealed significantly lower *pcsk9* mRNA levels in homozygous *pcsk9*[tpu-13/tpu-13] and *pcsk9*[tpu-2,+15/tpu-2,+15] mutants (residual expression medians of 15.9% and 8.0%; *P* = .008 in both comparisons) compared with their WT siblings (Figure 1D). Importantly, although earlier knock-down studies using morpholinos in zebrafish have indicated a crucial role for *pcsk9* in neural development,[35] *pcsk9* KO zebrafish did not have any apparent developmental abnormalities during the first 7 dpf (Figure S1). Furthermore, as adults, *pcsk9*[tpu-13/tpu-13] and *pcsk9*[tpu-2,+15/tpu-2,+15] mutants were morphologically similar to the WT fish (Figure 1E).
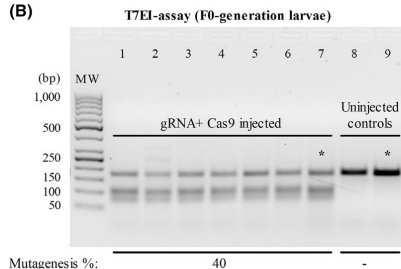
3.2 | *pcsk9* deficiency is dispensable for the survival of zebrafish upon a systemic pneumococcal infection

Both experimental and clinical data about the harmful/beneficial effects of PCSK9 in sepsis are contradictory.[14,17-21,36] To study the significance of the *pcsk9* gene in a systemic *S pneumoniae* infection of adult zebrafish,[23] we inoculated bacteria (4 700 000 CFU; SD 990 000 CFU) into the abdominal cavity of fish from both *pcsk9* mutation carrying lines; *pcsk9*[tpu-13] and *pcsk9*[tpu-2,+15]. After the 7-day follow-up, we observed average mortalities of 31.8% and 15.6% in the *pcsk9*[tpu-13] and *pcsk9*[tpu-2,+15] zebrafish lines respectively (Figure 2A and 2B). However, we did not observe any statistically significant difference in the survival of homozygous *pcsk9*[tpu-13/tpu-13] mutants (76.2% survival) compared with the corresponding heterozygous *pcsk9*[tpu-13/+] (70.8% survival; *P* = .31) and WT siblings (57.7%; *P* = .16) (Figure 2A), nor when comparing *pcsk9*[tpu-2,+15/tpu-2,+15] mutants (80.0% survival) with their sibling controls (90.7% of *pcsk9*[tpu-2,+15/+]; *P* = .30 and 82.6% of WT fish; *P* = .79) (Figure 2B).
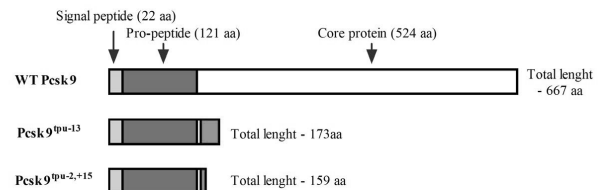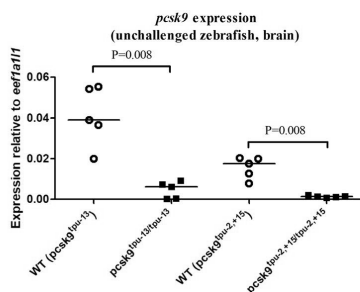
(A)

Zebrafish _pcsk9_ (ENSDARG00000074185)

pcsk9 nucleotide sequence

5´- ...TACATTGAAGAGGATTCCTCAATCTTTGCCCAAA GCATCCCATGGAACCTGCAGCGGGTCCTTCAAAATAAACATGAGGCTGGAAAATAC...-3´

gRNA target site   Protospacer adjacent motif (PAM) site
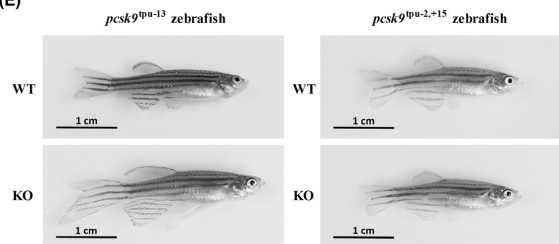
(B)

(C)

(D)

(E)

FIGURE 1 Homozygous _pcsk9_^tpu-13/tpu-13 and _pcsk9_^tpu-2,+15/tpu-2,+15 mutant zebrafish show reduced _pcsk9_ expression but normal morphology. A, A schematic representation of zebrafish _pcsk9_ (ENSDARG00000074185), and the gRNA target site for CRISPR/Cas9 mutagenesis in the third exon. B, The in vivo mutagenesis efficiency was estimated in the gRNA and Cas9 protein injected F0-generation embryos and in the uninjected controls using a T7 endonuclease I (T7EI) assay and 2.5% agarose TAE gel electrophoresis. The uninjected controls: a 169-bp WT PCR product (lanes 8 and 9); the gRNA and Cas9-injected mutant embryos: three bands of 169 bp (WT), ~100 bp and ~70 bp (lanes 1-7). The mutagenesis efficiency was calculated as described previously.[27] C, A schematic representation of the indel mutations (−13 bp deletion, _pcsk9_^tpu-13 and −2 bp deletion, +15 bp insertion, _pcsk9_^tpu-2,+15), leading to truncated protein products of 173 and 159 amino acids (aa) respectively. Red boxes indicate altered amino acids caused by the frameshift. D, The expression of _pcsk9_ was determined in the brain of _pcsk9_^tpu-13/tpu-13 (n = 5; 2 females, 3 males) and _pcsk9_^tpu-2,+15/tpu-2,+15 zebrafish (n = 5; 2 females, 3 males) and in the WT siblings (n = 5 in both control groups; 2 females, 3 males) with qPCR. Gene expression levels were normalized to _eef1a1l1_ and a 2-tailed Mann-Whitney test was used for statistics. E, Anesthetized WT and homozygous _pcsk9_ mutant zebrafish were imaged using a Canon EOS 7D Mark II camera with an exposure time of 17 ms. Fish were kept submerged in water during image acquisition. Images in (B) and (E) were cropped to exclude empty background from the figure

The host defense against pneumococcus is critically dependent on the innate immune response.[22] Consequently, we next used zebrafish larvae to specifically address if PCSK9 is important for the protective innate immunity in a pneumococcal infection. To this end, we microinjected _S pneumoniae_ (240 CFU; SD 76 CFU) into the blood circulation valley of the F2-generation progeny of heterozygous _pcsk9_^tpu-13/+ and _pcsk9_^tpu-2,+15/+ zebrafish at 2 dpf and followed their survival for 5 days. At the end of the experiment, an average of 25.7% (_pcsk9_^tpu-13 background) and 77.7% (_pcsk9_^tpu-2,+15 background) survival was observed (Figure 2C and 2D). More

specifically, 20.8% of the _pcsk9_^tpu-13/tpu-13, 39.6% of the _pcsk9_^tpu-13/+ and 16.7% of the WT (_pcsk9_^tpu-13 background) fish (Figure 2C) had survived, whereas survival fractions of 58.8% in the _pcsk9_^tpu-2,+15/tpu-2,+15, 87.5% in the _pcsk9_^tpu-2,+15/+ and 86.7% in the WT (_pcsk9_^tpu-2,+15) fish were seen (Figure 2D). Similarly to our experiments in adult zebrafish, no statistically significant differences in the survival rates of the _pcsk9_ KO and WT larvae were observed (P = .57 and P = .078 in _pcsk9_^tpu-13 and _pcsk9_^tpu-2,+15 lines respectively), although the difference between _pcsk9_ KO and heterozygous _pcsk9_^tpu-2,+15/+ larvae was significant (P = .038). Overall, we conclude that _pcsk9_ is
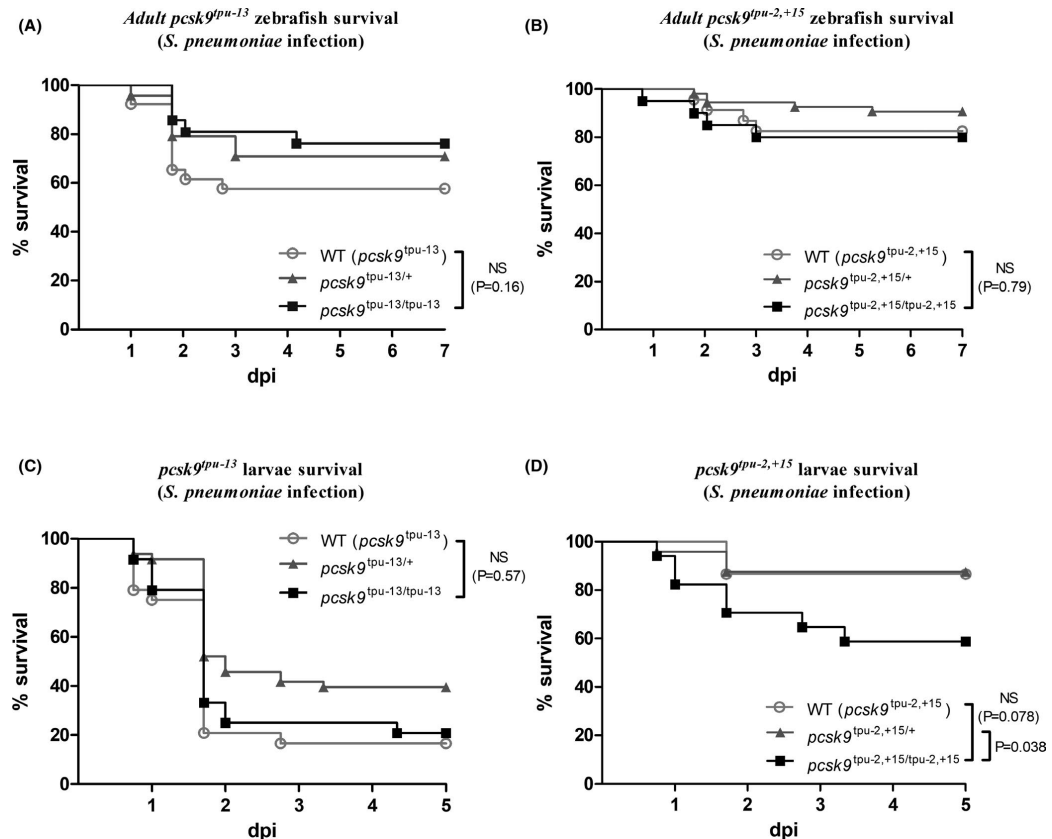
FIGURE 2 Nonsense mutations in *pcsk9* do not affect zebrafish survival upon an *S pneumoniae* infection. *S pneumoniae* (4 700 000 CFU; SD 990 000 CFU) was injected into the abdominal cavity of (A) *pcsk9*tpu-13/tpu-13 (n = 21; 8 females, 13 males; survived: n = 16; 8 females, 8 males), *pcsk9*tpu-13/+ (n = 24; 7 females, 17 males; survived: n = 17; 6 females, 11 males) and WT (*pcsk9*tpu-13) (n = 26; 5 females, 21 males; survived: n = 15; 4 females, 11 males) as well as (B) *pcsk9*tpu-2,+15/tpu-2,+15 (n = 20; 4 females, 16 males; survived: n = 16; 3 females, 13 males), *pcsk9*tpu-2,+15/+ (n = 54; 10 females, 44 males; survived: n = 49; 9 females, 40 males) and WT (*pcsk9*tpu-2,+15) (n = 23; 12 females, 11 males; survived: n = 19; 10 females, 9 males) adult zebrafish, and their survival was followed for 7 days. *Pneumococcus* infected (240 CFU; SD 76 CFU) zebrafish larvae from both the (C) *pcsk9*tpu-13 and (D) *pcsk9*tpu-2,+15 background were followed until 5 dpi and their survival was recorded. Group sizes; *pcsk9*tpu-13/tpu-13 (n = 24; survived: n = 5), *pcsk9*tpu-13/+ (n = 48; survived n = 19), WT (*pcsk9*tpu-13) (n = 24; survived n = 4) and *pcsk9*tpu-2,+15/tpu-2,+15 (n = 17; survived n = 10), *pcsk9*tpu-2,+15/+ (n = 24; survived n = 21), WT (*pcsk9*tpu-2,+15) (n = 15; survived n = 13). The data were collected from single experiments. A log-rank (Mantel-Cox) test was used for statistics. dpi, days post infection

not critical for the adult or larvae zebrafish survival on a *S pneumoniae* infection.

3.3 | Expression of *pcsk9* is upregulated on a *S pneumoniae* infection, and it is required for a normal acute-phase response

Previously, it has been shown that hepatic PCSK9 expression is increased in LPS-induced inflammation,[37] and that plasma PCSK9 levels are upregulated in a liver-dependent manner in bacteraemia patients.[21] To directly test whether hepatic PCSK9 is upregulated in

a pneumococcal infection, we injected adult WT zebrafish (AB line) with PBS or *S pneumoniae* (635 000 CFU; SD 276 000 CFU) into the abdominal cavity and quantified the expression of *pcsk9* in the liver at 7 dpi. Our qPCR analysis revealed a 4.5-fold increase (P = .008) in the relative levels of *pcsk9* mRNA in the pneumococcus infected zebrafish (Figure 3A), suggesting that the inflammation-mediated inducibility of hepatic PCSK9 is evolutionarily conserved.

To gain a genome-wide perspective on the PCSK9-dependent liver-specific transcriptional response in a *S pneumoniae* infection, we performed RNA sequencing on the livers of unchallenged, PBS injected and *S pneumoniae* infected (1 dpi, 3 370 000 CFU; SD 840 000 CFU) adult *pcsk9*tpu-13/tpu-13 zebrafish and their WT siblings.

The principal component analysis revealed that the experimental group was the largest variant affecting the sample clustering (Figure S2). In addition, the pcsk9^{tpu-13/tpu-13} mutants and the WT (pcsk9^{t-pu-13}) controls grouped separately among the unchallenged and the pneumococcus infected fish, indicating pcsk9-mediated effects also on gene expression in the liver. In fact, a comparison of transcript levels in pcsk9^{tpu-13/tpu-13} and WT fish using DESeq2, revealed a total of 828 differentially expressed genes, of which 609 (adjusted P-value < .05) were differentially expressed at steady-state, 81 on a PBS injection and 241 in a S pneumoniae infection (Figure 3B, Tables S2-S4). Although 87 genes were expressed differentially in at least two different experimental groups, most of the identified transcripts were specific for a particular treatment; 526 transcripts in unchallenged zebrafish, 25 in the PBS-injected group and 190 in infected fish.

To decipher the immunoregulatory functions of PCSK9 at a molecular level in vivo on infection, we next focused on the 112 up- and 77 down-regulated protein coding genes in the S pneumoniae challenged pcsk9^{tpu-13/tpu-13} mutants compared with the WT controls. To this end, gene ontology (GO) enrichment analysis of the induced transcripts in the pcsk9 KO zebrafish, revealed a total of 15 enriched processes that were related to hormonal responses, such

FIGURE 3 pcsk9 is up-regulated on a pneumococcal infection and associated with the expression of acute-phase reactants. A, The relative expression of pcsk9 was determined in the liver of PBS injected (n = 5; all males) and S pneumoniae infected (635 000 CFU; SD 276 000 CFU, n = 5; all males) WT AB zebrafish at 7 dpi using qPCR. Gene expression levels were normalized to eef1a1l1 expression and target genes were run once as technical duplicates. A 2-tailed Mann-Whitney test was used for statistics. B-C, RNA was isolated from the liver of unchallenged (n = 2 in both groups; 2 females/group), PBS injected (n = 3 in both groups; 3 females/group) and S pneumoniae infected (3 370 000 CFU; SD 840 000 CFU, n = 3 in both groups; 3 females/group) adult pcsk9^{tpu-13/tpu-13} and WT (pcsk9^{tpu-13}) zebrafish at 1 dpi and the transcriptome was analysed using RNA sequencing. B, Venn diagram for the differentially expressed genes within treatment groups. C, The top 25 up- and down-regulated genes in S pneumoniae infected pcsk9^{tpu-13/tpu-13} zebrafish in comparison with the WT controls are depicted using a heat-map. Statistics were done using DESeq2 and adjusted using the Benjamini-Hochberg (BH) method. D, The relative expression of selected genes up- or down-regulated in the RNA sequencing data (ldlrap1a, hamp and socs3a) was quantified using qPCR. Gene expression levels were normalized to eef1a1l1 expression and target genes were run once as technical duplicates
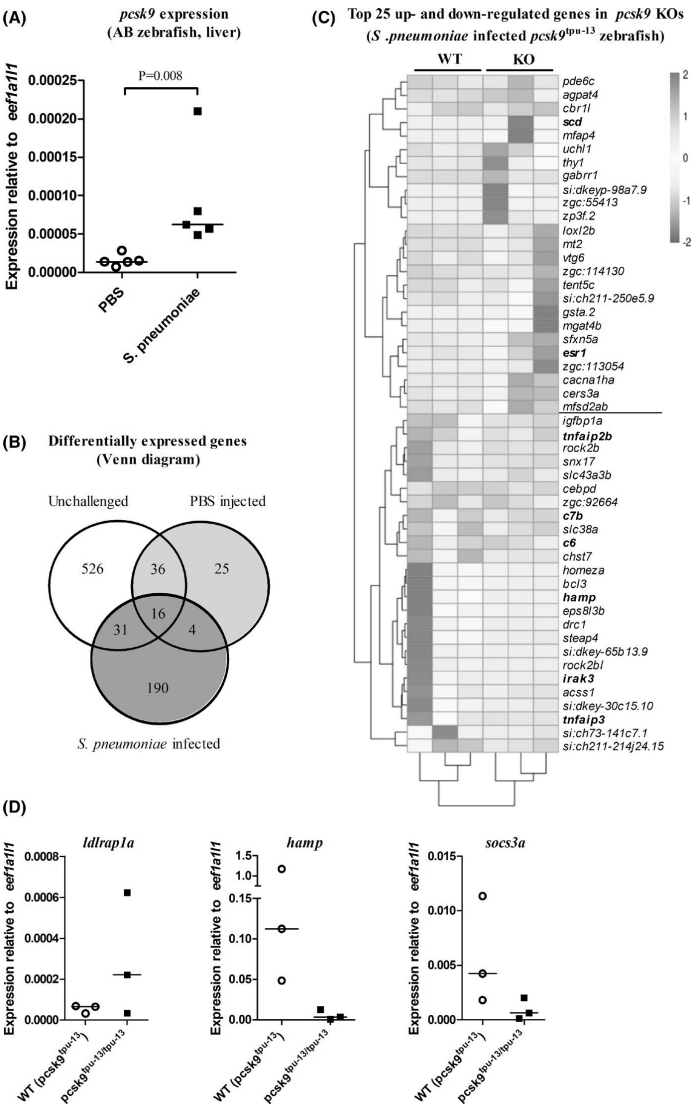
as the cellular response to an estrogen stimulus (GO:0071391), but also to a lipid metabolism, e.g., the response to lipids (GO:0033993) and lipid transport (GO:0006869) (Table 1). Among the up-regulated genes in *pcsk9* KO fish, we found *stearoyl-CoA desaturase* (*scd*, log 2-fold change 5.1, *P* < .001), *estrogen receptor 1* (*esr1*, log 2-fold change 3.5, *P* < .001) as well as several *vitellogenin* (eg *vtg3*, log 2-fold change 2.3, *P* = .010) genes (Figure 3C, Table S5). It is additionally important to note that the *PCSK9* promoter region contains estrogen response elements (EREs),[38] which can in principle explain the effects on *esr1* expression in the *pcsk9*[tpu-13/tpu-13] mutants. Interestingly, among the genes induced in *pcsk9*[tpu-13/tpu-13] zebrafish we also observed a 2.5-fold induction (log 2 change, *P* = .049) in the low-density *lipoprotein receptor adaptor protein 1a* (*ldlrap1a*) gene, encoding a homologue of the human mediator of LDLR endocytosis.[39]

Importantly, the GO-analysis of the down-regulated genes showed that from a total of six processes two were directly related to the immune system; the immune system process (GO:0002376) and the humoral immune response (GO:0006959) (Table 2). In fact, among the 78 genes whose expression levels were reduced in the *pcsk9*[tpu-13/tpu-13] fish, we found at least 18 genes (23%) with immunological functions, including *hepcidin antimicrobial peptide* (*hamp*, log 2-fold change −5.8, *P* < .001), *complement component 7b* (*c7b*, log 2-fold change −3.53, *P* < .001), *interleukin-1 receptor-associated kinase 3* (*irak3*, log 2-fold change −3.29, *P* < .001), *tumour necrosis factor, alpha-induced protein 3* (*tnfaip3*, log 2 fold change −3.02, *P* < .001) and *suppressor of cytokine signalling 3a* (*socs3a*, log 2 fold change −2.97, *P* = .008) (Figure 3C, Table S5). We replicated our RNA sequencing analysis for *ldlrap1a* (3.4-fold increase in median), *hamp* (residual expression median of 3.1%), and *socs3a* (residual expression median of 15.0%) using qPCR (Figure 3D). Overall, our findings indicate that upon a *S pneumoniae* infection *pcsk9* expression becomes up-regulated in vivo in the zebrafish liver, and that the lack of *pcsk9* favours the expression of genes associated with lipid and estrogen metabolism, whereas several liver-expressed acute-phase reaction (APR) genes are down-regulated.

3.4 | PCSK9 regulates the expression of innate immunity genes in human HepG2 cells

Suggesting a direct regulatory function for PCSK9 in the immune response in the absence of a microbial insult, in vitro administration of recombinant PCSK9 into a mouse and human macrophage culture was shown to induce the expression of genes coding for pro-inflammatory cytokines such as TNF, IL6 and IL1B.[13] To address whether PCSK9 controls the expression of the above identified innate immunity genes also in human hepatocytes, we knocked-down *PCSK9* expression in HepG2 cells (residual expression median of 41.8% compared with controls) (Figure 4, Figure S3A), and quantified the expression of *HAMP, C7, SOCS3, TNF, TNFAIP3, C6* and *LDLRAP1* using qPCR (Figure 4). In these experiments the mRNA levels of *HAMP* (25% decrease in median, *P* < .001), *C7* (1.41-fold increase in median, *P* = .008), *SOCS3* (1.29-fold increase in median

1.29, *P* = .019) and *TNF* (2.52-fold increase in median, *P* = .017) were significantly affected by the reduced PCSK9 expression. In addition, western blot analysis confirmed the down-regulation of HAMP also at the protein level (Figure S3B), underscoring the direct immunoregulatory role of PCSK9 also in a human hepatocyte cell line.

4 | DISCUSSION

PCSK9 antibodies efficiently lower cholesterol and provide protection against CHD, but whether inhibiting PCSK9 could also be leveraged to prevent an exacerbated immune response in septic patients remains under investigation. Here, we used the CRISPR/Cas9 system to create two zebrafish lines with nonsense *pcsk9* mutations (*pcsk9*[tpu-13] and *pcsk9*[tpu-2,+15]) and demonstrated that the mutant zebrafish have a normal morphology and development. Infecting *pcsk9* mutant fish with *S pneumoniae* did not reveal any differences in the mortality of either the larvae or the adult fish compared with controls. Nevertheless, the expression of *pcsk9* was induced on a pneumococcal challenge, and the genome-wide expression analysis of zebrafish liver revealed the down-regulation of several genes associated with the innate immunity, suggesting a role in the innate host response against a pneumococcus infection. Accordingly, silencing *PCSK9* in a human hepatocarcinoma cell line (HepG2) led to decreased *HAMP* expression as well as to alterations in the expression of other innate immune genes such as *TNF, C7* and *SOCS3*.

In mammals, PCSK9 is expressed not only in the liver but also in, e.g., the pancreas and brain.[40,41] Our previous analysis of genes of the *pcsk* family in adult zebrafish tissues revealed high relative *pcsk9* expression in the fish brain,[42] which is in accordance with an earlier report, where *pcsk9* was inhibited with morpholinos and a critical role for PCSK9 in neural tissues and early fish development were described.[35] By creating targeted nonsense mutations, we have demonstrated that the CRISPR/Cas9 mutagenesis method can be efficiently used to knock out genes of interest in zebrafish.[26,29] Accordingly, we created 2 *pcsk9* KO zebrafish lines; *pcsk9*[tpu-13] and *pcsk9*[tpu-2,+15], with disrupted open reading frames (residual expression medians of the mutated mRNAs in the brain; 15.9% and 8.0%, respectively). However, in contrast with previously published data demonstrating the absence of tectum and midbrain-hindbrain boundary in the *pcsk9* morphants at 24 hours post fertilization,[35] homozygous *pcsk9*[tpu-13/tpu-13] and *pcsk9*[tpu-2,+15/tpu-2,+15] mutants did not show morphological abnormalities during embryogenesis prior to 7 dpf. Moreover, adult fish were obtained in predicted Mendelian ratios, a result that is in line with the normal development of *Pcsk9* KO mouse and humans with null *PCSK9* alleles.[43] Clarity to whether the differing developmental results in zebrafish are indicative of morpholino off-target effects caused by p53-mediated neural cell death[44] or genetic compensation observed in experimental KO animals[45] could add to our understanding of the extra-hepatic functions of PCSK9.

TABLE 1 Enriched processes from a gene ontology (GO) analysis of up-regulated genes in *S pneumoniae* infected zebrafish

GO term	Description	P value
GO:0071391	Cellular response to estrogen stimulus	6.03 E−12
GO:0043627	Response to estrogen	1.63 E−11
GO:0032355	Response to estradiol	1.67 E−10
GO:0033993	Response to lipid	8.23 E−08
GO:0014070	Response to organic cyclic compound	2.00 E−06
GO:1901700	Response to oxygen-containing compound	5.72 E−06
GO:0009719	Response to endogenous stimulus	7.62 E−06
GO:0009725	Response to hormone	2.31 E−05
GO:0070887	Cellular response to chemical stimulus	2.49 E−05
GO:0042221	Response to chemical	3.12 E−05
GO:0010033	Response to organic substance	4.49 E−05
GO:0006869	Lipid transport	1.70 E−04
GO:0009082	Branched-chain amino acid biosynthetic process	2.91 E−04
GO:0046394	Carboxylic acid biosynthetic process	5.21 E−04
GO:0016053	Organic acid biosynthetic process	5.40 E−04

Note: A genome-wide transcriptome analysis in zebrafish liver was performed using RNA sequencing and a GO enrichment analysis was used to study the up-regulated transcripts in the *pcsk9*[tpu-13/tpu-13] mutants challenged with *S pneumoniae* compared with the WT controls. A target list of differentially expressed genes (adj. *P* < .05) was compared with a background list (adj. *P* ≥ .05).

Abbreviation: GO term, gene ontology term.

TABLE 2 Enriched processes from a gene ontology (GO) analysis of down-regulated genes in *S pneumoniae* infected zebrafish

GO term	Description	P value
GO:0070589	Cellular component macromolecule biosynthetic process	5.89 E−05
GO:0044038	Cell wall macromolecule biosynthetic process	5.89 E−05
GO:0044036	Cell wall macromolecule metabolic process	1.18 E−04
GO:0002376	Immune system process	1.34 E−04
GO:0051241	Negative regulation of multicellular organismal process	4.20 E−04
GO:0006959	Humoral immune response	6.42 E−04

Note: A genome-wide transcriptome analysis in zebrafish liver was performed using RNA sequencing and a GO enrichment analysis was used to study the down-regulated transcripts in the *pcsk9*[tpu-13/tpu-13] mutants challenged with *S pneumoniae* compared with the WT controls. A target list of differentially expressed genes (adj. *P* < .05) was compared with a background list (adj. *P* ≥ .05).

Abbreviation: GO term, gene ontology term.

Sepsis is a clinical syndrome caused by the interplay of microorganisms and an exacerbated immune reaction leading to multiple organ failure.[46] Although mammalian sepsis models remain highly important for pre-clinical drug development, they are laborious, expensive and raise ethical concerns. Zebrafish is a non-mammalian alternative for studying host-pathogen interactions in vivo. As it takes several weeks for lymphocytes and the adaptive immune system to develop in zebrafish, the fish larvae can be used to specifically study the innate immunity.[24] Importantly, adult zebrafish have a highly similar immune system compared with humans with both innate immune cells, lymphocytes [24] as well as humoral components like complement components.[47] To assess how the KO of *pcsk9* affects zebrafish mortality on a pneumococcal challenge, we infected both

zebrafish larvae and adult fish with *S pneumoniae* and followed their survival until 5 or 7 dpi respectively. Similarly to studies using LPS-induced endotoxemia in *Pcsk9* KO mice,[36] the mortality of pneumococcus infected homozygous *pcsk9*[tpu-13/tpu-13] and *pcsk9*[tpu-2,+15/tpu-2,+15] mutants was comparable with the WT controls in both the larvae and adult zebrafish. Overall, we conclude that PCSK9 is not essential for zebrafish survival in a systemic *S pneumoniae* infection.

More than 70% of the human genes have zebrafish orthologues,[48] and consequently gene KO zebrafish accompanied with genome-wide transcriptome analysis can be used to model both systemic and tissue-specific functions of human genes.[25,26] Here, our genome-wide transcriptomic analysis of pneumococcus infected *pcsk9*[tpu-13/tpu-13] mutants and WT fish revealed a substantial proportion (18/78 genes)
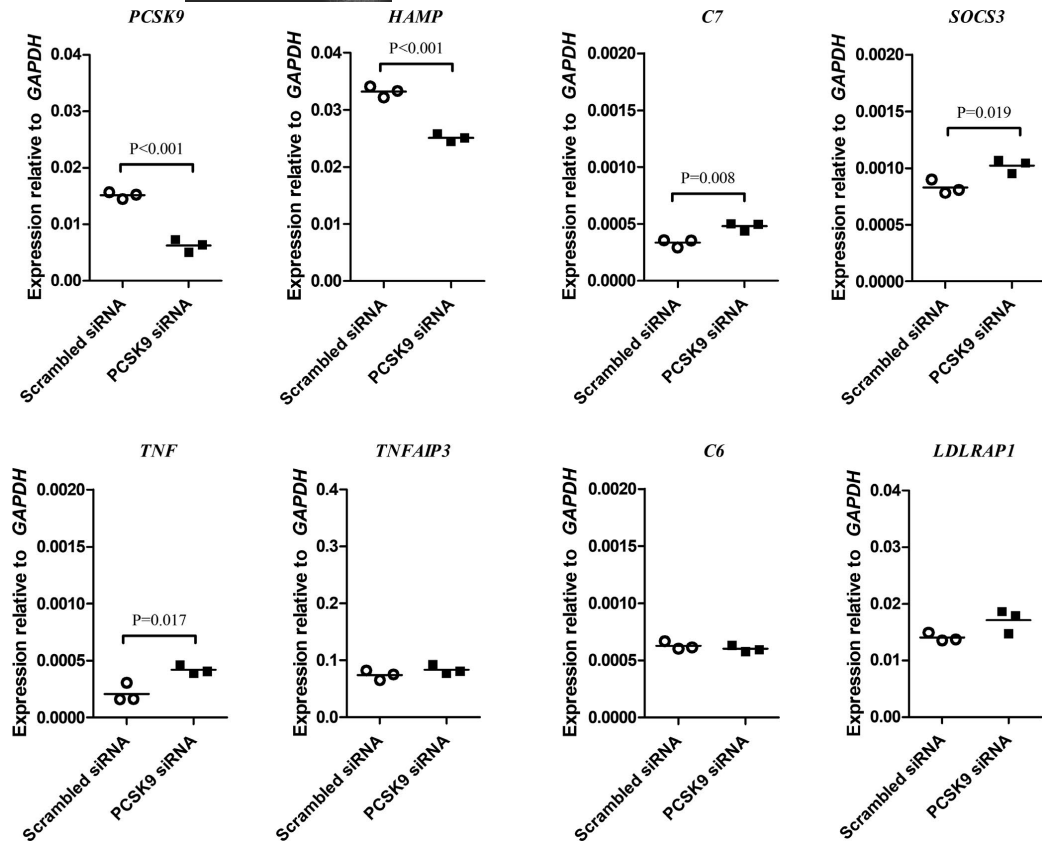
FIGURE 4 Silencing *PCSK9* influences the expression of genes of the innate immune response in HepG2 cells. The relative expression levels of *PCSK9*, *HAMP*, *C7*, *SOCS3*, *TNF*, *TNFAIP3*, *C6* and *LDLRAP1* were determined in control (n = 3) and *PCSK9* siRNA (n = 3) transfected HepG2 cells using qPCR. Gene expression levels were normalized to *GAPDH* expression and target genes were run once as technical duplicates. A 2-tailed *t* test was used for statistics

of immunological genes among the down-regulated transcripts in *pcsk9* KOs. From these genes, two complement system protein coding genes *c6* and *c7b* had significantly lower levels of mRNA in the *pcsk9*[t-pu-13/tpu-13] mutants in comparison with the WT controls. Additionally, we identified down-regulation of well-known immunoregulatory genes such as *tnfaip2b*, *nuclear factor kappa B subunit 2* (*nfkb2*), *irak3*, *socs3a* and *tnfaip3* [49-51] in the *pcsk9* KO zebrafish. In a human hepatocellular carcinoma cell line, we demonstrate that silencing *PCSK9* directly impacts the expression of innate immunity genes such as *C7*, *SOCS3* and *TNF*. However, there were notable differences between the zebrafish and HepG2 data, which can probably be attributed to the facts that the liver contains several different cell types,[13] and that there was no infectious insult in our in vitro model system.

HAMP encodes a liver-produced antimicrobial peptide, also known as hepcidin, that can reduce the concentration of iron in the blood and subsequently deprive it from micro-organisms.[52] Our RNA sequencing data of zebrafish liver indicated that *hamp* expression is induced on a

S pneumoniae challenge in zebrafish, and that *hamp* mRNA levels in the infected *pcsk9* KO zebrafish were reduced compared with the WT controls at 1 dpi. Furthermore, in line with previously published data that the in vitro administration of recombinant PCSK9 can regulate the expression of pro-inflammatory cytokine genes in the absence of inflammatory stimuli,[13] silencing *PCSK9* in vitro in HepG2 cells reduced *HAMP* expression levels. Since HAMP is a major regulator of iron homeostasis and its levels are linked to different forms of anaemias,[53] the positive correlation between *PCSK9* and *HAMP* expression also at steady-state could have clinical implications. In fact, a recent study in mice demonstrated that non-hematopoietic anaemia, independent of LDLR expression, was more severe in *Pcsk9* KO mice.[54] It is important to note that conventional PCSK enzymes FURIN, PCSK5, PCSK6 and PCSK7 have been demonstrated to directly process pro-hepcidin,[55] whereas FURIN has been reported to process PCSK9.[56] It remains to be confirmed whether there is a direct causal relationship between lowered HAMP levels and PCSK9 or if this is also affected by the other PCSK family members. Collectively, our

gene expression analyses unravel that the lack of *pcsk9/PCSK9* transcriptionally impacts APR, arguing for an immunostimulatory role for PCSK9 on a bacterial challenge and independent of infection.

The dual role of PCSK9 in regulating hepatocytic lipoprotein uptake [3,4] and the inflammatory response [13,14] has made this proprotein convertase an attractive candidate for studying sepsis. Although some data indicate that normal PCSK9 levels are associated with a better prognosis,[20,21] and that this effect could be age dependent,[19] other studies support the idea that blocking PCSK9 activity could improve the outcome of treatment in septic patients.[14,15,17] In fact, the PCSK9 inhibiting antibodies alirocumab (Praluent, Sanofi-Regeneron) and evolocumab (Repatha, Amgen) are being tested in clinical trials to treat septic patients (NCT03634293 and NCT03869073 respectively). Although we did not see any difference in the survival of *S pneumoniae* infected *pcsk9* KO and WT zebrafish, our transcriptomic data show that PCSK9 regulates the production of acute-phase reactants such as hepcidin and complement components. Although the direct role of LDLR-signalling remains to be investigated, inhibition of PCSK9 may cause immunodeficiency by dampening APR. Further studies are clearly warranted to decipher the role of PCSK9 in *S pneumoniae* host responses in tissue-specific infections such as pneumonia as well as in the context of infections in which an optimal liver immune response is necessary.

CONFLICT OF INTEREST

The authors declare no conflicts of interest.

DATA AVAILABILITY STATEMENT

RNA sequencing data has been submitted to Gene Expression Omnibus (GEO) repository (identifier code: GSE165508). Other generated and analyzed data are available on reasonable request from the corresponding author.

ORCID

Markus J. T. Ojanen https://orcid.org/0000-0001-6623-844X

REFERENCES

1. Siegfried G, Descarpentrie J, Evrard S, Khatib A. Proprotein convertases: key players in inflammation-related malignancies and metastasis. *Cancer Lett.* 2020;473:50-61.

2. Seidah NG, Prat A. The biology and therapeutic targeting of the proprotein convertases. *Nat Rev Drug Discov.* 2012;11(5):367-383.

3. Benjannet S, Rhainds D, Essalmani R, et al. NARC-1/PCSK9 and its natural mutants: zymogen cleavage and effects on the low density lipoprotein (LDL) receptor and LDL cholesterol. *J Biol Chem.* 2004;279(47):48865-48875.

4. Zhang D, Lagace TA, Garuti R, et al. Binding of proprotein convertase subtilisin/kexin type 9 to epidermal growth factor-like repeat A of low density lipoprotein receptor decreases receptor recycling and increases degradation. *J Biol Chem.* 2007;282(25):18602-18612.

5. Cohen JC, Boerwinkle E, Mosley TH, Hobbs HH. Sequence variations in PCSK9, low LDL, and protection against coronary heart disease. *N Engl J Med.* 2006;354(12):1264-1272.

6. Abifadel M, Varret M, Rabès J, et al. Mutations in PCSK9 cause autosomal dominant hypercholesterolemia. *Nat Genet.* 2003;34(2):154-156.

7. Stein EA, Mellis S, Yancopoulos GD, et al. Effect of a monoclonal antibody to PCSK9 on LDL cholesterol. *N Engl J Med.* 2012;366(12):1108-1118.

8. Sabatine MS, Giugliano RP, Keech AC, et al. Evolocumab and clinical outcomes in patients with cardiovascular disease. *N Engl J Med.* 2017;376(18):1713-1722.

9. Fitzgerald K, White S, Borodovsky A, et al. A highly durable RNAi therapeutic inhibitor of PCSK9. *N Engl J Med.* 2017;376(1):41-51.

10. Gan ES, Tan HC, Le DHT, et al. Dengue virus induces PCSK9 expression to alter antiviral responses and disease outcomes. *J Clin Invest.* 2020;130(10):5223-5234.

11. Stiekema LCA, Stroes ESG, Verweij SL, et al. Persistent arterial wall inflammation in patients with elevated lipoprotein(a) despite strong low-density lipoprotein cholesterol reduction by proprotein convertase subtilisin/kexin type 9 antibody treatment. *Eur Heart J.* 2019;40(33):2775-2781.

12. Giunzioni I, Tavori H, Covarrubias R, et al. Local effects of human PCSK9 on the atherosclerotic lesion. *J Pathol.* 2016;238(1):52-62.

13. Ricci C, Ruscica M, Camera M, et al. PCSK9 induces a proinflammatory response in macrophages. *Sci Rep.* 2018;8(1):1-10.

14. Walley KR, Thain KR, Russell JA, et al. PCSK9 is a critical regulator of the innate immune response and septic shock outcome. *Sci Transl Med.* 2014;6(258):258ra143.

15. Leung AKK, Genga KR, Topchiy E, et al. Reduced proprotein convertase subtilisin/kexin 9 (PCSK9) function increases lipoteichoic acid clearance and improves outcomes in gram positive septic shock patients. *Sci Rep.* 2019;9(1):1-8.

16. Trinder M, Boyd JH, Brunham LR. Molecular regulation of plasma lipid levels during systemic inflammation and sepsis. *Curr Opin Lipidol.* 2019;30(2):108-116.

17. Boyd JH, Fjell CD, Russell JA, Sirounis D, Cirstea MS, Walley KR. Increased plasma PCSK9 levels are associated with reduced endotoxin clearance and the development of acute organ failures during sepsis. *J Innate Immun.* 2016;8(2):211-220.

18. Feng Q, Wei W, Chaugai S, et al. A genetic approach to the association between PCSK9 and sepsis. *JAMA Netw Open.* 2019;2(9):e1911130.

19. Atreya MR, Whitacre BE, Cvijanovich NZ, et al. Proprotein convertase subtilisin/kexin type 9 loss-of-function is detrimental to the juvenile host with septic shock. *Crit Care Med.* 2020;48(10):1513-1520.

20. Vecchié A, Bonaventura A, Meessen J, et al. PCSK9 is associated with mortality in patients with septic shock: data from the ALBIOS study. *J Intern Med.* 2021;289:179-192.

21. Rannikko J, Sanz DJ, Ortutay Z, et al. Reduced plasma PCSK9 response in patients with bacteraemia is associated with mortality. *J Intern Med.* 2019;286(5):553-561.

22. Rouroja S, Saralahti A, Rantala L, et al. Defense of zebrafish embryos against streptococcus pneumoniae infection is dependent on the phagocytic activity of leukocytes. *Dev Comp Immunol.* 2012;36(2):342-348.

23. Saralahti A, Piippo H, Parikka M, Henriques-Normark B, Rämet M, Rounioja S. Adult zebrafish model for pneumococcal pathogenesis. *Dev Comp Immunol*. 2014;42(2):345-353.

24. Renshaw SA, Trede NS. A model 450 million years in the making: Zebrafish and vertebrate immunity. *Dis Model Mech*. 2012;5(1):38-47.

25. Harjula SE, Saralahti AK, Ojanen MJT, et al. Characterization of immune response against mycobacterium marinum infection in the main hematopoietic organ of adult zebrafish (danio rerio). *Dev Comp Immunol*. 2020;103:103523.

26. Ojanen MJT, Uusi-Mäkelä MIE, Harjula SE, et al. Intelectin 3 is dispensable for resistance against a mycobacterial infection in zebrafish (danio rerio). *Sci Rep*. 2019;9(1):995.

27. Ran FA, Hsu PD, Wright J, Agarwala V, Scott DA, Zhang F. Genome engineering using the CRISPR-Cas9 system. *Nat Protoc*. 2013;8(11):2281-2308.

28. Artimo P, Jonnalagedda M, Arnold K, et al. ExPASy: SIB bioinformatics resource portal. *Nucleic Acids Res*. 2012;40(W1):W597-W603

29. Uusi-Mäkelä MIE, Barker HR, Bäuerlein CA, Häkkinen T, Nykter M, Rämet M. Chromatin accessibility is associated with CRISPR-Cas9 efficiency in the zebrafish (danio rerio). *PLoS One*. 2018;13(4):e0196238.

30. Labun K, Montague TG, Gagnon JA, Thyme SB, Valen E. CHOPCHOP v2: a web tool for the next generation of CRISPR genome engineering. *Nucleic Acids Res*. 2016;44(W1):W272-W276.

31. Staahl BT, Benekareddy M, Coulon-Bainier C, et al. Efficient genome editing in the mouse brain by local delivery of engineered Cas9 ribonucleoprotein complexes. *Nat Biotechnol*. 2017;35(5):431-434.

32. Tang R, Dodd A, Lai D, McNabb WC, Love DR. Validation of zebrafish (danio rerio) reference genes for quantitative real-time RT-PCR normalization. *Acta Biochim Biophys Sin (Shanghai)*. 2007;39(5):384-390.

33. Harjula SE, Ojanen MJT, Taavitsainen S, Nykter M, Rämet M. Interleukin 10 mutant zebrafish have an enhanced interferon gamma response and improved survival against a mycobacterium marinum infection. *Sci Rep*. 2018;8(1):10360.

34. Jinek M, Chylinski K, Fonfara I, Hauer M, Doudna JA, Charpentier E. A programmable dual-RNA-guided DNA endonuclease in adaptive bacterial immunity. *Science*. 2012;337(6096):816-821.

35. Poirier S, Prat A, Marcinkiewicz E, et al. Implication of the proprotein convertase NARC-1/PCSK9 in the development of the nervous system. *J Neurochem*. 2006;98(3):838-850.

36. Berger J, Loza Valdes A, Gromada J, Anderson N, Horton JD. Inhibition of PCSK9 does not improve lipopolysaccharide-induced mortality in mice. *J Lipid Res*. 2017;58(8):1661-1669.

37. Feingold KR, Moser AH, Shigenaga JK, Patzek SM, Grunfeld C. Inflammation stimulates the expression of PCSK9. *Biochem Biophys Res Commun*. 2008;374(2):341-344.

38. Maarouf N, Chen Y, Shi C, et al. Unlike estrogens that increase PCSK9 levels post-menopause HSP27 vaccination lowers cholesterol levels and atherogenesis due to divergent effects on PCSK9 and LDLR. *Pharmacol Res*. 2020;161:105222.

39. He G, Gupta S, Yi M, Michaely P, Hobbs HH, Cohen JC. ARH is a modular adaptor protein that interacts with the LDL receptor, clathrin, and AP-2. *J Biol Chem*. 2002;277(46):44044-44049.

40. Seidah NG, Benjannet S, Wickham L, et al. The secretory proprotein convertase neural apoptosis-regulated convertase 1 (NARC-1): liver regeneration and neuronal differentiation. *Proc Natl Acad Sci USA*. 2003;100(3):928-933.

41. Langhi C, Le May C, Gmyr V, et al. PCSK9 is expressed in pancreatic delta-cells and does not alter insulin secretion. *Biochem Biophys Res Commun*. 2009;390(4):1288-1293.

42. Turpeinen H, Oksanen A, Kivinen V, et al. Proprotein convertase subtilisin/kexin type 7 (PCSK7) is essential for the zebrafish development and bioavailability of transforming growth factor β1a (TGFβ1a). *J Biol Chem*. 2013;288(51):36610-36623.

43. Rashid S, Curtis DE, Garuti R, et al. Decreased plasma cholesterol and hypersensitivity to statins in mice lacking Pcsk9. *Proc Natl Acad Sci USA*. 2005;102(15):5374-5379.

44. Robu ME, Larson JD, Nasevicius A, et al. P53 activation by knock-down technologies. *PLoS Genet*. 2007;3(5):e78.

45. Rossi A, Kontarakis Z, Gerri C, et al. Genetic compensation induced by deleterious mutations but not gene knockdowns. *Nature*. 2015;524(7564):230-233.

46. van der Poll T. Immunotherapy of sepsis. *Lancet Infect Dis*. 2001;1(3):165-174.

47. Seeger A, Mayer WE, Klein J. A complement factor B-like cDNA clone from the zebrafish (brachydanio rerio). *Mol Immunol*. 1996;33(6):511-520.

48. Kettleborough RN, Busch-Nentwich EM, Harvey SA, et al. A systematic genome-wide analysis of zebrafish protein-coding gene function. *Nature*. 2013;496(7446):494-497.

49. Ruscica M, Ricci C, Macchi C, et al. Suppressor of cytokine signaling-3 (SOCS-3) induces proprotein convertase subtilisin kexin type 9 (PCSK9) expression in hepatic HepG2 cell line. *J Biol Chem*. 2016;291(7):3508-3519.

50. Macchi C, Greco MF, Botta M, et al. Leptin, resistin, and proprotein convertase subtilisin/kexin type 9: The role of STAT3. *Am J Pathol*. 2020;190(11):2226-2236.

51. Shembade N, Harhaj EW. Regulation of NF-κB signaling by the A20 deubiquitinase. *Cell Mol Immunol*. 2012;9(2):123-130.

52. Ganz T, Nemeth E. Hepcidin and iron homeostasis. *Biochim Biophys Acta*. 2012;1823(9):1434-1443.

53. Pagani A, Nai A, Silvestri L, Camaschella C. Hepcidin and anemia: a tight relationship. *Front Physiol*. 2019;10:1294.

54. Venugopal J, Wang J, Guo C, Lu H, Chen YE, Eitzman DT. Non-hematopoietic deficiency of proprotein convertase subtilisin/kexin type 9 deficiency leads to more severe anemia in a murine model of sickle cell disease. *Sci Rep*. 2020;10:16514.

55. Scamuffa N, Basak A, Lalou C, et al. Regulation of prohepcidin processing and activity by the subtilisin-like proprotein convertases furin, PC5, PACE4 and PC7. *Gut*. 2008;57(11):1573-1582.

56. Lipari MT, Li W, Moran P, et al. Furin-cleaved proprotein convertase subtilisin/kexin type 9 (PCSK9) is active and modulates low density lipoprotein receptor and serum cholesterol levels. *J Biol Chem*. 2012;287(52):43482-43491.

SUPPORTING INFORMATION

Additional supporting information may be found online in the Supporting Information section.

Supplementary Information

Title: Proprotein Convertase Subtilisin/Kexin Type 9 (PCSK9) Regulates the Production of Acute-Phase Reactants from the Liver

Authors: Dafne Jacome Sanz[1], Anni K. Saralahti[2,*], Meeri Pekkarinen[3,*], Juha Kesseli[3], Matti Nykter[3], Mika Rämet[2,4,5,6], Markus J.T. Ojanen[1,+,#], Marko Pesu[1,7,+]

[*,+] equal contribution

Affiliations:

[1]Laboratory of Immunoregulation, Faculty of Medicine and Health Technology, Tampere University, Tampere FI-33014, Finland;

[2]Laboratory of Experimental Immunology, Faculty of Medicine and Health Technology, Tampere University, Tampere FI-33014, Finland;

[3]Laboratory of Computational Biology, Faculty of Medicine and Health Technology, Tampere University, Tampere FI-33014, Finland;

[4]Vaccine Research Center, Faculty of Medicine and Health Technology, Tampere University, Tampere FI-33014, Finland

[5]PEDEGO Research Unit, Medical Research Center, University of Oulu, Oulu FI-90014, Finland;

[6]Department of Children and Adolescents, Oulu University Hospital, Oulu FI-90029, Finland

[7]Fimlab laboratories Ltd, Tampere, Finland

[#]**Corresponding author:** Correspondence to Dr. Markus Ojanen, Faculty of Medicine and Health Technology, Tampere University, Arvo Ylpön katu 34, FI-33520 Tampere, Finland, Email address: markus.ojanen@tuni.fi, ORCID ID: 0000-0001-6623-844X

Supplementary Methods

Production of recombinant Cas9 protein

Expression of recombinant Cas9 protein was made in *E. coli* using 1xNLS-pMJ915v2 plasmid

(1) which was a kind gift from Jennifer Doudna (Addgene plasmid #39312;

http://n2t.net/addgene:39312; RRID:Addgene_39312). The plasmid was transformed into One

Shot® BL21 Star DE3 competent cells (Invitrogen, California, USA) using a standard heat

shock protocol (2). Single colony was used for pre-culture seed that was further used to

inoculate culture by diluting it with ratio of 1:50 to the 1000 ml of lysogeny broth (LB)

supplemented with 5 mM glucose and 50 µg/ml kanamycin. Bacteria was grown at 37 °C under

90 rpm shaking until optical density reached 0.6 after which the temperature was dropped to

18°C and after 30 minutes induced with 0.2 mM IPTG. Cells were harvested after 25 hour

incubation by centrifugation, washed with 50 mM Tris, 0.5 M NaCl, 10 mM imidazole (pH

8.0) buffer and frozen at -20 °C. Eventually, the cells were lysed in 50 mM Tris, 0.5 M NaCl,

10 mM imidazole (pH 8.0) buffer, supernatant clarified with centrifugation at 20 000 x g for

20 minutes and the soluble protein from cleared supernatant bound to 4 ml of Ni-NTA agarose

(Macherey-Nagel, Düren, Germany) at 4 °C. Impurities were washed with 30 ml of binding

buffer and the bound protein eluted from column using 50 mM Tris, 0.5 M NaCl, 500 mM

imidazole, 10 mM EDTA (pH 8.0) buffer. Protein was concentrated and buffer-changed to 20

mM HEPES, 150 mM KCl, 1% sucrose (pH 7.5) using MacroSep 30K Ultrafiltration Units

(PALL Lice Sciences, New York, USA).

Differential gene expression analysis

RNA sequencing data quality control steps and alignment against GRCz11 (ENSEMBL release

97) were performed with Spliced Transcripts Alignment to a Reference (STAR) (3) and

Snakemake (v. 5.6.0) combining the relevant modules from the Snakemake-wrapper release

0.38.0 with in-house scripts (4). After the pre-processing, the analyses were performed in the R-environment (v. 3.6.0) (5) as follows. While the sample clustering and within-group variation was examined by principal component analysis (PCA) using the regularized log (rlog)-transformed gene counts and DESeq2 (v. 1.24.0) (6), we could simultaneously analyze the differentially expressed genes (DEGs) between homozygous $pcsk9^{tpu-13/tpu-13}$ mutant zebrafish and the WT controls within each treatment group. Results were annotated with biomaRt (v. 2.40.5) (7), and the transcripts with Benjamini-Hochberg (BH) adjusted p-values smaller than 0.05 were considered differentially expressed and chosen for further analysis (8). Expression of protein-coding DEGs were visualized with pheatmap using the rlog-transformed gene counts as the input (9). Gene ontology was examined using GOrilla (10, 11) with two unranked lists of genes using the standard Hyper Geometric statistics (Target list: adjusted P-value <0.05, Background list: adjusted P-value ≥0.05) using the *Danio rerio* genome assembly.

Western blotting

HepG2 cell lysates were boiled in 4x Laemmli sample buffer (Bio-Rad Laboratories, California, USA) containing 2-Mercaptoethanol (Sigma-Aldrich, Missouri, USA) for 5min at 98°C and loaded on in-house prepared 7.5% or 12% gels for SDS-PAGE. Gels were blotted using Trans-Blot® Turbo™ Midi Nitrocellulose Transfer Packs (Bio-Rad) and the Trans-Blot® Turbo™ Transfer System (Bio-Rad). Membranes were blocked using 0.05% Tween, 4% BSA in TBS. 0.05% Tween, 0.5% BSA and 0.02% NaN3 in TBS was used for the staining solutions. Proteins were detected using the following antibodies; anti-PCSK9 (1/1000 dilution; #85813; Cell Signaling Technology, Massachusetts, USA), anti-HAMP (1/10 dilution #30760; Abcam, Cambridge, UK), anti-β-tubulin (1/1000 dilution; #166729; Santa Cruz Biotechnology, Texas, USA), IRDye® 680LT Goat anti-Rabbit (1/10,000 dilution; #925-68021; LI-COR Biosciences, Nebraska, USA) and IRDye® 800CW Goat anti-Mouse

(1/10,000 dilution; #925-32210; LI-COR Biosciences). Odyssey® CLx imaging system (LI-COR Biosciences) was used for imaging.

Supplementary Figures
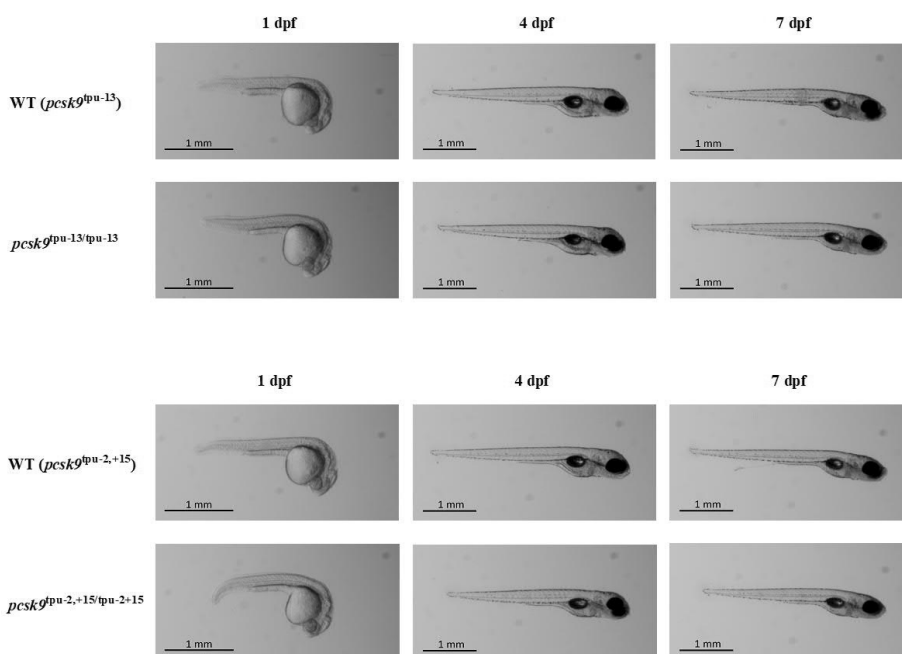
Supplementary Figure 1. *pcsk9* KO zebrafish are morphologically similar to WT controls during development. Ungenotyped F2-progeny of *pcsk9*[tpu-13/+] and *pcsk9*[tpu-2+15/+] zebrafish were imaged at 1, 4 and 7 dpf. At 4 and 7 dpf, the larvae were anesthetized for imaging with 0.02% 3-amino benzoic acid ethyl ester (Sigma-Aldrich), and eventually collected for genotyping at 7 dpf. Sanger sequencing and PCR product size was used for genotyping these larvae. Representative images of *pcsk9*[tpu-13/tpu-13] and *pcsk9*[tpu-2+15/tpu-2+15] embryos/larvae are shown together with corresponding WT controls. Micrographs were taken with Zeiss Lumar V12 fluorescence microscope and Axiocam MRm digital camera using a bright field exposure of 2 ms. A 22x-magnification was used at 1 dpf and a 17x-magnification at 4 and 7 dpf.
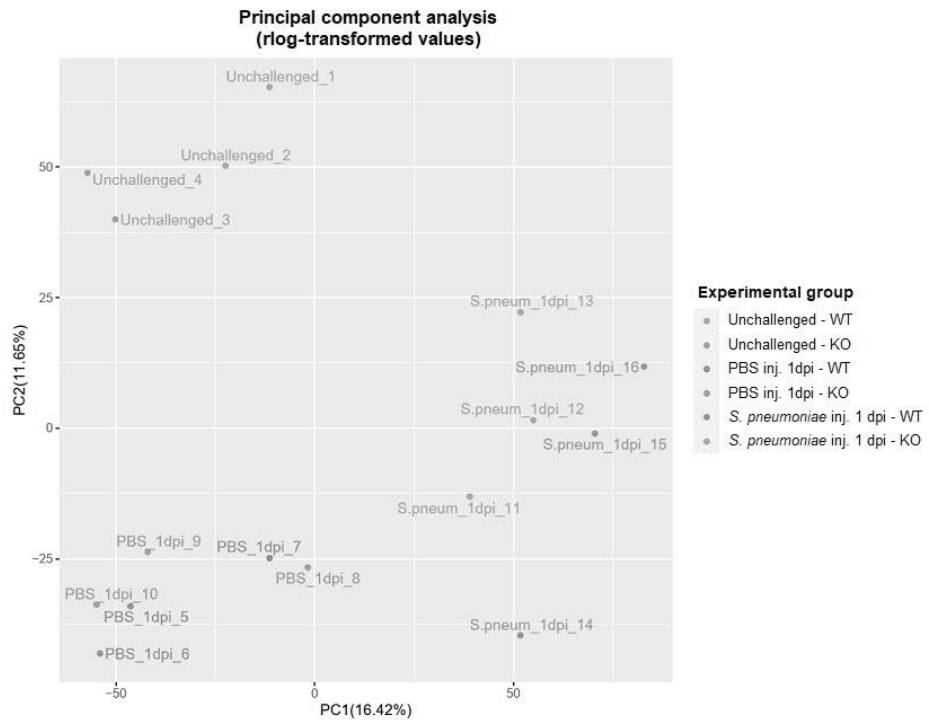
Supplementary Figure 2. Genome-wide transcriptome analysis using principal component analysis (PCA). RNA was isolated from the liver of unchallenged (n=2 in both groups), PBS injected (n=3 in both groups) and *S. pneumoniae* infected (3,370,000 CFU; SD 840,000 CFU, n=3 in both groups) adult *pcsk9*[tpu-13/tpu-13] and WT zebrafish at 1 dpi and the transcriptome analyzed using RNA sequencing. The sample clustering between and within rlog transformed gene counts are depicted using PCA.

A

B
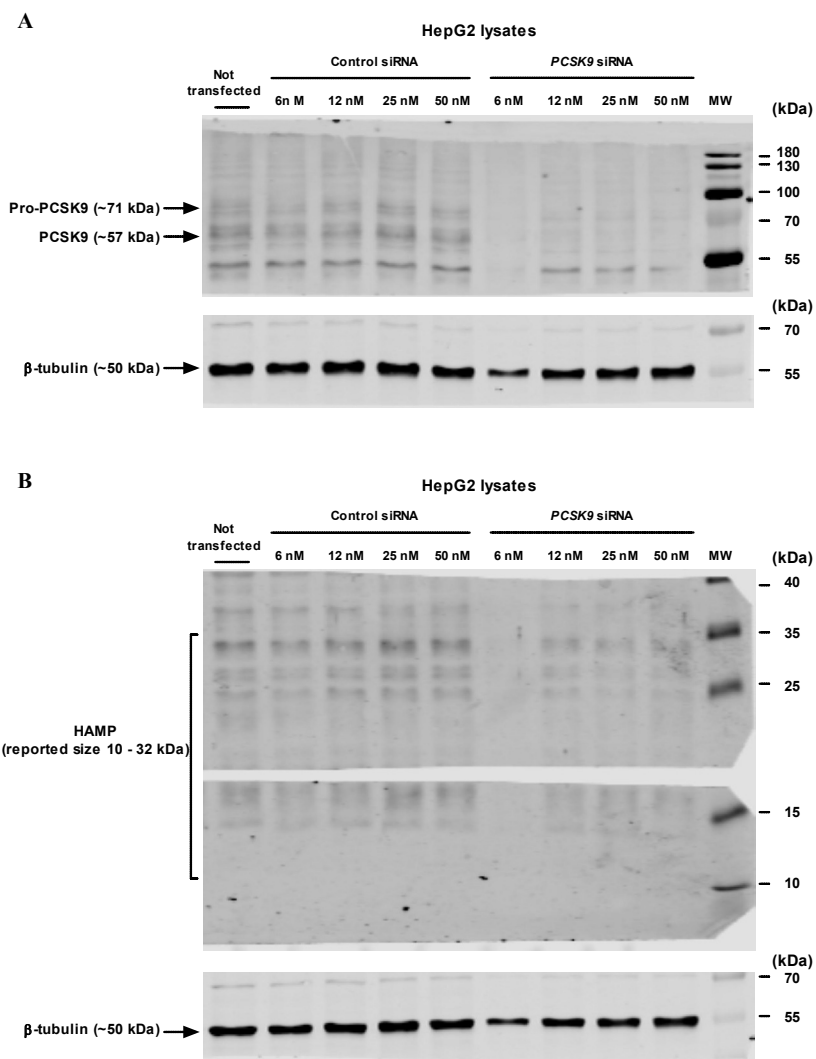
Supplementary Figure 3. PCSK9 and HAMP protein levels are decreased in HepG2 cells after a siRNA-mediated silencing of *PCSK9*. Human PCSK9 A) and HAMP B) were detected from the cell lysates of untreated HepG2 cells and control or PCSK9 siRNA transfected cells using western blotting. Working concentrations between 6 and 50 nM were used for siRNAs, and β-tubulin was used as a control protein in the detection. MW=PageRuler™ Prestained Protein Ladder, 10 to 180 kDa (#26616; Thermo Fisher Scientific, Massachusetts, USA).

Supplementary References

1. Staahl BT, Benekareddy M, Coulon-Bainier C, Banfal AA, Floor SN, Sabo JK, Urnes C, et al. Efficient genome editing in the mouse brain by local delivery of engineered Cas9 ribonucleoprotein complexes. Nat Biotechnol 2017; 35(5): 431-434.

2. Eschbach S, Hofmann C, Maerz M, Maier U-, Sitte P. Molecular Cloning. A Laboratory Manual. 2. Auflage. Hrsg. Von J. Sambrook, E. F. Fritsch, T. Maniatis, Cold Spring Harbor Laboratory Press, Cold Spring Harbour 1989, ISBN 0-87969-309-6, 1990:285-285.

3. Dobin A, Davis CA, Schlesinger F, Drenkow J, Zaleski C, Jha S, Batut P, et al. STAR: Ultrafast universal RNA-seq aligner. Bioinformatics 2013; 29(1): 15-21.

4. Köster J, Rahmann S. Snakemake—a scalable bioinformatics workflow engine. Bioinformatics 2012; 28(19): 2520-2522.

5. R Core Team. R: A language and environment for statistical computing. 2019; 2020(17.11.).

6. Love MI, Huber W, Anders S. Moderated estimation of fold change and dispersion for RNA-seq data with DESeq2. Genome Biol 2014; 15(12): 550.

7. Durinck S, Spellman PT, Birney E, Huber W. Mapping identifiers for the integration of genomic datasets with the R/bioconductor package biomaRt. Nat Protoc 2009; 4(8): 1184-1191.

8. Benjamini Y, Hochberg Y. Controlling the false discovery rate: A practical and powerful approach to multiple testing. Journal of the Royal Statistical Society: Series B (Methodological) 1995; 57(1): 289-300.

9. Kolde Raivo. R. pheatmap: Pretty heatmaps. 2019.

10. Eden E, Navon R, Steinfeld I, Lipson D, Yakhini Z. GOrilla: A tool for discovery and visualization of enriched GO terms in ranked gene lists. BMC Bioinformatics 2009; 10: 48.

11. Eden E, Lipson D, Yogev S, Yakhini Z. Discovering motifs in ranked lists of DNA sequences. PLoS Comput Biol 2007; 3(3): e39.

Supplementary Table 1. Oligonucleotide primer sequences for qPCR analysis. Organism and gene information together with Ensembl identification code and the primer sequence is described.

Organism	Gene symbol	Ensembl ID*	Sequence 5´- 3´
Danio rerio	pcsk9	ENSDARG00000074185	F: CACAGGCAGGCCAGTCAGTG
			R: GCTGAGAGGCCAGAGATGAC
Danio rerio	ldlrap1a	ENSDARG00000004311	F: ACTGCACAGCTGACAAGACG
			R: AGAACTCGAAGGCCACTCTG
Danio rerio	hamp	ENSDARG00000102175	F: GATGAGCATCATGTGGAGAG
			R: GTATCCGCAGCCTTTATTGC
Danio rerio	socs3a	ENSDARG00000025428	F: AGCCGAGACTCGACACTCTG
			R: CCTTGGAGCTGAAGGTCTTG
Danio rerio	eef1a1l1 (ef1a)	ENSDARG00000020850	F: CTGGAGGCCAGCTCAAACAT
			R: ATCAAGAAGAGTAGTACCGCTAGCATTAC
Homo sapiens	PCSK9	ENSG00000169174	F: GACACCAGCATACAGAGTGACC
			R: GTGCCATGACTGTCACACTTGC
Homo sapiens	HAMP	ENSG00000105697	F: CTGACCAGTGGCTCTGTTTTCC
			R: AAGTGGGTGTCTCGCCTCCTTC
Homo sapiens	C7	ENSG00000112936	F: GTGGTTTGGCTACTGTTGAGGG
			R: TCCAAGAGGACCAGCAACTCCA
Homo sapiens	SOCS3	ENSG00000184557	F: CATCTCTGTCGGAAGACCGTCA
			R: GCATCGTACTGGTCCAGGAACT
Homo sapiens	TNF	ENSG00000232810	F: CTCTTCTGCCTGCTGCACTTTG
			R: ATGGGCTACAGGCTTGTCACTC
Homo sapiens	TNFAIP3	ENSG00000118503	F: CTCAACTGGTGTCGAGAAGTCC
			R: TTCCTTGAGCGTGCTGAACAGC
Homo sapiens	C6	ENSG00000039537	F: GTGTCAGAGTGGCACCTATGGT
			R: GTAGCATCACAGGTACTCCAGG
Homo sapiens	LDLRAP1	ENSG00000157978	F: CCATCAAGAGGATCGTGGCTAC
			R: GGACACGTTCTCAATGAGCTGG
Homo sapiens	GAPDH	ENSG00000111640	F: GTCTCCTCTGACTTCAACAGCG
			R: ACCACCCTGTTGCTGTAGCCAA

* ID= Identification code

Supplementary Table 2. Differentially expressed genes in unchallenged *pcsk9* KO zebrafish. Gene expression in unchallenged *pcsk9*$^{tpu-13/tpu-13}$ (n=2) zebrafish liver was compared to WT siblings (n=2). RNA sequencing was performed using Illumina PE150 platform (50M reads).

Up-regulated transcripts

Gene ID (Ensembl)	Gene symbol	Gene Name	Average log2 Fold Change	Adj. P-value
ENSDARG00000077058	cela1.5	chymotrypsin like elastase family member 1, tandem duplicate 5 [Source:ZFIN;Acc:ZDB-GENE-040801-186]	23,70	1,03E-04
ENSDARG00000093173	si:dkey-93m18.6	si:dkey-93m18.6 [Source:ZFIN;Acc:ZDB-GENE-091204-133]	11,26	1,73E-10
ENSDARG00000055331	aldh9a1a.2	aldehyde dehydrogenase 9 family, member A1a, tandem duplicate 2 [Source:ZFIN;Acc:ZDB-GENE-081104-507]	8,22	6,74E-10
ENSDARG00000079997	si:zfos-223e1.2	si:zfos-223e1.2 [Source:ZFIN;Acc:ZDB-GENE-110411-269]	7,62	4,01E-03
ENSDARG00000070132	aste1a	asteroid homolog 1a [Source:ZFIN;Acc:ZDB-GENE-060503-520]	7,59	1,18E-03
ENSDARG00000011171	si:ch211-12m10.1	si:ch211-12m10.1 [Source:ZFIN;Acc:ZDB-GENE-060503-100]	7,57	1,41E-03
ENSDARG00000103060	ly6m7	lymphocyte antigen 6 family member M7 [Source:ZFIN;Acc:ZDB-GENE-131121-290]	7,55	1,40E-03
ENSDARG00000093477	zgc:123299	cytochrome P450 family 46 subfamily A member 1 [Source:HGNC Symbol;Acc:HGNC:2641]	7,14	5,24E-03
ENSDARG00000037122	si:dkey-34l15.2	teneurin transmembrane protein 2 [Source:HGNC Symbol;Acc:HGNC:29943]	6,92	7,25E-06
ENSDARG00000078069	rrm2	ribonucleotide reductase M2 polypeptide [Source:ZFIN;Acc:ZDB-GENE-990415-25]	6,57	3,86E-02
ENSDARG00000027529	hmox1a	heme oxygenase 1a [Source:ZFIN;Acc:ZDB-GENE-030131-3102]	6,55	3,14E-38
ENSDARG00000095193	si:dkey-23c22.7	si:dkey-23c22.7 [Source:ZFIN;Acc:ZDB-GENE-081105-139]	6,55	2,73E-02
ENSDARG00000052037	trim35-1	tripartite motif containing 35-1 [Source:ZFIN;Acc:ZDB-GENE-050522-17]	5,97	2,65E-04
ENSDARG00000060350	apoda.2	apolipoprotein Da, duplicate 2 [Source:ZFIN;Acc:ZDB-GENE-070912-551]	5,96	8,05E-03
ENSDARG00000103642	pglyrp6	peptidoglycan recognition protein 6 [Source:ZFIN;Acc:ZDB-GENE-071227-2]	5,42	3,27E-03
ENSDARG00000093449		heat shock cognate 70-kd protein, tandem duplicate 3 [Source:ZFIN;Acc:ZDB-GENE-110713-1]	4,92	2,52E-03
ENSDARG00000021924	hsp70.3		4,42	1,68E-10
ENSDARG00000093844	zgc:136461	zgc:136461 [Source:ZFIN;Acc:ZDB-GENE-060519-7]	4,38	1,93E-02
ENSDARG00000013856	amy2a	amylase alpha 2A (pancreatic) [Source:ZFIN;Acc:ZDB-GENE-040426-2393]	4,13	3,43E-02

Gene ID	Symbol	Description	Value	p-value
ENSDARG00000056210	si:ch211-199o1.2	si:ch211-199o1.2 [Source:ZFIN;Acc:ZDB-GENE-060503-867]	4,00	3,01E-03
ENSDARG00000043171	cela1.4	chymotrypsin like elastase family member 1, tandem duplicate 4 [Source:ZFIN;Acc:ZDB-GENE-050626-127]	3,97	2,28E-04
ENSDARG00000105046	ccnf	cyclin F [Source:ZFIN;Acc:ZDB-GENE-021030-2]	3,92	1,58E-06
ENSDARG00000077236	hspb6	heat shock protein, alpha-crystallin-related, b6 [Source:ZFIN;Acc:ZDB-GENE-080214-7]	3,80	5,32E-03
ENSDARG00000029822	cel.2	carboxyl ester lipase, tandem duplicate 2 [Source:ZFIN;Acc:ZDB-GENE-061110-10]	3,72	9,68E-07
ENSDARG00000095462	cela1.2	chymotrypsin like elastase family member 1, tandem duplicate 2 [Source:ZFIN;Acc:ZDB-GENE-050208-732]	3,65	1,24E-05
ENSDARG00000098191	si:dkey-16l2.20	si:dkey-16l2.20 [Source:ZFIN;Acc:ZDB-GENE-141212-380]	3,58	2,45E-02
ENSDARG00000021339	cpa5	carboxypeptidase A5 [Source:ZFIN;Acc:ZDB-GENE-020514-1]	3,57	2,48E-05
ENSDARG00000004262	cyp46a1.2	cytochrome P450, family 46, subfamily A, polypeptide 1, tandem duplicate 2 [Source:ZFIN;Acc:ZDB-GENE-040426-1184]	3,56	2,44E-11
ENSDARG00000052290	rab33ba	RAB33B, member RAS oncogene family a [Source:ZFIN;Acc:ZDB-GENE-050809-122]	3,53	6,43E-03
ENSDARG00000039730	zgc:112160	zgc:112160 [Source:ZFIN;Acc:ZDB-GENE-050417-229]	3,52	4,08E-05
ENSDARG00000030915	cpa1	carboxypeptidase A1 (pancreatic) [Source:ZFIN;Acc:ZDB-GENE-050522-438]	3,50	4,95E-05
ENSDARG00000079274	prss59.1	serine protease 59, tandem duplicate 1 [Source:ZFIN;Acc:ZDB-GENE-030131-1173]	3,40	1,78E-04
ENSDARG00000038500	cep41	centrosomal protein 41 [Source:ZFIN;Acc:ZDB-GENE-040704-35]	3,36	2,83E-02
ENSDARG00000044204	endou	endonuclease, polyU-specific [Source:ZFIN;Acc:ZDB-GENE-070112-2012]	3,35	7,72E-04
ENSDARG00000076313	si:ch211-240l19.7	si:ch211-240l19.7 [Source:ZFIN;Acc:ZDB-GENE-041210-329]	3,34	1,20E-04
ENSDARG00000090428	ctrb1	chymotrypsinogen B1 [Source:ZFIN;Acc:ZDB-GENE-030131-1171]	3,34	5,19E-05
ENSDARG00000042993	prss1	serine protease 1 [Source:ZFIN;Acc:ZDB-GENE-010131-7]	3,32	1,94E-04
ENSDARG00000007276	ela3l	elastase 3 like [Source:ZFIN;Acc:ZDB-GENE-060710-2]	3,26	2,36E-04
ENSDARG00000073742	prss59.2	serine protease 59, tandem duplicate 2 [Source:ZFIN;Acc:ZDB-GENE-110408-10]	3,23	3,65E-04
ENSDARG00000071585	stard15	StAR-related lipid transfer (START) domain containing 15 [Source:ZFIN;Acc:ZDB-GENE-070424-267]	3,15	1,65E-07
ENSDARG00000078259	bnip1a	BCL2 interacting protein 1a [Source:ZFIN;Acc:ZDB-GENE-081107-44]	3,14	4,49E-03
ENSDARG00000043175	cela1.1	chymotrypsin like elastase family member 1, tandem duplicate 1 [Source:ZFIN;Acc:ZDB-GENE-050522-187]	3,12	2,18E-04
ENSDARG00000052578	c6ast4	six-cysteine containing astacin protease 4 [Source:ZFIN;Acc:ZDB-GENE-050626-100]	3,11	1,74E-03
ENSDARG00000071658	ywhag2	3-monooxygenase/tryptophan 5-monooxygenase activation protein, gamma polypeptide 2 [Source:ZFIN;Acc:ZDB-GENE-061023-2]	3,10	1,85E-02
ENSDARG00000056744	ela2	elastase 2 [Source:ZFIN;Acc:ZDB-GENE-041117-1]	3,09	1,20E-04

Gene ID	Symbol	Description	Value	p-value
ENSDARG00000018263	pdia2	protein disulfide isomerase family A, member 2 [Source:ZFIN;Acc:ZDB-GENE-040426-705]	3,07	1,79E-03
ENSDARG00000098108	dusp2	dual specificity phosphatase 2 [Source:ZFIN;Acc:ZDB-GENE-040801-188]	3,07	5,19E-05
ENSDARG00000017314	cela1.6	chymotrypsin like elastase family member 1, tandem duplicate 6 [Source:ZFIN;Acc:ZDB-GENE-040808-55]	3,05	6,57E-04
ENSDARG00000043173	cela1.3	chymotrypsin like elastase family member 1, tandem duplicate 3 [Source:ZFIN;Acc:ZDB-GENE-040801-12]	2,91	8,16E-04
ENSDARG00000042548	tpd52l1	tpd52 like 1 [Source:ZFIN;Acc:ZDB-GENE-050522-121]	2,89	3,73E-06
ENSDARG00000016886	dnajb9b	DnaJ heat shock protein family (Hsp40) member B9b [Source:ZFIN;Acc:ZDB-GENE-050522-76]	2,86	5,44E-05
ENSDARG00000012539	dnase1	deoxyribonuclease I [Source:ZFIN;Acc:ZDB-GENE-040718-423]	2,84	2,55E-02
ENSDARG00000069113	dbn1	drebrin 1 [Source:ZFIN;Acc:ZDB-GENE-091204-284]	2,82	1,72E-03
ENSDARG00000040039	pttg1ipb	PTTG1 interacting protein b [Source:ZFIN;Acc:ZDB-GENE-041010-10]	2,82	5,26E-03
ENSDARG00000036074	cebpa	CCAAT enhancer binding protein alpha [Source:ZFIN;Acc:ZDB-GENE-020111-2]	2,80	2,30E-03
ENSDARG00000093619	sult3st2	sulfotransferase family 3, cytosolic sulfotransferase 2 [Source:ZFIN;Acc:ZDB-GENE-030131-1135]	2,78	8,56E-05
ENSDARG00000009153	pla2g1b	phospholipase A2, group IB (pancreas) [Source:ZFIN;Acc:ZDB-GENE-070117-1]	2,77	3,78E-03
ENSDARG00000009001	pdia6	protein disulfide isomerase family A, member 6 [Source:ZFIN;Acc:ZDB-GENE-030131-879]	2,76	7,56E-09
ENSDARG00000075930	adamts2	ADAM metallopeptidase with thrombospondin type 1 motif, 2 [Source:ZFIN;Acc:ZDB-GENE-070816-3]	2,74	7,62E-04
ENSDARG00000024759	inhbab	inhibin subunit beta Ab [Source:ZFIN;Acc:ZDB-GENE-050525-2]	2,71	7,62E-04
ENSDARG00000062943	taco1	translational activator of mitochondrially encoded cytochrome c oxidase I [Source:ZFIN;Acc:ZDB-GENE-070410-35]	2,70	6,47E-04
ENSDARG00000061621	them4	thioesterase superfamily member 4 [Source:ZFIN;Acc:ZDB-GENE-070112-982]	2,66	2,43E-03
ENSDARG00000015822	sesn3	sestrin 3 [Source:ZFIN;Acc:ZDB-GENE-040426-2924]	2,65	1,95E-04
ENSDARG00000019302	mid1ip1b	MID1 interacting protein 1b [Source:ZFIN;Acc:ZDB-GENE-040426-1720]	2,63	2,44E-05
ENSDARG00000023498	gmppab	GDP-mannose pyrophosphorylase Ab [Source:ZFIN;Acc:ZDB-GENE-040426-1550]	2,63	1,06E-04
ENSDARG00000063079	ago3b	argonaute RISC catalytic component 3b [Source:ZFIN;Acc:ZDB-GENE-060503-452]	2,62	2,91E-04
ENSDARG00000079369	si:ch211-212g7.6	si:ch211-212g7.6 [Source:ZFIN;Acc:ZDB-GENE-030131-4695]	2,61	1,64E-07
ENSDARG00000002745	tdh	L-threonine dehydrogenase [Source:ZFIN;Acc:ZDB-GENE-040426-2379]	2,52	8,93E-05
ENSDARG00000044098	egr2a	early growth response 2a [Source:ZFIN;Acc:ZDB-GENE-030723-6]	2,48	4,51E-03
ENSDARG00000010146	cpa2	carboxypeptidase A2 (pancreatic) [Source:ZFIN;Acc:ZDB-GENE-040801-182]	2,45	3,64E-02
ENSDARG00000110325	zgc:153733	zgc:153733 [Source:ZFIN;Acc:ZDB-GENE-060825-273]	2,43	1,42E-03

Gene ID	Symbol	Description	Value 1	Value 2
ENSDARG00000015709	hsd17b12a	hydroxysteroid (17-beta) dehydrogenase 12a [Source:ZFIN;Acc:ZDB-GENE-030131-5628]	2,42	2,52E-03
ENSDARG00000024746	hsp90aa1.2	heat shock protein 90, alpha (cytosolic), class A member 1, tandem duplicate 2 [Source:ZFIN;Acc:ZDB-GENE-031001-3]	2,39	2,21E-03
ENSDARG00000043168	cela1.5	chymotrypsin like elastase family member 1, tandem duplicate 5 [Source:ZFIN;Acc:ZDB-GENE-040801-186]	2,38	1,56E-04
ENSDARG00000016607	echdc2	enoyl CoA hydratase domain containing 2 [Source:ZFIN;Acc:ZDB-GENE-030219-147]	2,37	8,59E-05
ENSDARG00000059308	golt1bb	golgi transport 1Bb [Source:ZFIN;Acc:ZDB-GENE-050913-94]	2,37	2,36E-04
ENSDARG00000069843	kctd12.1	potassium channel tetramerisation domain containing 12.1 [Source:ZFIN;Acc:ZDB-GENE-030902-5]	2,35	7,44E-03
ENSDARG00000101139	agpat2	1-acylglycerol-3-phosphate O-acyltransferase 2 (lysophosphatidic acid acyltransferase, beta) [Source:ZFIN;Acc:ZDB-GENE-061103-541]	2,35	3,45E-05
ENSDARG00000052703	cisd2	CDGSH iron sulfur domain 2 [Source:ZFIN;Acc:ZDB-GENE-040426-1381]	2,31	6,22E-05
ENSDARG00000069681	pcgf6	polycomb group ring finger 6 [Source:ZFIN;Acc:ZDB-GENE-060526-178]	2,31	1,21E-04
ENSDARG00000044692	eri1	exoribonuclease 1 [Source:ZFIN;Acc:ZDB-GENE-050522-39]	2,27	3,48E-06
ENSDARG00000042873	slc25a27	solute carrier family 25 member 27 [Source:ZFIN;Acc:ZDB-GENE-040426-1290]	2,27	5,07E-03
ENSDARG00000035565	atp6v0a2b	ATPase H+ transporting V0 subunit a2b [Source:ZFIN;Acc:ZDB-GENE-060526-4]	2,26	2,42E-03
ENSDARG00000002792	arcn1a	archain 1a [Source:ZFIN;Acc:ZDB-GENE-021031-2]	2,23	4,46E-06
ENSDARG00000052537	cptp	ceramide-1-phosphate transfer protein [Source:ZFIN;Acc:ZDB-GENE-040801-240]	2,22	7,67E-04
ENSDARG00000035905	slc25a44b	solute carrier family 25 member 44b [Source:ZFIN;Acc:ZDB-GENE-050320-89]	2,20	1,53E-02
ENSDARG00000023160	snrnp40	small nuclear ribonucleoprotein 40 (U5) [Source:ZFIN;Acc:ZDB-GENE-040426-978]	2,18	3,27E-03
ENSDARG00000098746	dhrs13l1	dehydrogenase/reductase (SDR family) member 13 like 1 [Source:ZFIN;Acc:ZDB-GENE-040426-1907]	2,18	2,45E-02
ENSDARG00000030465	tmem263	transmembrane protein 263 [Source:ZFIN;Acc:ZDB-GENE-040426-2155]	2,17	7,01E-06
ENSDARG00000055760	srm	spermidine synthase [Source:ZFIN;Acc:ZDB-GENE-040426-1183]	2,16	1,69E-05
ENSDARG00000035167	mrpl48	mitochondrial ribosomal protein L48 [Source:ZFIN;Acc:ZDB-GENE-041008-125]	2,15	3,44E-03
ENSDARG00000099996	rhot1a	ras homolog family member T1a [Source:ZFIN;Acc:ZDB-GENE-030131-5354]	2,14	1,73E-05
ENSDARG00000010169	myd88	MYD88 innate immune signal transduction adaptor [Source:ZFIN;Acc:ZDB-GENE-040219-3]	2,14	1,49E-03
ENSDARG00000097155	zgc:153343	GDP-D-glucose phosphorylase 1 [Source:HGNC Symbol;Acc:HGNC:34360]	2,13	3,78E-03
ENSDARG00000011769	cpm	carboxypeptidase M [Source:ZFIN;Acc:ZDB-GENE-041210-191]	2,10	4,08E-02
ENSDARG00000098838	sdr42e1	short chain dehydrogenase/reductase family 42E, member 1 [Source:ZFIN;Acc:ZDB-GENE-051120-63]	2,06	3,93E-02
ENSDARG00000099195	ier2a	immediate early response 2a [Source:ZFIN;Acc:ZDB-GENE-030131-9126]	2,05	2,96E-03

Ensembl ID	Gene	Description	Fold	p-value
ENSDARG00000075618	slc36a1	solute carrier family 36 member 1 [Source:ZFIN;Acc:ZDB-GENE-061117-1]	2,04	1,07E-02
ENSDARG00000031496	ap1ar	adaptor related protein complex 1 associated regulatory protein [Source:ZFIN;Acc:ZDB-GENE-130530-580]	2,04	2,66E-03
ENSDARG00000074169	gpam	glycerol-3-phosphate acyltransferase, mitochondrial [Source:ZFIN;Acc:ZDB-GENE-101026-1]	2,03	4,78E-03
ENSDARG00000037042	ddhd1b	DDHD domain containing 1b [Source:ZFIN;Acc:ZDB-GENE-040724-18]	2,02	1,13E-02
ENSDARG00000011600	epha4b	eph receptor A4b [Source:ZFIN;Acc:ZDB-GENE-030826-6]	2,01	4,01E-02
ENSDARG00000076765	ddhd2	DDHD domain containing 2 [Source:ZFIN;Acc:ZDB-GENE-080519-4]	1,99	2,50E-02
ENSDARG00000056059	rangap1b	Ran GTPase activating protein 1b [Source:ZFIN;Acc:ZDB-GENE-040426-1921]	1,98	2,83E-03
ENSDARG00000061354	foxred2	FAD-dependent oxidoreductase domain containing 2 [Source:ZFIN;Acc:ZDB-GENE-060929-1026]	1,97	1,90E-04
ENSDARG00000098646	mthfd2	methylenetetrahydrofolate dehydrogenase (NADP+ dependent) 2, methenyltetrahydrofolate cyclohydrolase [Source:ZFIN;Acc:ZDB-GENE-040704-20]	1,96	1,78E-02
ENSDARG00000042708	tuba8l	tubulin, alpha 8 like [Source:ZFIN;Acc:ZDB-GENE-030131-9167]	1,96	5,16E-05
ENSDARG00000071426	lrrc59	leucine rich repeat containing 59 [Source:ZFIN;Acc:ZDB-GENE-040426-2547]	1,95	1,56E-04
ENSDARG00000091836	casp7	caspase 7, apoptosis-related cysteine peptidase [Source:ZFIN;Acc:ZDB-GENE-050522-506]	1,94	4,95E-04
ENSDARG00000019355	coa7	cytochrome c oxidase assembly factor 7 [Source:ZFIN;Acc:ZDB-GENE-041014-16]	1,92	2,15E-03
ENSDARG00000045254	zmp:0000000624	zmp:0000000624 [Source:ZFIN;Acc:ZDB-GENE-130530-627]	1,91	2,52E-03
ENSDARG00000056600	papss2b	3'-phosphoadenosine 5'-phosphosulfate synthase 2b [Source:ZFIN;Acc:ZDB-GENE-010323-5]	1,90	4,32E-04
ENSDARG00000105195	dnajc21	DnaJ heat shock protein family (Hsp40) member C21 [Source:ZFIN;Acc:ZDB-GENE-030131-8928]	1,89	2,06E-03
ENSDARG00000010432	eaf2	ELL associated factor 2 [Source:ZFIN;Acc:ZDB-GENE-040625-179]	1,88	3,50E-04
ENSDARG00000017199	elp2	elongator acetyltransferase complex subunit 2 [Source:ZFIN;Acc:ZDB-GENE-060503-525]	1,88	1,35E-02
ENSDARG00000074807	tbrg4	transforming growth factor beta regulator 4 [Source:ZFIN;Acc:ZDB-GENE-091020-8]	1,88	8,16E-04
ENSDARG00000041220	ftr53	finTRIM family, member 53 [Source:ZFIN;Acc:ZDB-GENE-030616-515]	1,87	4,54E-02
ENSDARG00000056367	mpv17l2	MPV17 mitochondrial membrane protein-like 2 [Source:ZFIN;Acc:ZDB-GENE-040718-306]	1,87	2,77E-04
ENSDARG00000008548	arhgap12a	Rho GTPase activating protein 12a [Source:ZFIN;Acc:ZDB-GENE-050809-38]	1,87	2,61E-02
ENSDARG00000103902	nde1	nudE neurodevelopment protein 1 [Source:ZFIN;Acc:ZDB-GENE-050913-61]	1,87	2,15E-02
ENSDARG00000063177	manf	mesencephalic astrocyte-derived neurotrophic factor [Source:ZFIN;Acc:ZDB-GENE-060929-640]	1,86	3,28E-05
ENSDARG00000057184	zgc:55781	zgc:55781 [Source:ZFIN;Acc:ZDB-GENE-030131-4704]	1,85	3,54E-03
ENSDARG00000006786	copz2	coatomer protein complex, subunit zeta 2 [Source:ZFIN;Acc:ZDB-GENE-000406-5]	1,84	2,61E-03

Ensembl ID	Symbol	Description	Value	p-value
ENSDARG00000043666	abt1	activator of basal transcription 1 [Source:ZFIN;Acc:ZDB-GENE-050522-127]	1,84	9,41E-03
ENSDARG00000008840	hmbsa	hydroxymethylbilane synthase a [Source:ZFIN;Acc:ZDB-GENE-040426-1375]	1,84	8,22E-04
ENSDARG00000076251	irf3	interferon regulatory factor 3 [Source:ZFIN;Acc:ZDB-GENE-071120-7]	1,84	3,61E-02
ENSDARG00000044899	tmem183a	transmembrane protein 183A [Source:ZFIN;Acc:ZDB-GENE-050327-5]	1,82	1,72E-03
ENSDARG00000028367	sult2st3	sulfotransferase family 2, cytosolic sulfotransferase 3 [Source:ZFIN;Acc:ZDB-GENE-061117-4]	1,81	4,72E-02
ENSDARG00000030038	grcc10	gene rich cluster, C10 gene [Source:ZFIN;Acc:ZDB-GENE-030131-2279]	1,81	4,16E-02
ENSDARG00000004517	ppat	phosphoribosyl pyrophosphate amidotransferase [Source:ZFIN;Acc:ZDB-GENE-041210-323]	1,81	1,87E-03
ENSDARG00000042539	ywhaqa	tyrosine 3-monooxygenase/tryptophan 5-monooxygenase activation protein, theta polypeptide a [Source:ZFIN;Acc:ZDB-GENE-040122-5]	1,80	2,04E-03
ENSDARG00000029695	pgp	phosphoglycolate phosphatase [Source:ZFIN;Acc:ZDB-GENE-030131-6240]	1,80	4,37E-02
ENSDARG00000044405	ttc4	tetratricopeptide repeat domain 4 [Source:ZFIN;Acc:ZDB-GENE-040426-1021]	1,79	7,25E-03
ENSDARG00000016093	qtrt2	queuine tRNA-ribosyltransferase accessory subunit 2 [Source:ZFIN;Acc:ZDB-GENE-060427-4]	1,78	5,37E-03
ENSDARG00000074533	slc25a38b	solute carrier family 25 member 38b [Source:ZFIN;Acc:ZDB-GENE-110214-1]	1,78	2,49E-02
ENSDARG00000043542	zpr1	ZPR1 zinc finger [Source:ZFIN;Acc:ZDB-GENE-040426-2110]	1,78	5,31E-04
ENSDARG00000012572	polr3f	polymerase (RNA) III (DNA directed) polypeptide F [Source:ZFIN;Acc:ZDB-GENE-040426-972]	1,77	8,85E-03
ENSDARG00000007377	odc1	ornithine decarboxylase 1 [Source:ZFIN;Acc:ZDB-GENE-010816-1]	1,76	7,87E-05
ENSDARG00000004017	spag1a	sperm associated antigen 1a [Source:ZFIN;Acc:ZDB-GENE-030131-9443]	1,76	5,33E-03
ENSDARG00000043304	nop2	NOP2 nucleolar protein homolog (yeast) [Source:ZFIN;Acc:ZDB-GENE-050309-7]	1,76	2,23E-04
ENSDARG00000029071	creld2	cysteine-rich with EGF-like domains 2 [Source:ZFIN;Acc:ZDB-GENE-040426-1626]	1,75	7,78E-03
ENSDARG00000015343	pgd	phosphogluconate dehydrogenase [Source:ZFIN;Acc:ZDB-GENE-040426-2807]	1,74	3,21E-02
ENSDARG00000031098	timm50	translocase of inner mitochondrial membrane 50 homolog (S. cerevisiae) [Source:ZFIN;Acc:ZDB-GENE-040426-1618]	1,74	3,27E-03
ENSDARG00000060150	psmd11a	proteasome 26S subunit, non-ATPase 11a [Source:ZFIN;Acc:ZDB-GENE-030131-2711]	1,74	2,04E-03
ENSDARG00000071669	smyd5	SMYD family member 5 [Source:ZFIN;Acc:ZDB-GENE-040912-39]	1,74	6,11E-03
ENSDARG00000093006	rarres3	retinoic acid receptor responder 3 [Source:ZFIN;Acc:ZDB-GENE-060929-616]	1,73	4,48E-03
ENSDARG00000058992	cers2b	ceramide synthase 2b [Source:ZFIN;Acc:ZDB-GENE-110408-40]	1,71	5,49E-03
ENSDARG00000057672	plpp5	phospholipid phosphatase 5 [Source:ZFIN;Acc:ZDB-GENE-040704-54]	1,71	3,79E-02
ENSDARG00000100498		myeloid-associated differentiation marker-like [Source:NCBI gene;Acc:100536607]	1,71	3,02E-02
ENSDARG00000062864	gk5	glycerol kinase 5 [Source:ZFIN;Acc:ZDB-GENE-061110-49]	1,70	2,11E-03

Ensembl ID	Symbol	Description	Value	p-value
ENSDARG00000010445	trabd	TraB domain containing [Source:ZFIN;Acc:ZDB-GENE-030131-1301]	1,70	2,28E-04
ENSDARG00000012222	nup35	nucleoporin 35 [Source:ZFIN;Acc:ZDB-GENE-030131-9407]	1,70	2,15E-02
ENSDARG00000022340	ufc1	ubiquitin-fold modifier conjugating enzyme 1 [Source:ZFIN;Acc:ZDB-GENE-040801-268]	1,70	3,27E-03
ENSDARG00000013004	tdg.1	thymine DNA glycosylase, tandem duplicate 1 [Source:ZFIN;Acc:ZDB-GENE-050522-44]	1,69	4,98E-02
ENSDARG00000017874	dnajc3b	DnaJ (Hsp40) homolog, subfamily C, member 3b [Source:ZFIN;Acc:ZDB-GENE-000831-4]	1,68	1,87E-02
ENSDARG00000100025	si:ch211-231f6.6	si:ch211-231f6.6 [Source:ZFIN;Acc:ZDB-GENE-141216-156]	1,68	4,46E-02
ENSDARG00000058734	prdx1	peroxiredoxin 1 [Source:ZFIN;Acc:ZDB-GENE-050320-35]	1,67	9,38E-03
ENSDARG00000036489	zgc:112356	zgc:112356 [Source:ZFIN;Acc:ZDB-GENE-050913-28]	1,66	2,50E-02
ENSDARG00000033320	sar1ab	secretion associated, Ras related GTPase 1Ab [Source:ZFIN;Acc:ZDB-GENE-050417-437]	1,66	2,25E-02
ENSDARG00000037158	rcc1	regulator of chromosome condensation 1 [Source:ZFIN;Acc:ZDB-GENE-040426-2216]	1,66	4,21E-03
ENSDARG00000098312	scarb2a	scavenger receptor class B, member 2a [Source:ZFIN;Acc:ZDB-GENE-020419-29]	1,66	8,96E-04
ENSDARG00000102850			1,65	4,60E-02
ENSDARG00000059634	thumpd3	THUMP domain containing 3 [Source:ZFIN;Acc:ZDB-GENE-030131-9745]	1,64	2,96E-03
ENSDARG00000012274	eif4e1c	eukaryotic translation initiation factor 4E family member 1c [Source:ZFIN;Acc:ZDB-GENE-050417-398]	1,63	2,21E-03
ENSDARG00000042401	derl2	derlin 2 [Source:ZFIN;Acc:ZDB-GENE-050522-90]	1,63	2,29E-03
ENSDARG00000031382	reep2	receptor accessory protein 2 [Source:ZFIN;Acc:ZDB-GENE-050706-125]	1,62	2,15E-02
ENSDARG00000089787	crebzf	CREB/ATF bZIP transcription factor [Source:ZFIN;Acc:ZDB-GENE-030131-8015]	1,62	1,11E-02
ENSDARG00000013505	ube2kb	ubiquitin-conjugating enzyme E2Kb (UBC1 homolog, yeast) [Source:ZFIN;Acc:ZDB-GENE-980605-9]	1,62	6,79E-03
ENSDARG00000036076	heatr3	HEAT repeat containing 3 [Source:ZFIN;Acc:ZDB-GENE-040426-1876]	1,62	3,44E-03
ENSDARG00000100317	ahsa1b	AHA1, activator of heat shock protein ATPase homolog 1b [Source:ZFIN;Acc:ZDB-GENE-030131-664]	1,60	7,63E-03
ENSDARG00000042851	srp9	signal recognition particle 9 [Source:ZFIN;Acc:ZDB-GENE-040426-1106]	1,60	1,60E-03
ENSDARG00000000542	gtf2e1	general transcription factor IIE, polypeptide 1, alpha [Source:ZFIN;Acc:ZDB-GENE-041210-221]	1,59	2,05E-02
ENSDARG00000016163	usp33	ubiquitin specific peptidase 33 [Source:ZFIN;Acc:ZDB-GENE-040426-2323]	1,58	1,87E-02
ENSDARG00000038141	atf4b	activating transcription factor 4b [Source:ZFIN;Acc:ZDB-GENE-070928-23]	1,58	9,33E-03
ENSDARG00000052641	kpna3	karyopherin alpha 3 (importin alpha 4) [Source:ZFIN;Acc:ZDB-GENE-030616-541]	1,58	1,46E-03
ENSDARG00000043856	amd1	adenosylmethionine decarboxylase 1 [Source:ZFIN;Acc:ZDB-GENE-040426-760]	1,57	3,27E-02
ENSDARG00000109830		Scm like with four mbt domains 1 [Source:HGNC Symbol;Acc:HGNC:20255]	1,57	9,20E-03
ENSDARG00000087048	si:dkey-165n16.1	si:dkey-165n16.1 [Source:ZFIN;Acc:ZDB-GENE-100922-224]	1,56	3,65E-02
ENSDARG00000070472	arf5	ADP-ribosylation factor 5 [Source:ZFIN;Acc:ZDB-GENE-030910-5]	1,56	7,29E-04

Ensembl ID	Gene	Description	Value	p-value
ENSDARG00000017741	g3bp1	GTPase activating protein (SH3 domain) binding protein 1 [Source:ZFIN;Acc:ZDB-GENE-030131-7452]	1,56	2,11E-03
ENSDARG00000018106	eif2b3	eukaryotic translation initiation factor 2B, subunit 3 gamma [Source:ZFIN;Acc:ZDB-GENE-040426-1039]	1,56	2,05E-02
ENSDARG00000038785	abcf2a	ATP-binding cassette, sub-family F (GCN20), member 2a [Source:ZFIN;Acc:ZDB-GENE-030131-8714]	1,56	2,11E-03
ENSDARG00000078391	fam98a	family with sequence similarity 98 member A [Source:ZFIN;Acc:ZDB-GENE-091202-6]	1,55	2,22E-02
ENSDARG00000041991	rrp9	ribosomal RNA processing 9, U3 small nucleolar RNA binding protein [Source:ZFIN;Acc:ZDB-GENE-060427-1]	1,55	6,51E-03
ENSDARG00000012407	mgat1a	mannosyl (alpha-1,3-)-glycoprotein beta-1,2-N-acetylglucosaminyltransferase a [Source:ZFIN;Acc:ZDB-GENE-040426-1515]	1,55	2,83E-03
ENSDARG00000016496	cdk8	cyclin-dependent kinase 8 [Source:ZFIN;Acc:ZDB-GENE-030903-2]	1,55	1,83E-02
ENSDARG00000070545	top1l	DNA topoisomerase I, like [Source:ZFIN;Acc:ZDB-GENE-060616-217]	1,54	3,27E-02
ENSDARG00000090557	si:ch1073-110a20.7	si:ch1073-110a20.7 [Source:ZFIN;Acc:ZDB-GENE-121214-133]	1,54	4,67E-02
ENSDARG00000006963	cse1l	CSE1 chromosome segregation 1-like (yeast) [Source:ZFIN;Acc:ZDB-GENE-990603-1]	1,54	5,53E-03
ENSDARG00000057987	uba3	ubiquitin-like modifier activating enzyme 3 [Source:ZFIN;Acc:ZDB-GENE-040426-2825]	1,54	3,05E-02
ENSDARG00000100060	exosc7	exosome component 7 [Source:ZFIN;Acc:ZDB-GENE-050417-47]	1,54	1,83E-02
ENSDARG00000070798	pmvk	phosphomevalonate kinase [Source:ZFIN;Acc:ZDB-GENE-070410-91]	1,53	3,24E-02
ENSDARG00000031434	rcor1	REST corepressor 1 [Source:ZFIN;Acc:ZDB-GENE-050506-79]	1,53	1,75E-02
ENSDARG00000089626	ptges3b	prostaglandin E synthase 3b (cytosolic) [Source:ZFIN;Acc:ZDB-GENE-040625-144]	1,53	2,65E-02
ENSDARG00000052928	arf6b	ADP-ribosylation factor 6b [Source:ZFIN;Acc:ZDB-GENE-030131-9056]	1,53	1,48E-02
ENSDARG00000035131	surf4l	surfeit 4, like [Source:ZFIN;Acc:ZDB-GENE-040718-172]	1,53	3,25E-02
ENSDARG00000005738	rpf1	ribosome production factor 1 homolog [Source:ZFIN;Acc:ZDB-GENE-040625-177]	1,53	1,25E-02
ENSDARG00000004774	wdr36	WD repeat domain 36 [Source:ZFIN;Acc:ZDB-GENE-030131-464]	1,52	3,64E-02
ENSDARG00000012723	rbm14a	RNA binding motif protein 14a [Source:ZFIN;Acc:ZDB-GENE-050522-496]	1,52	3,27E-03
ENSDARG00000038635	magoh	mago homolog, exon junction complex subunit [Source:ZFIN;Acc:ZDB-GENE-041216-1]	1,52	1,34E-02
ENSDARG00000087346	rap1ab	RAP1A, member of RAS oncogene family b [Source:ZFIN;Acc:ZDB-GENE-040426-2738]	1,51	7,84E-03
ENSDARG00000007387	irf2a	interferon regulatory factor 2a [Source:ZFIN;Acc:ZDB-GENE-030131-4135]	1,51	1,78E-02
ENSDARG00000043734	trmu	tRNA 5-methylaminomethyl-2-thiouridylate methyltransferase [Source:ZFIN;Acc:ZDB-GENE-050522-540]	1,50	2,85E-02
ENSDARG00000022303	higd1a	HIG1 hypoxia inducible domain family, member 1A [Source:ZFIN;Acc:ZDB-GENE-030826-15]	1,50	2,50E-02
ENSDARG00000059711	nol6	nucleolar protein 6 (RNA-associated) [Source:ZFIN;Acc:ZDB-GENE-030131-6294]	1,49	4,64E-03
ENSDARG00000002720	utp15	UTP15 small subunit processome component [Source:ZFIN;Acc:ZDB-GENE-030131-3831]	1,49	4,15E-03

Gene ID	Symbol	Description	Value	p-value
ENSDARG00000029663	rab1ab	RAB1A, member RAS oncogene family b [Source:ZFIN;Acc:ZDB-GENE-030616-564]	1,49	3,73E-03
ENSDARG00000006392	exosc9	exosome component 9 [Source:ZFIN;Acc:ZDB-GENE-041010-180]	1,48	3,17E-02
ENSDARG00000018953	gclm	glutamate-cysteine ligase, modifier subunit [Source:ZFIN;Acc:ZDB-GENE-030131-5906]	1,48	2,37E-02
ENSDARG00000012369	rdh10b	retinol dehydrogenase 10b [Source:ZFIN;Acc:ZDB-GENE-030909-7]	1,48	2,86E-02
ENSDARG00000077839	dhx30	DEAH (Asp-Glu-Ala-His) box helicase 30 [Source:ZFIN;Acc:ZDB-GENE-130530-833]	1,47	4,67E-02
ENSDARG00000052536	tia1	TIA1 cytotoxic granule-associated RNA binding protein [Source:ZFIN;Acc:ZDB-GENE-030131-1506]	1,47	9,77E-03
ENSDARG00000058865	endog	endonuclease G [Source:ZFIN;Acc:ZDB-GENE-050522-402]	1,47	1,25E-02
ENSDARG00000056127	polr2gl	polymerase (RNA) II (DNA directed) polypeptide G-like [Source:ZFIN;Acc:ZDB-GENE-030131-2808]	1,47	8,42E-03
ENSDARG00000100374	txnrd3	thioredoxin reductase 3 [Source:ZFIN;Acc:ZDB-GENE-030327-3]	1,47	2,88E-02
ENSDARG00000013670	hyou1	hypoxia up-regulated 1 [Source:ZFIN;Acc:ZDB-GENE-030131-5344]	1,46	2,05E-02
ENSDARG00000008395	snupn	snurportin 1 [Source:ZFIN;Acc:ZDB-GENE-030131-3464]	1,46	3,65E-02
ENSDARG00000010281	xpo4	exportin 4 [Source:ZFIN;Acc:ZDB-GENE-030131-3062]	1,46	1,46E-02
ENSDARG00000019326	prpsap2	phosphoribosyl pyrophosphate synthetase-associated protein 2 [Source:ZFIN;Acc:ZDB-GENE-040426-2077]	1,45	4,82E-03
ENSDARG00000038213	slc35b1	solute carrier family 35 member B1 [Source:ZFIN;Acc:ZDB-GENE-040912-148]	1,45	1,11E-02
ENSDARG00000017093	emc8	ER membrane protein complex subunit 8 [Source:ZFIN;Acc:ZDB-GENE-040426-2692]	1,45	4,36E-03
ENSDARG00000013095	gclc	glutamate-cysteine ligase, catalytic subunit [Source:ZFIN;Acc:ZDB-GENE-030131-5056]	1,45	5,56E-03
ENSDARG00000105293	srsf4	serine and arginine rich splicing factor 4 [Source:ZFIN;Acc:ZDB-GENE-030131-591]	1,44	1,64E-02
ENSDARG00000026767	nol11	nucleolar protein 11 [Source:ZFIN;Acc:ZDB-GENE-030131-419]	1,44	3,39E-02
ENSDARG00000032535	praf2	PRA1 domain family, member 2 [Source:ZFIN;Acc:ZDB-GENE-050417-190]	1,43	1,13E-02
ENSDARG00000005057	dimt1l	DIM1 dimethyladenosine transferase 1-like (S. cerevisiae) [Source:ZFIN;Acc:ZDB-GENE-040801-75]	1,43	7,63E-03
ENSDARG00000031907	ptbp1b	polypyrimidine tract binding protein 1b [Source:ZFIN;Acc:ZDB-GENE-030131-9796]	1,43	4,35E-02
ENSDARG00000100564	sil1	SIL1 nucleotide exchange factor [Source:ZFIN;Acc:ZDB-GENE-160113-49]	1,42	2,02E-02
ENSDARG00000003068	gorasp1a	golgi reassembly stacking protein 1a [Source:ZFIN;Acc:ZDB-GENE-030826-23]	1,42	1,38E-02
ENSDARG00000063663	clp1	cleavage and polyadenylation factor I subunit 1 [Source:ZFIN;Acc:ZDB-GENE-030131-5306]	1,42	4,43E-02
ENSDARG00000074287	sptlc2b	serine palmitoyltransferase, long chain base subunit 2b [Source:ZFIN;Acc:ZDB-GENE-080305-8]	1,42	7,99E-03
ENSDARG00000005593	rxrga	retinoid x receptor, gamma a [Source:ZFIN;Acc:ZDB-GENE-980526-36]	1,41	3,05E-02
ENSDARG00000055743	ankrd54	ankyrin repeat domain 54 [Source:ZFIN;Acc:ZDB-GENE-040718-318]	1,41	4,07E-02
ENSDARG00000053447	ppp4r2b	protein phosphatase 4, regulatory subunit 2b [Source:ZFIN;Acc:ZDB-GENE-030131-3008]	1,41	2,54E-02

ENSDARG ID	Symbol	Description		
ENSDARG00000011648	snrpd1	small nuclear ribonucleoprotein D1 polypeptide [Source:ZFIN;Acc:ZDB-GENE-020419-14]	1,39	3,94E-02
ENSDARG00000037283	plrg1	pleiotropic regulator 1 [Source:ZFIN;Acc:ZDB-GENE-040426-2787]	1,39	1,48E-02
ENSDARG00000011049	slc17a9b	solute carrier family 17 member 9b [Source:ZFIN;Acc:ZDB-GENE-040718-380]	1,39	4,74E-03
ENSDARG00000038225	nras	NRAS proto-oncogene, GTPase [Source:ZFIN;Acc:ZDB-GENE-990415-166]	1,38	3,94E-02
ENSDARG00000069909	si:dkey-33c12.12	si:dkey-33c12.12 [Source:ZFIN;Acc:ZDB-GENE-081028-30]	1,38	3,79E-02
ENSDARG00000017835	brf1a	BRF1 RNA polymerase III transcription initiation factor subunit a [Source:ZFIN;Acc:ZDB-GENE-030131-6334]	1,38	4,21E-02
ENSDARG00000032103	mapk6	mitogen-activated protein kinase 6 [Source:ZFIN;Acc:ZDB-GENE-050420-7]	1,38	4,57E-02
ENSDARG00000006900	impdh2	IMP (inosine 5'-monophosphate) dehydrogenase 2 [Source:ZFIN;Acc:ZDB-GENE-030114-5]	1,37	9,04E-03
ENSDARG00000004754	hspa4a	heat shock protein 4a [Source:ZFIN;Acc:ZDB-GENE-040426-2832]	1,37	1,46E-02
ENSDARG00000015524	prps1a	phosphoribosyl pyrophosphate synthetase 1A [Source:ZFIN;Acc:ZDB-GENE-011212-5]	1,37	1,28E-02
ENSDARG00000045565	noc4l	nucleolar complex associated 4 homolog [Source:ZFIN;Acc:ZDB-GENE-050522-98]	1,37	4,08E-02
ENSDARG00000077396	tlcd2	TLC domain containing 2 [Source:ZFIN;Acc:ZDB-GENE-080204-81]	1,37	3,37E-02
ENSDARG00000029058	rbbp4	retinoblastoma binding protein 4 [Source:ZFIN;Acc:ZDB-GENE-030131-445]	1,37	2,52E-02
ENSDARG00000060748	tsfm	Ts translation elongation factor, mitochondrial [Source:ZFIN;Acc:ZDB-GENE-061215-17]	1,36	4,61E-02
ENSDARG00000071566	ppp1cab	protein phosphatase 1, catalytic subunit, alpha isozyme b [Source:ZFIN;Acc:ZDB-GENE-030131-5512]	1,36	2,08E-02
ENSDARG00000012234	psme3	proteasome activator subunit 3 [Source:ZFIN;Acc:ZDB-GENE-991110-19]	1,36	1,38E-02
ENSDARG00000012261	eftud2	elongation factor Tu GTP binding domain containing 2 [Source:ZFIN;Acc:ZDB-GENE-040426-1569]	1,36	2,04E-02
ENSDARG00000058148	dnajc7	DnaJ (Hsp40) homolog, subfamily C, member 7 [Source:ZFIN;Acc:ZDB-GENE-040426-2483]	1,35	6,88E-03
ENSDARG00000052734	hmgcra	3-hydroxy-3-methylglutaryl-CoA reductase a [Source:ZFIN;Acc:ZDB-GENE-040401-2]	1,35	1,46E-02
ENSDARG00000038422	entpd4	ectonucleoside triphosphate diphosphohydrolase 4 [Source:ZFIN;Acc:ZDB-GENE-040718-116]	1,35	3,31E-02
ENSDARG00000054446	ccdc43	coiled-coil domain containing 43 [Source:ZFIN;Acc:ZDB-GENE-040426-1587]	1,35	4,97E-02
ENSDARG00000058365	hspb8	heat shock protein b8 [Source:ZFIN;Acc:ZDB-GENE-030131-2480]	1,35	8,28E-03
ENSDARG00000004836	dnajc5ab	DnaJ (Hsp40) homolog, subfamily C, member 5ab [Source:ZFIN;Acc:ZDB-GENE-081021-2]	1,34	3,61E-02
ENSDARG00000034060	elac2	elaC ribonuclease Z 2 [Source:ZFIN;Acc:ZDB-GENE-041111-227]	1,34	2,66E-02
ENSDARG00000012603	eif3ja	eukaryotic translation initiation factor 3, subunit Ja [Source:ZFIN;Acc:ZDB-GENE-040426-1266]	1,34	2,45E-02
ENSDARG00000071203	sptssa	serine palmitoyltransferase, small subunit A [Source:ZFIN;Acc:ZDB-GENE-050320-26]	1,33	3,43E-02
ENSDARG00000038074	ergic3	ERGIC and golgi 3 [Source:ZFIN;Acc:ZDB-GENE-040426-795]	1,32	1,91E-02

Ensembl ID	Symbol	Description	Fold	p-value
ENSDARG00000099667	snrpg	small nuclear ribonucleoprotein polypeptide G [Source:ZFIN;Acc:ZDB-GENE-040912-105]	1,32	2,25E-02
ENSDARG00000059360	srsf3b	serine and arginine rich splicing factor 3b [Source:ZFIN;Acc:ZDB-GENE-071005-2]	1,31	2,59E-02
ENSDARG00000014770	usp4	ubiquitin specific peptidase 4 (proto-oncogene) [Source:ZFIN;Acc:ZDB-GENE-041008-187]	1,31	4,07E-02
ENSDARG00000007923	ptpn1	protein tyrosine phosphatase non-receptor type 1 [Source:ZFIN;Acc:ZDB-GENE-980605-23]	1,31	9,85E-03
ENSDARG00000042900	gtpbp1l	GTP binding protein 1, like [Source:ZFIN;Acc:ZDB-GENE-041007-2]	1,31	4,24E-02
ENSDARG00000054540	imp4	IMP U3 small nucleolar ribonucleoprotein 4 [Source:ZFIN;Acc:ZDB-GENE-040718-474]	1,31	2,58E-02
ENSDARG00000025033	stx5a	syntaxin 5A [Source:ZFIN;Acc:ZDB-GENE-040718-18]	1,31	3,25E-02
ENSDARG00000014329	npm1a	nucleophosmin 1a [Source:ZFIN;Acc:ZDB-GENE-021028-1]	1,29	6,79E-03
ENSDARG00000035595	ficd	FIC domain containing [Source:ZFIN;Acc:ZDB-GENE-030131-6588]	1,29	3,97E-02
ENSDARG00000008032	sart3	spliceosome associated factor 3, U4/U6 recycling protein [Source:ZFIN;Acc:ZDB-GENE-040724-10]	1,29	4,24E-02
ENSDARG00000027825	naa50	N(alpha)-acetyltransferase 50, NatE catalytic subunit [Source:ZFIN;Acc:ZDB-GENE-040801-142]	1,28	4,82E-02
ENSDARG00000024602	zgc:162964	zgc:162964 [Source:ZFIN;Acc:ZDB-GENE-030131-9798]	1,28	3,44E-02
ENSDARG00000104353	nop58	NOP58 ribonucleoprotein homolog (yeast) [Source:ZFIN;Acc:ZDB-GENE-040426-2140]	1,28	2,64E-02
ENSDARG00000059630	mlec	malectin [Source:ZFIN;Acc:ZDB-GENE-081105-187]	1,27	3,22E-02
ENSDARG00000036721	tomm40l	translocase of outer mitochondrial membrane 40 homolog, like [Source:ZFIN;Acc:ZDB-GENE-040426-2319]	1,26	4,62E-02
ENSDARG00000033597	api5	apoptosis inhibitor 5 [Source:ZFIN;Acc:ZDB-GENE-030131-395]	1,26	3,78E-02
ENSDARG00000021433	asmtl	acetylserotonin O-methyltransferase-like [Source:ZFIN;Acc:ZDB-GENE-030131-2854]	1,26	2,54E-02
ENSDARG00000055561	c1galt1b	core 1 synthase, glycoprotein-N-acetylgalactosamine 3-beta-galactosyltransferase, 1b [Source:ZFIN;Acc:ZDB-GENE-030131-9075]	1,25	4,67E-02
ENSDARG00000039363	dnajb12a	DnaJ heat shock protein family (Hsp40) member B12a [Source:ZFIN;Acc:ZDB-GENE-030131-2725]	1,25	2,36E-02
ENSDARG00000035870	laptm4b	lysosomal protein transmembrane 4 beta [Source:ZFIN;Acc:ZDB-GENE-030616-616]	1,25	4,34E-02
ENSDARG00000101877	rbm34	RNA binding motif protein 34 [Source:ZFIN;Acc:ZDB-GENE-040718-77]	1,24	4,90E-02
ENSDARG00000074858	stard7	StAR-related lipid transfer (START) domain containing 7 [Source:ZFIN;Acc:ZDB-GENE-030131-2310]	1,24	2,35E-02
ENSDARG00000024026	sdf2	stromal cell-derived factor 2 [Source:ZFIN;Acc:ZDB-GENE-030131-8823]	1,23	2,25E-02
ENSDARG00000009484	arf1	ADP-ribosylation factor 1 [Source:ZFIN;Acc:ZDB-GENE-010724-5]	1,23	3,04E-02
ENSDARG00000044304	prrc1	proline-rich coiled-coil 1 [Source:ZFIN;Acc:ZDB-GENE-041024-9]	1,23	3,98E-02
ENSDARG00000103364	cs	citrate synthase [Source:ZFIN;Acc:ZDB-GENE-030131-1058]	1,22	3,31E-02

Gene ID (Ensembl)	Gene symbol	Gene Name	Average log2 Fold Change	Adj. P-value
ENSDARG00000025972	mcts1	MCTS1 re-initiation and release factor [Source:ZFIN;Acc:ZDB-GENE-040426-957]	1,22	4,15E-02
ENSDARG00000038473	ube2d3	ubiquitin-conjugating enzyme E2D 3 [Source:ZFIN;Acc:ZDB-GENE-030131-551]	1,21	3,88E-02
ENSDARG00000037109	pwp2h	PWP2 small subunit processome component [Source:ZFIN;Acc:ZDB-GENE-021031-3]	1,21	3,24E-02
ENSDARG00000019360	sec23b	SEC23 homolog B, coat complex II component [Source:ZFIN;Acc:ZDB-GENE-030131-5479]	1,21	1,46E-02
ENSDARG00000103714	rab6a	RAB6A, member RAS oncogene family [Source:ZFIN;Acc:ZDB-GENE-040426-2849]	1,20	3,25E-02
ENSDARG00000042533	gstm.1	glutathione S-transferase mu, tandem duplicate 1 [Source:ZFIN;Acc:ZDB-GENE-030911-2]	1,20	3,67E-02
ENSDARG00000045146	tomm22	translocase of outer mitochondrial membrane 22 homolog (yeast) [Source:ZFIN;Acc:ZDB-GENE-030131-9810]	1,20	4,99E-02
ENSDARG00000057855	mrps31	mitochondrial ribosomal protein S31 [Source:ZFIN;Acc:ZDB-GENE-030131-3715]	1,19	4,81E-02
ENSDARG00000035631	sdf2l1	stromal cell-derived factor 2-like 1 [Source:ZFIN;Acc:ZDB-GENE-040808-46]	1,19	3,97E-02
ENSDARG00000006260	tuba8l4	tubulin, alpha 8 like 4 [Source:ZFIN;Acc:ZDB-GENE-040426-860]	1,18	2,16E-02
ENSDARG00000004806	grwd1	glutamate-rich WD repeat containing 1 [Source:ZFIN;Acc:ZDB-GENE-030131-9844]	1,18	4,08E-02
ENSDARG00000056160	hspd1	heat shock 60 protein 1 [Source:ZFIN;Acc:ZDB-GENE-021206-1]	1,18	3,17E-02
ENSDARG00000040666	nifk	nucleolar protein interacting with the FHA domain of MKI67 [Source:ZFIN;Acc:ZDB-GENE-021131-4]	1,16	4,21E-02
ENSDARG00000074129	edem3	ER degradation enhancer, mannosidase alpha-like 3 [Source:ZFIN;Acc:ZDB-GENE-070801-5]	1,15	4,35E-02
ENSDARG00000090352		uncharacterized LOC101883708 [Source:NCBI gene;Acc:101883708]	1,15	4,46E-02
ENSDARG00000101341	si:ch211-26i1.6	si:ch211-26i1.6 [Source:ZFIN;Acc:ZDB-GENE-030131-6242]	1,15	4,67E-02
ENSDARG00000093425			1,15	2,66E-02
ENSDARG00000039082	zgc:123010	zgc:123010 [Source:ZFIN;Acc:ZDB-GENE-051120-15]	1,14	4,10E-02
ENSDARG00000023299	snu13b	SNU13 homolog, small nuclear ribonucleoprotein b (U4/U6.U5) [Source:ZFIN;Acc:ZDB-GENE-030131-9670]	1,13	4,57E-02

Down-regulated transcripts

Gene ID (Ensembl)	Gene symbol	Gene Name	Average log2 Fold Change	Adj. P-value
ENSDARG00000008275	klhl24b	kelch-like family member 24b [Source:ZFIN;Acc:ZDB-GENE-040426-1185]	-4,30	8,88E-23
ENSDARG00000045132	vdac1	voltage-dependent anion channel 1 [Source:ZFIN;Acc:ZDB-GENE-030131-6514]	-4,00	1,02E-16
ENSDARG00000055510	ypel3	yippee-like 3 [Source:ZFIN;Acc:ZDB-GENE-030516-4]	-5,19	5,08E-16
ENSDARG00000096234	tac4	tachykinin 4 (hemokinin) [Source:ZFIN;Acc:ZDB-GENE-120215-159]	-8,09	6,00E-13

Gene ID	Symbol	Description	Fold	p-value
ENSDARG00000069251	zpax1	zona pellucida protein AX 1 [Source:ZFIN;Acc:ZDB-GENE-030131-5968]	-5,80	1,53E-11
ENSDARG00000013775	si:dkey-246g23.4	si:dkey-246g23.4 [Source:ZFIN;Acc:ZDB-GENE-050419-234]	-4,64	6,05E-11
ENSDARG00000090768	zgc:173556	zona pellucida glycoprotein 3, tandem duplicate 2 [Source:ZFIN;Acc:ZDB-GENE-050626-121]	-5,78	8,44E-11
ENSDARG00000042129	zp3a.1	zona pellucida glycoprotein 3a, tandem duplicate 1 [Source:ZFIN;Acc:ZDB-GENE-040727-1]	-4,84	9,26E-10
ENSDARG00000095281	zgc:152652	zgc:152652 [Source:ZFIN;Acc:ZDB-GENE-060818-27]	-6,21	3,86E-09
ENSDARG00000016868	rhobtb4	Rho related BTB domain containing 4 [Source:ZFIN;Acc:ZDB-GENE-060315-11]	-2,83	4,78E-09
ENSDARG00000079034	zpax4	zona pellucida protein AX 4 [Source:ZFIN;Acc:ZDB-GENE-030131-6199]	-7,16	4,78E-09
ENSDARG00000099776	glula	glutamate-ammonia ligase (glutamine synthase) a [Source:ZFIN;Acc:ZDB-GENE-030131-688]	-3,81	6,02E-09
ENSDARG00000114958	zp3.2	zona pellucida glycoprotein 3 [Source:ZFIN;Acc:ZDB-GENE-991129-7]	-4,73	6,02E-09
ENSDARG00000016908	zp3e	zona pellucida glycoprotein 3e [Source:ZFIN;Acc:ZDB-GENE-071004-38]	-5,02	7,56E-09
ENSDARG00000104760	si:ch211-1i11.3	si:ch211-1i11.3 [Source:ZFIN;Acc:ZDB-GENE-030131-8638]	-3,36	1,22E-08
ENSDARG00000092924	zgc:171474	zgc:171474 [Source:ZFIN;Acc:ZDB-GENE-080215-16]	-5,92	1,25E-08
ENSDARG00000077741	zgc:175135	zgc:175135 [Source:ZFIN;Acc:ZDB-GENE-080214-1]	-5,53	2,81E-08
ENSDARG00000061660		carnitine O-palmitoyltransferase 1, liver isoform-like [Source:NCBI gene;Acc:100333227]	-2,85	4,62E-08
ENSDARG00000035088	si:ch211-254c8.3	si:ch211-254c8.3 [Source:ZFIN;Acc:ZDB-GENE-100922-130]	-10,08	1,35E-07
ENSDARG00000028517	hbp1	HMG-box transcription factor 1 [Source:ZFIN;Acc:ZDB-GENE-050522-414]	-2,76	1,64E-07
ENSDARG00000077782	acer2	alkaline ceramidase 2 [Source:ZFIN;Acc:ZDB-GENE-121026-1]	-2,59	1,92E-07
ENSDARG00000099060	zgc:111868	zgc:111868 [Source:ZFIN;Acc:ZDB-GENE-050809-138]	-5,86	2,26E-07
ENSDARG00000027316	tcp11l2	t-complex 11, testis-specific-like 2 [Source:ZFIN;Acc:ZDB-GENE-040426-1956]	-2,47	2,35E-07
ENSDARG00000105499	zgc:175135	zgc:175135 [Source:ZFIN;Acc:ZDB-GENE-080214-1]	-9,66	2,35E-07
ENSDARG00000028017	tp53inp1	tumor protein p53 inducible nuclear protein 1 [Source:ZFIN;Acc:ZDB-GENE-031018-3]	-3,32	4,22E-07
ENSDARG00000071871	glod5	glyoxalase domain containing 5 [Source:ZFIN;Acc:ZDB-GENE-050522-174]	-3,49	4,27E-07
ENSDARG00000062518	ulk1a	unc-51 like autophagy activating kinase 1a [Source:ZFIN;Acc:ZDB-GENE-080723-31]	-3,89	6,92E-07
ENSDARG00000088444		selenoprotein L [Source:NCBI gene;Acc:100462964]	-8,94	7,65E-07
ENSDARG00000093216	si:ch211-146I10.7	si:ch211-146I10.7 [Source:ZFIN;Acc:ZDB-GENE-091112-4]	-5,83	8,26E-07
ENSDARG00000045423	si:ch211-146I10.8	si:ch211-146I10.8 [Source:ZFIN;Acc:ZDB-GENE-160113-6]	-6,52	8,31E-07
ENSDARG00000045424	zgc:173856	zgc:173856 [Source:ZFIN;Acc:ZDB-GENE-030131-5358]	-7,20	1,58E-06
ENSDARG00000031426	csrnp1a	cysteine-serine-rich nuclear protein 1a [Source:ZFIN;Acc:ZDB-GENE-070912-475]	-4,26	2,27E-06
ENSDARG00000034989	retsatl	retinol saturase (all-trans-retinol 13,14-reductase) like [Source:ZFIN;Acc:ZDB-GENE-051113-252]	-5,89	2,27E-06

Ensembl ID	Symbol	Description	Fold	p-value
ENSDARG00000099221	ppp2r2bb	protein phosphatase 2, regulatory subunit B, beta b [Source:ZFIN;Acc:ZDB-GENE-041010-39]	-4,90	2,61E-06
ENSDARG00000055415	zp2l1	zona pellucida glycoprotein 2, like 1 [Source:ZFIN;Acc:ZDB-GENE-060818-3]	-4,68	3,48E-06
ENSDARG00000032156	zgc:171776	zgc:171776 [Source:ZFIN;Acc:ZDB-GENE-071004-36]	-5,03	3,48E-06
ENSDARG00000094392	si:dkey-229d11.5	si:dkey-229d11.5 [Source:ZFIN;Acc:ZDB-GENE-030131-5342]	-5,23	4,01E-06
ENSDARG00000013946	ivns1abpb	influenza virus NS1A binding protein b [Source:ZFIN;Acc:ZDB-GENE-030131-6266]	-2,78	4,08E-06
ENSDARG00000115457	zp3.2	zona pellucida glycoprotein 3, tandem duplicate 2 [Source:ZFIN;Acc:ZDB-GENE-050626-121]	-5,80	5,20E-06
ENSDARG00000074289	tuba4l	tubulin, alpha 4 like [Source:ZFIN;Acc:ZDB-GENE-030131-5588]	-4,11	6,15E-06
ENSDARG00000092885	zgc:171977	zgc:171977 [Source:ZFIN;Acc:ZDB-GENE-070822-24]	-4,93	6,15E-06
ENSDARG00000096095	buc	bucky ball [Source:ZFIN;Acc:ZDB-GENE-070117-694]	-5,26	6,15E-06
ENSDARG00000092057	si:dkey-90l23.1	si:dkey-90l23.1 [Source:ZFIN;Acc:ZDB-GENE-030131-5242]	-8,37	8,36E-06
ENSDARG00000013252	tmc5	transmembrane channel like 5 [Source:ZFIN;Acc:ZDB-GENE-120411-6]	-2,59	1,14E-05
ENSDARG00000077862	si:dkey-16i9l5.4	si:dkey-16i9l5.4 [Source:ZFIN;Acc:ZDB-GENE-030131-8695]	-8,74	1,29E-05
ENSDARG00000023176	tdo2b	tryptophan 2,3-dioxygenase b [Source:ZFIN;Acc:ZDB-GENE-030131-6014]	-2,36	1,34E-05
ENSDARG00000088713	si:ch211-226h8.14	si:ch211-226h8.14 [Source:ZFIN;Acc:ZDB-GENE-050208-470]	-4,94	1,34E-05
ENSDARG00000078638	zgc:171750	zgc:171750 [Source:ZFIN;Acc:ZDB-GENE-071004-30]	-8,95	1,59E-05
ENSDARG00000051923	ccnb1	cyclin B1 [Source:ZFIN;Acc:ZDB-GENE-000406-10]	-3,52	1,69E-05
ENSDARG00000102892	h1m	linker histone H1M [Source:ZFIN;Acc:ZDB-GENE-030131-5614]	-4,03	1,73E-05
ENSDARG00000058699	tmeff2b	transmembrane protein with EGF-like and two follistatin-like domains 2b [Source:ZFIN;Acc:ZDB-GENE-101001-4]	-4,03	1,74E-05
ENSDARG00000070709	wu:fi42e03	wu:fi42e03 [Source:ZFIN;Acc:ZDB-GENE-030131-6284]	-5,08	1,89E-05
ENSDARG00000105265	zgc:171534	zgc:171534 [Source:ZFIN;Acc:ZDB-GENE-080218-6]	-25,47	1,96E-05
ENSDARG00000075737	zgc:165518	zgc:165518 [Source:ZFIN;Acc:ZDB-GENE-070720-15]	-6,52	2,87E-05
ENSDARG00000035056	fgf13a	fibroblast growth factor 13a [Source:ZFIN;Acc:ZDB-GENE-041114-101]	-5,41	3,45E-05
ENSDARG00000095741	ddx41	si:ch1073-75o15.3 [Source:ZFIN;Acc:ZDB-GENE-100921-22]	-4,90	4,17E-05
ENSDARG00000074526	zbtb16b	zinc finger and BTB domain containing 16b [Source:ZFIN;Acc:ZDB-GENE-100923-1]	-2,36	5,19E-05
ENSDARG00000020711	rrm2	ribonucleotide reductase M2 polypeptide [Source:ZFIN;Acc:ZDB-GENE-990415-25]	-8,45	5,65E-05
ENSDARG00000055792	foxo4	forkhead box O4 [Source:ZFIN;Acc:ZDB-GENE-150311-1]	-2,13	6,88E-05
ENSDARG00000061544	ano6	anoctamin 6 [Source:ZFIN;Acc:ZDB-GENE-081104-64]	-2,87	6,88E-05
ENSDARG00000038720	zp3f.1	zona pellucida glycoprotein 3f, tandem duplicate 1 [Source:ZFIN;Acc:ZDB-GENE-030616-590]	-4,32	6,88E-05

Gene ID	Symbol	Description	Fold	p-value
ENSDARG00000076118	cdip1	cell death-inducing p53 target 1 [Source:ZFIN;Acc:ZDB-GENE-070720-18]	-2,03	7,72E-05
ENSDARG00000027639	zgc:165539	zgc:165539 [Source:ZFIN;Acc:ZDB-GENE-030131-5478]	-8,38	7,74E-05
ENSDARG00000061952	ecpas	Ecm29 proteasome adaptor and scaffold [Source:ZFIN;Acc:ZDB-GENE-061207-66]	-2,55	1,01E-04
ENSDARG00000092498	si:dkeyp-46h3.2	si:dkeyp-46h3.2 [Source:ZFIN;Acc:ZDB-GENE-030131-7351]	-8,25	1,09E-04
ENSDARG00000099229		protein ABHD15-like [Source:NCBI gene;Acc:110437708]	-2,21	1,22E-04
ENSDARG00000062080	shc2	SHC (Src homology 2 domain containing) transforming protein 2 [Source:ZFIN;Acc:ZDB-GENE-050208-666]	-2,55	1,25E-04
ENSDARG00000098739		H2A histone family member 1a like [Source:NCBI gene;Acc:100332229]	-3,83	1,31E-04
ENSDARG00000088989	si:dkey-24l7.5	si:dkey-24l7.5 [Source:ZFIN;Acc:ZDB-GENE-041014-237]	-3,70	1,50E-04
ENSDARG00000090870	si:ch1073-263o8.2	si:ch1073-263o8.2 [Source:ZFIN;Acc:ZDB-GENE-030131-5362]	-5,75	1,50E-04
ENSDARG00000105043	si:dkey-152b24.6	si:dkey-152b24.6 [Source:ZFIN;Acc:ZDB-GENE-100922-31]	-5,08	1,51E-04
ENSDARG00000038587		uncharacterized LOC100004199 [Source:NCBI gene;Acc:100004199]	-2,74	1,62E-04
ENSDARG00000086859	qdprb2	quinoid dihydropteridine reductase b2 [Source:ZFIN;Acc:ZDB-GENE-070720-19]	-6,53	1,68E-04
ENSDARG00000057328	cth1	cysteine three histidine 1 [Source:ZFIN;Acc:ZDB-GENE-990806-20]	-5,01	1,85E-04
ENSDARG00000042130	zp3a.2	zona pellucida glycoprotein 3a, tandem duplicate 2 [Source:ZFIN;Acc:ZDB-GENE-040727-2]	-4,04	1,88E-04
ENSDARG00000089478	si:dkey-24l7.4	si:dkey-24l7.4 [Source:ZFIN;Acc:ZDB-GENE-041014-238]	-6,19	1,93E-04
ENSDARG00000027169	kpna7	karyopherin alpha 7 (importin alpha 8) [Source:ZFIN;Acc:ZDB-GENE-040426-2023]	-4,83	1,95E-04
ENSDARG00000067806	zgc:158432	zgc:158432 [Source:ZFIN;Acc:ZDB-GENE-061201-57]	-2,09	1,96E-04
ENSDARG00000063126	gusb	glucuronidase, beta [Source:ZFIN;Acc:ZDB-GENE-070705-256]	-1,94	2,11E-04
ENSDARG00000103024	zgc:175136	zgc:175136 [Source:ZFIN;Acc:ZDB-GENE-080204-122]	-7,51	2,18E-04
ENSDARG00000073704	si:dkeyp-72g9.4	si:dkeyp-72g9.4 [Source:ZFIN;Acc:ZDB-GENE-031204-23]	-2,02	2,18E-04
ENSDARG00000006580	cldnd	claudin d [Source:ZFIN;Acc:ZDB-GENE-010328-4]	-3,77	2,23E-04
ENSDARG00000036848	slc43a2a	solute carrier family 43 member 2a [Source:ZFIN;Acc:ZDB-GENE-040426-964]	-2,32	2,28E-04
ENSDARG00000079862	kl	klotho [Source:ZFIN;Acc:ZDB-GENE-110221-1]	-3,31	2,37E-04
ENSDARG00000068199	pld3	phospholipase D family, member 3 [Source:ZFIN;Acc:ZDB-GENE-050419-212]	-2,79	2,65E-04
ENSDARG00000089567	patl2	PAT1 homolog 2 [Source:ZFIN;Acc:ZDB-GENE-121214-350]	-7,99	2,72E-04
ENSDARG00000015164	mknk2b	MAPK interacting serine/threonine kinase 2b [Source:ZFIN;Acc:ZDB-GENE-030829-2]	-2,73	2,91E-04
ENSDARG00000003197	wdr21	WD repeat domain 21 [Source:ZFIN;Acc:ZDB-GENE-040109-2]	-7,91	3,07E-04
ENSDARG00000060515	zdhhc9	zinc finger, DHHC-type containing 9 [Source:ZFIN;Acc:ZDB-GENE-071004-8]	-2,12	3,58E-04
ENSDARG00000016404	ptch1	patched 1 [Source:ZFIN;Acc:ZDB-GENE-980526-196]	-3,12	3,71E-04

Ensembl ID	Gene	Description	Value	p-value
ENSDARG00000018266	mthfd1a	methylenetetrahydrofolate dehydrogenase (NADP+ dependent) 1a, methenyltetrahydrofolate cyclohydrolase, formyltetrahydrofolate synthetase [Source:ZFIN;Acc:ZDB-GENE-041001-127]	-2,88	3,89E-04
ENSDARG00000098821	sec14l1	SEC14-like lipid binding 1 [Source:ZFIN;Acc:ZDB-GENE-040426-801]	-2,06	4,18E-04
ENSDARG00000002670	zgc:113944	autophagy related 14 [Source:HGNC Symbol;Acc:HGNC:19962]	-2,75	4,95E-04
ENSDARG00000116290	si:ch211-250e5.16	si:ch211-250e5.16 [Source:ZFIN;Acc:ZDB-GENE-030131-6052]	-6,03	5,30E-04
ENSDARG00000003701	cldng	claudin g [Source:ZFIN;Acc:ZDB-GENE-010328-7]	-3,29	5,35E-04
ENSDARG00000031336	hsd20b2	hydroxysteroid (20-beta) dehydrogenase 2 [Source:ZFIN;Acc:ZDB-GENE-030804-21]	-2,83	5,37E-04
ENSDARG00000054087	irs1	insulin receptor substrate 1 [Source:ZFIN;Acc:ZDB-GENE-030131-872]	-3,65	6,07E-04
ENSDARG00000062101	iffo2a	intermediate filament family orphan 2a [Source:ZFIN;Acc:ZDB-GENE-090313-342]	-2,20	6,41E-04
ENSDARG00000060393	fibcd1	fibrinogen C domain containing 1 [Source:ZFIN;Acc:ZDB-GENE-070424-245]	-4,16	6,57E-04
ENSDARG00000094370	si:ch211-125e6.13	si:ch211-125e6.13 [Source:ZFIN;Acc:ZDB-GENE-070912-37]	-4,46	6,64E-04
ENSDARG00000093841	zgc:152936	si:ch211-12h2.6 [Source:ZFIN;Acc:ZDB-GENE-091117-31]	-5,98	7,10E-04
ENSDARG00000008541	chia.4	chitinase, acidic.4 [Source:ZFIN;Acc:ZDB-GENE-030131-9279]	-7,03	7,53E-04
ENSDARG00000104576	si:ch211-152c8.5	si:ch211-152c8.5 [Source:ZFIN;Acc:ZDB-GENE-030131-5764]	-2,55	7,61E-04
ENSDARG00000061896	slco2a1	solute carrier organic anion transporter family, member 2A1 [Source:ZFIN;Acc:ZDB-GENE-060606-3]	-2,86	7,87E-04
ENSDARG00000038398	pmm1	phosphomannomutase 1 [Source:ZFIN;Acc:ZDB-GENE-180314-1]	-1,87	7,96E-04
ENSDARG00000015805	cgnl1	cingulin-like 1 [Source:ZFIN;Acc:ZDB-GENE-071009-2]	-2,92	8,16E-04
ENSDARG00000079681	mucin-5AC	mucin-5AC [Source:NCBI gene;Acc:100332822]	-5,91	8,17E-04
ENSDARG00000076474	org	oogenesis-related gene [Source:ZFIN;Acc:ZDB-GENE-050208-584]	-4,61	9,20E-04
ENSDARG00000020123	coq8aa	coenzyme Q8A, genome duplicate a [Source:ZFIN;Acc:ZDB-GENE-040718-487]	-2,27	1,01E-03
ENSDARG00000090980	apof	apolipoprotein F [Source:ZFIN;Acc:ZDB-GENE-031204-36]	-1,83	1,04E-03
ENSDARG00000021789	myoc	myocilin [Source:ZFIN;Acc:ZDB-GENE-050425-2]	-4,70	1,08E-03
ENSDARG00000008454	cpeb1b	cytoplasmic polyadenylation element binding protein 1b [Source:ZFIN;Acc:ZDB-GENE-990927-1]	-5,22	1,29E-03
ENSDARG00000021896	asap3	ArfGAP with SH3 domain, ankyrin repeat and PH domain 3 [Source:ZFIN;Acc:ZDB-GENE-050913-39]	-2,56	1,35E-03
ENSDARG00000006301	wu:fj59g11	Ras association (RalGDS/AF-6) and pleckstrin homology domains 1a [Source:ZFIN;Acc:ZDB-GENE-070912-156]	-2,51	1,44E-03
ENSDARG00000020239	lpin1	lipin 1 [Source:ZFIN;Acc:ZDB-GENE-080722-2]	-1,58	1,45E-03
ENSDARG00000103991	sec14l1	SEC14-like lipid binding 1 [Source:ZFIN;Acc:ZDB-GENE-040426-801]	-1,76	1,49E-03
ENSDARG00000105346	zp2.2	zona pellucida glycoprotein 2, tandem duplicate 2 [Source:ZFIN;Acc:ZDB-GENE-010622-1]	-5,71	1,59E-03

ENSDARG ID	Gene	Description	Fold	p-value
ENSDARG00000041607	eif4ebp3l	eukaryotic translation initiation factor 4E binding protein 3, like [Source:ZFIN;Acc:ZDB-GENE-030826-26]	-1,89	1,59E-03
ENSDARG00000116005	zgc:171446	zgc:171446 [Source:ZFIN;Acc:ZDB-GENE-080205-1]	-5,87	1,68E-03
ENSDARG00000074425	si:busm1-57f23.1	si:busm1-57f23.1 [Source:ZFIN;Acc:ZDB-GENE-030616-512]	-3,03	1,73E-03
ENSDARG00000020749	caprin2	caprin family member 2 [Source:ZFIN;Acc:ZDB-GENE-040812-2]	-4,06	1,86E-03
ENSDARG00000040059	gbp	glycogen synthase kinase binding protein [Source:ZFIN;Acc:ZDB-GENE-990714-7]	-2,04	1,94E-03
ENSDARG00000086529	si:dkey-90l23.2	si:dkey-90l23.2 [Source:ZFIN;Acc:ZDB-GENE-041008-200]	-5,54	1,94E-03
ENSDARG00000016749	slco1c1	solute carrier organic anion transporter family, member 1C1 [Source:ZFIN;Acc:ZDB-GENE-041210-50]	-3,56	1,97E-03
ENSDARG00000018782	kdm4aa	lysine (K)-specific demethylase 4A, genome duplicate a [Source:ZFIN;Acc:ZDB-GENE-110609-4]	-2,87	2,04E-03
ENSDARG00000022413	ing5a	inhibitor of growth family, member 5a [Source:ZFIN;Acc:ZDB-GENE-031016-1]	-1,96	2,05E-03
ENSDARG00000062304	pdpk1a	3-phosphoinositide dependent protein kinase 1a [Source:ZFIN;Acc:ZDB-GENE-061013-109]	-3,67	2,13E-03
ENSDARG00000115205	zgc:171445	zgc:171445 [Source:ZFIN;Acc:ZDB-GENE-080205-2]	-6,76	2,15E-03
ENSDARG00000068465	zgc:136254	zgc:136254 [Source:ZFIN;Acc:ZDB-GENE-060421-3062]	-4,79	2,17E-03
ENSDARG00000059252	zpcx	zona pellucida protein C [Source:ZFIN;Acc:ZDB-GENE-040824-1]	-5,10	2,30E-03
ENSDARG00000070166	zgc:153499	zgc:153499 [Source:ZFIN;Acc:ZDB-GENE-060825-234]	-7,47	2,32E-03
ENSDARG00000038405	zgc:153921	zgc:153921 [Source:ZFIN;Acc:ZDB-GENE-060929-816]	-1,73	2,36E-03
ENSDARG00000078917	zgc:195245	zgc:195245 [Source:ZFIN;Acc:ZDB-GENE-081022-200]	-5,72	2,36E-03
ENSDARG00000095463	si:ch73-90k17.1	si:ch73-90k17.1 [Source:ZFIN;Acc:ZDB-GENE-090312-218]	-7,48	2,42E-03
ENSDARG00000078394			-6,75	2,88E-03
ENSDARG00000053820	pcmtd2a	protein-L-isoaspartate (D-aspartate) O-methyltransferase domain containing 2a [Source:ZFIN;Acc:ZDB-GENE-060312-14]	-3,89	2,96E-03
ENSDARG00000105693		insulin receptor substrate 2-B-like [Source:NCBI gene;Acc:794462]	-1,74	2,97E-03
ENSDARG00000061311	znf438	zinc finger protein 438 [Source:ZFIN;Acc:ZDB-GENE-060929-868]	-3,93	2,97E-03
ENSDARG00000105452	plxna1a	plexin A1a [Source:ZFIN;Acc:ZDB-GENE-140106-137]	-4,52	3,14E-03
ENSDARG00000008803	marcksb	myristoylated alanine-rich protein kinase C substrate b [Source:ZFIN;Acc:ZDB-GENE-030131-1921]	-6,56	3,17E-03
ENSDARG00000001857	aff4	AF4/FMR2 family, member 4 [Source:ZFIN;Acc:ZDB-GENE-100910-5]	-1,52	3,22E-03
ENSDARG00000076564	hspg2	heparan sulfate proteoglycan 2 [Source:ZFIN;Acc:ZDB-GENE-080807-4]	-2,18	3,27E-03
ENSDARG00000019763	acp5a	acid phosphatase 5a, tartrate resistant [Source:ZFIN;Acc:ZDB-GENE-040426-2864]	-3,58	3,27E-03
ENSDARG00000103285	si:dkey-167k11.5	coiled-coil domain containing 134 [Source:HGNC Symbol;Acc:26185]	-7,25	3,34E-03

Gene ID	Symbol	Description	Fold change	p-value
ENSDARG00000055731	si:dkeyp-69e1.8	si:dkeyp-69e1.8 [Source:ZFIN;Acc:ZDB-GENE-070912-676]	-3,07	3,44E-03
ENSDARG00000071583	gtf3ab	general transcription factor IIIA, b [Source:ZFIN;Acc:ZDB-GENE-030131-7698]	-5,04	3,44E-03
ENSDARG00000044525	pparda	peroxisome proliferator-activated receptor delta a [Source:ZFIN;Acc:ZDB-GENE-990415-212]	-1,63	3,53E-03
ENSDARG00000002271	zfand5b	zinc finger, AN1-type domain 5b [Source:ZFIN;Acc:ZDB-GENE-040426-875]	-2,31	3,54E-03
ENSDARG00000016464	cdc42bpab	CDC42 binding protein kinase alpha (DMPK-like) b [Source:ZFIN;Acc:ZDB-GENE-080219-17]	-4,17	3,71E-03
ENSDARG00000059294	marco	macrophage receptor with collagenous structure [Source:ZFIN;Acc:ZDB-GENE-120514-2]	-1,80	3,80E-03
ENSDARG00000073787	si:ch73-303b9.1	si:ch73-303b9.1 [Source:ZFIN;Acc:ZDB-GENE-131127-391]	-6,71	3,80E-03
ENSDARG00000094557	nupr1b	nuclear protein 1b [Source:ZFIN;Acc:ZDB-GENE-030131-4653]	-2,38	3,89E-03
ENSDARG00000003968	larp6b	La ribonucleoprotein domain family, member 6b [Source:ZFIN;Acc:ZDB-GENE-041008-244]	-6,55	4,15E-03
ENSDARG00000042737	slc52a3	solute carrier family 52 member 3 [Source:ZFIN;Acc:ZDB-GENE-060421-4490]	-4,59	4,32E-03
ENSDARG00000093704	si:dkeyp-46h3.8	si:dkeyp-46h3.8 [Source:ZFIN;Acc:ZDB-GENE-060503-183]	-7,23	4,32E-03
ENSDARG00000041248	si:dkey-24i17.6	si:dkey-24i17.6 [Source:ZFIN;Acc:ZDB-GENE-041014-235]	-3,63	4,43E-03
ENSDARG00000038121	si:ch211-13k12.2	si:ch211-13k12.2 [Source:ZFIN;Acc:ZDB-GENE-061207-5]	-1,83	4,45E-03
ENSDARG00000095486	si:dkey-172k15.19	si:dkey-172k15.19 [Source:NCBI gene;Acc:108179095]	-7,39	5,05E-03
ENSDARG00000037532	mcm3l	MCM3 minichromosome maintenance deficient 3 (S. cerevisiae), like [Source:ZFIN;Acc:ZDB-GENE-040121-2]	-7,18	5,24E-03
ENSDARG00000035680	zgc:113424	zgc:113424 [Source:ZFIN;Acc:ZDB-GENE-050227-9]	-7,26	5,31E-03
ENSDARG00000115870			-1,73	5,33E-03
ENSDARG00000038938	itprid2	ITPR interacting domain containing 2 [Source:ZFIN;Acc:ZDB-GENE-090824-1]	-1,83	5,33E-03
ENSDARG00000054814	ptp4a3b	protein tyrosine phosphatase 4A3b [Source:ZFIN;Acc:ZDB-GENE-030131-2635]	-1,92	5,37E-03
ENSDARG00000019706	zar1	zygote arrest 1 [Source:ZFIN;Acc:ZDB-GENE-030818-1]	-3,44	5,39E-03
ENSDARG00000094616	zgc:113984	zgc:113984 [Source:ZFIN;Acc:ZDB-GENE-050626-82]	-5,40	5,63E-03
ENSDARG00000023479	lrp13	low-density lipoprotein receptor related-protein 13 [Source:ZFIN;Acc:ZDB-GENE-130729-1]	-7,49	5,65E-03
ENSDARG00000025615	prr15la	proline rich 15 like a [Source:ZFIN;Acc:ZDB-GENE-040801-218]	-2,90	5,77E-03
ENSDARG00000060096	tbc1d10ab	TBC1 domain family, member 10Ab [Source:ZFIN;Acc:ZDB-GENE-081105-145]	-3,78	5,82E-03
ENSDARG00000100167		cold shock domain containing C2 [Source:HGNC Symbol;Acc:HGNC:30359]	-1,69	5,90E-03
ENSDARG00000043257	ckbb	creatine kinase, brain b [Source:ZFIN;Acc:ZDB-GENE-020103-2]	-2,53	6,03E-03
ENSDARG00000086221	si:ch211-226h8.4	si:ch211-226h8.4 [Source:ZFIN;Acc:ZDB-GENE-050208-376]	-3,35	6,15E-03
ENSDARG00000088923	si:ch211-12h2.8	si:ch211-12h2.8 [Source:ZFIN;Acc:ZDB-GENE-091118-43]	-3,56	

Ensembl ID	Gene	Description	Value	p-value
ENSDARG00000001879	nav2b	neuron navigator 2b [Source:ZFIN;Acc:ZDB-GENE-061207-13]	-1,67	6,18E-03
ENSDARG00000089913	cacna1g	calcium channel, voltage-dependent, T type, alpha 1G subunit [Source:ZFIN;Acc:ZDB-GENE-090514-2]	-6,04	6,31E-03
ENSDARG00000105114	crebrf	creb3 regulatory factor [Source:ZFIN;Acc:ZDB-GENE-120203-3]	-3,01	6,67E-03
ENSDARG00000020645	slc7a3a	solute carrier family 7 member 3a [Source:ZFIN;Acc:ZDB-GENE-041114-206]	-2,21	7,12E-03
ENSDARG00000059824	soat2	sterol O-acyltransferase 2 [Source:ZFIN;Acc:ZDB-GENE-061013-742]	-2,45	7,25E-03
ENSDARG00000092919	zp3c	zona pellucida glycoprotein 3c [Source:ZFIN;Acc:ZDB-GENE-060817-5]	-4,83	7,25E-03
ENSDARG00000020693	sesn1	sestrin 1 [Source:ZFIN;Acc:ZDB-GENE-040718-408]	-2,27	7,32E-03
ENSDARG00000086247	si:ch73-189n23.1	si:ch73-189n23.1 [Source:ZFIN;Acc:ZDB-GENE-070705-217]	-3,43	7,43E-03
ENSDARG00000105545	si:dkey-165a24.10	si:dkey-165a24.10 [Source:ZFIN;Acc:ZDB-GENE-160728-16]	-6,24	7,69E-03
ENSDARG00000088143	sema4gb	sema domain, immunoglobulin domain (Ig), transmembrane domain (TM) and short cytoplasmic domain, (semaphorin) 4Gb [Source:ZFIN;Acc:ZDB-GENE-111117-1]	-1,66	7,78E-03
ENSDARG00000029766	nr1i2	nuclear receptor subfamily 1, group I, member 2 [Source:ZFIN;Acc:ZDB-GENE-030903-3]	-2,21	7,83E-03
ENSDARG00000000730	slc6a22.1	solute carrier family 6 member 22, tandem duplicate 1 [Source:ZFIN;Acc:ZDB-GENE-030616-629]	-2,54	7,87E-03
ENSDARG00000086856	stk35	serine/threonine kinase 35 [Source:ZFIN;Acc:ZDB-GENE-061103-553]	-1,99	8,86E-03
ENSDARG00000055250	cntd2	cyclin N-terminal domain containing 2 [Source:ZFIN;Acc:ZDB-GENE-030131-5453]	-3,99	9,04E-03
ENSDARG00000087961	avd	avidin [Source:ZFIN;Acc:ZDB-GENE-140205-1]	-7,17	9,20E-03
ENSDARG00000075113	nanog	nanog homeobox [Source:ZFIN;Acc:ZDB-GENE-030131-5486]	-6,32	9,33E-03
ENSDARG00000025386	lsm14b	LSM family member 14B [Source:ZFIN;Acc:ZDB-GENE-040426-779]	-4,25	9,37E-03
ENSDARG00000093019	si:dkey-83k24.5	si:dkey-83k24.5 [Source:ZFIN;Acc:ZDB-GENE-081104-440]	-4,12	9,38E-03
ENSDARG00000068152	malt3	MALT paracaspase 3 [Source:ZFIN;Acc:ZDB-GENE-050419-182]	-1,81	9,45E-03
ENSDARG00000007449	slc25a39	solute carrier family 25 member 39 [Source:ZFIN;Acc:ZDB-GENE-040426-1250]	-2,08	9,45E-03
ENSDARG00000076104	sema4bb	sema domain, immunoglobulin domain (Ig), transmembrane domain (TM) and short cytoplasmic domain, (semaphorin) 4Bb [Source:ZFIN;Acc:ZDB-GENE-120503-1]	-2,03	9,68E-03
ENSDARG00000025032	nr3c1	nuclear receptor subfamily 3, group C, member 1 (glucocorticoid receptor) [Source:ZFIN;Acc:ZDB-GENE-050522-503]	-1,76	9,89E-03
ENSDARG00000007682	ppdpfa	pancreatic progenitor cell differentiation and proliferation factor a [Source:ZFIN;Acc:ZDB-GENE-030219-204]	-1,33	9,93E-03
ENSDARG00000117285	mucin-17-like	mucin-17-like [Source:NCBI gene;Acc:108191474]	-5,67	1,00E-02
ENSDARG00000030687	phka2	phosphorylase kinase, alpha 2 (liver) [Source:ZFIN;Acc:ZDB-GENE-130422-1]	-1,48	1,01E-02

Gene ID	Symbol	Description	Fold	p-value
ENSDARG00000020057	bmpr2b	bone morphogenetic protein receptor, type II b (serine/threonine kinase) [Source:ZFIN;Acc:ZDB-GENE-070618-2]	-1,77	1,02E-02
ENSDARG00000099885	trim105	tripartite motif containing 105 [Source:ZFIN;Acc:ZDB-GENE-060810-140]	-2,49	1,02E-02
ENSDARG00000040469	enpp6	ectonucleotide pyrophosphatase/phosphodiesterase 6 [Source:ZFIN;Acc:ZDB-GENE-031205-1]	-1,52	1,03E-02
ENSDARG00000060702	npffr2b	neuropeptide FF receptor 2b [Source:ZFIN;Acc:ZDB-GENE-070705-159]	-4,18	1,07E-02
ENSDARG00000089390	pnpla2	patatin-like phospholipase domain containing 2 [Source:ZFIN;Acc:ZDB-GENE-120913-3]	-1,67	1,09E-02
ENSDARG00000011122	pptc7a	PTC7 protein phosphatase homolog a [Source:ZFIN;Acc:ZDB-GENE-041114-74]	-1,74	1,10E-02
ENSDARG00000004697	rxrgb	retinoid X receptor, gamma b [Source:ZFIN;Acc:ZDB-GENE-040718-34]	-1,65	1,10E-02
ENSDARG00000056639	carmil2	capping protein regulator and myosin 1 linker 2 [Source:ZFIN;Acc:ZDB-GENE-050419-197]	-1,97	1,11E-02
ENSDARG00000091558	si:ch211-251f6.7	si:ch211-251f6.7 [Source:ZFIN;Acc:ZDB-GENE-091113-57]	-4,08	1,11E-02
ENSDARG00000096628	buc2l	bucky ball 2-like [Source:ZFIN;Acc:ZDB-GENE-030131-6407]	-6,23	1,11E-02
ENSDARG00000036102	ctdsp2	CTD (carboxy-terminal domain, RNA polymerase II, polypeptide A) small phosphatase 2 [Source:ZFIN;Acc:ZDB-GENE-061009-25]	-2,02	1,15E-02
ENSDARG00000037836	igfals	insulin-like growth factor binding protein, acid labile subunit [Source:ZFIN;Acc:ZDB-GENE-030131-184]	-1,43	1,16E-02
ENSDARG00000010423	npsn	nephrosin [Source:ZFIN;Acc:ZDB-GENE-040420-2]	-3,64	1,17E-02
ENSDARG00000088807	klhl22	kelch-like family member 22 [Source:ZFIN;Acc:ZDB-GENE-081104-154]	-3,19	1,20E-02
ENSDARG00000035519	histh1l	histone H1 like [Source:ZFIN;Acc:ZDB-GENE-050417-145]	-1,76	1,22E-02
ENSDARG00000098583	wbp1	WW domain binding protein 1 [Source:ZFIN;Acc:ZDB-GENE-040426-1830]	-1,60	1,26E-02
ENSDARG00000062837	spata13	spermatogenesis associated 13 [Source:ZFIN;Acc:ZDB-GENE-091116-25]	-1,26	1,31E-02
ENSDARG00000079534	zgc:175135	zgc:175135 [Source:ZFIN;Acc:ZDB-GENE-080214-1]	-7,11	1,31E-02
ENSDARG00000006251	ell2	elongation factor, RNA polymerase II, 2 [Source:ZFIN;Acc:ZDB-GENE-030131-1717]	-1,48	1,33E-02
ENSDARG00000078172		prostaglandin F2 receptor inhibitor [Source:NCBI gene;Acc:101883373]	-2,01	1,33E-02
ENSDARG00000093886	tmsb5	thymosin beta 5 [Source:ZFIN;Acc:ZDB-GENE-090313-198]	-4,80	1,33E-02
ENSDARG00000036695	calcoco1a	calcium binding and coiled-coil domain 1a [Source:ZFIN;Acc:ZDB-GENE-030131-6911]	-1,89	1,41E-02
ENSDARG00000060841	pik3c2a	phosphatidylinositol-4-phosphate 3-kinase, catalytic subunit type 2 alpha [Source:ZFIN;Acc:ZDB-GENE-030328-39]	-1,71	1,46E-02
ENSDARG00000069428	slbp2	stem-loop binding protein 2 [Source:ZFIN;Acc:ZDB-GENE-070112-1722]	-3,55	1,46E-02
ENSDARG00000095867	si:ch73-132k15.2	si:ch73-132k15.2 [Source:ZFIN;Acc:ZDB-GENE-110411-191]	-6,00	1,48E-02
ENSDARG00000116193		uncharacterized LOC100334068 [Source:NCBI gene;Acc:100334068]	-6,21	1,49E-02

ENSDARG ID	Gene	Description	Fold change	p-value
ENSDARG00000039828	zp3b	zona pellucida glycoprotein 3b [Source:ZFIN;Acc:ZDB-GENE-031214-2]	-2,66	1,53E-02
ENSDARG00000104742	hnf4b	hepatic nuclear factor 4, beta [Source:ZFIN;Acc:ZDB-GENE-030131-2730]	-1,87	1,54E-02
ENSDARG00000008835	si:dkey-46g23.5	si:dkey-46g23.5 [Source:ZFIN;Acc:ZDB-GENE-030131-9306]	-4,56	1,54E-02
ENSDARG00000060813	plekha7a	pleckstrin homology domain containing, family A member 7a [Source:ZFIN;Acc:ZDB-GENE-050419-75]	-2,51	1,61E-02
ENSDARG00000003615	slc26a3.2	solute carrier family 26 member 3, tandem duplicate 2 [Source:ZFIN;Acc:ZDB-GENE-041210-179]	-1,87	1,65E-02
ENSDARG00000007383	kcnk6	potassium channel, subfamily K, member 6 [Source:ZFIN;Acc:ZDB-GENE-050309-213]	-1,33	1,68E-02
ENSDARG00000029524	impdh1b	IMP (inosine 5'-monophosphate) dehydrogenase 1b [Source:ZFIN;Acc:ZDB-GENE-030219-206]	-1,64	1,74E-02
ENSDARG00000040465	irf2	interferon regulatory factor 2 [Source:ZFIN;Acc:ZDB-GENE-041212-38]	-1,84	1,74E-02
ENSDARG00000028721	mapk14b	mitogen-activated protein kinase 14b [Source:ZFIN;Acc:ZDB-GENE-021007-1]	-1,79	1,88E-02
ENSDARG00000054323	pparab	peroxisome proliferator-activated receptor alpha b [Source:ZFIN;Acc:ZDB-GENE-990415-211]	-1,57	1,89E-02
ENSDARG00000098121			-3,38	1,93E-02
ENSDARG00000037528	si:ch211-191a24.4	si:ch211-191a24.4 [Source:ZFIN;Acc:ZDB-GENE-030131-4489]	-3,61	2,03E-02
ENSDARG00000103505	fbxl3a	F-box and leucine-rich repeat protein 3a [Source:ZFIN;Acc:ZDB-GENE-030912-5]	-1,86	2,08E-02
ENSDARG00000100528	map1lc3c	microtubule-associated protein 1 light chain 3 gamma [Source:ZFIN;Acc:ZDB-GENE-040426-1080]	-4,44	2,10E-02
ENSDARG00000117458			-2,65	2,14E-02
ENSDARG00000061994	acacb	acetyl-CoA carboxylase beta [Source:ZFIN;Acc:ZDB-GENE-060526-132]	-1,38	2,15E-02
ENSDARG00000040081	zp3d.1	zona pellucida glycoprotein 3d tandem duplicate 1 [Source:ZFIN;Acc:ZDB-GENE-030131-5827]	-6,68	2,15E-02
ENSDARG00000043236	ccna1	cyclin A1 [Source:ZFIN;Acc:ZDB-GENE-040311-2]	-3,81	2,17E-02
ENSDARG00000036180	ccnb2	cyclin B2 [Source:ZFIN;Acc:ZDB-GENE-030429-12]	-3,39	2,22E-02
ENSDARG00000087392	si:ch73-160p18.3	si:ch73-160p18.3 [Source:ZFIN;Acc:ZDB-GENE-141212-268]	-5,90	2,24E-02
ENSDARG00000094002	ccl34b.4	chemokine (C-C motif) ligand 34b, duplicate 4 [Source:ZFIN;Acc:ZDB-GENE-091204-344]	-2,45	2,25E-02
ENSDARG00000059337	tgif1	TGFB-induced factor homeobox 1 [Source:ZFIN;Acc:ZDB-GENE-030131-475]	-1,42	2,27E-02
ENSDARG00000011299	blzf1	basic leucine zipper nuclear factor 1 [Source:ZFIN;Acc:ZDB-GENE-010724-1]	-1,58	2,27E-02
ENSDARG00000036864	slc34a2b	solute carrier family 34 member 2b [Source:ZFIN;Acc:ZDB-GENE-030709-1]	-1,98	2,28E-02
ENSDARG00000022767	apobb.1	apolipoprotein Bb, tandem duplicate 1 [Source:ZFIN;Acc:ZDB-GENE-030131-9732]	-1,47	2,31E-02
ENSDARG00000103503	dgat1a	diacylglycerol O-acyltransferase 1a [Source:ZFIN;Acc:ZDB-GENE-030131-4600]	-1,92	2,38E-02
ENSDARG00000026294	erbb2	erb-b2 receptor tyrosine kinase 2 [Source:ZFIN;Acc:ZDB-GENE-031118-121]	-1,79	2,39E-02

Gene ID	Gene symbol	Description	log2FC	p-value
ENSDARG00000103699	ptpn13	protein tyrosine phosphatase non-receptor type 13 [Source:ZFIN;Acc:ZDB-GENE-070410-72]	-1,77	2,42E-02
ENSDARG00000004823	asz1	ankyrin repeat, SAM and basic leucine zipper domain containing 1 [Source:ZFIN;Acc:ZDB-GENE-040426-988]	-6,64	2,46E-02
ENSDARG00000099044		pregnancy zone protein-like [Source:NCBI gene;Acc:103909927]	-6,87	2,47E-02
ENSDARG00000100979	h1fx	H1 histone family, member X [Source:ZFIN;Acc:ZDB-GENE-030131-1228]	-6,59	2,54E-02
ENSDARG00000054058	efna1a	ephrin-A1a [Source:ZFIN;Acc:ZDB-GENE-040426-1135]	-1,65	2,58E-02
ENSDARG00000030326	tmem131l	transmembrane 131 like [Source:ZFIN;Acc:ZDB-GENE-030131-6110]	-2,69	2,60E-02
ENSDARG00000096655	si:ch211-85n16.4	si:ch211-85n16.4 [Source:ZFIN;Acc:ZDB-GENE-030131-7043]	-2,66	2,61E-02
ENSDARG00000079434	pabpc1l	poly(A) binding protein, cytoplasmic 1-like [Source:ZFIN;Acc:ZDB-GENE-030131-5836]	-1,70	2,65E-02
ENSDARG00000077040	taok1b	TAO kinase 1b [Source:ZFIN;Acc:ZDB-GENE-141024-1]	-1,86	2,73E-02
ENSDARG00000002597	dscama	Down syndrome cell adhesion molecule a [Source:ZFIN;Acc:ZDB-GENE-050310-7]	-4,01	2,80E-02
ENSDARG00000098304	arrdc2	arrestin domain containing 2 [Source:ZFIN;Acc:ZDB-GENE-030131-7146]	-1,45	2,80E-02
ENSDARG00000024865	si:dkey-18a10.3	si:dkey-18a10.3 [Source:ZFIN;Acc:ZDB-GENE-091204-174]	-1,34	2,83E-02
ENSDARG00000020761	scrn2	secernin 2 [Source:ZFIN;Acc:ZDB-GENE-040724-75]	-1,42	2,85E-02
ENSDARG00000090814	tmem110l	transmembrane protein 110, like [Source:ZFIN;Acc:ZDB-GENE-040426-912]	-1,30	2,97E-02
ENSDARG00000043497	mtss1	MTSS I-BAR domain containing 1 [Source:ZFIN;Acc:ZDB-GENE-081105-141]	-1,53	2,97E-02
ENSDARG00000045518			-2,12	2,97E-02
ENSDARG00000059604			-1,27	3,01E-02
ENSDARG00000117023			-6,53	3,05E-02
ENSDARG00000070187	dyrk1b	dual-specificity tyrosine-(Y)-phosphorylation regulated kinase 1B [Source:ZFIN;Acc:ZDB-GENE-060503-499]	-2,25	3,05E-02
ENSDARG00000045557	socs2	suppressor of cytokine signaling 2 [Source:ZFIN;Acc:ZDB-GENE-041210-171]	-2,27	3,05E-02
ENSDARG00000076949	zgc:173837	zgc:173837 [Source:ZFIN;Acc:ZDB-GENE-080213-12]	-5,90	3,07E-02
ENSDARG00000099247	si:dkey-68o6.5	si:dkey-68o6.5 [Source:ZFIN;Acc:ZDB-GENE-030131-5416]	-6,65	3,22E-02
ENSDARG00000053535	lmo7b	LIM domain 7b [Source:ZFIN;Acc:ZDB-GENE-060825-242]	-6,55	3,26E-02
ENSDARG00000100826	hif1al	hypoxia inducible factor 1 subunit alpha, like [Source:ZFIN;Acc:ZDB-GENE-040426-1315]	-1,36	3,27E-02
ENSDARG00000103739	bahcc1a	BAH domain and coiled-coil containing 1a [Source:ZFIN;Acc:ZDB-GENE-170301-1]	-2,60	3,31E-02
ENSDARG00000054748	cuedc1b	CUE domain containing 1b [Source:ZFIN;Acc:ZDB-GENE-070424-29]	-1,88	3,37E-02
ENSDARG00000104773	junbb	JunB proto-oncogene, AP-1 transcription factor subunit b [Source:ZFIN;Acc:ZDB-GENE-040426-2666]	-4,81	3,46E-02
ENSDARG00000074675	pan2	poly(A) specific ribonuclease subunit PAN2 [Source:ZFIN;Acc:ZDB-GENE-030131-3113]	-2,07	3,50E-02

ENSDARG ID	Gene	Description	Value	p-value
ENSDARG00000071724	ankha	ANKH inorganic pyrophosphate transport regulator a [Source:ZFIN;Acc:ZDB-GENE-050913-33]	-2,43	3,60E-02
ENSDARG00000025174	zgc:103482	zgc:103482 [Source:ZFIN;Acc:ZDB-GENE-041010-115]	-5,82	3,75E-02
ENSDARG00000079723	si:dkey-46g23.1	si:dkey-46g23.1 [Source:ZFIN;Acc:ZDB-GENE-070705-475]	-2,20	3,78E-02
ENSDARG00000033614	rasgef1ba	RasGEF domain family, member 1Ba [Source:ZFIN;Acc:ZDB-GENE-030131-5783]	-1,37	3,79E-02
ENSDARG00000015749	hps3	HPS3 biogenesis of lysosomal organelles complex 2 subunit 1 [Source:ZFIN;Acc:ZDB-GENE-061110-115]	-1,49	3,98E-02
ENSDARG00000012485	aurka	aurora kinase A [Source:ZFIN;Acc:ZDB-GENE-040801-161]	-4,13	3,98E-02
ENSDARG00000002347	cyp11a1	cytochrome P450, family 11, subfamily A, polypeptide 1 [Source:ZFIN;Acc:ZDB-GENE-010306-1]	-6,56	4,12E-02
ENSDARG00000027572	as3mt	arsenite methyltransferase [Source:ZFIN;Acc:ZDB-GENE-060312-15]	-1,26	4,16E-02
ENSDARG00000010655	ppm1k	protein phosphatase, Mg2+/Mn2+ dependent, 1K [Source:ZFIN;Acc:ZDB-GENE-050306-8]	-1,90	4,35E-02
ENSDARG00000092887	si:dkeyp-46h3.3	si:dkeyp-46h3.3 [Source:ZFIN;Acc:ZDB-GENE-060503-748]	-6,41	4,46E-02
ENSDARG00000070721	vdrb	vitamin D receptor b [Source:ZFIN;Acc:ZDB-GENE-080403-10]	-2,36	4,51E-02
ENSDARG00000020876	pdk2a	pyruvate dehydrogenase kinase, isozyme 2a [Source:ZFIN;Acc:ZDB-GENE-120910-1]	-1,32	4,54E-02
ENSDARG00000101452		sushi domain containing 2 [Source:HGNC Symbol;Acc:HGNC:30667]	-1,23	4,55E-02
ENSDARG00000078183	zgc:165453	zgc:165453 [Source:ZFIN;Acc:ZDB-GENE-070720-13]	-5,60	4,56E-02
ENSDARG00000030981	tmem127	transmembrane protein 127 [Source:ZFIN;Acc:ZDB-GENE-050522-97]	-1,58	4,60E-02
ENSDARG00000061560	stim1b	stromal interaction molecule 1b [Source:ZFIN;Acc:ZDB-GENE-060531-4]	-1,53	4,61E-02
ENSDARG00000104835	map3k4	mitogen-activated protein kinase kinase kinase 4 [Source:ZFIN;Acc:ZDB-GENE-990603-4]	-1,83	4,64E-02
ENSDARG00000002299	arsh	arylsulfatase H [Source:ZFIN;Acc:ZDB-GENE-081104-120]	-1,26	4,72E-02
ENSDARG00000103271	pla2g15	phospholipase A2, group XV [Source:ZFIN;Acc:ZDB-GENE-030131-6948]	-1,20	4,72E-02
ENSDARG00000080009	bahcc1b	BAH domain and coiled-coil containing 1b [Source:ZFIN;Acc:ZDB-GENE-100716-2]	-2,41	4,75E-02
ENSDARG00000055973	zar1l	zygote arrest 1-like [Source:ZFIN;Acc:ZDB-GENE-060810-119]	-4,78	4,75E-02
ENSDARG00000075564	fam13a	family with sequence similarity 13 member A [Source:ZFIN;Acc:ZDB-GENE-050208-102]	-1,32	4,87E-02
ENSDARG00000055655	birc5b	baculoviral IAP repeat containing 5b [Source:ZFIN;Acc:ZDB-GENE-030826-2]	-5,64	4,87E-02
ENSDARG00000086269	ndst2a	N-deacetylase/N-sulfotransferase (heparan glucosaminyl) 2a [Source:ZFIN;Acc:ZDB-GENE-060810-182]	-1,38	4,91E-02
ENSDARG00000098103	tefb	TEF transcription factor, PAR bZIP family member b [Source:ZFIN;Acc:ZDB-GENE-050522-224]	-1,44	4,97E-02

Supplementary Table 3. Differentially expressed genes in PBS injected *pcsk9* KO zebrafish. Gene expression in PBS injected *pcsk9* [tpu-13/tpu-13] (n=3) zebrafish liver was compared to WT siblings (n=3). RNA sequencing was perfomed using Illumina PE150 platform (50M reads).

Up-regulated transcripts

Gene ID (Ensembl)	Gene symbol	Gene Name	Average log2 Fold Change	Adj. P-value
ENSDARG00000078069	rrm2	ribonucleotide reductase M2 polypeptide [Source:ZFIN;Acc:ZDB-GENE-990415-25]	7,55	7,16E-08
ENSDARG00000094696	si:dkey-201c13.2	si:dkey-201c13.2 [Source:ZFIN;Acc:ZDB-GENE-060526-243]	3,96	9,17E-05
ENSDARG00000103277	cyp24a1	cytochrome P450, family 24, subfamily A, polypeptide 1 [Source:ZFIN;Acc:ZDB-GENE-060825-1]	3,67	1,26E-11
ENSDARG00000028396	fkbp5	FKBP prolyl isomerase 5 [Source:ZFIN;Acc:ZDB-GENE-030616-630]	3,39	9,74E-20
ENSDARG00000068194	klf9	Kruppel-like factor 9 [Source:ZFIN;Acc:ZDB-GENE-060526-244]	3,34	1,58E-05
ENSDARG00000038398	pmm1	phosphomannomutase 1 [Source:ZFIN;Acc:ZDB-GENE-180314-1]	3,10	9,54E-05
ENSDARG00000009001	pdia6	protein disulfide isomerase family A, member 6 [Source:ZFIN;Acc:ZDB-GENE-030131-879]	3,00	1,26E-23
ENSDARG00000016607	echdc2	enoyl CoA hydratase domain containing 2 [Source:ZFIN;Acc:ZDB-GENE-030219-147]	2,35	1,89E-05
ENSDARG00000097205	ulk2	unc-51 like autophagy activating kinase 2 [Source:ZFIN;Acc:ZDB-GENE-090218-30]	2,33	2,63E-08
ENSDARG00000017665	snrkb	SNF related kinase b [Source:ZFIN;Acc:ZDB-GENE-040426-1724]	2,16	2,73E-05
ENSDARG00000004262	cyp46a1.2	cytochrome P450, family 46, subfamily A, polypeptide 1, tandem duplicate 2 [Source:ZFIN;Acc:ZDB-GENE-040426-1184]	2,01	1,71E-04
ENSDARG00000054076	tatdn3	TatD DNase domain containing 3 [Source:ZFIN;Acc:ZDB-GENE-050522-192]	1,91	4,91E-05
ENSDARG00000061368	klf13	Kruppel-like factor 13 [Source:ZFIN;Acc:ZDB-GENE-060929-1274]	1,87	7,55E-05
ENSDARG00000042630	hebp2	heme binding protein 2 [Source:ZFIN;Acc:ZDB-GENE-040426-914]	1,86	1,11E-05
ENSDARG00000011373	mknk2a	MAPK interacting serine/threonine kinase 2a [Source:ZFIN;Acc:ZDB-GENE-060526-244]	1,69	1,57E-04
ENSDARG00000103038	pik3r3a	phosphoinositide-3-kinase, regulatory subunit 3a (gamma) [Source:ZFIN;Acc:ZDB-GENE-040426-1978]	1,69	6,74E-06
ENSDARG00000102048	slc25a43	solute carrier family 25 member 43 [Source:ZFIN;Acc:ZDB-GENE-030616-69]	1,53	5,92E-05
ENSDARG00000035120	gldc	glycine dehydrogenase (decarboxylating) [Source:ZFIN;Acc:ZDB-GENE-030131-340]	1,31	3,89E-05
ENSDARG00000020143	pah	phenylalanine hydroxylase [Source:ZFIN;Acc:ZDB-GENE-031006-2]	1,25	1,90E-04
ENSDARG00000105403	abcc6b.1	ATP-binding cassette, sub-family C (CFTR/MRP), member 6b, tandem duplicate 1 [Source:ZFIN;Acc:ZDB-GENE-050517-19]	1,17	1,66E-05

Down-regulated transcripts

Gene ID (Ensembl)	Gene symbol	Gene Name	Average log2 Fold Change	Adj. P-value
ENSDARG00000088444		selenoprotein L [Source:NCBI gene;Acc:100462964]	-8,63	2,31E-14
ENSDARG00000068256	rwdd	RWD domain containing 4 [Source:ZFIN;Acc:ZDB-GENE-041010-61]	-8,43	1,26E-05
ENSDARG00000098525	si:dkeyp-98a7.4	si:dkeyp-98a7.4 [Source:ZFIN;Acc:ZDB-GENE-050208-760]	-7,81	5,48E-07
ENSDARG00000035680	zgc:113424	zgc:113424 [Source:ZFIN;Acc:ZDB-GENE-050227-9]	-6,58	1,59E-05
ENSDARG00000087392	si:ch73-160p18.3	si:ch73-160p18.3 [Source:ZFIN;Acc:ZDB-GENE-141212-268]	-6,57	4,27E-06
ENSDARG00000099599	pigrl2.3	polymeric immunoglobulin receptor-like 2.3 [Source:ZFIN;Acc:ZDB-GENE-150409-2]	-5,99	1,78E-04
ENSDARG00000096097	si:dkeyp-98a7.4	si:dkeyp-98a7.4 [Source:ZFIN;Acc:ZDB-GENE-050208-760]	-5,61	2,24E-07
ENSDARG00000088276	si:ch211-190p8.2	zgc:92591 [Source:ZFIN;Acc:ZDB-GENE-040718-483]	-4,64	2,03E-04
ENSDARG00000020711	rrm2	ribonucleotide reductase M2 polypeptide [Source:ZFIN;Acc:ZDB-GENE-990415-25]	-4,63	2,34E-07
ENSDARG00000055833	lectin	lectin [Source:ZFIN;Acc:ZDB-GENE-070912-438]	-4,32	1,21E-05
ENSDARG00000035171	btg4	B-cell translocation gene 4 [Source:ZFIN;Acc:ZDB-GENE-031008-1]	-3,84	1,93E-04
ENSDARG00000089478	si:dkey-241l7.4	si:dkey-241l7.4 [Source:ZFIN;Acc:ZDB-GENE-041014-238]	-3,71	5,97E-07
ENSDARG00000105043	si:dkey-152b24.6	si:dkey-152b24.6 [Source:ZFIN;Acc:ZDB-GENE-100922-31]	-3,68	9,06E-08
ENSDARG00000002597	pabpc1l	poly(A) binding protein, cytoplasmic 1-like [Source:ZFIN;Acc:ZDB-GENE-030131-5836]	-3,66	1,98E-04
ENSDARG00000086522	zp2.5	zona pellucida glycoprotein 2, tandem duplicate 5 [Source:ZFIN;Acc:ZDB-GENE-090306-1]	-3,64	3,82E-05
ENSDARG00000092090	si:ch211-125e6.12	si:ch211-125e6.12 [Source:ZFIN;Acc:ZDB-GENE-070912-36]	-3,63	4,46E-07
ENSDARG00000036180	ccnb2	cyclin B2 [Source:ZFIN;Acc:ZDB-GENE-030429-12]	-3,60	1,12E-04
ENSDARG00000012485	aurka	aurora kinase A [Source:ZFIN;Acc:ZDB-GENE-040801-161]	-3,49	6,01E-05
ENSDARG00000086221	si:ch211-226h8.4	si:ch211-226h8.4 [Source:ZFIN;Acc:ZDB-GENE-050208-376]	-3,33	1,07E-04
ENSDARG00000043236	ccna1	cyclin A1 [Source:ZFIN;Acc:ZDB-GENE-040311-2]	-3,32	6,59E-05
ENSDARG00000096017		si:ch211-250e5.3 [Source:NCBI gene;Acc:561392]	-3,28	2,14E-04
ENSDARG00000105499	zgc:175135	zgc:175135 [Source:ZFIN;Acc:ZDB-GENE-080214-1]	-3,25	1,45E-07
ENSDARG00000099060	zgc:111868	zgc:111868 [Source:ZFIN;Acc:ZDB-GENE-050809-138]	-3,12	6,80E-07
ENSDARG00000045423	si:ch211-146i10.8	si:ch211-146i10.8 [Source:ZFIN;Acc:ZDB-GENE-160113-6]	-3,11	2,21E-05
ENSDARG00000072169	kpna7	karyopherin alpha 7 (importin alpha 8) [Source:ZFIN;Acc:ZDB-GENE-040426-2023]	-3,11	1,63E-06
ENSDARG00000074764	zgc:171426	zgc:171426 [Source:ZFIN;Acc:ZDB-GENE-080212-2]	-3,10	2,02E-05
ENSDARG00000003701	cldng	claudin g [Source:ZFIN;Acc:ZDB-GENE-010328-7]	-3,10	9,09E-06
ENSDARG00000076474	org	oogenesis-related gene [Source:ZFIN;Acc:ZDB-GENE-050208-584]	-3,01	2,98E-05
ENSDARG00000115457	zp3.2	zona pellucida glycoprotein 3, tandem duplicate 2 [Source:ZFIN;Acc:ZDB-GENE-050626-121]	-2,99	7,51E-05
ENSDARG00000038296	tmem86b	transmembrane protein 86B [Source:ZFIN;Acc:ZDB-GENE-060825-132]	-2,97	1,99E-06
ENSDARG00000096095	buc	bucky ball [Source:ZFIN;Acc:ZDB-GENE-070117-694]	-2,95	3,41E-05
ENSDARG00000038720	zp3f.1	zona pellucida glycoprotein 3f, tandem duplicate 1 [Source:ZFIN;Acc:ZDB-GENE-030616-590]	-2,89	3,40E-05
ENSDARG00000092885	zgc:171977	zgc:171977 [Source:ZFIN;Acc:ZDB-GENE-070822-24]	-2,87	2,28E-04
ENSDARG00000090768	zgc:173556	zona pellucida glycoprotein 3, tandem duplicate 2 [Source:ZFIN;Acc:ZDB-GENE-050626-121]	-2,86	4,81E-06
ENSDARG00000051923	ccnb1	cyclin B1 [Source:ZFIN;Acc:ZDB-GENE-000406-10]	-2,84	8,03E-05
ENSDARG00000008541	chia.4	chitinase, acidic.4 [Source:ZFIN;Acc:ZDB-GENE-030131-9279]	-2,83	1,97E-05
ENSDARG00000034989	retsatl	retinol saturase (all-trans-retinol 13,14-reductase) like [Source:ZFIN;Acc:ZDB-GENE-051113-252]	-2,83	1,65E-06
ENSDARG00000041248	si:dkey-241l7.6	si:dkey-241l7.6 [Source:ZFIN;Acc:ZDB-GENE-041014-235]	-2,80	1,24E-04
ENSDARG00000100528	map1lc3c	microtubule-associated protein 1 light chain 3 gamma [Source:ZFIN;Acc:ZDB-GENE-040426-1080]	-2,73	2,37E-04
ENSDARG00000095741	ddx41	si:ch1073-75o15.3 [Source:ZFIN;Acc:ZDB-GENE-100921-22]	-2,73	6,66E-05
ENSDARG00000069251	zpax1	zona pellucida protein AX 1 [Source:ZFIN;Acc:ZDB-GENE-030131-5968]	-2,72	2,22E-06
ENSDARG00000098739		H2A histone family member 1a like [Source:NCBI gene;Acc:100332229]	-2,72	7,23E-05
ENSDARG00000075737	zgc:165518	zgc:165518 [Source:ZFIN;Acc:ZDB-GENE-070720-15]	-2,70	1,33E-04
ENSDARG00000078638	zgc:171750	zgc:171750 [Source:ZFIN;Acc:ZDB-GENE-071004-30]	-2,69	6,01E-05
ENSDARG00000077741	zgc:175135	zgc:175135 [Source:ZFIN;Acc:ZDB-GENE-080214-1]	-2,69	1,05E-05
ENSDARG00000045424	zgc:173856	zgc:173856 [Source:ZFIN;Acc:ZDB-GENE-030131-5358]	-2,69	2,34E-05
ENSDARG00000094370	si:ch211-125e6.13	si:ch211-125e6.13 [Source:ZFIN;Acc:ZDB-GENE-070912-37]	-2,67	2,29E-04
ENSDARG00000016908	zp3e	zona pellucida glycoprotein 3e [Source:ZFIN;Acc:ZDB-GENE-071004-38]	-2,62	1,83E-05
ENSDARG00000092057	si:dkey-90l23.1	si:dkey-90l23.1 [Source:ZFIN;Acc:ZDB-GENE-030131-5242]	-2,61	2,12E-04
ENSDARG00000006580	cldnd	claudin d [Source:ZFIN;Acc:ZDB-GENE-010328-4]	-2,61	2,54E-04
ENSDARG00000032156	zgc:171776	zgc:171776 [Source:ZFIN;Acc:ZDB-GENE-071004-36]	-2,61	1,57E-05
ENSDARG00000116005	zgc:171446	zgc:171446 [Source:ZFIN;Acc:ZDB-GENE-080205-1]	-2,54	2,11E-04
ENSDARG00000079034	zpax4	zona pellucida protein AX 4 [Source:ZFIN;Acc:ZDB-GENE-030131-6199]	-2,52	7,57E-05
ENSDARG00000095281	zgc:152652	zgc:152652 [Source:ZFIN;Acc:ZDB-GENE-060818-27]	-2,51	5,17E-06
ENSDARG00000090870	si:ch1073-263o8.2	si:ch1073-263o8.2 [Source:ZFIN;Acc:ZDB-GENE-030131-5362]	-2,48	1,53E-04
ENSDARG00000074289	tuba4l	tubulin, alpha 4 like [Source:ZFIN;Acc:ZDB-GENE-030131-5588]	-2,45	1,40E-04
ENSDARG00000068465	zgc:136254	zgc:136254 [Source:ZFIN;Acc:ZDB-GENE-060421-3062]	-2,26	1,72E-04
ENSDARG00000079979	fam89a	family with sequence similarity 89 member A [Source:ZFIN;Acc:ZDB-GENE-111019-1]	-2,17	8,17E-06
ENSDARG00000043257	ckbb	creatine kinase, brain b [Source:ZFIN;Acc:ZDB-GENE-020103-2]	-1,81	1,16E-05
ENSDARG00000039943	tent5ba	terminal nucleotidyltransferase 5ba [Source:ZFIN;Acc:ZDB-GENE-061110-129]	-1,42	9,09E-06
ENSDARG00000018266	mthfd1a	methylenetetrahydrofolate dehydrogenase (NADP+ dependent) 1a, methenyltetrahydrofolate cyclohydrolase, formyltetrahydrofolate synthetase [Source:ZFIN;Acc:ZDB-GENE-041001-127]	-1,42	1,26E-04

Supplementary Table 4. Differentially expressed genes in *S. pneumoniae* infected *pcsk9* KO zebrafish. Gene expression in pneumococcus infected *pcsk9*$^{tpu-13/tpu-13}$ (n=3) zebrafish liver was compared to WT siblings (n=3). RNA sequencing was performed using Illumina PE150 platform (50M reads).

Up-regulated transcripts

Gene ID (Ensembl)	Gene symbol	Gene Name	Average log2 Fold Change	Adj. P-value
ENSDARG00000087873	eevs	2-epi-5-epi-valiolone synthase [Source:ZFIN;Acc:ZDB-GENE-131121-365]	8,50	4,89E-05
ENSDARG00000003706	ryr2b	ryanodine receptor 2b (cardiac) [Source:ZFIN;Acc:ZDB-GENE-061226-3]	7,51	1,51E-05
ENSDARG00000054313	zp3f.2	zona pellucida glycoprotein 3f, tandem duplicate 2 [Source:ZFIN;Acc:ZDB-GENE-030616-589]	7,21	8,35E-06
ENSDARG00000043902	gabrr1	gamma-aminobutyric acid (GABA) A receptor, rho 1 [Source:ZFIN;Acc:ZDB-GENE-040724-212]	7,04	1,45E-06
ENSDARG00000116066		microfibril-associated glycoprotein 4-like [Source:NCBI gene;Acc:100334800]	7,00	1,57E-10
ENSDARG00000092028	si:dkey-4c23.3	si:dkey-4c23.3 [Source:ZFIN;Acc:ZDB-GENE-050208-668]	6,67	1,26E-04
ENSDARG00000096447			6,58	4,77E-07
ENSDARG00000074653	si:ch211-233m11.1	si:ch211-233m11.1 [Source:ZFIN;Acc:ZDB-GENE-081028-16]	6,57	2,59E-05
ENSDARG00000071103	si:dkey-222p3.1	si:dkey-222p3.1 [Source:ZFIN;Acc:ZDB-GENE-050208-374]	6,44	6,41E-05
ENSDARG00000096017		si:ch211-250e5.3 [Source:NCBI gene;Acc:561392]	6,33	1,10E-06
ENSDARG00000010727	ttyh2l	tweety homolog 2, like [Source:NCBI gene;Acc:406540]	6,27	1,91E-04
ENSDARG00000006008	dct	dopachrome tautomerase [Source:ZFIN;Acc:ZDB-GENE-000508-1]	6,26	3,94E-04
ENSDARG00000077741	zgc:175135	zgc:175135 [Source:ZFIN;Acc:ZDB-GENE-080214-1]	6,06	3,52E-04
ENSDARG00000102926	si:dkey-223p19.2	si:dkey-223p19.2 [Source:ZFIN;Acc:ZDB-GENE-120215-157]	6,04	5,43E-04
ENSDARG00000043446	efhd1	EF-hand domain family, member D1 [Source:ZFIN;Acc:ZDB-GENE-030131-7461]	5,87	4,21E-04
ENSDARG00000087584	si:dkeyp-98a7.9	si:dkeyp-98a7.9 [Source:ZFIN;Acc:ZDB-GENE-050208-680]	5,84	3,30E-06
ENSDARG00000040732	elavl2	ELAV like neuron-specific RNA binding protein 2 [Source:ZFIN;Acc:ZDB-GENE-040704-9]	5,81	1,88E-05
ENSDARG00000076391	npm2a	nucleophosmin/nucleoplasmin, 2a [Source:ZFIN;Acc:ZDB-GENE-060810-57]	5,60	1,27E-04
ENSDARG00000039832	gsta.2	glutathione S-transferase, alpha tandem duplicate 2 [Source:ZFIN;Acc:ZDB-GENE-070822-30]	5,55	8,04E-06
ENSDARG00000089802	akap1a	A kinase (PRKA) anchor protein 1a [Source:ZFIN;Acc:ZDB-GENE-030131-5980]	5,34	9,20E-05
ENSDARG00000038720	zp3f.1	zona pellucida glycoprotein 3f, tandem duplicate 1 [Source:ZFIN;Acc:ZDB-GENE-050208-470]	5,27	3,24E-06
ENSDARG00000088713	si:ch211-226h8.14	si:ch211-226h8.14 [Source:ZFIN;Acc:ZDB-GENE-030616-590]	5,18	1,44E-06
ENSDARG00000037002	zgc:152968	zgc:152968 [Source:ZFIN;Acc:ZDB-GENE-061013-448]	5,16	5,89E-04

ENSDARG00000067964	slc6a5	solute carrier family 6 member 5 [Source:ZFIN;Acc:ZDB-GENE-050105-2]	5,12	4,00E-05
ENSDARG00000033662	scd	stearoyl-CoA desaturase (delta-9-desaturase) [Source:ZFIN;Acc:ZDB-GENE-031106-3]	5,10	9,99E-08
ENSDARG00000036247	tmem144b	transmembrane protein 144b [Source:ZFIN;Acc:ZDB-GENE-041010-58]	5,09	4,79E-05
ENSDARG00000008541	chia.4	chitinase, acidic.4 [Source:ZFIN;Acc:ZDB-GENE-030131-9279]	5,04	4,21E-06
ENSDARG00000004874	spata6l	spermatogenesis associated 6-like [Source:ZFIN;Acc:ZDB-GENE-040426-1369]	5,04	4,81E-05
ENSDARG00000095867	si:ch73-132k15.2	si:ch73-132k15.2 [Source:ZFIN;Acc:ZDB-GENE-110411-191]	5,04	4,49E-06
ENSDARG00000004115	mgat4b	alpha-1,3-mannosyl-glycoprotein 4-beta-N-acetylglucosaminyltransferase B [Source:NCBI gene;Acc:4317227]	4,95	1,66E-07
ENSDARG00000041699	piwil1	piwi-like RNA-mediated gene silencing 1 [Source:NCBI gene;Acc:368200]	4,84	1,40E-04
ENSDARG00000053483	zgc:113054	zgc:113054 [Source:ZFIN;Acc:ZDB-GENE-050320-9]	4,77	1,04E-08
ENSDARG00000070618	tatdn2	TatD DNase domain containing 2 [Source:ZFIN;Acc:ZDB-GENE-081022-51]	4,74	4,92E-04
ENSDARG00000111240	dhrs13a.2	dehydrogenase/reductase (SDR family) member 13a, tandem duplicate 2 [Source:ZFIN;Acc:ZDB-GENE-040912-69]	4,70	2,48E-05
ENSDARG00000086522	zp2.5	zona pellucida glycoprotein 2, tandem duplicate 5 [Source:ZFIN;Acc:ZDB-GENE-090306-1]	4,66	1,09E-05
ENSDARG00000014208	zgc:55413	zgc:55413 [Source:ZFIN;Acc:ZDB-GENE-040426-2909]	4,65	2,31E-06
ENSDARG00000075113	nanog	nanog homeobox [Source:ZFIN;Acc:ZDB-GENE-030131-5486]	4,61	1,05E-04
ENSDARG00000075737	zgc:165518	zgc:165518 [Source:ZFIN;Acc:ZDB-GENE-070720-15]	4,56	2,50E-05
ENSDARG00000104170	si:dkey-208k4.2	si:dkey-208k4.2 [Source:ZFIN;Acc:ZDB-GENE-030131-6124]	4,55	4,95E-04
ENSDARG00000051923	ccnb1	cyclin B1 [Source:ZFIN;Acc:ZDB-GENE-000406-10]	4,52	6,45E-06
ENSDARG00000054374	alg13	ALG13 UDP-N-acetylglucosaminyltransferase subunit [Source:ZFIN;Acc:ZDB-GENE-060307-1]	4,50	3,83E-04
ENSDARG00000079455	nlgn4xa	neuroligin 4 X-linked a [Source:ZFIN;Acc:ZDB-GENE-100309-2]	4,43	1,96E-04
ENSDARG00000018871	henmt1	HEN methyltransferase 1 [Source:NCBI gene;Acc:550540]	4,40	7,00E-04
ENSDARG00000090768	zp3.2	zona pellucida glycoprotein 3, tandem duplicate 2 [Source:ZFIN;Acc:ZDB-GENE-050626-121]	4,38	7,10E-05
ENSDARG00000088923	si:ch211-12h2.8	si:ch211-12h2.8 [Source:ZFIN;Acc:ZDB-GENE-091118-43]	4,37	9,32E-05
ENSDARG00000055655	birc5b	baculoviral IAP repeat containing 5b [Source:ZFIN;Acc:ZDB-GENE-030826-2]	4,35	5,78E-05
ENSDARG00000092090	si:ch211-125e6.12	si:ch211-125e6.12 [Source:ZFIN;Acc:ZDB-GENE-070912-36]	4,34	1,06E-04
ENSDARG00000093216	si:ch211-146l10.7	si:ch211-146l10.7 [Source:ZFIN;Acc:ZDB-GENE-091112-4]	4,31	1,13E-04
ENSDARG00000092885	zgc:171977	zgc:171977 [Source:ZFIN;Acc:ZDB-GENE-070822-24]	4,31	3,22E-06
ENSDARG00000035018	thy1	Thy-1 cell surface antigen [Source:ZFIN;Acc:ZDB-GENE-030131-8561]	4,30	1,33E-14
ENSDARG00000019233	nln	neurolysin (metallopeptidase M3 family) [Source:ZFIN;Acc:ZDB-GENE-041010-216]	4,30	4,71E-05
ENSDARG00000041248	si:dkey-24l17.6	si:dkey-24l17.6 [Source:ZFIN;Acc:ZDB-GENE-041014-235]	4,26	3,12E-04

Gene ID	Symbol	Description	Value	p-value
ENSDARG00000093841	si:ch211-12h2.6	zgc:152936 [Source:ZFIN;Acc:ZDB-GENE-060825-355]	4,23	6,22E-05
ENSDARG00000053877	cpdb	carboxypeptidase D, b [Source:ZFIN;Acc:ZDB-GENE-060929-1270]	4,22	2,54E-04
ENSDARG00000034989	retsatl	retinol saturase (all-trans-retinol 13,14-reductase) like [Source:NCBI gene;Acc:677660]	4,22	2,94E-04
ENSDARG00000100979		pregnancy zone protein-like [Source:NCBI gene;Acc:103909927]	4,20	1,14E-04
ENSDARG00000103595	sfxn5a	sideroflexin 5a [Source:ZFIN;Acc:ZDB-GENE-090312-174]	4,13	1,62E-06
ENSDARG00000060702	npffr2b	neuropeptide FF receptor 2b [Source:ZFIN;Acc:ZDB-GENE-070705-159]	4,12	1,26E-05
ENSDARG00000103024	zgc:175136	zgc:175136 [Source:ZFIN;Acc:ZDB-GENE-080204-122]	4,07	1,04E-04
ENSDARG00000007751	lmnl3	lamin L3 [Source:ZFIN;Acc:ZDB-GENE-020424-4]	4,07	4,92E-04
ENSDARG00000076949	zgc:173837	zgc:173837 [Source:ZFIN;Acc:ZDB-GENE-080213-12]	4,05	7,11E-04
ENSDARG00000011239	ppp1r14aa	protein phosphatase 1, regulatory (inhibitor) subunit 14Aa [Source:ZFIN;Acc:ZDB-GENE-050417-413]	4,04	7,12E-04
ENSDARG00000003968	larp6b	La ribonucleoprotein 6, translational regulator b [Source:ZFIN;Acc:ZDB-GENE-041008-244]	4,00	2,39E-04
ENSDARG00000069744	mos	v-mos Moloney murine sarcoma viral oncogene homolog [Source:ZFIN;Acc:ZDB-GENE-040428-3]	3,98	2,85E-04
ENSDARG00000002330	lhx8a	LIM homeobox 8a [Source:ZFIN;Acc:ZDB-GENE-031008-2]	3,95	6,57E-04
ENSDARG00000002597	pabpc1l	poly(A) binding protein, cytoplasmic 1-like [Source:ZFIN;Acc:ZDB-GENE-030131-5836]	3,94	1,87E-04
ENSDARG00000020749	caprin2	caprin family member 2 [Source:NCBI gene;Acc:407729]	3,93	5,55E-06
ENSDARG00000079034	zpax4	zona pellucida protein AX 4 [Source:ZFIN;Acc:ZDB-GENE-030131-6199]	3,91	9,59E-05
ENSDARG00000040725	zgc:114130	zgc:114130 [Source:ZFIN;Acc:ZDB-GENE-050913-48]	3,90	5,12E-07
ENSDARG00000094747	si:ch211-197g15.6	si:ch211-197g15.6 [Source:ZFIN;Acc:ZDB-GENE-050208-457]	3,90	6,26E-04
ENSDARG00000016733	psat1	phosphoserine aminotransferase 1 [Source:ZFIN;Acc:ZDB-GENE-030131-5723]	3,89	3,08E-04
ENSDARG00000059252	zpcx	zona pellucida protein C [Source:ZFIN;Acc:ZDB-GENE-040824-1]	3,89	5,37E-04
ENSDARG00000063670	gtf2a1l	general transcription factor IIA, 1-like [Source:ZFIN;Acc:ZDB-GENE-060929-28]	3,84	2,30E-05
ENSDARG00000100528	map1lc3c	microtubule-associated protein 1 light chain 3 gamma [Source:ZFIN;Acc:ZDB-GENE-040426-1080]	3,82	5,09E-04
ENSDARG00000075421	pttg1	PTTG1 regulator of sister chromatid separation, securin [Source:ZFIN;Acc:ZDB-GENE-081104-345]	3,77	7,36E-05
ENSDARG00000037961	rcn3	reticulocalbin 3, EF-hand calcium binding domain [Source:ZFIN;Acc:ZDB-GENE-040625-175]	3,74	2,13E-05
ENSDARG00000042130	zp3a.2	zona pellucida glycoprotein 3a, tandem duplicate 2 [Source:ZFIN;Acc:ZDB-GENE-040727-2]	3,69	5,77E-04
ENSDARG00000088989	si:dkey-24l7.5	si:dkey-24l7.5 [Source:ZFIN;Acc:ZDB-GENE-041014-237]	3,63	3,25E-04
ENSDARG00000093019	si:dkey-83k24.5	si:dkey-83k24.5 [Source:ZFIN;Acc:ZDB-GENE-081104-440]	3,60	3,51E-05

Gene ID	Symbol	Description	Value	p-value
ENSDARG00000039828	zp3b	zona pellucida glycoprotein 3b [Source:ZFIN;Acc:ZDB-GENE-031124-2]	3,57	1,69E-06
ENSDARG00000104175			3,56	1,13E-04
ENSDARG00000003854	acsl1b	acyl-CoA synthetase long chain family member 1b [Source:ZFIN;Acc:ZDB-GENE-040801-88]	3,52	8,10E-05
ENSDARG00000098004	ftr91	finTRIM family, member 91 [Source:ZFIN;Acc:ZDB-GENE-131125-31]	3,50	1,60E-04
ENSDARG00000004111	esr1	estrogen receptor 1 [Source:NCBI gene;Acc:259252]	3,48	1,86E-10
ENSDARG00000041623	mt2	metallothionein 2 [Source:NCBI gene;Acc:100174951]	3,47	1,71E-19
ENSDARG00000089478	si:dkey-24I7.4	si:dkey-24I7.4 [Source:ZFIN;Acc:ZDB-GENE-041014-238]	3,44	1,22E-04
ENSDARG00000044074	loxl2b	lysyl oxidase-like 2b [Source:NCBI gene;Acc:791144]	3,39	3,80E-07
ENSDARG00000019763	acp5a	acid phosphatase 5a, tartrate resistant [Source:ZFIN;Acc:ZDB-GENE-040426-2864]	3,38	2,23E-04
ENSDARG00000100397	pde6c	phosphodiesterase 6C, cGMP-specific, cone, alpha prime [Source:ZFIN;Acc:ZDB-GENE-040426-1664]	3,25	1,47E-06
ENSDARG00000026871	uchl1	ubiquitin carboxyl-terminal esterase L1 (ubiquitin thiolesterase) [Source:ZFIN;Acc:ZDB-GENE-030131-3844]	3,24	8,97E-08
ENSDARG00000006003	mycla	MYCL proto-oncogene, bHLH transcription factor a [Source:NCBI gene;Acc:405873]	3,18	1,07E-04
ENSDARG00000044362	unc119b	unc-119 homolog b (C. elegans) [Source:ZFIN;Acc:ZDB-GENE-050201-2]	3,16	6,07E-04
ENSDARG00000059993	trpm4a	transient receptor potential cation channel, subfamily M, member 4a [Source:ZFIN;Acc:ZDB-GENE-090302-3]	3,11	4,64E-04
ENSDARG00000069966	alox5b.3	arachidonate 5-lipoxygenase b, tandem duplicate 3 [Source:ZFIN;Acc:ZDB-GENE-050522-330]	3,09	2,69E-04
ENSDARG00000007129	slc6a16a	solute carrier family 6 member 16a [Source:ZFIN;Acc:ZDB-GENE-061009-43]	3,08	2,77E-04
ENSDARG00000060496	cacna1ha	calcium channel, voltage-dependent, T type, alpha 1H subunit a [Source:ZFIN;Acc:ZDB-GENE-130103-1]	3,08	6,02E-06
ENSDARG00000078541	cers3a	ceramide synthase 3a [Source:ZFIN;Acc:ZDB-GENE-130320-1]	3,07	1,49E-06
ENSDARG00000005355	larp6a	La ribonudeoprotein 6, translational regulator a [Source:ZFIN;Acc:ZDB-GENE-030131-6403]	2,96	2,77E-04
ENSDARG00000023950	znhit3	zinc finger, HIT-type containing 3 [Source:NCBI gene;Acc:393243]	2,91	7,80E-05
ENSDARG00000100227		solute carrier family 7 member 1b [Source:NCBI gene;Acc:406380]	2,87	6,63E-07
ENSDARG00000035859	angptl4	angiopoietin-like 4 [Source:ZFIN;Acc:ZDB-GENE-041111-222]	2,85	2,97E-04
ENSDARG00000069044	agpat4	1-acylglycerol-3-phosphate O-acyltransferase 4 (lysophosphatidic acid acyltransferase, delta) [Source:ZFIN;Acc:ZDB-GENE-040426-1924]	2,84	1,53E-13
ENSDARG00000101557	scarb1	scavenger receptor class B, member 1 [Source:ZFIN;Acc:ZDB-GENE-031126-1]	2,83	2,22E-04
ENSDARG00000023768	mfsd4aa	major facilitator superfamily domain containing 4Aa [Source:NCBI gene;Acc:393503]	2,83	6,95E-04
ENSDARG00000069441	lpar6b	lysophosphatidic acid receptor 6b [Source:ZFIN;Acc:ZDB-GENE-110408-67]	2,77	1,25E-04

Gene ID	Symbol	Description	Value	p-value
ENSDARG00000037000	fkbp11	FKBP prolyl isomerase 11 [Source:ZFIN;Acc:ZDB-GENE-030616-357]	2,73	2,81E-05
ENSDARG00000009001	pdia6	protein disulfide isomerase family A, member 6 [Source:ZFIN;Acc:ZDB-GENE-030131-879]	2,66	7,80E-07
ENSDARG00000007099	cx43.4	connexin 43.4 [Source:NCBI gene;Acc:30276]	2,65	2,65E-04
ENSDARG00000032010	slc15a2	solute carrier family 15 member 2 [Source:NCBI gene;Acc:556684]	2,65	2,05E-04
ENSDARG00000006497	rtn1a	reticulon 1a [Source:ZFIN;Acc:ZDB-GENE-030131-2426]	2,61	9,92E-05
ENSDARG00000060325	fam20cl	family with sequence similarity 20 member C, like [Source:ZFIN;Acc:ZDB-GENE-070705-319]	2,60	4,94E-04
ENSDARG00000114552	siva1	SIVA1, apoptosis-inducing factor [Source:ZFIN;Acc:ZDB-GENE-050506-57]	2,57	3,80E-04
ENSDARG00000010437	tent5c	terminal nucleotidyltransferase 5C [Source:NCBI gene;Acc:327154]	2,55	5,77E-06
ENSDARG00000018145	mid1ip1l	MID1 interacting protein 1, like [Source:NCBI gene;Acc:322977]	2,53	2,41E-04
ENSDARG00000004311	ldlrap1a	low density lipoprotein receptor adaptor protein 1a [Source:ZFIN;Acc:ZDB-GENE-030328-13]	2,51	6,85E-04
ENSDARG00000006427	fabp2	fatty acid binding protein 2, intestinal [Source:ZFIN;Acc:ZDB-GENE-991019-5]	2,49	1,72E-05
ENSDARG00000075368	mrm2	mitochondrial rRNA methyltransferase 2 [Source:ZFIN;Acc:ZDB-GENE-030131-5205]	2,49	6,06E-04
ENSDARG00000063218	ppm1la	protein phosphatase, Mg2+/Mn2+ dependent, 1La [Source:ZFIN;Acc:ZDB-GENE-061103-118]	2,45	2,07E-04
ENSDARG00000028295	mkrn4	makorin, ring finger protein, 4 [Source:ZFIN;Acc:ZDB-GENE-030131-5954]	2,44	5,41E-04
ENSDARG00000008491	si:ch211-107o10.3	si:ch211-107o10.3 [Source:ZFIN;Acc:ZDB-GENE-030131-4716]	2,40	1,44E-04
ENSDARG00000069278	trmt5	tRNA methyltransferase 5 [Source:NCBI gene;Acc:564078]	2,31	1,43E-04
ENSDARG00000016448	vtg3	vitellogenin 3, phosvitinless [Source:ZFIN;Acc:ZDB-GENE-991019-2]	2,27	6,82E-05
ENSDARG00000015765	iah1	isoamyl acetate hydrolyzing esterase 1 (putative) [Source:NCBI gene;Acc:449926]	2,22	3,61E-04
ENSDARG00000012199	gpt2	glutamic pyruvate transaminase (alanine aminotransferase) 2 [Source:ZFIN;Acc:ZDB-GENE-030729-8]	2,21	5,25E-04
ENSDARG00000014599	slc5a6b	solute carrier family 5 member 6 [Source:ZFIN;Acc:ZDB-GENE-050913-86]	2,21	2,60E-05
ENSDARG00000035909	mfsd2ab	major facilitator superfamily domain containing 2ab [Source:NCBI gene;Acc:445176]	2,14	1,12E-07
ENSDARG00000033771	hspbap1	hspb associated protein 1 [Source:NCBI gene;Acc:445320]	2,06	1,40E-04
ENSDARG00000016825	vtg6	vitellogenin 6 [Source:ZFIN;Acc:ZDB-GENE-001201-5]	2,05	1,18E-06
ENSDARG00000079216	dpep2	dipeptidase 2 [Source:ZFIN;Acc:ZDB-GENE-120419-2]	2,03	7,03E-04
ENSDARG00000004262	cyp46a1.2	cytochrome P450, family 46, subfamily A, polypeptide 1, tandem duplicate 2 [Source:ZFIN;Acc:ZDB-GENE-040426-1184]	1,98	6,01E-04
ENSDARG00000020000	sh3bp4a	SH3-domain binding protein 4a [Source:NCBI gene;Acc:403082]	1,95	5,93E-05
ENSDARG00000054916	eif4ebp3	eukaryotic translation initiation factor 4E binding protein 3 [Source:ZFIN;Acc:ZDB-GENE-041114-44]	1,94	1,20E-04
ENSDARG00000037393	slc43a1a	solute carrier family 43 member 1a [Source:ZFIN;Acc:ZDB-GENE-030131-6327]	1,94	6,13E-04

Gene ID (Ensembl)	Gene symbol	Gene Name	Average log2 Fold Change	Adj. P-value
ENSDARG00000045129	fkbp10b	FKBP prolyl isomerase 10b [Source:ZFIN;Acc:ZDB-GENE-030131-3101]	1,93	1,42E-04
ENSDARG00000101089	gart	phosphoribosylglycinamide formyltransferase [Source:ZFIN;Acc:ZDB-GENE-000616-14]	1,90	2,36E-04
ENSDARG00000011371	zgc:64106	zgc:64106 [Source:ZFIN;Acc:ZDB-GENE-040426-1370]	1,88	1,63E-05
ENSDARG00000104906	mtr	5-methyltetrahydrofolate-homocysteine methyltransferase [Source:ZFIN;Acc:ZDB-GENE-031001-5]	1,83	1,33E-04
ENSDARG00000021149	cbr1l	carbonyl reductase 1-like [Source:ZFIN;Acc:ZDB-GENE-030131-9642]	1,81	1,00E-05
ENSDARG00000041372	zgc:136564	zgc:136564 [Source:ZFIN;Acc:ZDB-GENE-070410-3]	1,81	6,02E-05
ENSDARG00000090690	nell2a	neural EGFL like 2 [Source:HGNC Symbol;Acc:HGNC:7751]	1,79	4,01E-04
ENSDARG00000074698	sdsl	serine dehydratase-like [Source:ZFIN;Acc:ZDB-GENE-131121-410]	1,78	2,17E-04
ENSDARG00000045568	bcat1	branched chain amino-acid transaminase 1, cytosolic [Source:ZFIN;Acc:ZDB-GENE-030131-9358]	1,78	3,82E-05
ENSDARG00000092126	vtg5	vitellogenin 5 [Source:ZFIN;Acc:ZDB-GENE-001201-4]	1,69	1,14E-04
ENSDARG00000092419	vtg7	vitellogenin 7 [Source:ZFIN;Acc:ZDB-GENE-001201-6]	1,67	1,16E-04
ENSDARG00000098639	pycr1b	pyrroline-5-carboxylate reductase 1b [Source:ZFIN;Acc:ZDB-GENE-050522-26]	1,57	6,25E-04
ENSDARG00000078429	vtg4	vitellogenin 4 [Source:ZFIN;Acc:ZDB-GENE-001201-3]	1,55	2,82E-04
ENSDARG00000031325	tmed1a	transmembrane p24 trafficking protein 1a [Source:ZFIN;Acc:ZDB-GENE-040801-229]	1,53	4,66E-04
ENSDARG00000033539	paics	phosphoribosylaminoimidazole carboxylase, phosphoribosylaminoimidazole succinocarboxamide synthetase [Source:ZFIN;Acc:ZDB-GENE-030131-9762]	1,49	6,96E-04
ENSDARG00000074169	gpam	glycerol-3-phosphate acyltransferase, mitochondrial [Source:ZFIN;Acc:ZDB-GENE-101026-1]	1,48	6,15E-05
ENSDARG00000045776	cnbpa	CCHC-type zinc finger, nucleic acid binding protein a [Source:ZFIN;Acc:ZDB-GENE-030131-5045]	1,07	2,19E-04

Down-regulated transcripts

Gene ID (Ensembl)	Gene symbol	Gene Name	Average log2 Fold Change	Adj. P-value
ENSDARG00000003197	wdr21	WD repeat domain 21 [Source:ZFIN;Acc:ZDB-GENE-040109-2]	-9,35	1,28E-12
ENSDARG00000020711	rrm2	ribonucleotide reductase regulatory subunit M2 [Source:NCBI gene;Acc:100330864]	-7,75	1,13E-08
ENSDARG00000102317	rpl26	ribosomal protein L26 [Source:ZFIN;Acc:ZDB-GENE-040426-2117]	-6,26	5,85E-05
ENSDARG00000042182	drc1	dynein regulatory complex subunit 1 homolog (Chlamydomonas) [Source:NCBI gene;Acc:100034551]	-5,97	2,18E-09
ENSDARG00000102175	hamp	hepcidin antimicrobial peptide [Source:NCBI gene;Acc:402837]	-5,83	8,59E-12

Ensembl ID	Gene	Description	Fold change	p-value
ENSDARG00000027940	kcnf1a	potassium voltage-gated channel, subfamily F, member 1a [Source:ZFIN;Acc:ZDB-GENE-041001-217]	-5,48	5,93E-04
ENSDARG00000105249	si:dkey-65b13.9	si:dkey-65b13.9 [Source:ZFIN;Acc:ZDB-GENE-041014-335]	-5,34	4,10E-11
ENSDARG00000100381	rock2bl	rho-associated, coiled-coil containing protein kinase 2b, like [Source:ZFIN;Acc:ZDB-GENE-071005-1]	-5,23	2,39E-07
ENSDARG00000042285	atp8b3	ATPase phospholipid transporting 8B3 [Source:ZFIN;Acc:ZDB-GENE-050208-424]	-5,06	2,02E-04
ENSDARG00000016464	cdc42bpab	CDC42 binding protein kinase alpha (DMPK-like) b [Source:ZFIN;Acc:ZDB-GENE-080219-17]	-4,92	2,66E-05
ENSDARG00000077058	cela1.5	chymotrypsin like elastase family member 1, tandem duplicate 5 [Source:ZFIN;Acc:ZDB-GENE-040801-186]	-4,61	8,95E-05
ENSDARG00000029688	hsp70.1	heat shock cognate 70-kd protein, tandem duplicate 1 [Source:ZFIN;Acc:ZDB-GENE-990415-91]	-4,57	7,21E-04
ENSDARG00000078970	il7r	interleukin 7 receptor [Source:ZFIN;Acc:ZDB-GENE-080110-7]	-4,47	9,97E-05
ENSDARG00000091042	sacs	sacsin molecular chaperone [Source:ZFIN;Acc:ZDB-GENE-110411-146]	-4,46	2,12E-04
ENSDARG00000096433	rock2b	rho-associated, coiled-coil containing protein kinase 2b [Source:ZFIN;Acc:ZDB-GENE-060125-2]	-4,14	3,57E-13
ENSDARG00000005704	eps8l3b	EPS8-like 3b [Source:ZFIN;Acc:ZDB-GENE-040426-1335]	-3,83	1,59E-05
ENSDARG00000055723	hsp70l	heat shock cognate 70-kd protein, like [Source:ZFIN;Acc:ZDB-GENE-050321-1]	-3,79	1,92E-05
ENSDARG00000087832	bcl3	BCL3 transcription coactivator [Source:ZFIN;Acc:ZDB-GENE-061013-1]	-3,76	1,14E-05
ENSDARG00000043729	plac8.1	placenta associated 8, tandem duplicate 1 [Source:ZFIN;Acc:ZDB-GENE-050809-124]	-3,75	7,74E-05
ENSDARG00000089075	si:ch73-173p19.1	si:ch73-173p19.1 [Source:ZFIN;Acc:ZDB-GENE-130530-952]	-3,68	3,43E-05
ENSDARG00000055901	steap4	STEAP family member 4 [Source:ZFIN;Acc:ZDB-GENE-070424-244]	-3,62	5,79E-08
ENSDARG00000057121	c7b	complement component 7b [Source:ZFIN;Acc:ZDB-GENE-021120-1]	-3,53	8,72E-09
ENSDARG00000037528	si:ch211-191a24.4	si:ch211-191a24.4 [Source:ZFIN;Acc:ZDB-GENE-030131-4489]	-3,50	9,44E-09
ENSDARG00000043581	gadd45aa	growth arrest and DNA-damage-inducible, alpha, a [Source:ZFIN;Acc:ZDB-GENE-040426-1501]	-3,43	2,38E-05
ENSDARG00000054304	homeza	homeobox and leucine zipper encoding a [Source:ZFIN;Acc:ZDB-GENE-030616-592]	-3,40	5,93E-06
ENSDARG00000088130	si:dkey-30c15.10	si:dkey-30c15.10 [Source:ZFIN;Acc:ZDB-GENE-060503-826]	-3,38	1,99E-08
ENSDARG00000097528	si:dkey-7j14.5	si:dkey-7j14.5 [Source:ZFIN;Acc:ZDB-GENE-030131-8110]	-3,36	1,97E-05
ENSDARG00000053131	irak3	interleukin-1 receptor-associated kinase 3 [Source:ZFIN;Acc:ZDB-GENE-060503-710]	-3,29	1,03E-06
ENSDARG00000028478	si:ch211-173n18.3	si:ch211-173n18.3 [Source:ZFIN;Acc:ZDB-GENE-120215-62]	-3,10	1,21E-04
ENSDARG00000099351	igfbp1a	insulin-like growth factor binding protein 1a [Source:ZFIN;Acc:ZDB-GENE-021231-1]	-3,06	5,12E-11
ENSDARG00000013926	slc16a9a	solute carrier family 16 member 9a [Source:ZFIN;Acc:ZDB-GENE-040426-1364]	-3,04	4,76E-04
ENSDARG00000027777	tnfaip3	tumor necrosis factor, alpha-induced protein 3 [Source:ZFIN;Acc:ZDB-GENE-100212-2]	-3,03	8,10E-10
ENSDARG00000063481	si:ch211-214j24.15	si:ch211-214j24.15 [Source:ZFIN;Acc:ZDB-GENE-110914-85]	-3,02	3,53E-06

Ensembl ID	Gene	Description	Value	p-value
ENSDARG00000044142	acss1	acyl-CoA synthetase short chain family member 1 [Source:ZFIN;Acc:ZDB-GENE-050320-139]	-2,99	2,18E-06
ENSDARG00000025428	socs3a	suppressor of cytokine signaling 3a [Source:ZFIN;Acc:ZDB-GENE-030131-7349]	-2,97	4,96E-05
ENSDARG00000091111	si:ch211-15b10.6	si:ch211-15b10.6 [Source:ZFIN;Acc:ZDB-GENE-160728-113]	-2,97	1,11E-04
ENSDARG00000055252	snap23.2	synaptosome associated protein 23.2 [Source:ZFIN;Acc:ZDB-GENE-051030-75]	-2,96	9,55E-05
ENSDARG00000044341	chst7	carbohydrate (N-acetylglucosamine 6-O) sulfotransferase 7 [Source:ZFIN;Acc:ZDB-GENE-131121-150]	-2,92	3,97E-06
ENSDARG00000074501	tnip2	TNFAIP3 interacting protein 2 [Source:ZFIN;Acc:ZDB-GENE-120913-2]	-2,92	4,83E-05
ENSDARG00000058160	tnfaip2b	tumor necrosis factor, alpha-induced protein 2b [Source:ZFIN;Acc:ZDB-GENE-081107-56]	-2,88	1,94E-06
ENSDARG00000040623	fosl2	fos-like antigen 2 [Source:ZFIN;Acc:ZDB-GENE-070209-164]	-2,85	3,53E-04
ENSDARG00000071015	pbxip1a	pre-B-cell leukemia homeobox interacting protein 1a [Source:ZFIN;Acc:ZDB-GENE-060503-871]	-2,83	5,32E-05
ENSDARG00000031683	fosab	v-fos FBJ murine osteosarcoma viral oncogene homolog Ab [Source:ZFIN;Acc:ZDB-GENE-031222-4]	-2,71	1,74E-05
ENSDARG00000087303	cebpd	CCAAT enhancer binding protein delta [Source:ZFIN;Acc:ZDB-GENE-020111-4]	-2,71	4,78E-12
ENSDARG00000009040	si:ch73-141c7.1	si:ch73-141c7.1 [Source:NCBI gene;Acc:393762]	-2,70	1,28E-06
ENSDARG00000117262			-2,64	1,49E-04
ENSDARG00000037593	prickle2b	prickle homolog 2b [Source:ZFIN;Acc:ZDB-GENE-030724-6]	-2,57	2,55E-05
ENSDARG00000061804	si:ch211-194e15.5	si:ch211-194e15.5 [Source:NCBI gene;Acc:100034579]	-2,54	2,73E-04
ENSDARG00000006760	slc24a3	solute carrier family 24 member 3 [Source:ZFIN;Acc:ZDB-GENE-090312-67]	-2,48	3,95E-04
ENSDARG00000059824	soat2	sterol O-acyltransferase 2 [Source:ZFIN;Acc:ZDB-GENE-061013-742]	-2,47	1,61E-04
ENSDARG00000075045	cxcl18b	chemokine (C-X-C motif) ligand 18b [Source:ZFIN;Acc:ZDB-GENE-090313-165]	-2,45	5,62E-05
ENSDARG00000093052	c6	complement component 6 [Source:ZFIN;Acc:ZDB-GENE-040426-1358]	-2,45	3,10E-06
ENSDARG00000025522	sgk1	serum/glucocorticoid regulated kinase 1 [Source:NCBI gene;Acc:324140]	-2,43	4,25E-05
ENSDARG00000103277	cyp24a1	cytochrome P450, family 24, subfamily A, polypeptide 1 [Source:ZFIN;Acc:ZDB-GENE-060825-1]	-2,42	5,98E-05
ENSDARG00000001807	tnfrsf21	tumor necrosis factor receptor superfamily, member 21 [Source:ZFIN;Acc:ZDB-GENE-030131-5971]	-2,35	5,40E-04
ENSDARG00000032868	pde4ba	phosphodiesterase 4B, cAMP-specific a [Source:ZFIN;Acc:ZDB-GENE-030131-9570]	-2,31	3,24E-04
ENSDARG00000007693	nfkbiab	nuclear factor of kappa light polypeptide gene enhancer in B-cells inhibitor, alpha b [Source:ZFIN;Acc:ZDB-GENE-030131-1819]	-2,27	2,11E-04
ENSDARG00000015161	zgc:92664	zgc:92664 [Source:ZFIN;Acc:ZDB-GENE-040718-119]	-2,26	3,44E-06
ENSDARG00000071012	ifit14	interferon-induced protein with tetratricopeptide repeats 14 [Source:ZFIN;Acc:ZDB-GENE-131120-20]	-2,25	3,48E-04

ENSDARG00000032859	lratd2	LRAT domain containing 2 [Source:ZFIN;Acc:ZDB-GENE-060929-1130]	-2,25	6,45E-05
ENSDARG00000062080	shc2	SHC (Src homology 2 domain containing) transforming protein 2 [Source:ZFIN;Acc:ZDB-GENE-050208-666]	-2,21	1,46E-05
ENSDARG00000068182	crb3b	crumbs homolog 3b [Source:ZFIN;Acc:ZDB-GENE-060610-3]	-2,14	1,52E-04
ENSDARG00000004877	rock2b	rho-associated, coiled-coil containing protein kinase 2b [Source:ZFIN;Acc:ZDB-GENE-060125-2]	-2,13	2,06E-05
ENSDARG00000005481	nfkbiaa	nuclear factor of kappa light polypeptide gene enhancer in B-cells inhibitor, alpha a [Source:ZFIN;Acc:ZDB-GENE-040426-2227]	-2,12	6,57E-04
ENSDARG00000057949	slc43a3b	solute carrier family 43 member 3b [Source:ZFIN;Acc:ZDB-GENE-060312-28]	-2,12	1,84E-06
ENSDARG00000089390	pnpla2	patatin-like phospholipase domain containing 2 [Source:ZFIN;Acc:ZDB-GENE-120913-3]	-2,11	2,14E-05
ENSDARG00000091418	snx17	sorting nexin 17 [Source:NCBI gene;Acc:568263]	-2,07	1,40E-08
ENSDARG00000087814	mfrp	membrane frizzled-related protein [Source:ZFIN;Acc:ZDB-GENE-160728-150]	-2,07	4,43E-04
ENSDARG00000038687	nfkb2	nuclear factor of kappa light polypeptide gene enhancer in B-cells 2 (p49/p100) [Source:ZFIN;Acc:ZDB-GENE-030131-6701]	-2,06	2,76E-05
ENSDARG00000069135	ppp1r15a	protein phosphatase 1, regulatory subunit 15A [Source:ZFIN;Acc:ZDB-GENE-030131-4408]	-2,03	5,96E-04
ENSDARG00000062552	lpar6a	lysophosphatidic acid receptor 6a [Source:ZFIN;Acc:ZDB-GENE-061013-343]	-1,98	1,03E-04
ENSDARG00000069484	dab2ipa	DAB2 interacting protein a [Source:ZFIN;Acc:ZDB-GENE-081104-516]	-1,95	5,08E-05
ENSDARG00000078676	myrf	myelin regulatory factor [Source:ZFIN;Acc:ZDB-GENE-080204-57]	-1,93	3,75E-05
ENSDARG00000043317	kita	KIT proto-oncogene, receptor tyrosine kinase a [Source:NCBI gene;Acc:30256]	-1,89	4,28E-04
ENSDARG00000045886	slc38a2	solute carrier family 38 member 2 [Source:NCBI gene;Acc:566537]	-1,87	6,99E-06
ENSDARG00000042329	si:dkey-91m11.5	si:dkey-91m11.5 [Source:ZFIN;Acc:ZDB-GENE-060503-932]	-1,86	3,71E-05
ENSDARG00000058666	dennd2da	DENN/MADD domain containing 2Da [Source:ZFIN;Acc:ZDB-GENE-061013-542]	-1,85	2,57E-04
ENSDARG00000059906	sdc4	syndecan 4 [Source:ZFIN;Acc:ZDB-GENE-061111-1]	-1,82	3,13E-05
ENSDARG00000100731	zgc:101540	zgc:101540 [Source:ZFIN;Acc:ZDB-GENE-041212-67]	-1,82	5,75E-04
ENSDARG00000036695	calcoco1a	calcium binding and coiled-coil domain 1a [Source:NCBI gene;Acc:334971]	-1,74	3,67E-04
ENSDARG00000017312	lmbrd2b	LMBR1 domain containing 2b [Source:NCBI gene;Acc:335257]	-1,73	3,48E-05
ENSDARG00000076903	bend3	BEN domain containing 3 [Source:ZFIN;Acc:ZDB-GENE-090312-181]	-1,66	4,79E-04
ENSDARG00000023933	skila	SKI-like proto-oncogene a [Source:ZFIN;Acc:ZDB-GENE-070912-548]	-1,59	4,02E-04
ENSDARG00000056976	ifit16	interferon-induced protein with tetratricopeptide repeats 16 [Source:ZFIN;Acc:ZDB-GENE-131120-86]	-1,55	1,71E-04
ENSDARG00000023176	tdo2b	tryptophan 2,3-dioxygenase b [Source:NCBI gene;Acc:334082]	-1,51	5,24E-04
ENSDARG00000102610	r3hdm2	R3H domain containing 2 [Source:ZFIN;Acc:ZDB-GENE-180313-1]	-1,47	3,69E-04

Gene ID	Symbol	Description	Value	p-value
ENSDARG00000028017	tp53inp1	tumor protein p53 inducible nuclear protein 1 [Source:ZFIN;Acc:ZDB-GENE-031018-3]	-1,45	4,38E-04
ENSDARG00000057113	c6	complement component 6 [Source:ZFIN;Acc:ZDB-GENE-040426-1358]	-1,38	2,17E-04
ENSDARG00000100499	cpeb4b	cytoplasmic polyadenylation element binding protein 4b [Source:ZFIN;Acc:ZDB-GENE-170601-167]	-1,32	4,98E-04
ENSDARG00000028614	mospd1	motile sperm domain containing 1 [Source:ZFIN;Acc:ZDB-GENE-040426-2691]	-1,28	4,18E-04
ENSDARG00000043497	scrn2	secernin 2 [Source:NCBI gene;Acc:558306]	-1,08	3,57E-04

Supplementary Table 5. Differentially expressed protein coding genes specific for *S. pneumoniae* infected *pcsk9* KO zebrafish. Gene expression in pneumococcus infected *pcsk9*[tpu-13/tpu-13] zebrafish was compared to WT siblings and genes expressed differentially in pneumococcus infected fish (n=3 in both groups) listed. RNA sequencing was perfomed using Illumina PE150 platform (50M reads).

Up-regulated transcripts

Gene ID (Ensembl)	Gene symbol	Gene Name	Average log2 Fold Change	Adj. P-value
ENSDARG00000087873	eevs	2-epi-5-epi-valiolone synthase	8,50	4,89E-05
ENSDARG00000003706	ryr2b	ryanodine receptor 2b (cardiac)	7,51	1,51E-05
ENSDARG00000054313	zp3f.2	zona pellucida glycoprotein 3f, tandem duplicate 2	7,21	8,35E-06
ENSDARG00000043902	gabrr1	gamma-aminobutyric acid (GABA) A receptor, rho 1	7,04	1,45E-06
ENSDARG00000116066		microfibril-associated glycoprotein 4-like	7,00	1,57E-10
ENSDARG00000092028	si:dkey-4c23.3	si:dkey-4c23.3	6,67	1,26E-04
ENSDARG00000074653	si:ch211-233m11.1	si:ch211-233m11.1	6,57	2,59E-05
ENSDARG00000071103	si:dkey-222p3.1	si:dkey-222p3.1	6,44	6,41E-05
ENSDARG00000010727	ttyh2l	tweety homolog 2, like	6,27	1,91E-04
ENSDARG00000006008	dct	dopachrome tautomerase	6,26	3,94E-04
ENSDARG00000102926	si:dkey-223p19.2	si:dkey-223p19.2	6,04	5,43E-04
ENSDARG00000043446	efhd1	EF-hand domain family, member D1	5,87	4,21E-04
ENSDARG00000087584	si:dkeyp-98a7.9	si:dkeyp-98a7.9	5,84	3,30E-06
ENSDARG00000040732	elavl2	ELAV like neuron-specific RNA binding protein 2	5,81	1,88E-05
ENSDARG00000076391	npm2a	nucleophosmin/nucleoplasmin, 2a	5,60	1,27E-04
ENSDARG00000039832	gsta.2	glutathione S-transferase, alpha tandem duplicate 2	5,55	8,04E-06
ENSDARG00000089802	akap1a	A kinase (PRKA) anchor protein 1a	5,34	9,20E-05
ENSDARG00000037002	zgc:152968	zgc:152968	5,16	5,89E-04
ENSDARG00000067964	slc6a5	solute carrier family 6 member 5	5,12	4,00E-05

Ensembl ID	Gene	Description	Value	p-value
ENSDARG00000033662	scd	stearoyl-CoA desaturase (delta-9-desaturase)	5,10	9,99E-08
ENSDARG00000036247	tmem144b	transmembrane protein 144b	5,09	4,79E-05
ENSDARG00000004874	spata6l	spermatogenesis associated 6-lik	5,04	4,81E-05
ENSDARG00000004115	mgat4b	alpha-1,3-mannosyl-glycoprotein 4-beta-N-acetylglucosaminyltransferase B	4,95	1,66E-07
ENSDARG00000041699	piwil1	piwi-like RNA-mediated gene silencing 1	4,84	1,40E-04
ENSDARG00000053483	zgc:113054	zgc:113054	4,77	1,04E-08
ENSDARG00000070618	tatdn2	TatD DNase domain containing 2	4,74	4,92E-04
ENSDARG00000111240	dhrs13a.2	dehydrogenase/reductase (SDR family) member 13a, tandem duplicate 2	4,70	2,48E-05
ENSDARG00000014208	zgc:55413	zgc:55413	4,65	2,31E-06
ENSDARG00000104170	si:dkey-208k4.2	si:dkey-208k4.2	4,55	4,95E-04
ENSDARG00000054374	alg13	ALG13 UDP-N-acetylglucosaminyltransferase subunit	4,50	3,83E-04
ENSDARG00000079455	nlgn4xa	neuroligin 4 X-linked a	4,43	1,96E-04
ENSDARG00000018871	henmt1	HEN methyltransferase 1	4,40	7,00E-04
ENSDARG00000035018	thy1	Thy-1 cell surface antigen	4,30	1,33E-14
ENSDARG00000019233	nln	neurolysin (metallopeptidase M3 family)	4,30	4,71E-05
ENSDARG00000053877	cpdb	carboxypeptidase D, b	4,22	2,54E-04
ENSDARG00000103595	sfxn5a	sideroflexin 5a	4,13	1,62E-06
ENSDARG00000007751	lmnl3	lamin L3	4,07	4,92E-04
ENSDARG00000011239	ppp1r14aa	protein phosphatase 1, regulatory (inhibitor) subunit 14Aa	4,04	7,12E-04
ENSDARG00000069744	mos	v-mos Moloney murine sarcoma viral oncogene homolog	3,98	2,85E-04
ENSDARG00000002330	lhx8a	LIM homeobox 8a	3,95	6,57E-04
ENSDARG00000040725	zgc:114130	zgc:114130	3,90	5,12E-07
ENSDARG00000094747	si:ch211-197g15.6	si:ch211-197g15.6	3,90	6,26E-04
ENSDARG00000016733	psat1	phosphoserine aminotransferase 1	3,89	3,08E-04
ENSDARG00000063670	gtf2a1l	general transcription factor IIA, 1-like	3,84	2,30E-05
ENSDARG00000075421	pttg1	PTTG1 regulator of sister chromatid separation, securin	3,77	7,36E-05

Ensembl ID	Gene	Description	Fold	p-value
ENSDARG00000037961	rcn3	reticulocalbin 3, EF-hand calcium binding domain	3,74	2,13E-05
ENSDARG00000104175			3,56	1,13E-04
ENSDARG00000003854	acsl1b	acyl-CoA synthetase long chain family member 1b	3,52	8,10E-05
ENSDARG00000098004	ftr91	finTRIM family, member 91	3,50	1,60E-04
ENSDARG00000004111	esr1	estrogen receptor 1	3,48	1,86E-10
ENSDARG00000041623	mt2	metallothionein 2	3,47	1,71E-19
ENSDARG00000044074	loxl2b	lysyl oxidase-like 2b	3,39	3,80E-07
ENSDARG00000100397	pde6c	phosphodiesterase 6C, cGMP-specific, cone, alpha prime	3,25	1,47E-06
ENSDARG00000026871	uchl1	ubiquitin carboxyl-terminal esterase L1 (ubiquitin thiolesterase)	3,24	8,97E-08
ENSDARG00000006003	mycla	MYCL proto-oncogene, bHLH transcription factor a	3,18	1,07E-04
ENSDARG00000044362	unc119b	unc-119 homolog b (C. elegans)	3,16	6,07E-04
ENSDARG00000059993	trpm4a	transient receptor potential cation channel, subfamily M, member 4a	3,11	4,64E-04
ENSDARG00000069966	alox5b.3	arachidonate 5-lipoxygenase b, tandem duplicate 3	3,09	2,69E-04
ENSDARG00000007129	slc6a16a	solute carrier family 6 member 16a	3,08	2,77E-04
ENSDARG00000060496	cacna1ha	calcium channel, voltage-dependent, T type, alpha 1H subunit a	3,08	6,02E-06
ENSDARG00000078541	cers3a	ceramide synthase 3a	3,07	1,49E-06
ENSDARG00000005355	larp6a	La ribonucleoprotein 6, translational regulator a	2,96	2,77E-04
ENSDARG00000023950	znhit3	zinc finger, HIT-type containing 3	2,91	7,80E-05
ENSDARG00000100227		solute carrier family 7 member 1b	2,87	6,63E-07
ENSDARG00000035859	angptl4	angiopoietin-like 4	2,85	2,97E-04
ENSDARG00000069044	agpat4	1-acylglycerol-3-phosphate O-acyltransferase 4 (lysophosphatidic acid acyltransferase, delta)	2,84	1,53E-13
ENSDARG00000101557	scarb1	scavenger receptor class B, member 1	2,83	2,22E-04
ENSDARG00000023768	mfsd4aa	major facilitator superfamily domain containing 4Aa	2,83	6,95E-04
ENSDARG00000069441	lpar6b	lysophosphatidic acid receptor 6b	2,77	1,25E-04
ENSDARG00000037000	fkbp11	FKBP prolyl isomerase 11	2,73	2,81E-05

Ensembl ID	Gene	Description	Fold	p-value
ENSDARG00000007099	cx43.4	connexin 43.4	2,65	2,65E-04
ENSDARG00000032010	slc15a2	solute carrier family 15 member 2	2,65	2,05E-04
ENSDARG00000006497	rtn1a	reticulon 1a	2,61	9,92E-05
ENSDARG00000060325	fam20cl	family with sequence similarity 20 member C, like	2,60	4,94E-04
ENSDARG00000114552	siva1	SIVA1, apoptosis-inducing factor	2,57	3,80E-04
ENSDARG00000010437	tent5c	terminal nucleotidyltransferase 5C	2,55	5,77E-06
ENSDARG00000018145	mid1ip1l	MID1 interacting protein 1, like	2,53	2,41E-04
ENSDARG00000004311	ldlrap1a	low density lipoprotein receptor adaptor protein 1a	2,51	6,85E-04
ENSDARG00000006427	fabp2	fatty acid binding protein 2, intestinal	2,49	1,72E-05
ENSDARG00000075368	mrm2	mitochondrial rRNA methyltransferase 2	2,49	6,06E-04
ENSDARG00000063218	ppm1la	protein phosphatase, Mg2+/Mn2+ dependent, 1La	2,45	2,07E-04
ENSDARG00000028295	mkrn4	makorin, ring finger protein, 4	2,44	5,41E-04
ENSDARG00000008491	si:ch211-107o10.3	si:ch211-107o10.3	2,40	1,44E-04
ENSDARG00000069278	trmt5	tRNA methyltransferase 5	2,31	1,43E-04
ENSDARG00000016448	vtg3	vitellogenin 3, phosvitinless	2,27	6,82E-05
ENSDARG00000015765	iah1	isoamyl acetate hydrolyzing esterase 1 (putative)	2,22	3,61E-04
ENSDARG00000012199	gpt2	glutamic pyruvate transaminase (alanine aminotransferase) 2	2,21	5,25E-04
ENSDARG00000014599	slc5a6b	solute carrier family 5 member 6	2,21	2,60E-05
ENSDARG00000035909	mfsd2ab	major facilitator superfamily domain containing 2ab	2,14	1,12E-07
ENSDARG00000033771	hspbap1	hspb associated protein 1	2,06	1,40E-04
ENSDARG00000016825	vtg6	vitellogenin 6	2,05	1,18E-06
ENSDARG00000079216	dpep2	dipeptidase 2	2,03	7,03E-04
ENSDARG00000020000	sh3bp4a	SH3-domain binding protein 4a	1,95	5,93E-05
ENSDARG00000054916	eif4ebp3	eukaryotic translation initiation factor 4E binding protein 3	1,94	1,20E-04
ENSDARG00000037393	slc43a1a	solute carrier family 43 member 1a	1,94	6,13E-04
ENSDARG00000045129	fkbp10b	FKBP prolyl isomerase 10b	1,93	1,42E-04
ENSDARG00000101089	gart	phosphoribosylglycinamide formyltransferase	1,90	2,36E-04
ENSDARG00000011371	zgc:64106	zgc:64106	1,88	1,63E-05

Gene ID (Ensembl)	Gene symbol	Gene Name	Average log2 Fold Change	Adj. P-value
ENSDARG00000104906	mtr	5-methyltetrahydrofolate-homocysteine methyltransferase	1,83	1,33E-04
ENSDARG00000021149	cbr1l	carbonyl reductase 1-like	1,81	1,00E-05
ENSDARG00000041372	zgc:136564	zgc:136564	1,81	6,02E-05
ENSDARG00000090690	nell2a	neural EGFL like 2	1,79	4,01E-04
ENSDARG00000074698	sdsl	serine dehydratase-like	1,78	2,17E-04
ENSDARG00000045568	bcat1	branched chain amino-acid transaminase 1, cytosolic	1,78	3,82E-05
ENSDARG00000092126	vtg5	vitellogenin 5	1,69	1,14E-04
ENSDARG00000092419	vtg7	vitellogenin 7	1,67	1,16E-04
ENSDARG00000098639	pycr1b	pyrroline-5-carboxylate reductase 1b	1,57	6,25E-04
ENSDARG00000078429	vtg4	vitellogenin 4	1,55	2,82E-04
ENSDARG00000031325	tmed1a	transmembrane p24 trafficking protein 1a	1,53	4,66E-04
ENSDARG00000033539	paics	phosphoribosylaminoimidazole carboxylase, phosphoribosylaminoimidazole succinocarboxamide synthetase	1,49	6,96E-04
ENSDARG00000045776	cnbpa	CCHC-type zinc finger, nucleic acid binding protein a	1,07	2,19E-04

Down-regulated transcripts

Gene ID (Ensembl)	Gene symbol	Gene Name	Average log2 Fold Change	Adj. P-value
ENSDARG00000102317	rpl26	ribosomal protein L26	-6,26	5,85E-05
ENSDARG00000042182	drc1	dynein regulatory complex subunit 1 homolog (Chlamydomonas)	-5,97	2,18E-09
ENSDARG00000102175	hamp	hepcidin antimicrobial peptide	-5,83	8,59E-12
ENSDARG00000027940	kcnf1a	potassium voltage-gated channel, subfamily F, member 1a	-5,48	5,93E-04
ENSDARG00000105249	si:dkey-65b13.9	si:dkey-65b13.9	-5,34	4,10E-11
ENSDARG00000100381	rock2bl	rho-associated, coiled-coil containing protein kinase 2b, like	-5,23	2,39E-07
ENSDARG00000042285	atp8b3	ATPase phospholipid transporting 8B3	-5,06	2,02E-04

Ensembl ID	Gene	Description	Value	p-value
ENSDARG00000029688	hsp70.1	heat shock cognate 70-kd protein, tandem duplicate 1	-4,57	7,21E-04
ENSDARG00000078970	il7r	interleukin 7 receptor	-4,47	9,97E-05
ENSDARG00000091042	sacs	sacsin molecular chaperone	-4,46	2,12E-04
ENSDARG00000096433	rock2b	rho-associated, coiled-coil containing protein kinase 2b	-4,14	3,57E-13
ENSDARG00000005704	eps8l3b	EPS8-like 3b	-3,83	1,59E-05
ENSDARG00000055723	hsp70l	heat shock cognate 70-kd protein, like	-3,79	1,92E-05
ENSDARG00000087832	bcl3	BCL3 transcription coactivator	-3,76	1,14E-05
ENSDARG00000043729	plac8.1	placenta associated 8, tandem duplicate 1	-3,75	7,74E-05
ENSDARG00000089075	si:ch73-173p19.1	si:ch73-173p19.1	-3,68	3,43E-05
ENSDARG00000055901	steap4	STEAP family member 4	-3,62	5,79E-08
ENSDARG00000057121	c7b	complement component 7b	-3,53	8,72E-09
ENSDARG00000043581	gadd45aa	growth arrest and DNA-damage-inducible, alpha, a	-3,43	2,38E-05
ENSDARG00000054304	homeza	homeobox and leucine zipper encoding a	-3,40	5,93E-06
ENSDARG00000088130	si:dkey-30c15.10	si:dkey-30c15.10	-3,38	1,99E-08
ENSDARG00000097528	si:dkey-7j14.5	si:dkey-7j14.5	-3,36	1,97E-05
ENSDARG00000053131	irak3	interleukin-1 receptor-associated kinase 3	-3,29	1,03E-06
ENSDARG00000028478	si:ch211-173n18.3	si:ch211-173n18.3	-3,10	1,21E-04
ENSDARG00000099351	igfbp1a	insulin-like growth factor binding protein 1a	-3,06	5,12E-11
ENSDARG00000013926	slc16a9a	solute carrier family 16 member 9a	-3,04	4,76E-04
ENSDARG00000027777	tnfaip3	tumor necrosis factor, alpha-induced protein 3	-3,03	8,10E-10
ENSDARG00000063481	si:ch211-214j24.15	si:ch211-214j24.15	-3,02	3,53E-06
ENSDARG00000044142	acss1	acyl-CoA synthetase short chain family member 1	-2,99	2,18E-06
ENSDARG00000025428	socs3a	suppressor of cytokine signaling 3a	-2,97	4,96E-05
ENSDARG00000091111	si:ch211-15b10.6	si:ch211-15b10.6	-2,97	1,11E-04
ENSDARG00000055252	snap23.2	synaptosome associated protein 23.2	-2,96	9,55E-05
ENSDARG00000044341	chst7	carbohydrate (N-acetylglucosamine 6-O) sulfotransferase 7	-2,92	3,97E-06
ENSDARG00000074501	tnip2	TNFAIP3 interacting protein 2	-2,92	4,83E-05
ENSDARG00000058160	tnfaip2b	tumor necrosis factor, alpha-induced protein 2b	-2,88	1,94E-06

Ensembl ID	Gene	Description	Value	p-value
ENSDARG00000040623	fosl2	fos-like antigen 2	-2,85	3,53E-04
ENSDARG00000071015	pbxip1a	pre-B-cell leukemia homeobox interacting protein 1a	-2,83	5,32E-05
ENSDARG00000031683	fosab	v-fos FBJ murine osteosarcoma viral oncogene homolog Ab	-2,71	1,74E-05
ENSDARG00000087303	cebpd	CCAAT enhancer binding protein delta	-2,71	4,78E-12
ENSDARG00000009040	si:ch73-141c7.1	si:ch73-141c7.1	-2,70	1,28E-06
ENSDARG00000037593	prickle2b	prickle homolog 2b	-2,57	2,55E-05
ENSDARG00000061804	si:ch211-194e15.5	si:ch211-194e15.5	-2,54	2,73E-04
ENSDARG00000006760	slc24a3	solute carrier family 24 member 3	-2,48	3,95E-04
ENSDARG00000075045	cxcl18b	chemokine (C-X-C motif) ligand 18b	-2,45	5,62E-05
ENSDARG00000093052	c6	complement component 6	-2,45	3,10E-06
ENSDARG00000025522	sgk1	serum/glucocorticoid regulated kinase 1	-2,43	4,25E-05
ENSDARG00000001807	tnfrsf21	tumor necrosis factor receptor superfamily, member 21	-2,35	5,40E-04
ENSDARG00000032868	pde4ba	phosphodiesterase 4B, cAMP-specific a	-2,31	3,24E-04
ENSDARG00000007693	nfkbiab	nuclear factor of kappa light polypeptide gene enhancer in B-cells inhibitor, alpha b	-2,27	2,11E-04
ENSDARG00000015161	zgc:92664	zgc:92664	-2,26	3,44E-06
ENSDARG00000071012	ifit14	interferon-induced protein with tetratricopeptide repeats 14	-2,25	3,48E-04
ENSDARG00000032859	lratd2	LRAT domain containing 2	-2,25	6,45E-05
ENSDARG00000068182	crb3b	crumbs homolog 3b	-2,14	1,52E-04
ENSDARG00000004877	rock2b	rho-associated, coiled-coil containing protein kinase 2b	-2,13	2,06E-05
ENSDARG00000005481	nfkbiaa	nuclear factor of kappa light polypeptide gene enhancer in B-cells inhibitor, alpha a	-2,12	6,57E-04
ENSDARG00000057949	slc43a3b	solute carrier family 43 member 3b	-2,12	1,84E-06
ENSDARG00000091418	snx17	sorting nexin 17	-2,07	1,40E-08
ENSDARG00000087814	mfrp	membrane frizzled-related protein	-2,07	4,43E-04
ENSDARG00000038687	nfkb2	nuclear factor of kappa light polypeptide gene enhancer in B-cells 2 (p49/p100)	-2,06	2,76E-05

Ensembl ID	Symbol	Description	Value	p-value
ENSDARG00000069135	ppp1r15a	protein phosphatase 1, regulatory subunit 15A	-2,03	5,96E-04
ENSDARG00000062552	lpar6a	lysophosphatidic acid receptor 6a	-1,98	1,03E-04
ENSDARG00000069484	dab2ipa	DAB2 interacting protein a	-1,95	5,08E-05
ENSDARG00000078676	myrf	myelin regulatory factor	-1,93	3,75E-05
ENSDARG00000043317	kita	KIT proto-oncogene, receptor tyrosine kinase a	-1,89	4,28E-04
ENSDARG00000045886	slc38a2	solute carrier family 38 member 2	-1,87	6,99E-06
ENSDARG00000042329	si:dkey-91m11.5	si:dkey-91m11.5	-1,86	3,71E-05
ENSDARG00000058666	dennd2da	DENN/MADD domain containing 2Da	-1,85	2,57E-04
ENSDARG00000059906	sdc4	syndecan 4	-1,82	3,13E-05
ENSDARG00000100731	zgc:101540	zgc:101540	-1,82	5,75E-04
ENSDARG00000017312	lmbrd2b	LMBR1 domain containing 2b	-1,73	3,48E-05
ENSDARG00000076903	bend3	BEN domain containing 3	-1,66	4,79E-04
ENSDARG00000023933	skila	SKI-like proto-oncogene a	-1,59	4,02E-04
ENSDARG00000056976	ifit16	interferon-induced protein with tetratricopeptide repeats 16	-1,55	1,71E-04
ENSDARG00000102610	r3hdm2	R3H domain containing 2	-1,47	3,69E-04
ENSDARG00000057113	c6	complement component 6	-1,38	2,17E-04
ENSDARG00000100499	cpeb4b	cytoplasmic polyadenylation element binding protein 4b	-1,32	4,98E-04
ENSDARG00000028614	mospd1	motile sperm domain containing 1	-1,28	4,18E-04

PUBLICATION
III

Evaluating targeted therapies in ovarian cancer metabolism: novel role for PCSK9 and second generation of mTOR inhibitors

Dafne Jacome Sanz, Juuli Raivola, Hanna Karvonen, Mariliina Arjama, Harlan Barker, Astrid Murumägi and Daniela Ungureanu

Evaluating Targeted Therapies in Ovarian Cancer Metabolism: Novel Role for PCSK9 and Second Generation mTOR Inhibitors

Dafne Jacome Sanz [1,†], Juuli Raivola [2,†], Hanna Karvonen [3], Mariliina Arjama [4], Harlan Barker [5,6], Astrid Murumägi [4] and Daniela Ungureanu [2,3,*]

1   Laboratory of Immunoregulation, Faculty of Medicine and Health Technology, Tampere University, FI-33014 Tampere, Finland; dafne.jacomesanz@tuni.fi
2   Applied Tumor Genomics, Faculty of Medicine, University of Helsinki, FI-00014 Helsinki, Finland; juuli.raivola@helsinki.fi
3   Cancer Signaling, Faculty of Medicine and Health Technology, Tampere University, FI-33014 Tampere, Finland; hanna.karvonen@tuni.fi
4   Institute for Molecular Medicine, FIMM, University of Helsinki, FI-00014 Helsinki, Finland; mariliina.arjama@helsinki.fi (M.A.); astrid.murumagi@helsinki.fi (A.M.)
5   Clinical Medicine 5, Faculty of Medicine and Health Technology, Tampere University, FI-33014 Tampere, Finland; harlan.barker@tuni.fi
6   Fimlab Ltd., Tampere University Hospital, FI-33520 Tampere, Finland
*   Correspondence: daniela.ungureanu@helsinki.fi
†   These authors contributed equally to this work.

Simple Summary: Ovarian cancer (OC) is known for its poor prognosis, due to the absence of reliable biomarkers and its late diagnosis, since the early-stage disease is almost asymptomatic. Lipid metabolism plays an important role in OC progression due to the development of omental metastasis in the abdominal cavity. The aim of our study was to assess the therapeutic role of various enzymes involved in lipid metabolism regulation or synthesis, in different subtypes of OC represented by cell lines as well as patient-derived cancer cell cultures (PDCs). We show that proprotein convertase subtilisin/kexin type 9 (PCSK9), a cholesterol-regulating enzyme, plays a pro-survival role in OC and targeting its expression impairs cancer cell growth. We also tested a small library of metabolic and mTOR-targeting drugs to identify drug vulnerabilities specific to various subtypes of OC. Our results show that in OC cell lines and PDCs the second generation of mTOR inhibitors such as AZD8055, vistusertib, dactolisib and sapanisertib, have higher cytotoxic activity compared to the first generation mTOR inhibitors such as rapalogs. These results suggest that, in the era of precision medicine, it is possible to target the metabolic pathway in OC and identify subtype-specific drug vulnerabilities that could be advanced to the clinic.

Abstract: Background: Dysregulated lipid metabolism is emerging as a hallmark in several malignancies, including ovarian cancer (OC). Specifically, metastatic OC is highly dependent on lipid-rich omentum. We aimed to investigate the therapeutic value of targeting lipid metabolism in OC. For this purpose, we studied the role of PCSK9, a cholesterol-regulating enzyme, in OC cell survival and its downstream signaling. We also investigated the cytotoxic efficacy of a small library of metabolic (n = 11) and mTOR (n = 10) inhibitors using OC cell lines (n = 8) and ex vivo patient-derived cell cultures (PDCs, n = 5) to identify clinically suitable drug vulnerabilities. Targeting PCSK9 expression with siRNA or PCSK9 specific inhibitor (PF-06446846) impaired OC cell survival. In addition, overexpression of PCSK9 induced robust AKT phosphorylation along with increased expression of ERK1/2 and MEK1/2, suggesting a pro-survival role of PCSK9 in OC cells. Moreover, our drug testing revealed marked differences in cytotoxic responses to drugs targeting metabolic pathways of high-grade serous ovarian cancer (HGSOC) and low-grade serous ovarian cancer (LGSOC) PDCs. Our results show that targeting PCSK9 expression could impair OC cell survival, which warrants further investigation to address the dependency of this cancer on lipogenesis and omental metastasis. Moreover, the differences in metabolic gene expression and drug responses of OC PDCs indicate the

existence of a metabolic heterogeneity within OC subtypes, which should be further explored for therapeutic improvements.

1. Introduction

Ovarian cancer (OC) continues to be the second most common gynecological cancer in the world, due to its late diagnosis and poor prognosis [1]. Molecular profiling has identified several histological subtypes with distinct biological and molecular properties; therefore, tailoring patient treatment is often complicated [2]. High-grade serous ovarian cancer (HGSOC) is the most common epithelial ovarian cancer (EOC) subtype, and is characterized by aberrant TP53, genomic instability, and homologous recombination (HR) defects in the DNA repair pathway in 50% of cases [3]. Other less common subtypes are low-grade serous ovarian cancer (LGSOC), mucinous, clear cell and endometrioid carcinoma, which are mostly driven by specific kinase mutations. KRAS and BRAF mutation are more common in LGSOC, KRAS mutation and HER2 amplification are found in mucinous EOC, and ARID1A mutations are found in clear cell EOC [4]. Platinum-based chemotherapy coupled with debulking surgery is the first-line of OC treatment; however, development of chemoresistance is highly prevalent among OC patients [3].

Altered cellular metabolism is one of the hallmarks of tumorigenesis, directly or indirectly connected to the accumulated genomic aberrations [5]. The metabolic fitness acquired by cancer cells will influence not just tumor evolution and plasticity, but also the tumor microenvironment, metastasis, and treatment outcome [6]. Cancer cells have enhanced metabolic efficiency and flexibility, allowing acquisition of necessary nutrients and the ability to use them effectively to sustain tumor growth, differentiation, and the development of metastasis [7]. This metabolic flexibility could be observed, for instance, during lipid scavenging in metastasis. Scavenging extracellular lipids, rather than increased lipogenesis, has emerged as an important adaptive mechanism bypassing the need to supply carbon to promote cancer cell growth [7]. This mechanism is commonly observed during omental metastasis, in which adipocytes provide fatty acids to tumor cells as a source of nutrients, particularly in OC [8,9].

A common site for metastatic disease arising from intraperitoneal tumors is the omental tissue which favors metastatic tumor growth [10]. Omentum, an organ primarily composed of adipocytes, provides a homing niche for abdominal tumor cell proliferation and metastasis [11]. Omental metastasis typically represents the largest intra-abdominal tumor for patients with advanced OC and 80% of all women with serous ovarian carcinoma present with omental metastases [8]. The adipocyte-rich omentum provides a proliferative advantage and transfers fatty acids to cancer cells as indicated by the high lipid content found in OC cells bordering the adipocytes in omental metastasis. Moreover, advanced OC patients are commonly presented with ascites, a reservoir of a complex mixture of soluble factors and cellular components, which provide a pro-inflammatory and tumor-promoting microenvironment for the tumor cells [12]. The ascites also facilitates omental metastasis, becoming a major source of morbidity and mortality for OC patients [13].

In this study, we investigated the role of PCSK9, the proprotein convertase subtilisin/kexin type-9 regulating cholesterol and lipid metabolism, in OC cell survival and its intracellular signaling, in cell lines ($n = 8$) and PDCs ($n = 5$). Our OC models are comprised of subtype-specific cell lines such as HGSOC and endometrioid, including paired cell-lines pre- and post- acquisition of cisplatin resistance, whereas PDCs were also chosen as representative models of HGSOC and LGSOC. We also analyzed the efficacy of a small library of anti-metabolic ($n = 11$) and first and second generation of mTOR inhibitors ($n = 10$) in order to identify metabolic vulnerabilities that could be therapeutically useful in OC treatment.

2. Materials and Methods

2.1. Cell Culture and Transfections

Human ovarian cancer (OC) cell lines OVCAR3 and OVCAR3cis were cultured in RPMI 1640 (Lonza, Basel, Switzerland) supplemented with 20% fetal bovine serum (Thermo Fisher Scientific, Waltham, MA, USA), 2 mM L-glutamine (Thermo Fisher Scientific) and penicillin/streptomycin (Thermo Fisher Scientific). The cisplatin resistant phenotype, OVCAR3cis, cells were cultured with 1 μM cisplatin (SelleckChem, Houston, TX, USA). The endometrial subtype OC cell lines A2780 and A2780cis, were cultured in RPMI 1640, supplemented with 10% fetal bovine serum, 2 mM L-glutamine and Primocin^{TM}. The cisplatin resistant phenotype, A2780cis, cells were cultured with 1 μM cisplatin (Selleckchem). JHOS2 cells were cultured in DMEM/F-12 (Gibco^{TM}, Thermo Fisher Scientific) supplemented with 10% fetal bovine serum, 1× MEM-NEAA (Thermo Fisher Scientific, Waltham, MA, USA) and Primocin^{TM} (InvivoGen, San Diego, CA, USA). Kuramochi and Ovsaho cell lines were cultured in RPMI 1640 supplemented with 10% fetal bovine serum, 2 mM L-glutamine and Primocin^{TM}. COV362, HEK293T and HeLa cells were cultured in DMEM (Lonza), supplemented with 10% fetal bovine serum, 2mM L-glutamine and Primocin^{TM}. All cell lines were kept and incubated at 37 °C and 5% CO2.

Small interference RNA (siRNA) transfections were performed with Transfection Reagent 1 or 4 (GE Dharmacon, Lafayette, CO, USA) cells and with small interference RNA (siRNA) ON-TARGETplus Non-targeting Control Pool (GE Dharmacon) acting as a control or ON-TARGET plus Human PCSK9 siRNA—SMART pool 10 nM (GE Dharmacon) were used to silence PCSK9 in ovarian cancer. The final concentration of siRNA used in transfection was 6 nM for OVCAR3 cells and 25 nM for HeLa cells

Human PCSK9/NARC1 plasmid (HG15813-CM) was transfected to HEK293T or JHOS2 cells with TurboFect^{TM} Transfection Reagent (Thermo Fisher Scientific) and reduced serum media Opti-MEM I (Gibco^{TM}, Thermo Fisher Scientific). pCINEO expression vector (Promega, Madison, WI, USA) was used as transfection control.

2.2. Cell Viability and Inhibitor Treatment

CellTiter-Glo (CTG) 2.0 (Promega) assay was used to measure cell viability, according to manufacturer's instructions. Cells were plated to 96-well plates and untreated or treated with increasing concentrations of the PCSK9 inhibitor (PCSK9i) PF-06446846 hydrochloride (MedChemExpress, Monmouth Junction, USA) and viability was analyzed after 48 h. The luminescence was measured with Envision plate reader (PerkinElmer, Waltham, MA, USA).

2.3. Western Blot

Cells were lysed with 50 mM Tris-HCl (pH 7.5) containing 1 mM EDTA, 50 mM NaF, 150 mM NaCl, 1% Triton X-100, 10% glycerol plus 1% phosphatase and protease inhibitor cocktails (Bimake, Houston, TX, USA). Proteins were separated using SDS-PAGE and were transferred onto nitrocellulose membrane (Bio-Rad Laboratories, CA, USA). The following primary antibodies were used: anti-PCSK9 antibody (85813, Cell Signaling Technology, Danvers, MA, USA), pERK1/2 (T202/Y204) (Cell Signaling Technology, 9101), ERK1/2 (Cell Signaling Technology, 4696), pAKT (Ser473) (Cell Signaling Technology, 4060), AKT (Cell Signaling Technology, 2920), pMEK Ser217/221 (Cell Signaling Technology, 9121), MEK (Cell Signaling Technology, 4694) and anti β-tubulin (Santa Cruz Biotech sc-166729, Dallas, TX, USA). Specific LI-COR secondary antibodies IRDye® 680RD Donkey anti-Goat IgG, IRDye® 800CW Donkey anti-Mouse IgG, or IRDye® 680RD Donkey anti-Rabbit IgG (LI-COR, Lincoln, NE, USA) were used before detection with Odyssey® CLx Imaging System (LI-COR). Image analysis was performed using Image Studio ™ Lite software (LI-COR).

2.4. Drug Testing

Drug testing was performed for OC cell lines and PDCs with dose-dependent concentration of drugs for 72 h. Briefly, 1000–1500 cells were added to wells of 384-well

plates with drugs pre-plated over a 10,000-fold concentration range (in five concentrations). After a 3-day incubation at 37 °C, cell viability was measured using the Cell Titer-Glo reagent (Promega) and plates were read with PHERAstar FS (BMG Labtech, Ortenberg, Germany). For each drug, dose–response curves were generated and DSS were calculated as previously described [14]. In short, DSS is a measure of drug–response based on the area under the dose–response curve that captures both the potency and the efficacy of the drug effect. It integrates complementary information extracted by half-maximal inhibitory concentration (IC50), slope and minimal and maximum asymptotes. Analysis of hierarchical clustering and similarity matrix of DSSs was performed using Morpheus software [15]. For drug combination, cells were pre-treated with 1 μM cisplatin before being added into drug-loaded 384 plates and cell survival was measured with Cell Titer-Glo after 72 h.

2.5. Gene Expression Analysis

Total RNA was isolated from PDCs using total RNeasy kit (Qiagen, Tübinge, Germany). Quantity and quality of the RNA samples were assessed by Qubit (Thermo Fisher Scientific, USA) and Bioanalyzer (Agilent Technologies, Santa Clara, CA, USA). RNA with an RNA integrity number (RIN) > 8 was used to derive libraries and the sequencing was performed with Illumina HiSeq system (Illumina, San Diego, CA, USA) as previously described [16]. The expression of lipid metabolism and PCSK family genes was derived from RNA-seq analysis. Hierarchical clustering analysis was performed using log2 transformation of transcripts per kilobase million (TPM) values derived from RNA-Seq data from samples of five PDCs. Clustering was performed on genes involved in the lipid-metabolism pathway and PCSK family based on KEGG pathway definitions [17]. Clustering was performed with the cluster module of the SciPy library [18], using a Euclidean distance metric and Ward linkage variance. Visualization of clusters were performed with Matplotlib [19] and Seaborn [20].

3. Results

3.1. Cholesterol Modulating pCSK9 Proprotein Is Expressed in OC Cell Lines and Patient Samples

Proprotein convertases (PCs) are serine proteases capable of specific proteolysis at the RXR/KR motif in a multitude of substrates such as growth factors and growth factor receptors and pro-angiogenic proteins [21]. This family of proteases consists of nine members: PC1/3, PC2, Furin, PC4, PC5/6, PACE4, PC7, SKI-1/S1P, and PCSK9 (NARC-1) [22]. The last member, PCSK9 (NARC-1) is expressed in adult liver, small intestine and ovary [23] and is known to regulate cholesterol metabolism through binding to low-density lipoprotein receptor (LDLR) and subsequent targeting of the receptor for lysosomal degradation [24,25]. Therefore, inhibition of PCSK9 plays an important role in hypercholesterolemia treatment [26]. Gain-of-function mutations in *PCSK9* increases LDLR degradation and, therefore, decreases the circulating LDL uptake and clearance [27]. Since lipid metabolism is highly deregulated in OC and acts as major mediator of omental metastasis, we wanted to assess whether PCSK9 expression could play a role in OC cell survival, both in cell lines and PDCs. For this purpose, we investigated PCSK9 expression in six OC cell lines (Table 1), comprised of HGSOC subtype cell lines (JHOS2, Ovsaho, Kuramochi, COV362, OVCAR3) as well as the endometrioid subtype A2780 cell line.

Table 1. Summary of cell lines and patient-derived cell lines used in these studies. Abbreviations: mut: mutation, amp: amplification, fs: frameshift, del: deletion.

Name	Cell Type	Main Genomic Aberrations
HeLa	Endometrial carcinoma	
JHOS2	High grade ovarian serous adenocarcinoma.	*TP53* mut; BRCA1 mut [28,29]
Kuramochi	High grade ovarian serous adenocarcinoma	*TP53* mut; BRCA2 mut; MYC amp; KRAS amp
COV362	High grade ovarian serous adenocarcinoma	*TP53* mut; BRCA1 mut; MYC amp; RB1 del
Ovsaho	High grade ovarian serous adenocarcinoma	*TP53* mut; RB1 del; BRCA1 del [28,29]
OVCAR3	High grade ovarian serous adenocarcinoma	*TP53* mut [30]
OVCAR3cis	High grade ovarian serous adenocarcinoma, resistant to cisplatin	*TP53* mut [30,31]
A2780	Ovarian endometrioid adenocarcinoma.	PIK3CA mut; PTEN mut; BRAF mut; ARD1A mut
A2780cis	Ovarian endometrioid adenocarcinoma, resistant to cisplatin	[28,29]
PDC #1	Patient-derived cell culture (PDCs) from high grade serous OC tumor	*TP53* mut p.R175H; CCNE1 amp; PAX8 positive
PDC #2	Patient-derived cell culture (PDCs) from high grade serous OC tumor	*TP53* mut p. R283P; CCNE1 amp; PAX8 positive
PDC #3	Patient-derived cell culture (PDCs) from high grade serous OC tumor	*TP53* fs, MYC amp; KRAS amp; PAX8 positive
PDC #4	Patient-derived cell culture (PDCs) from low grade serous OC tumor	*TP53* WT; CDKN2A homozygous loss; PAX8 positive
PDC #5	Patient-derived cell culture (PDCs) from low grade serous OC tumor	*TP53* WT; CDKN2A homozygous loss; PAX8 positive

To date, there are not any known LGSOC representative cell lines. Moreover, for OVCAR3 and A2780 cell lines, we have included both parental and cisplatin-resistant clones, as platinum chemoresistance usually develops in OC patients and has therapeutic significance. Western blot analysis of OC cell line lysates identified variable expression of PCSK9 isoforms (uncleaved and cleaved) in comparison with cervical carcinoma HeLa cell line, which was previously shown to express PCSK9 [32] (Figure 1A,B and Figure S1, Table S1). The highest PCSK9 expression among OC cell lines was identified in OVCAR3 cell lysates, whereas the cisplatin-resistant OVCAR3cis cell lysates showed lower PCSK9 levels. This difference, however, was not observed in the endometrioid subtype of A2780/A2780cis cell line lysates. Since cleaved PCSK9 is known to be secreted, we also analyzed cell supernatants and found enriched expression of cleaved PCSK9 in OVCAR3 and HeLa cell lines (Figure 1C and Figure S1).

Furthermore, we wanted to evaluate PCSK9 expression in OC tumor samples and for this, we used PDCs derived from HGSOC and LGSOC patient tumors. Personalized cancer therapy using ex vivo pharmacogenomic testing of patient-derived cancer cells has already shown great potential and PDCs are currently used as models for tumor molecular profiling as excellent ex vivo representatives of patients' tumor [33]. We assessed PCSK9 expression levels in PDC cell lysates (Figure 1D,E and Figure S1) by Western blotting and observed that three out of five PDCs (PDC#2, PDC#4 and PDC#5) cell lysates were positive for uncleaved PCSK9, whereas LGSOC PDCs (PDC#4 and PDC#5) showed also detectable levels of cleaved PCSK9 (Figure 1D,E). Our results show for the first time that PCSK9 expression is detected in tumor-derived PDCs, indicating that modulation of cholesterol pathway could play a role in OC tumorigenesis. Moreover, we also analyzed the gene expression profile for both lipid-associated and PCSK family of proteins in PDCs. Hierarchical clustering of gene expression showed that the LGSOC PDCs (PDC#4 and PDC#5) clustered together while, likewise, expression values for HGSOC PDCs were more similar to each other (Figure 1F). Notably, we observed that compared to HGSOC, LGSOC PDCs had low expression of apolipoprotein family genes *APOA1, APOA4, APOH, APOC3* as well as *PCSK2, PCSK6* and *PCSK1*, suggesting a subtype specific metabolic gene expression profile of OC PDCs.
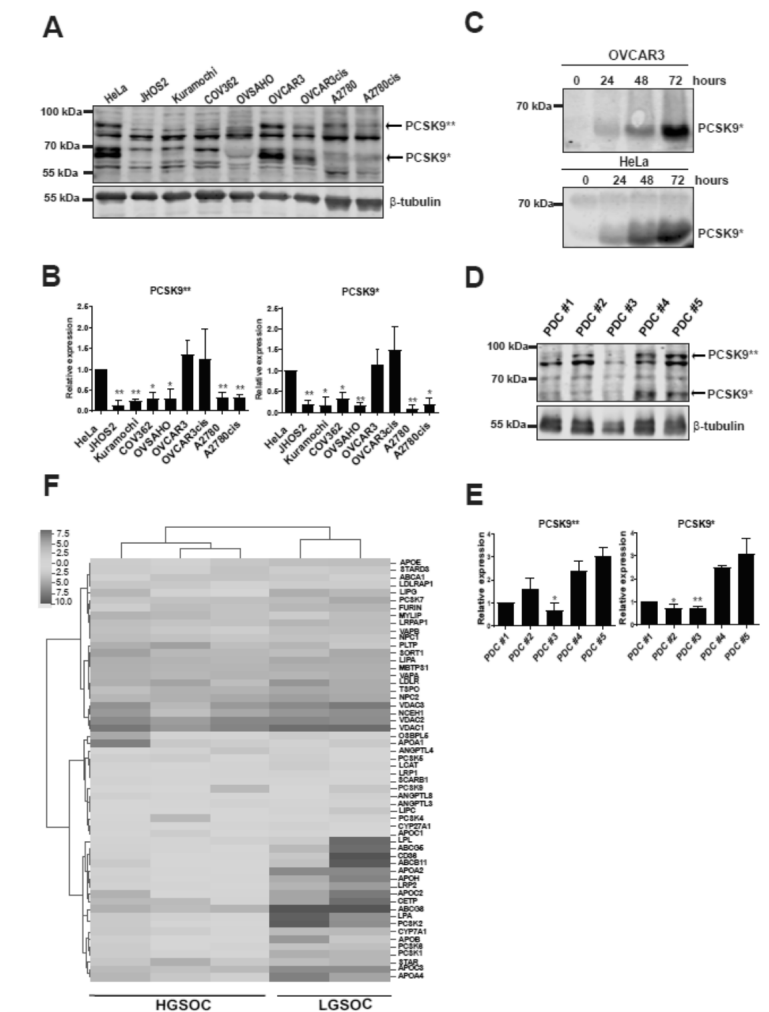
Figure 1. PCSK9 proprotein is expressed in OC. (**A**) PCSK9 protein expression in OC cell lines. Cervical carcinoma HeLa cell line served as positive control. Arrows indicate the molecular weight of cleaved (PCSK9*) and uncleaved (PCSK9**) isoforms. β-tubulin was used as loading control. (**B**) Quantification of PCSK9* and PCSK9** isoform levels from A. Protein levels were normalized to β-tubulin and then compared to PCSK9 isoform levels in HeLa cells (set to 1 for reference point, error bars indicate -/+ SEM of 3 independent experiments. Two-tailed student´s t-test was used to calculate statistical significance, which was indicated as * ($p \leq 0.05$) or ** ($p \leq 0.01$). (**C**) PCSK9* expression in supernatants of OVCAR3 and HeLa cells detected at various time points as indicated. (**D**) Western blot analysis of PCSK9* and PCSK9** isoform expression in lysates of OC PDCs. (**E**) Quantification of PCSK9* and PCSK9** isoform levels from (**D**). An arbitrary value of 1 was given to PCSK9 isoform levels in PDC#1. Error bars indicate −/+ SEM of 3 independent experiments. The statistical analysis was performed as in (**B**). (**F**) Hierarchical clustering of KEGG defined PCSK family and lipid-associated gene expression pathways of the low-grade serous ovarian carcinoma (LGSOC) and high-grade serous ovarian carcinoma (HGSOC) PDCs. Values are presented as log2 transformed transcripts per kilobase million (TPM) from RNA-seq from five PDCs. The uncropped Western Blot images can be found in Figure S1, and signal values are listed in Table S1.

3.2. Targeting PCSK9 Expression Impairs OC Cell Viability

Next, we wanted to assess whether targeting PCSK9 expression has any effect on OVCAR3 and HeLa cell viability. siRNA-mediated knockdown of PCSK9 expression resulted in a statistically significant reduction of cell survival (Figure 2A), and a robust downregulation of PCSK9 levels in cell lysates and the supernatant fraction of OVCAR3 cells (Figure 2B,C and Figure S2, Table S2). Next, we investigated whether targeting PCSK9 with a specific inhibitor would similarly impair cancer cell survival. As shown in Figure 2D, PCSK9 inhibitor PF-06446846 had a clear effect on cell proliferation at $100\mu M$ concentration in HeLa, OVCAR3 and OVCAR3cis cells, whereas JHSO2 cells that do not express PCSK9 showed minimal sensitivity (85% cell survival), indicating that PCSK9 plays a survival role in these cancer cells.

We also investigated whether overexpression of PCSK9 in JHOS2 cells that typically lack its expression will activate pro-survival signaling pathways such as AKT/ERK. Transient transfection of PCSK9 in JHOS2 cells resulted in increased phospho-AKT, phospho-ERK and phospho-MEK levels, as well as an increase in ERK and MEK basal expression (Figure 2E,F and Figure S2B). This could indicate that the pro-survival role of PCSK9 in OC is, at least in part, mediated by activating intracellular AKT/MEK/ERK signaling.

3.3. Anti-Metabolic Drugs Show OC Subtype-Specific Efficacies

Metabolic plasticity allows cancer cells to thrive in environments defined by harsh conditions and targeting cancer cell metabolism could, therefore, be seen as a treatment strategy to improve cancer therapy [34]. Since we observed that targeting cholesterol-modulating PCSK9 enzyme with its specific PF-06446846 inhibitor could impair OC cancer cell survival, we decided to investigate the cytotoxic effect of other compounds involved in lipid-metabolism (Table 2) in OC cell lines and PDCs. Consecutively, we assessed the cytotoxicity of atorvastatin, a statin involved in cholesterol synthesis and previously shown to reduce tumor cell proliferation as neoadjuvant agent; erastin, a ferroptosis activator that causes excessive lipid peroxidation and cell death due to cysteine and glutathione depletion; pevonedistat, an inhibitor of NEDD8-activating enzyme (NAE) with potential antineoplastic activity; AZD3965 an inhibitor of monocarboxylate transporter 1 (MCT1) leading to accumulation of glycolytic intermediates; disulfiram-(CuCl$_2$), an alcohol dehydrogenase inhibitor chelating copper ions selectively accumulated in cancer cells. We also focused on compounds that inhibit DNA or RNA synthesis by blocking the activity of various enzymes required for metabolic reactions, such as daporinad, AVN944, methotrexate, pemetrexed, TH588 and triapine (Table 2). Each compound was tested in 5 dilutions to generate a dose–response curve that was used to calculate a drug sensitivity score (DSS) [14], which is used for quantitative scoring of differential drug responses. A DSS ≥ 7 in at least one cell line was used as a threshold for drug efficacy evaluation.
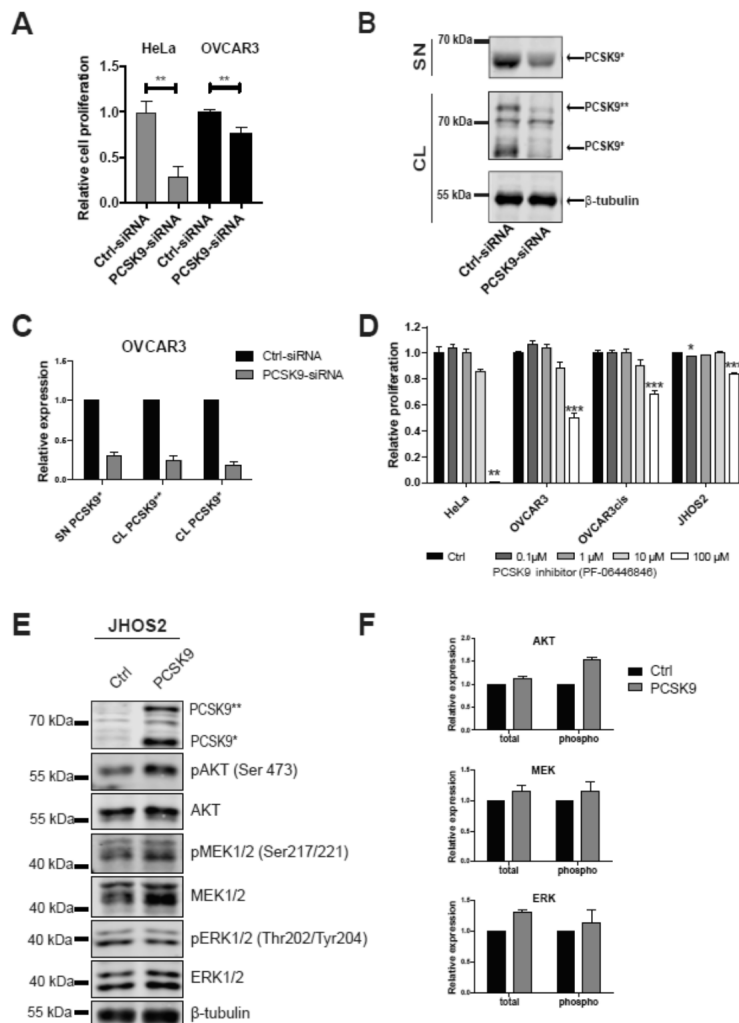
Figure 2. Targeting PCSK9 expression impairs OC cell viability. (**A**) Relative cell proliferation of OVCAR3 and HeLa cells treated with control or PCSK9-siRNA for 48 h. Statistical significance was tested using a two-tailed *t*-test (* indicates *p*-value < 0.05 and *** indicates *p*-value <0.001). (**B**) Western blot analysis of PCSK9 isoform levels following 48 h siRNA treatment from OVCAR3 supernatant (SN) and cell lysate (CL). (**C**) Quantification of PCSK9** and PCSK9* isoform levels from (B). An arbitrary value of 1 was given to PCSK9 isoform levels in control siRNA treated cells. Error bars indicate −/+ SEM of 3 independent experiments. (**D**) Relative cell survival of HeLa, OVCAR3, OVCAR3cis (PCSK9-positive) and JHOS2 cells (PCSK9-negative) treated with increasing amounts of PCSK9 inhibitor PF-06446846 for 48h. Statistical significance was calculated using two-tailed *t*-test (* indicates *p*-value < 0.05; ** indicates *p*-value < 0.01; *** indicates *p*-value < 0.001). (**E**) Western blot analysis of JHOS2 cell lysates non-transfected or transfected with PCSK9 for 48 h. (**F**) Quantification of phosphorylated and total AKT, ERK and MEK protein levels from (**E**). Arbitrary value of 1 was given to the indicated protein levels in control (non-transfected) sample. Error bars indicate -/+ SEM of 3 independent experiments. The uncropped Western Blot images can be found in Figure S2 and signal values are listed in Table S2.

Table 2. Metabolic modifiers and mTOR inhibitors investigated in this study. Selected reference, biochemical class and main clinical trials are also listed. Clinical trial data is from DrugBank database [35].

Drug Name	Mechanism/Targets	Biochemical Class	Clinical Trials (OC)
Daporinad [36]	Targets nicotinamide phosphoribosyltransferase (NAMPT), an intermediate in the biosynthesis of nicotinamide adenine dinucleotide (NAD)	Metabolic modifier	Melanoma (Phase II), B-cell Chronic Lymphocytic Leukemia (Phase I/II), T-cell Lymphoma (Phase II)
Pevonedistat [36]	Inhibitor of Nedd8 activating enzyme (NAE)	Metabolic modifier	Myelodysplastic Syndrome (Phase I), Acute Myeloid Leukemia (Phase I/2), Advanced/Solid Tumors (Phase I), Multiple Myeloma (Phase I), Melanoma (Phase I)
AVN944 [37]	Inhibitor of inosine monophosphate dehydrogenase (IMPDH), an enzyme involved in the de novo synthesis of GTP	Metabolic modifier	Hematological Malignancies (Phase I)
Erastin [38]	Activator of ferroptosis by acting as a voltage-dependent anion channel (VDAC) inhibitor; depletes cellular cysteine and glutathione, inducing excessive lipid peroxidation and cell death	Metabolic modifier	-
Methotrexate [39]	Inhibits dihydrofolate reductase enzyme, resulting in inhibition of purine nucleotide and thymidylate synthesis	Metabolic modifier	Ovarian cancer (Phase II), Acute Lymphoblastic Leukemia (Phase IV), Rheumatoid arthritis (Phase IV); Psoriasis (Phase IV), Breast Cancer (Phase II)
Atorvastatin [40]	Statin, inhibits hepatic hydroxymethyl-glutaryl coenzyme A (HMG-CoA) reductase involved in cholesterol synthesis	Metabolic modifier	Cardiovascular Disease (Phase IV), Cholesterol LDL (Phase IV), Type 2 Diabetes Mellitus (Phase IV), Alzheimer's Disease (Phase III)
Triapine [41]	Inhibitor of ribonucleotide reductase (RNR); DNA synthesis inhibitor	Metabolic modifier	Ovarian Epithelial Cancer (Phase II), Leukemia/ Myelodysplastic Syndromes (Phase I/II) Lung Cancer (Phase II), Prostate Cancer (Phase II), Adenocarcinoma (Phase II)
TH588 [42]	Inhibitor of mut-T homolog-1 (MTH1, also known as NUDT1) that eliminates oxidized dNTP pools to prevent incorporation of damaged bases during DNA replication; impairs mitotic progression and mitotic DNA synthesis	Metabolic modifier	-
AZD3965 [43]	Monocarboxylate transporter 1 (MCT1) inhibitor; impairs lactate efflux leading to accumulation of glycolytic intermediates	Metabolic modifier	-
Disulfiram (+CuCl2) [44]	Alcohol dehydrogenase inhibitor chelating Cu+ selectively accumulated in cancer cells; generates reactive oxygen species (ROS) and inhibits proteasome activity	Metabolic modifier	Alcohol Dependence (Phase IV), Opioid Dependence (Phase II), Melanomas (Phase II), Glioblastoma (Phase II/III), HIV Infections (Phase I/II)
Pemetrexed [45]	Inhibitor of thymidylate synthase (TS) enzyme involved in DNA synthesis	Metabolic modifier	Ovarian cancer (Phase II), Lung cancer (Phase I), Breast cancer (Phase I), Prostate cancer (Phase II).
Ridaforolimus [46]	mTORC1 inhibitor, binds peptidyl-prolyl cis-trans isomerase FKBP12	Rapalog	Ovarian Cancer (Phase I), Metastatic sarcomas (Phase III), Breast cancer (Phase II), Prostate cancer (Phase II), Lymphoma/Myeloma (Phase II), Lung Cancer (Phase II)
Temsirolimus [46]	mTORC1 inhibitor, binds peptidyl-prolyl cis-trans isomerase FKBP12	Rapalog	Ovarian cancer (Phase II), Pancreatic Cancer (Phase II), Acute Myeloid Leukemia (Phase II), Glioblastoma (Phase II), Sarcomas (Phase II), Renal Cancers (Phase I), Breast cancer (Phase I/II)
Everolimus [46]	mTORC1 inhibitor, binds peptidyl-prolyl cis-trans isomerase FKBP12	Rapalog	Ovarian Cancer (Phase II), Breast cancer (Phase IV), Allograft rejection (Phase IV),
Sirolimus [47]	mTORC1 inhibitor, binds peptidyl-prolyl cis-trans isomerase FKBP12	Rapalog	Ovarian cancer (Phase II), Allograft rejection (Phase IV), Leukemia (Phase III), Hepatocellular Carcinoma (Phase III), Breast Cancer (Phase II)

Drug Name	Mechanism/Targets	Biochemical Class	Clinical Trials (*OC*)
AZD8055 [48]	mTOR inhibitor	Kinase inhibitor	Advanced Solid Malignancies (Phase I)
Vistusertib [48]	mTOR inhibitor, ATP-competitive	Kinase inhibitor	Breast Cancer (Phase I), Prostate Cancer (Phase I), Lung Cancer (Phase I)
Dactolisib [49]	mTOR/(PI3K) inhibitor	Kinase inhibitor	Breast Cancer (Phase I), Prostate Cancer (Phase I)
Sapanisertib [50]	mTOR inhibitor	Kinase inhibitor	Breast Cancer (Phase I), Prostate Cancer (Phase I), Lung cancer (Phase I)
CC-115 [51]	mTOR/DNA-dependent protein kinase (DNA-PK) inhibitor	Kinase inhibitor	-
CC-223 [52]	mTOR inhibitor	Kinase inhibitor	Hepatocellular Carcinoma (Phase I/II), B-Cell Lymphoma (Phase I/II), Glioblastoma (Phase I/II), Lung Cancer (Phase I/II)

We observed variable responses among OC cell lines and PDCs to our diverse library of metabolic modifiers (Figure 3A,B and Figure S3A,B). Notably, high DSS values were observed for daporinad, pevonedistat and AVN944 in both cell lines and PDCs, whereas OC cell lines were also more sensitive to methotrexate and pemetrexed. Interestingly, a high sensitivity to erastin was observed in PDC#3 derived from a HGSOC patient as well as in the Kuramochi cell line, and these results we also confirmed by hierarchical clustering of all DSS values for metabolic modifiers (Figure 3C). A similarity matrix and PCA-plot analysis of DSSs from cell lines and PDCs indicated that OVCAR3/OVCAR3cis and A2780/A2780cis clustered together, as well as LGSOC PDC#4 and PDC#5 (Figure 3D,E). On the other hand, HGSOC representative cell lines such as Kuramochi, Ovsaho, and JHOS2, as well as PDC#1, PDC#2 and PDC#3 (also HGSOC) formed their own cluster, suggesting that similar drug responses could be expected in subtype-specific OC models.

3.4. mTOR Inhibitors Elicit Diverse Efficacies in OC Cell Lines and PDCs

The discovery and characterization of the mechanistic target of rapamycin (mTOR) pathway helped us to understand the molecular mechanisms that regulate eukaryotic cell growth, linking nutrient sensing to regulation of protein synthesis, metabolism, aging and disease development [53]. mTOR is a serine/threonine protein kinase that belongs to the PI3K-related kinase (PIKK) family and forms the catalytic subunit of two distinct protein complexes, known as mTOR Complex 1 (mTORC1) and 2 (mTORC2). mTORC1 consists of three core components: mTOR, Raptor (regulatory protein associated with mTOR), and mLST8 (mammalian lethal with Sec13 protein 8, also known as GßL) [54]. In addition, mTORC1 also contains two inhibitory subunits PRAS40 (proline-rich AKT substrate of 40 kDa) and DEPTOR (DEP domain containing mTOR interacting protein). mTORC2 contains mTOR, Rictor (rapamycin insensitive companion of mTOR) instead of Raptor, mLST8, and DEPTOR as well as the regulatory subunits mSin1 and Protor1/2 [54]. mTORC1 is a key regulator of the anabolic–catabolic balance in response to environmental conditions which acts by modulating protein, lipids and nucleotides synthesis to sustain cell growth [55]. On the other hand, mTORC2 controls cell proliferation and survival primarily by phosphorylating AKT, a key effector of insulin/PI3K signaling [56].
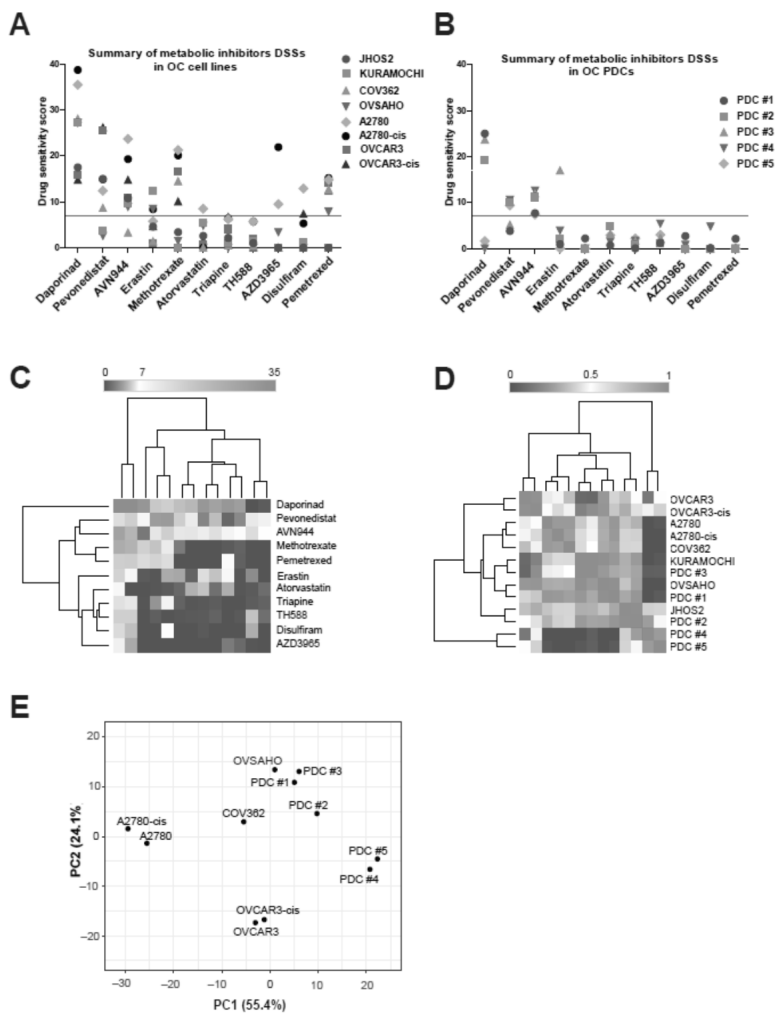
Figure 3. Evaluation of drug responses for anti-metabolic drugs (*n* = 11) in OC cell lines and PDCs. Comparison of DSS values for anti-metabolic drugs in OC cell lines (**A**) and PDCs (**B**). An arbitrary threshold of DSS 7 was chosen, as it indicates a moderate drug cytotoxicity. Analysis of drug responses based on hierarchical clustering (**C**), similarity matrix (**D**) and PCA plot (**E**) of combined DSS values from OC cell lines and PDCs (from patients #1 to #5).

Targeting the mTOR pathway has been extensively explored in cancer therapy and the first mTOR inhibitors approved were a class of rapamycin derivatives known as "rapalogs". Rapamycin, also known as sirolimus and one of the first generation mTOR inhibitors, exerts its effect by binding to FRBP-12 (12 kDa FK506-binding protein) to form a ternary complex with mTOR, leading to inactivation of mTORC1 [57]. Other rapalogs include everolimus, ridaforolimus, and temsirolimus, among others. We investigated the cytotoxic efficacies sirolimus, temsirolimus, everolimus, and ridaforolimus, as well as other tyrosine kinase inhibitors (second generation of rapalogs) targeting mTOR pathway, such as AZD8055, vistusertib, dactolisib, sapanisertib, CC-115 and CC-223 (Table 2) in OC cell lines

and PDCs. Comparison of DSS values for all mTOR inhibitors in OC cell lines and PDCs showed high sensitivity for AZD8055, vistusertib, dactolisib and sapanisertib in all models except the COV362 cell line, which is known for its drug-resistant phenotype (Figure 4A,B and Figure S4A,B). On the other hand, all rapalogs and CC-223 displayed moderate to low cytotoxic activity (Figure 4A,C). We also observed that LGSOC PDCs were in general more sensitive to mTOR inhibitors than HGSOC PDCs. Similarity matrix and principal component analysis (PCA) of cell lines and PDCs DSSs to mTOR inhibitors revealed that A2780/A2780cis and OVCAR3/OVCAR3cis clustered together, whereas LGSOC PDC#4 and PDC#5 clustered differently, indicating variable drug response profile within the same OC subtype (Figure 4D,E). In conclusion, the first generation of mTOR inhibitors, the rapalogs, did not show enhanced cytotoxic activity in OC cell lines and PDCs, whereas the more advanced mTOR inhibitors such as tyrosine kinase inhibitors were more efficient in killing OC cell lines and PDCs.
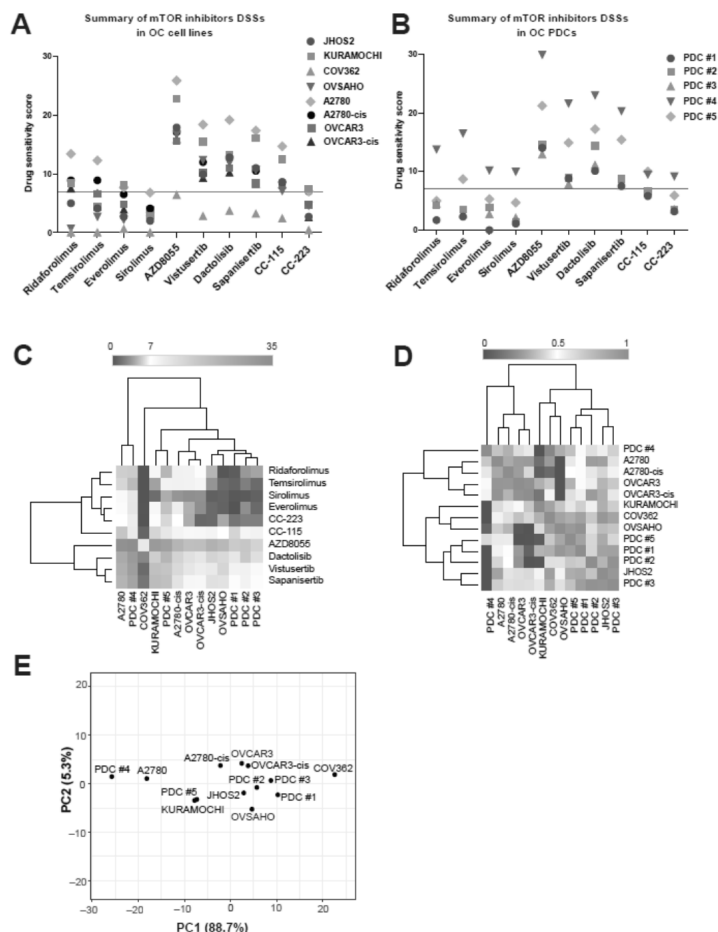
Figure 4. Evaluation of drug responses for mTOR inhibitors (*n* = 10) in OC cell lines and PDCs. Comparison of DSS values for mTOR inhibitors in OC cell lines (**A**) and PDCs (**B**). An arbitrary threshold of DSS 7 was chosen to define a moderate drug cytotoxicity. Analysis of drug responses based on hierarchical clustering (**C**), similarity matrix (**D**) and PCA plot (**E**) of combined DSS values from OC cell lines and PDCs (from patients #1 to #5).

4. Discussion

Many human diseases, including cancer, are the consequence of altered metabolic pathways. Cancer cells have distinctive metabolic phenotypes characterized by altered nutrient metabolism that supports the rapid manufacture of biomass required to sustain rapid cell proliferation [5]. OC is particularly known for its omental metastatic propensity and indeed, almost 80% of OC patients present metastasis in the omentum [8], suggesting a preferential site for metastatic OC tumors in this adipocyte-rich environment. Lipid-rich microenvironments such as omentum could provide cancer cells with a source of fatty acids for rapid tumor growth, and several studies have already provided ample evidence suggesting a strong role for fatty acid metabolism in tumorigenesis [58–60]. Furthermore, the expression and activity of various enzymes involved in the synthesis and catabolic pathways of fatty acids (phospholipids and cholesterol) are significantly dysregulated in cancers [61]. PCSK9, an enzyme involved in the regulation of LDL cholesterol homeostasis by targeting LDLR for degradation, plays an important role in the treatment of hypercholesterolemia [26]. Although dysregulated cholesterol levels are clearly associated with the pathogenesis of coronary artery disease, an association of cholesterol with cancer development has been already reported [62]. An early study indicated that women with high serum cholesterol levels have high risk of OC, suggesting a role for hypercholesterolemia in OC development [63].

In this study, we investigated expression levels and an anti-apoptotic role of PCSK9 in OC models including cell lines and PDCs from various subtypes of OC. We found variable PCSK9 expression in our OC cell lines, with OVCAR3 showing the highest level of PCSK9 (both, uncleaved and cleaved) compared to HeLa cells that are known to express PCSK9 (Figure 1A,B). Detectable levels of secreted PCSK9 were also observed in OVCAR3 and HeLa cell supernatants, suggesting that PCSK9 trafficking is intact in these cells (Figure 1C). Moreover, we also observed various levels of PCSK9 in PDCs, with three out of five PDCs showing detectable levels of uncleaved PCSK9, whereas in LGSOC PDC#4 and PDC#5 cell lysates we could also detect cleaved PCSK9 expression (Figures 1D and 2E). More importantly, targeting PCSK9 expression with siRNA or the PF-0446846 inhibitor impaired cell proliferation (Figure 2A,D), suggesting that PCSK9 has a survival role in OC cells. In addition to its therapeutic role in regulating cholesterol levels, PCSK9 has been previously shown to be involved in cancer. For instance, PCSK9 enhances liver metastasis by maintaining high circulating cholesterol levels [64], whereas in gastric cancers high PCSK9 expression could promote metastasis development by activating the MAPK signaling pathway [65]. In line with this, we also show that overexpressing PCSK9 in OC cells could activate the AKT/MEK/ERK pathway (Figure 2E,F). Our results show for the first time that PCSK9 expression is detected in OC tumor-derived cancer cells or PDCs. Moreover, PCSK9 has a survival role for OC cells, indicating that this proprotein convertase could directly or indirectly modulate tumorigenesis and should be further investigated in cancer therapy.

Our data also uncovered differences in lipid metabolism and PCSK family gene expression between LGSOC and HGSOC PDCs. Notably, lower levels of apolipoprotein family genes *APOA1*, *APOA4*, *APOH*, *APOC3* as well as *PCSK2*, *PCSK6*, *PCSK1* were observed in LGSOC PDCs compared to HGSOC PDCs (Figure 1E). Moreover, we also show detectable levels of cleaved PCSK9 in LGSOC PDCs (Figure 1D). Apolipoproteins are a family of multifunctional glycoproteins that bind and transport lipids in the circulatory system. Apolipoprotein A1 (ApoA1) is the major component of high-density lipoprotein (HDL) particles and is considered as atheroprotective [66] due to its role in fat and cholesterol clearance from blood. ApoA4, also known as Apoa-IV, is a lipid-binding protein and a component of HDL and chylomicrons with an active role in lipid absorption and metabolism, contributing to protection against diabetes and atherosclerosis [67]. Apolipoprotein H (ApoH), also known as β2-glycoprotein I (β2GPI) is a phospholipid-binding plasma protein that is involved in lipid metabolism, angiogenesis and atherogenesis, among others [68], whereas APOC3 or ApoC-III is an important regulator of triglyceride transport and dys-

lipidemia [69]. Taken together, our gene expression analyses show clear differences in lipid metabolism pathways in LGSOC versus HGSOC subtype. Low levels of apolipoproteins expression in LGSOC would indicate a lack of lipid binding and transport, which would result in impaired lipoproteins functions [70]. For instance, low ApoA1 levels have been observed before in LGSOC compared to HGSOC OC patient samples [71], which is in line with our current observation, and low levels of ApoA4 were also detected previously in the plasma levels of OC patients [72]. Our results are in line with recent studies on metabolic heterogeneity within OC subtypes, which identified clear differences of cellular metabolism between low-grade and high-grade disease, as well as between primary tumors and metastatic tissue [73,74].

Consequently, we sought to test a small library of anti-metabolic inhibitors as well as first and second generation mTOR inhibitors in various subtypes of OC models. Among our OC models, we included HGSOC and endometrioid cell lines, since LGSOC cell lines models have not been clearly identified thus far, as well as HGSOC and LGSOC PDCs that are closely related to the original tumor molecular profile. Our DSS analysis of metabolic inhibitors identified three drugs with overall good cytotoxic response in OC cell lines and PDCs: daporinad, pevonedistat and AVN944. Daporinad (APO866) is an inhibitor of nicotinamide phosphoribosyltransferase (NAMPT) specifically inhibiting the biosynthesis of NAD+ from niacinamide, which is essential for the cellular metabolism, protein modification and messenger synthesis [75]. Daporinad has been clinically investigated in advanced melanomas (NCT00432107, ClinicalTrials.gov) as well as chronic lymphocytic leukemia (CLL; NCT00435084, ClinicalTrials.gov) and cutaneous T-Cell Lymphoma (CTCL; NCT00431912). Interestingly, we observed high DSS values for daporinad with HGSOC PDCs but not LGSOC PDCs (Figure 3B), suggesting a subtype-specific response for this inhibitor in OC, and further studies should be conducted using more subtype OC models in order to substantiate our findings. AVN944 is an inhibitor of inosine monophosphate dehydrogenase (IMPDH) [37], an enzyme involved in the de novo synthesis of GTP required for DNA and RNA synthesis, resulting in cellular apoptosis due to lack of GTP [76]. AVN944 appears to have a selective effect on cancer cells that are more dependent on GTP production, whereas deprivation of GTP in normal cells results in a temporary slowing of cell growth only. AVN944 is being investigated for the treatment of patients with advanced hematologic malignancies (NCT00273936, ClinicalTrials.gov), since IMPDH is more expressed in hematological cancers, as well as for its anti-angiogenetic properties [77]. A recent study has documented that IMPDH2 is highly expressed in OC and may serve as a potential prognostic biomarker [78], suggesting that AVN944 could have good efficacy in OC treatment. Indeed, we observed a relatively good cytotoxic effect of AVN944 in all OC PDCs (DSS values $\geq$ 7, Figure 3B) as well as in all OC cell lines except COV362. Furthermore, we also observed enhanced cytotoxic activity of AVN944 in the presence of cisplatin treatment in PDC#2 and PDC#4 (Figure S5B), suggesting an additive cytotoxic activity that should be clinically relevant. Taken together, these findings strongly support the use of AVN944 for the treatment of OC and should be further investigated in a clinical setting. Pevonedistat (MLN4924) is a second-generation inhibitor that targets NAE and subsequently blocks the neddylation-dependent activation of Cullin-RING E3 ligases (CRLs), leading to apoptotic cell death [79]. Pevonedistat is currently explored (alone or in combination) in several clinical trials for the treatment of acute myeloid leukemia (AML; NCT03268954, NCT04712942, NCT04266795, ClinicalTrials.gov) as well as of solid tumors including OC (NCT01862328, ClinicalTrials.gov) and non-small cell lung carcinoma (NSCLC; NCT03228186, ClinicalTrials.gov) and others. Previous studies in OC preclinical models have shown that pevonedistat treatment of mice bearing ovarian tumor xenografts derived from A2780/A2780cis cells significantly increased the efficacy of cisplatin against both cisplatin-sensitive and -resistant xenograft tumors [80]. Phase I clinical studies have shown better efficacy of pevonedistat in combination with standard-of-care chemotherapy agents such as platinum-based and taxane drugs, suggesting that pevonedistat might re-sensitize platinum-resistant patients to cisplatin treatment [81]. We observed a moderate

sensitivity to pevonedistat treatment alone (DSS values ~10) in three out of five PDCs (both HGSOC and LGSOC), indicating a good starting point for combinatorial treatments including paclitaxel or cisplatin. In order to validate this hypothesis, we carried out a drug combination treatment of cisplatin and pevonedistat and noticed enhanced cytotoxic effect of this drug combination in PDC#2 and PDC#4 (Figure S5B) compared to either drug treatments alone. Interestingly, we observed no difference in DSS values for paired cisplatin-resistant cell lines compared to their parental cell line (A2780/A2780cis and OV-CAR3/OVCAR3cis), whereas HGSOC Kuramochi and Ovsaho cell lines were resistant to pevonedistat treatment (Figure 3A). Another interesting observation is the overall lack of cytotoxic effect of atorvastatin, a cholesterol lowering statin, in OC cell lines and PDCs (Figure 3A,B). Statins deplete intracellular cholesterol by reducing mevalonate synthesis, initiating transcriptional activation of sterol regulatory element-binding protein SREBP and, consequently, an increased membrane expression of LDLR, which leads to enhanced LDL cholesterol uptake from the bloodstream [82]. By contrast, PCSK9 controls LDLR turnover at the plasma membrane and inhibition of PCSK9 elicits the same cholesterol-lowering effect. The anti-tumor potential of statins has been highlighted in several studies showing reduced cancer risk, disease stage and recurrence in patients treated with statins [83]. However, not all cancer patients respond to statins treatment, suggesting that targeting the mevalonate pathway should be investigated in each cancer type as the complexity of this pathway regulation is cancer specific [84]. In our study, we observed that targeting PCSK9 expression impaired OC cell survival, suggesting that one way to efficiently kill PCSK9-expressing cancer cells is via its inhibition and this approach should be investigated in clinical trials in a similar way as statins.

Among the mTOR targeted drugs, our screen showed that the first generation of rapalogs had overall low DSS values in both OC cell lines and PDCs, except for PDC#4 which displayed good sensitivity to all rapalogs (Figure 4B). Previous studies have shown a modest therapeutic effect of temsirolimus monotherapy in OC preclinical and clinical studies, indicating that combining rapalogs with other therapies would render better results [85]. Indeed, our drug combination studies of cisplatin and temsirolimus treatment in two PDC models (PDC#2 and PDC#4) showed better cytotoxic effect than either drug treatments alone. The second generation of mTOR inhibitors, which are kinase inhibitors, showed high activity in both OC cell lines and PDCs. All OC cell lines and PDCs achieved high DSS values (DSS ≥ 7) with AZD8055, vistusertib, dactolisib and sapanisertib, except COV362 which is known to have an overall drug-resistant profile. AZD8055 is a new ATP-competitive mTOR kinase inhibitor shown to have cytotoxic activity in OC cell lines alone [86,87] or in combination with trametinib [88]. Vistusertib is a dual mTORC1/2 kinase inhibitor that has been positively evaluated in a phase I clinical trial in combination with paclitaxel for HGSOC patients [89]. Dactolisib (NVP-BEZ235) is a dual mTOR/PI3K kinase inhibitor with previously demonstrated activity on OC preclinical models [49,90]. Sapanisertib (TAK 228), also a dual mTORC1/2 kinase inhibitor, has been evaluated in a phase Ib trial in combination with serabelisib (TAK 117) and paclitaxel in patients with advanced solid tumors, including OC [91], indicating good anti-tumor activity and tolerability. Therefore, investigation of sapanisertib as a single agent and in novel treatment combinations is warranted.

5. Conclusions

Our study is the first to evaluate the expression and anti-apoptotic role of PCSK9 in OC. By investigating the efficacy of various metabolic and mTOR inhibitors ex vivo using tumor representative OC PDCs, our results showed differences in drug cytotoxic responses in LGSOC compared to HGSOC PDCs, which is in line with previous studies showing that OC subtypes display clear metabolic phenotypes [73]. As such, more studies should be directed towards a better understanding of the metabolic profile between various OC subtypes, which could help in tailoring better therapeutic benefits.

Abbreviations

A2780cis	Cis-platin resistant A2780
APO	Apolipoprotein
ARID1A	AT-Rich Interaction Domain 1A
BRAF	v-raf murine sarcoma viral oncogene homolog B1
CRLs	Cullin-RING E3 ligases
DEPTOR	DEP domain containing mTOR interacting protein
DSS	Drug sensitivity score
EOC	Epithelial ovarian cancer
FRBP-12	12 kDa FK506-binding protein
GTP	guanosine triphosphate
HDL	High-density lipoprotein
HeLa	Henrietta Lacks' cervical carcinoma cell line
HepG2	Hepatoma G2
HER2	Human epidermal growth factor receptor 2
HGSOC	High-grade serous ovarian cancer
HR	Homologous recombination
IMPDH	Inosine monophosphate dehydrogenase
IMPDH2	Inosine monophosphate dehydrogenase 2
KRAS	Kirsten Rat Sarcoma Viral Proto-Oncogene
LDLR	Low-density lipoprotein receptor
LGSOC	Low-grade serous ovarian cancer
MAPK	Mitogen-Activated Protein Kinase
MCT1	Monocarboxylate transporter 1
mLST8	Mammalian lethal with Sec13 protein 8

mSin	Regulatory subunit
mTOR	Mammalian target of Rapamycin
mTORC	Mammalian target of Rapamycin Complex
NAE	Nedd8 activating enzyme
NAMPT	Nicotinamide phosphoribosyltransferase
NARC-1	Neural Apoptosis-Regulated Convertase 1
Nedd8	Neural Precursor Cell Expressed, Developmentally Downregulated 8
OC	Ovarian cancer
OVCAR3cis	Cisplatin resistant OVCAR3
PACE4	Paired Basic Amino Acid Cleaving Enzyme 4
PC	Previously known as Proprotein Convertase Subtilisin/Kexin Type 5 or Proprotein Convertase Subtilisin/Kexin
PCA	Principal components analysis
PCs	Proprotein convertases
PCSK	Proprotein Convertase Subtilisin/Kexin
PDCs	Patient-derived cell cultures
PI3K	Phosphoinositide 3-kinase
PIKK	Phosphoinositide 3-kinase-related kinase family
PRAS40	Proline-Rich Akt Substrate
Protor1/2	Regulatory subunit
Rictor	Rapamycin insensitive companion of mTOR
RNA	Ribonucleic acid
ROS	Reactive oxygen species
RT-qPCR	Real time quantitative polymerase chain reaction
siRNA	Small interference RNA
SREBP	sterol regulatory element-binding protein
SKI-1/S1P	Subtilisin kexin isozyme 1
TAK 117	Serabelisib
TAK 228	Sapanisertib
TH588	Selective Human MutT Homolog 1 (NUDT1) inhibitor
TP53	Cellular Tumor Antigen P53

References

1. Narod, S. Can advanced-stage ovarian cancer be cured? *Nat. Rev. Clin. Oncol.* **2016**, *13*, 255–261. [CrossRef]
2. Lheureux, S.; Msc, M.B.; Oza, A.M. Epithelial ovarian cancer: Evolution of management in the era of precision medicine. *CA Cancer J. Clin.* **2019**, *69*, 280–304. [CrossRef]
3. Bowtell, D.D.; Böhm, S.; Ahmed, A.A.; Aspuria, P.-J.; Bast, R.C., Jr.; Beral, V.; Berek, J.S.; Birrer, M.J.; Blagden, S.; Bookman, M.A.; et al. Rethinking ovarian cancer II: Reducing mortality from high-grade serous ovarian cancer. *Nat. Rev. Cancer* **2015**, *15*, 668–679. [CrossRef]
4. Rojas, V.; Hirshfield, K.M.; Ganesan, S.; Rodriguez-Rodriguez, L. Molecular Characterization of Epithelial Ovarian Cancer: Implications for Diagnosis and Treatment. *Int. J. Mol. Sci.* **2016**, *17*, 2113. [CrossRef]
5. Pavlova, N.N.; Thompson, C.B. The Emerging Hallmarks of Cancer Metabolism. *Cell Metab.* **2016**, *23*, 27–47. [CrossRef]
6. Phan, L.M.; Yeung, S.J.; Lee, M.-H. Cancer metabolic reprogramming: Importance, main features, and potentials for precise targeted anti-cancer therapies. *Cancer Biol. Med.* **2014**, *11*, 1–19. [PubMed]
7. Boroughs, L.K.; DeBerardinis, R.J. Metabolic pathways promoting cancer cell survival and growth. *Nat. Cell Biol.* **2015**, *17*, 351–359. [CrossRef] [PubMed]
8. Nieman, K.M.; Kenny, H.A.; Penicka, C.V.; Ladanyi, A.; Buell-Gutbrod, R.; Zillhardt, M.R.; Romero, I.L.; Carey, M.S.; Mills, G.B.; Hotamisligil, G.S.; et al. Adipocytes promote ovarian cancer metastasis and provide energy for rapid tumor growth. *Nat. Med.* **2011**, *17*, 1498–1503. [CrossRef] [PubMed]
9. Ackerman, D.; Simon, M.C. Hypoxia, lipids, and cancer: Surviving the harsh tumor microenvironment. *Trends Cell Biol.* **2014**, *24*, 472–478. [CrossRef]
10. Liu, J.; Geng, X.; Li, Y. Milky spots: Omental functional units and hotbeds for peritoneal cancer metastasis. *Tumor Biol.* **2016**, *37*, 5715–5726. [CrossRef]
11. Clark, R.; Krishnan, V.; Schoof, M.; Rodriguez, I.; Theriault, B.; Chekmareva, M.; Rinker-Schaeffer, C. Milky Spots Promote Ovarian Cancer Metastatic Colonization of Peritoneal Adipose in Experimental Models. *Am. J. Pathol.* **2013**, *183*, 576–591. [CrossRef]
12. Ahmed, N.; Stenvers, K.L. Getting to Know Ovarian Cancer Ascites: Opportunities for Targeted Therapy-Based Translational Research. *Front. Oncol.* **2013**, *3*, 256. [CrossRef] [PubMed]
13. Adam, R.A.; Adam, Y.G. Malignant ascites: Past, present, and future. *J. Am. Coll. Surg.* **2004**, *198*, 999–1011. [CrossRef] [PubMed]

14. Yadav, B.; Pemovska, T.; Szwajda, A.; Kulesskiy, E.; Kontro, M.; Karjalainen, R.; Majumder, M.M.; Malani, D.; Murumägi, A.; Knowles, J.; et al. Quantitative scoring of differential drug sensitivity for individually optimized anticancer therapies. *Sci. Rep.* **2015**, *4*, 5193. [CrossRef] [PubMed]
15. Morpheus. Available online: https://software.broadinstitute.org/morpheus (accessed on 2 May 2021).
16. Kumar, A.; Kankainen, M.; Parsons, A.; Kallioniemi, O.; Matti, K.; Heckman, C.A. The impact of RNA sequence library construction protocols on transcriptomic profiling of leukemia. *BMC Genom.* **2017**, *18*, 629. [CrossRef]
17. Kanehisa, M.; Goto, S.; Furumichi, M.; Tanabe, M.; Hirakawa, M. KEGG for representation and analysis of molecular networks involving diseases and drugs. *Nucleic Acids Res.* **2010**, *38*, D355–D360. [CrossRef]
18. Oliphant, T.E. Python for Scientific Computing. *Comput. Sci. Eng.* **2007**, *9*, 10–20. [CrossRef]
19. Hunter, J.D. Matplotlib: A 2D Graphics Environment. *Comput. Sci. Eng.* **2007**, *9*, 90–95. [CrossRef]
20. Waskom, M.; Botvinnik, O.; Hobson, P.; Cole, J.B.; Halchenko, Y.; Hoyer, S.; Miles, A.; Augspurger, T.; Yarkoni, T.; Megies, T.; et al. Seaborn: V0.5.0 (November 2014) 2014. *Zenodo* **2014**. [CrossRef]
21. Page, R.E.; Klein-Szanto, A.J.P.; Litwin, S.; Nicolas, E.; Al-Jumaily, R.; Alexander, P.; Godwin, A.K.; Ross, E.A.; Schilder, R.J.; Bassi, D.E. Increased Expression of the Pro-Protein Convertase Furin Predicts Decreased Survival in Ovarian Cancer. *Cell. Oncol.* **2007**, *29*, 289–299. [CrossRef]
22. Seidah, N.G.; Sadr, M.S.; Chrétien, M.; Mbikay, M. The Multifaceted Proprotein Convertases: Their Unique, Redundant, Complementary, and Opposite Functions. *J. Biol. Chem.* **2013**, *288*, 21473–21481. [CrossRef]
23. Kwok, S.C.; Chakraborty, D.; Soares, M.J.; Dai, G. Relative expression of proprotein convertases in rat ovaries during pregnancy. *J. Ovarian Res.* **2013**, *6*, 91. [CrossRef]
24. Fan, D.; Yancey, P.G.; Qiu, S.; Ding, L.; Weeber, E.J.; Linton, M.F.; Fazio, S. Self-Association of Human PCSK9 Correlates with Its LDLR-Degrading Activity. *Biochemistry* **2008**, *47*, 1631–1639. [CrossRef]
25. Nassoury, N.; Blasiole, D.A.; Oler, A.T.; Benjannet, S.; Hamelin, J.; Poupon, V.; McPherson, P.S.; Attie, A.D.; Prat, A.; Seidah, N.G. The Cellular Trafficking of the Secretory Proprotein Convertase PCSK9 and Its Dependence on the LDLR. *Traffic* **2007**, *8*, 718–732. [CrossRef] [PubMed]
26. Sabatine, M.S.; Giugliano, R.; Wiviott, S.D.; Raal, F.J.; Blom, D.; Robinson, J.; Ballantyne, C.M.; Somaratne, R.; Legg, J.; Wasserman, S.M.; et al. Efficacy and Safety of Evolocumab in Reducing Lipids and Cardiovascular Events. *N. Engl. J. Med.* **2015**, *372*, 1500–1509. [CrossRef]
27. Fasano, T.; Sun, X.-M.; Patel, D.D.; Soutar, A.K. Degradation of LDLR protein mediated by 'gain of function' PCSK9 mutants in normal and ARH cells. *Atherosclerosis* **2009**, *203*, 166–171. [CrossRef]
28. Domcke, S.; Sinha, R.; Levine, D.A.; Sander, C.; Schultz, N. Evaluating cell lines as tumour models by comparison of genomic profiles. *Nat. Commun.* **2013**, *4*, 2126. [CrossRef]
29. Hernandez, L.; Kim, M.K.; Lyle, L.T.; Bunch, K.P.; House, C.D.; Ning, F.; Noonan, A.; Annunziata, C.M. Characterization of ovarian cancer cell lines as in vivo models for preclinical studies. *Gynecol. Oncol.* **2016**, *142*, 332–340. [CrossRef]
30. Bradbury, A.; O'Donnell, R.; Drew, Y.; Curtin, N.J.; Saha, S.S. Characterisation of Ovarian Cancer Cell Line NIH-OVCAR3 and Implications of Genomic, Transcriptomic, Proteomic and Functional DNA Damage Response Biomarkers for Therapeutic Targeting. *Cancers* **2020**, *12*, 1939. [CrossRef] [PubMed]
31. Karvonen, H.; Arjama, M.; Kaleva, L.; Niininen, W.; Barker, H.; Koivisto-Korander, R.; Tapper, J.; Pakarinen, P.; Lassus, H.; Loukovaara, M.; et al. Glucocorticoids induce differentiation and chemoresistance in ovarian cancer by promoting ROR1-mediated stemness. *Cell Death Dis.* **2020**, *11*, 790. [CrossRef] [PubMed]
32. Wang, Y.; Huang, Y.; Hobbs, H.H.; Cohen, J.C. Molecular characterization of proprotein convertase subtilisin/kexin type 9-mediated degradation of the LDLR. *J. Lipid Res.* **2012**, *53*, 1932–1943. [CrossRef] [PubMed]
33. Kodack, D.P.; Farago, A.F.; Dastur, A.; Held, M.A.; Dardaei, L.; Friboulet, L.; von Flotow, F.; Damon, L.J.; Lee, D.; Parks, M.; et al. Primary Patient-Derived Cancer Cells and Their Potential for Personalized Cancer Patient Care. *Cell Rep.* **2017**, *21*, 3298–3309. [CrossRef] [PubMed]
34. Germain, N.; Dhayer, M.; Boileau, M.; Fovez, Q.; Kluza, J.; Marchetti, P. Lipid Metabolism and Resistance to Anticancer Treatment. *Biol.* **2020**, *9*, 474. [CrossRef] [PubMed]
35. Wishart, D.S.; Knox, C.; Guo, A.C.; Shrivastava, S.; Hassanali, M.; Stothard, P.; Chang, Z.; Woolsey, J. DrugBank: A Comprehensive Resource for in Silico Drug Discovery and Exploration. *Nucleic Acids Res.* **2006**, *34*, D668–D672. [CrossRef]
36. Soucy, T.A.; Smith, P.G.; Milhollen, M.A.; Berger, A.J.; Gavin, J.M.; Adhikari, S.; Brownell, J.E.; Burke, K.E.; Cardin, D.P.; Critchley, S.; et al. An inhibitor of NEDD8-activating enzyme as a new approach to treat cancer. *Nat. Cell Biol.* **2009**, *458*, 732–736. [CrossRef]
37. Naffouje, R.; Grover, P.; Yu, H.; Sendilnathan, A.; Wolfe, K.; Majd, N.; Smith, E.P.; Takeuchi, K.; Senda, T.; Kofuji, S.; et al. Anti-Tumor Potential of IMP Dehydrogenase Inhibitors: A Century-Long Story. *Cancers* **2019**, *11*, 1346. [CrossRef]
38. Li, L.; Qiu, C.; Hou, M.; Wang, X.; Huang, C.; Zou, J.; Liu, T.; Qu, J. Ferroptosis in Ovarian Cancer: A Novel Therapeutic Strategy. *Front. Oncol.* **2021**, *11*, 1364. [CrossRef]
39. Li, P.; Zheng, Y.; Chen, X. Drugs for Autoimmune Inflammatory Diseases: From Small Molecule Compounds to Anti-TNF Biologics. *Front. Pharmacol.* **2017**, *8*, 460. [CrossRef]
40. Malhotra, H.S.; Goa, K.L. Atorvastatin. *Drugs* **2001**, *61*, 1835–1881. [CrossRef]

41. Finch, R.A.; Liu, M.-C.; Grill, S.P.; Rose, W.C.; Loomis, R.; Vasquez, K.M.; Cheng, Y.-C.; Sartorelli, A.C. Triapine (3-aminopyridine-2-carboxaldehyde-thiosemicarbazone): A potent inhibitor of ribonucleotide reductase activity with broad spectrum antitumor activity. *Biochem. Pharmacol.* **2000**, *59*, 983–991. [CrossRef]

42. Gad, H.; Koolmeister, T.; Jemth, A.-S.; Eshtad, S.; Jacques, S.A.; Ström, C.E.; Svensson, L.M.; Schultz, N.; Lundbäck, T.; Einarsdottir, B.; et al. MTH1 inhibition eradicates cancer by preventing sanitation of the dNTP pool. *Nat. Cell Biol.* **2014**, *508*, 215–221. [CrossRef]

43. Wang, N.; Jiang, X.; Zhang, S.; Zhu, A.; Yuan, Y.; Xu, H.; Lei, J.; Yan, C. Structural basis of human monocarboxylate transporter 1 inhibition by anti-cancer drug candidates. *Cell* **2021**, *184*, 370–383.e13. [CrossRef] [PubMed]

44. Papaioannou, M.; Mylonas, I.; Kast, R.E.; Bruning, A. Disulfiram/copper causes redox-related proteotoxicity and concomitant heat shock response in ovarian cancer cells that is augmented by auranofin-mediated thioredoxin inhibition. *Oncoscience* **2013**, *1*, 21–29. [CrossRef]

45. Egloff, H.; Jatoi, A. Pemetrexed for Ovarian Cancer: A Systematic Review of the Published Literature and a Consecutive Series of Patients Treated in a Nonclinical Trial Setting. *Case Rep. Oncol.* **2014**, *7*, 541–549. [CrossRef]

46. Porta, C.; Paglino, C.; Mosca, A. Targeting PI3K/Akt/mTOR Signaling in Cancer. *Front. Oncol.* **2014**, *4*, 64. [CrossRef]

47. Sehgal, S. Sirolimus: Its discovery, biological properties, and mechanism of action. *Transplant. Proc.* **2003**, *35*, S7–S14. [CrossRef]

48. Pike, K.G.; Malagu, K.; Hummersone, M.G.; Menear, K.A.; Duggan, H.M.; Gomez, S.; Martin, N.M.; Ruston, L.; Pass, S.L.; Pass, M. Optimization of potent and selective dual mTORC1 and mTORC2 inhibitors: The discovery of AZD8055 and AZD2014. *Bioorganic Med. Chem. Lett.* **2013**, *23*, 1212–1216. [CrossRef] [PubMed]

49. Oishi, T.; Itamochi, H.; Kudoh, A.; Nonaka, M.; Kato, M.; Nishimura, M.; Oumi, N.; Sato, S.; Naniwa, J.; Sato, S.; et al. The PI3K/mTOR dual inhibitor NVP-BEZ235 reduces the growth of ovarian clear cell carcinoma. *Oncol. Rep.* **2014**, *32*, 553–558. [CrossRef]

50. Williams, C.B.; Williams, K.A.; Krie, A.K.; De, P.; Dey, N.; Leyland-Jones, B.; Starks, D.; Rojas-Espaillat, L.A. Results of a phase Ib trial evaluating the safety and clinical activity of sapanisertib (TAK 228) in combination with serabelisib (TAK 117) and paclitaxel in patients with advanced ovarian, endometrial, or breast cancer. *J. Clin. Oncol.* **2020**, *38*, 3604. [CrossRef]

51. Mortensen, D.S.; Perrin-Ninkovic, S.M.; Shevlin, G.; Elsner, J.; Zhao, J.; Whitefield, B.; Tehrani, L.; Sapienza, J.; Riggs, J.R.; Parnes, J.S.; et al. Optimization of a Series of Triazole Containing Mammalian Target of Rapamycin (mTOR) Kinase Inhibitors and the Discovery of CC-115. *J. Med. Chem.* **2015**, *58*, 5599–5608. [CrossRef]

52. Mortensen, D.S.; Perrin-Ninkovic, S.M.; Shevlin, G.; Zhao, J.; Packard, G.; Bahmanyar, S.; Correa, M.; Elsner, J.; Harris, R.; Lee, B.G.S.; et al. Discovery of Mammalian Target of Rapamycin (mTOR) Kinase Inhibitor CC-223. *J. Med. Chem.* **2015**, *58*, 5323–5333. [CrossRef] [PubMed]

53. Saxton, R.A.; Sabatini, D.M. mTOR Signaling in Growth, Metabolism, and Disease. *Cell* **2017**, *168*, 960–976. [CrossRef]

54. Baretić, D.; Williams, R.L. The structural basis for mTOR function. *Semin. Cell Dev. Biol.* **2014**, *36*, 91–101. [CrossRef]

55. Zhang, Y.; Nicholatos, J.; Dreier, J.R.; Ricoult, S.J.H.; Widenmaier, S.; Hotamisligil, G.S.; Kwiatkowski, D.J.; Manning, B.D. Coordinated regulation of protein synthesis and degradation by mTORC1. *Nat. Cell Biol.* **2014**, *513*, 440–443. [CrossRef] [PubMed]

56. Sarbassov, D.D.; Guertin, D.A.; Ali, S.M.; Sabatini, D.M. Phosphorylation and Regulation of Akt/PKB by the Rictor-mTOR Complex. *Science* **2005**, *307*, 1098–1101. [CrossRef]

57. Abraham, R.T.; Wiederrecht, G.J. Immunopharmacology of rapamycin. *Annu. Rev. Immunol.* **1996**, *14*, 483–510. [CrossRef]

58. Liu, Y. Fatty acid oxidation is a dominant bioenergetic pathway in prostate cancer. *Prostate Cancer Prostatic Dis.* **2006**, *9*, 230–234. [CrossRef]

59. Zaugg, K.; Yao, Y.; Reilly, P.T.; Kannan, K.; Kiarash, R.; Mason, J.; Huang, P.; Sawyer, S.K.; Fuerth, B.; Faubert, B.; et al. Carnitine palmitoyltransferase 1C promotes cell survival and tumor growth under conditions of metabolic stress. *Genes Dev.* **2011**, *25*, 1041–1051. [CrossRef] [PubMed]

60. Hernlund, E.; Ihrlund, L.S.; Khan, O.; Ates, Y.O.; Linder, S.; Panaretakis, T.; Shoshan, M.C. Potentiation of chemotherapeutic drugs by energy metabolism inhibitors 2-deoxyglucose and etomoxir. *Int. J. Cancer* **2008**, *123*, 476–483. [CrossRef]

61. Ji, Z.; Shen, Y.; Feng, X.; Kong, Y.; Shao, Y.; Meng, J.; Zhang, X.; Yang, G. Deregulation of Lipid Metabolism: The Critical Factors in Ovarian Cancer. *Front. Oncol.* **2020**, *10*, 593017. [CrossRef]

62. Ding, X.; Zhang, W.; Li, S.; Yang, H. The role of cholesterol metabolism in cancer. *Am. J. Cancer Res.* **2019**, *9*, 219–227. [PubMed]

63. Helzlsouer, K.J.; Alberg, A.J.; Norkus, E.P.; Morris, J.S.; Hoffman, S.C.; Comstock, G.W. Prospective Study of Serum Micronutrients and Ovarian Cancer. *J. Natl. Cancer Inst.* **1996**, *88*, 32–37. [CrossRef]

64. Sun, X.; Essalmani, R.; Day, R.; Khatib, A.M.; Seidah, N.; Prat, A. Proprotein Convertase Subtilisin/Kexin Type 9 Deficiency Reduces Melanoma Metastasis in Liver. *Neoplasia* **2012**, *14*, 1122–1131. [CrossRef] [PubMed]

65. Xu, B.; Li, S.; Fang, Y.; Zou, Y.; Song, D.; Zhang, S.; Cai, Y. Proprotein Convertase Subtilisin/Kexin Type 9 Promotes Gastric Cancer Metastasis and Suppresses Apoptosis by Facilitating MAPK Signaling Pathway Through HSP70 Up-Regulation. *Front. Oncol.* **2021**, *10*, 609663. [CrossRef] [PubMed]

66. Chistiakov, D.A.; Orekhov, A.N.; Bobryshev, Y.V. ApoA1 and ApoA1-specific self-antibodies in cardiovascular disease. *Lab. Investig.* **2016**, *96*, 708–718. [CrossRef] [PubMed]

67. Qu, J.; Ko, C.-W.; Tso, P.; Bhargava, A. Apolipoprotein A-IV: A Multifunctional Protein Involved in Protection against Atherosclerosis and Diabetes. *Cells* **2019**, *8*, 319. [CrossRef]

68. Mather, K.A.; Thalamuthu, A.; Oldmeadow, C.; Song, F.; Armstrong, N.J.; Poljak, A.; Holliday, E.G.; McEvoy, M.; Kwok, J.B.; Assareh, A.A.; et al. Genome-wide significant results identified for plasma apolipoprotein H levels in middle-aged and older adults. *Sci. Rep.* **2016**, *6*, 23675. [CrossRef]

69. Wolska, A.; Reimund, M.; Remaley, A.T. Apolipoprotein C-II. *Curr. Opin. Lipidol.* **2020**, *31*, 147–153. [CrossRef] [PubMed]

70. Ren, L.; Yi, J.; Li, W.; Zheng, X.; Liu, J.; Wang, J.; Du, G. Apolipoproteins and cancer. *Cancer Med.* **2019**, *8*, 7032–7043. [CrossRef]

71. Su, F.; Lang, J.; Kumar, A.; Ng, C.; Hsieh, B.; Suchard, M.A.; Reddy, S.T.; Farias-Eisner, R. Validation of Candidate Serum Ovarian Cancer Biomarkers for Early Detection. *Biomark. Insights* **2007**, *2*, 369–375. [CrossRef]

72. Dieplinger, H.; Ankerst, D.; Burges, A.; Lenhard, M.; Lingenhel, A.; Fineder, L.; Buchner, H.; Stieber, P. Afamin and Apolipoprotein A-IV: Novel Protein Markers for Ovarian Cancer. *Cancer Epidemiol. Biomark. Prev.* **2009**, *18*, 1127–1133. [CrossRef] [PubMed]

73. Garg, G.; Yilmaz, A.; Kumar, P.; Turkoglu, O.; Mutch, D.G.; Powell, M.A.; Rosen, B.; Bahado-Singh, R.O.; Graham, S.F. Targeted metabolomic profiling of low and high grade serous epithelial ovarian cancer tissues: A pilot study. *Metabolomics* **2018**, *14*, 154. [CrossRef]

74. Elia, I.; Doglioni, G.; Fendt, S.-M. Metabolic Hallmarks of Metastasis Formation. *Trends Cell Biol.* **2018**, *28*, 673–684. [CrossRef]

75. Olesen, U.H.; Petersen, J.G.; Garten, A.; Kiess, W.; Yoshino, J.; Imai, S.-I.; Christensen, M.K.; Fristrup, P.; Thougaard, A.V.; Björkling, F.; et al. Target enzyme mutations are the molecular basis for resistance towards pharmacological inhibition of nicotinamide phosphoribosyltransferase. *BMC Cancer* **2010**, *10*, 677. [CrossRef]

76. Floryk, D.; Thompson, T.C. Antiproliferative effects of AVN944, a novel inosine 5-monophosphate dehydrogenase inhibitor, in prostate cancer cells. *Int. J. Cancer* **2008**, *123*, 2294–2302. [CrossRef]

77. Weaver, Z.; Strovel, J.; Chakiath, M.; Natarajan, P.; Lawrence, T.; Bol, D. Antiangiogenic properties of the IMPDH inhibitor AVN944. *Cancer Res.* **2007**, *67* (Suppl. 9), 3983. Available online: http://cancerres.aacrjournals.org/content/67/9_Supplement/3983.abstract (accessed on 14 June 2021).

78. Tian, Y.; Zhang, J.; Chen, L.; Zhang, X. The expression and prognostic role of IMPDH2 in ovarian cancer. *Ann. Diagn. Pathol.* **2020**, *46*, 151511. [CrossRef]

79. Xu, B.; Deng, Y.; Bi, R.; Guo, H.; Shu, C.; Shah, N.K.; Chang, J.; Liu, G.; Du, Y.; Wei, W.; et al. A first-in-class inhibitor, MLN4924 (pevonedistat), induces cell-cycle arrest, senescence, and apoptosis in human renal cell carcinoma by suppressing UBE2M-dependent neddylation modification. *Cancer Chemother. Pharmacol.* **2018**, *81*, 1083–1093. [CrossRef]

80. Nawrocki, S.T.; Kelly, K.R.; Smith, P.G.; Espitia, C.M.; Possemato, A.; Beausoleil, S.A.; Milhollen, M.; Blakemore, S.; Thomas, M.; Berger, A.; et al. Disrupting Protein NEDDylation with MLN4924 Is a Novel Strategy to Target Cisplatin Resistance in Ovarian Cancer. *Clin. Cancer Res.* **2013**, *19*, 3577–3590. [CrossRef] [PubMed]

81. Lockhart, A.C.; Bauer, T.M.; Aggarwal, C.; Lee, C.B.; Harvey, R.D.; Cohen, R.B.; Sedarati, F.; Nip, T.K.; Faessel, H.; Dash, A.B.; et al. Phase Ib study of pevonedistat, a NEDD8-activating enzyme inhibitor, in combination with docetaxel, carboplatin and paclitaxel, or gemcitabine, in patients with advanced solid tumors. *Investig. New Drugs* **2019**, *37*, 87–97. [CrossRef] [PubMed]

82. Longo, J.; Van Leeuwen, J.E.; Elbaz, M.; Branchard, E.; Penn, L.Z. Statins as Anticancer Agents in the Era of Precision Medicine. *Clin. Cancer Res.* **2020**, *26*, 5791–5800. [CrossRef] [PubMed]

83. Nielsen, S.F.; Nordestgaard, B.G.; Bojesen, S.E. Statin Use and Reduced Cancer-Related Mortality. *N. Engl. J. Med.* **2012**, *367*, 1792–1802. [CrossRef] [PubMed]

84. Mullen, P.J.; Yu, R.; Longo, J.; Archer, M.C.; Penn, L.Z. The interplay between cell signalling and the mevalonate pathway in cancer. *Nat. Rev. Cancer* **2016**, *16*, 718–731. [CrossRef] [PubMed]

85. Emons, G.; Kurzeder, C.; Schmalfeldt, B.; Neuser, P.; de Gregorio, N.; Pfisterer, J.; Park-Simon, T.-W.; Mahner, S.; Schröder, W.; Lück, H.-J.; et al. Temsirolimus in women with platinum-refractory/resistant ovarian cancer or advanced/recurrent endometrial carcinoma. A phase II study of the AGO-study group (AGO-GYN8). *Gynecol. Oncol.* **2016**, *140*, 450–456. [CrossRef]

86. Hisamatsu, T.; Mabuchi, S.; Matsumoto, Y.; Kawano, M.; Sasano, T.; Takahashi, R.; Sawada, K.; Ito, K.; Kurachi, H.; Schilder, R.J.; et al. Potential Role of mTORC2 as a Therapeutic Target in Clear Cell Carcinoma of the Ovary. *Mol. Cancer Ther.* **2013**, *12*, 1367–1377. [CrossRef]

87. Caumanns, J.J.; Berns, K.; Wisman, G.B.A.; Fehrmann, R.; Tomar, T.; Klip, H.; Meersma, G.J.; Hijmans, E.M.; Gennissen, A.M.; Duiker, E.; et al. Integrative Kinome Profiling Identifies mTORC1/2 Inhibition as Treatment Strategy in Ovarian Clear Cell Carcinoma. *Clin. Cancer Res.* **2018**, *24*, 3928–3940. [CrossRef]

88. Pétigny-Lechartier, C.; Duboc, C.; Jebahi, A.; Louis, M.-H.; Abeilard, E.; Denoyelle, C.; Gauduchon, P.; Poulain, L.; Villedieu, M. The mTORC1/2 Inhibitor AZD8055 Strengthens the Efficiency of the MEK Inhibitor Trametinib to Reduce the Mcl-1/[Bim and Puma] ratio and to Sensitize Ovarian Carcinoma Cells to ABT-737. *Mol. Cancer Ther.* **2016**, *16*, 102–115. [CrossRef]

89. Basu, B.; Krebs, M.; Sundar, R.; Wilson, R.; Spicer, J.; Jones, R.; Brada, M.; Talbot, D.; Steele, N.; Garces, A.I.; et al. Vistusertib (dual m-TORC1/2 inhibitor) in combination with paclitaxel in patients with high-grade serous ovarian and squamous non-small-cell lung cancer. *Ann. Oncol.* **2018**, *29*, 1918–1925. [CrossRef]

90. Kudoh, A.; Oishi, T.; Itamochi, H.; Sato, S.; Naniwa, J.; Sato, S.; Shimada, M.; Kigawa, J.; Harada, T. Dual Inhibition of Phosphatidylinositol 3′-Kinase and Mammalian Target of Rapamycin Using NVP-BEZ235 as a Novel Therapeutic Approach for Mucinous Adenocarcinoma of the Ovary. *Int. J. Gynecol. Cancer* **2014**, *24*, 444–453. [CrossRef]

91. Moore, K.N.; Bauer, T.M.; Falchook, G.S.; Chowdhury, S.; Patel, C.; Neuwirth, R.; Enke, A.; Zohren, F.; Patel, M.R. Phase I study of the investigational oral mTORC1/2 inhibitor sapanisertib (TAK-228): Tolerability and food effects of a milled formulation in patients with advanced solid tumours. *ESMO Open* **2018**, *3*, e000291. [CrossRef]
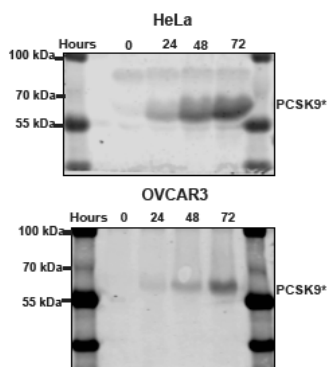
Supplementary Materials: Evaluating Targeted Therapies in Ovarian Cancer Metabolism: Novel Role for PCSK9 and Second Generation mTOR Inhibitors

Dafne Jacome Sanz, Juuli Raivola, Hanna Karvonen, Mariliina Arjama, Harlan Barker, Astrid Murumägi and Daniela Ungureanu
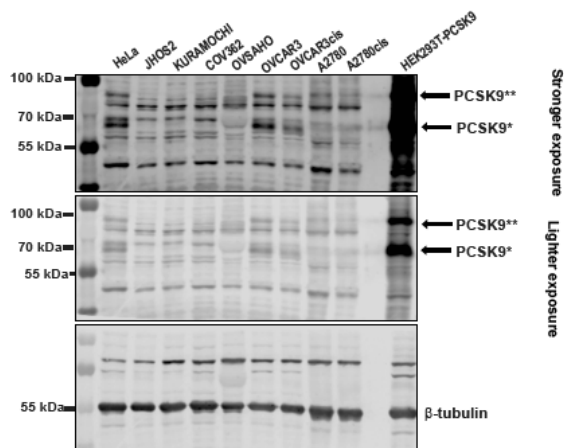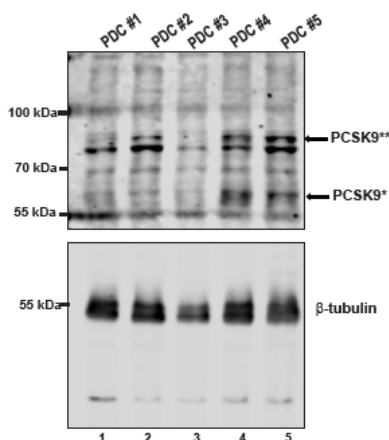

Figure S1. Analysis of PCSK9 isoforms in OC models. (**A**) Upper panel: Uncropped Western blot of Figure 1A showing PCSK9 expression in the OC cell lines. For an accurate analysis, a sample of over-expressed PCSK9 in HEK293T cells is shown as HEK293T-PCSK9. Lower panel: β-tubulin levels as loading control. (**B**) Uncropped Western blots from Figure 1C. (**C**) Uncropped Western blots from Figure 1D.
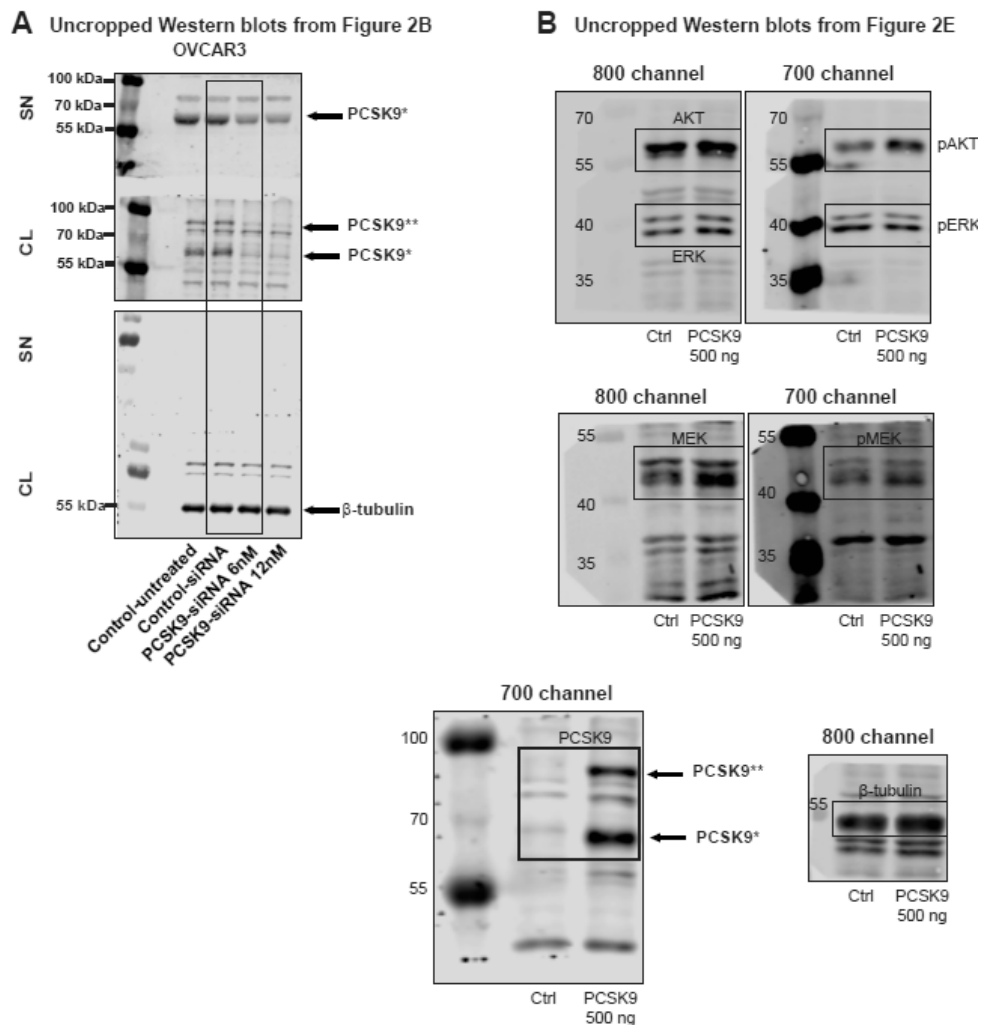
Figure S2. Analysis of PCSK9 targeting in OC cell line. (**A**) Upper panel: Uncropped Western blot of Figure 2B showing PCSK9 expression in OVCAR3 cells treated with Control-siRNA or PCSK9-siRNA for 48h, for supernatant (SN) and cell lysate fractions (CL). Lower panel: β-tubulin levels as loading control. (**B**) Uncropped Western blots for Figure 2E showing the expression of indicated protein from JHOS2 ctrl or PCSK9 (500 ng) transfection. Frames in blots indicate the bands shown in Figure 2E. Ladder molecular weights in kDas.
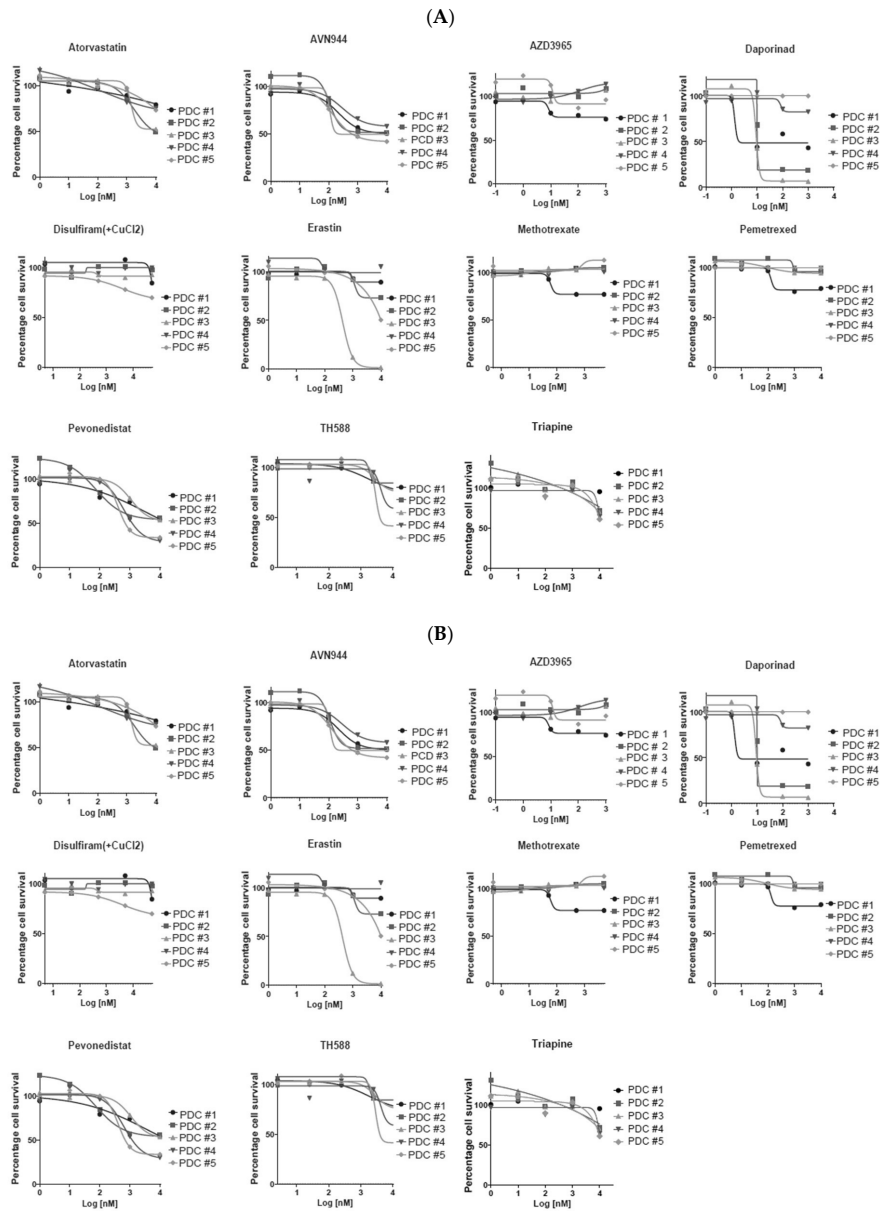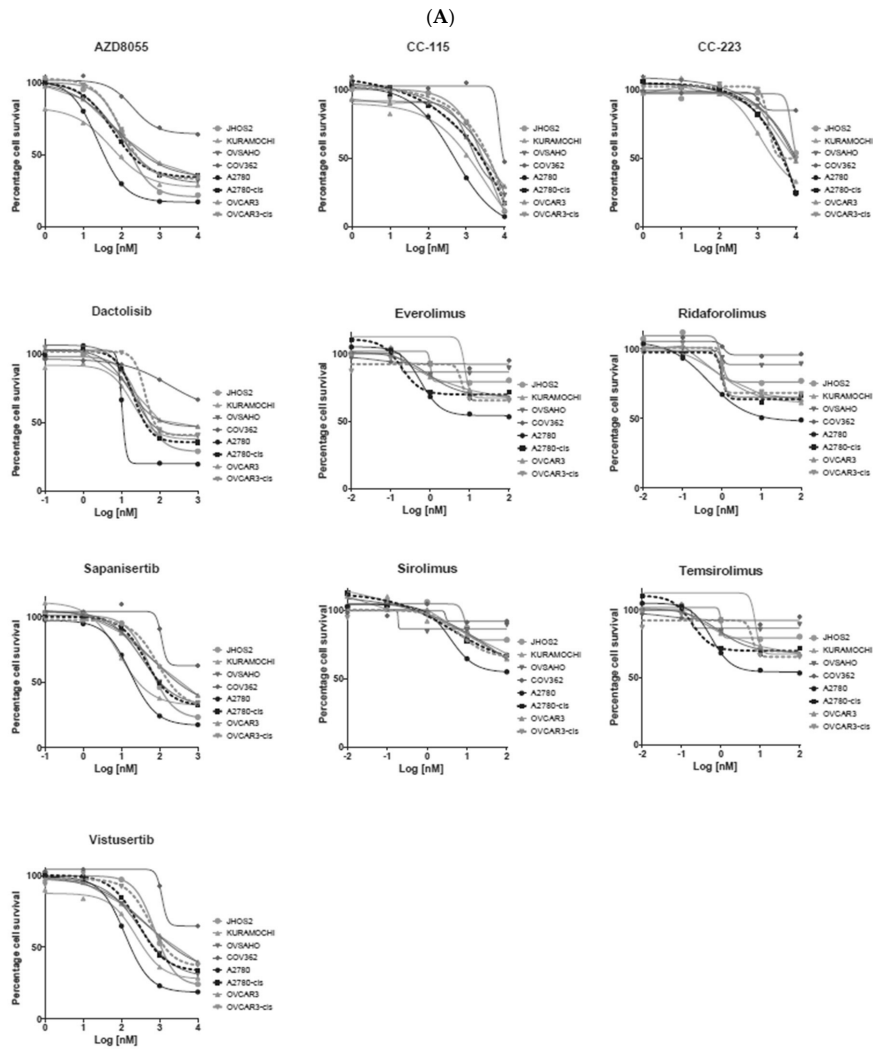
(A)

(B)

Figure S3. Original drug-response curves of anti-metabolic drugs (*n* = 11) in OC cell lines (**A**) and PDCs (**B**). For each drug, five concentrations are represented as log10 values, and cell viability is calculated as percentage inhibition, where the lowest drug concentration is given 100% percentage cell survival.

(A)

(B)

Figure S4. Original drug-response curves of mTOR targeting drugs (*n* = 10) in OC cell lines (**A**) and PDCs (**B**). For each drug, five concentrations are represented as log M values, and cell viability is calculated as percentage inhibition, where the lowest drug concentration is given 100% percentage cell survival.
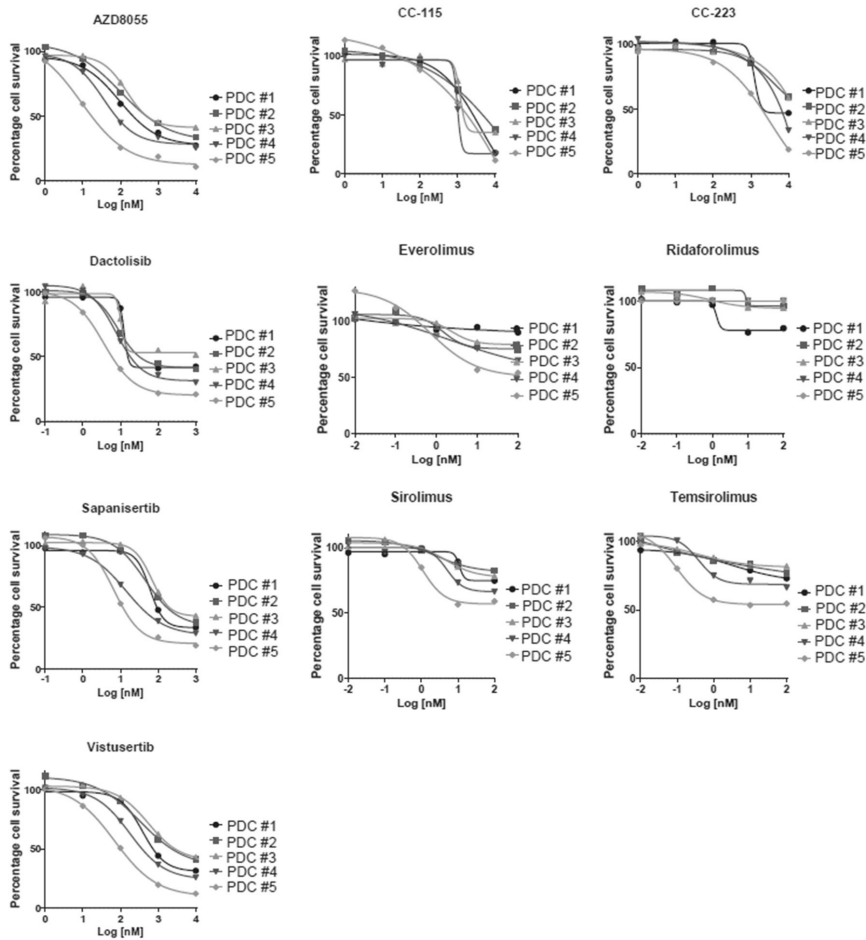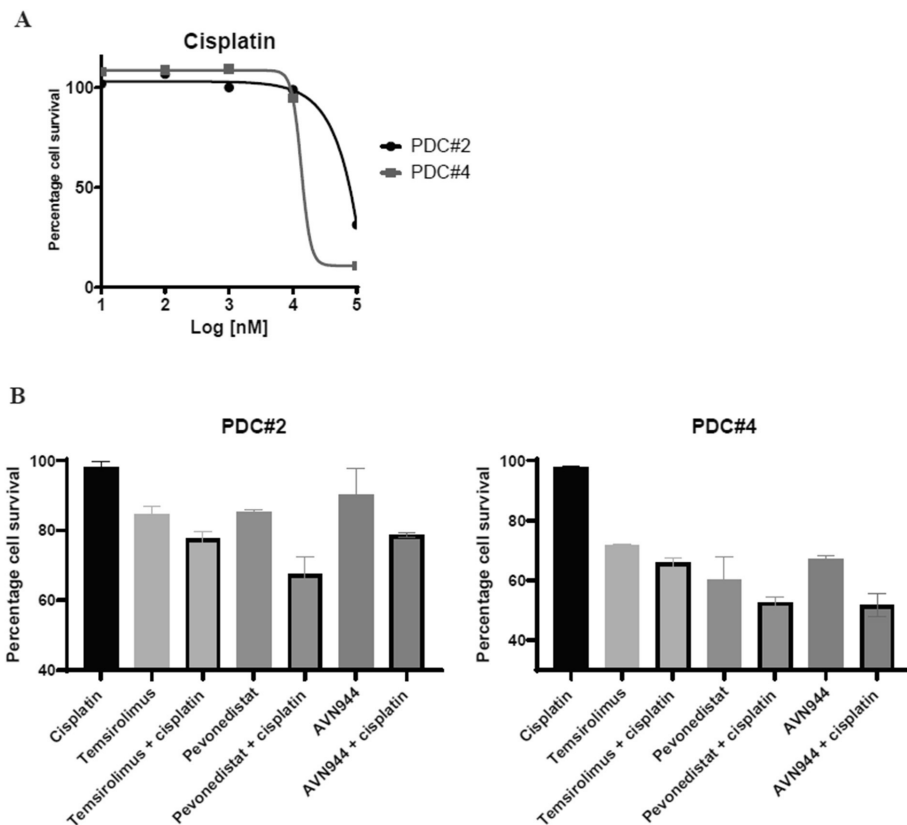
Figure S5. The effect of cisplatin (**A**) and cisplatin in combination with other drugs (**B**) on PDC#2 and PDC#4. (**A**) Drug response curves for cisplatin sensitivity in PDC#2 and PDC#4. Five concentrations of cisplatin are represented as log M values and cell viability is calculated as percentage inhibition, where the lowest cisplatin concentration is given 100% percentage cell survival. (**B**) Drug combination using cisplatin together with either temsirolimus, pevonedistat and AVN944 showed enhanced cytotoxic activity in both, PDC#2 and PDC#4 when both drugs were added, compared to either treatment alone. For drug combinations, a concentration of 1 μM cisplatin was chosen, as it had no effect on cell survival in (**A**). Other drugs were used at concentration of 1 nM (temsirolimus) and 100 nM (pevonedistat and AVN944). PDCs were treated with drugs or drug-combinations as indicated for 72 h and cell viability was calculated as percentage inhibition compared to vehicle (DMSO) control (100%). Each experiment was performed in duplicates and error bars indicate standard deviations.

Table S1. Signal values for of the Western blots in Figure 1.

	Channel	Name	Signal	Signal	Signal
	Figure 1A				
PCSK9**	Channel	Name	Signal	Signal	Signal
	700	HeLa	174	111	1540
	700	JHOS2	32,9	0,291	219
	700	Kuramochi	38,2	23,9	440
	700	COV362	57,6	35,9	729
	700	OVSAHO	66	6,13	152
	700	OVCAR3	213	216	1660
	700	OVCAR3cis	336	208	623
	700	A2780	41,3	35	716
	700	A2780cis	44,9	28,5	548
PCSK9*	Channel	Name	Signal	Signal	Signal
	700	HeLa	416	271	2720
	700	JHOS2	57,6	28,5	642
	700	Kuramochi	13,6	29	874
	700	COV362	203	84,7	1330
	700	OVSAHO	59,8	19	182
	700	OVCAR3	444	463	1280
	700	OVCAR3cis	951	652	716
	700	A2780	5,95	51,9	261
	700	A2780cis	11,1	67,9	428
Tubulin	Channel	Name	Signal	Signal	Signal
	800	HeLa	711	1390	5280
	800	JHOS2	583	1000	4200
	800	Kuramochi	616	1560	4280
	800	COV362	1190	2360	5220
	800	OVSAHO	372	749	3340
	800	OVCAR3	698	1550	3030
	800	OVCAR3cis	803	1610	3250
	800	A2780	647	1570	4610
	800	A2780cis	686	1010	4110

		Figure 1C		
		OVCAR3		
PCSK9**	Channel	Name		Signal
	700	0		4510
	700	24		13200
	700	48		47400
	700	72		166000
		HeLA		
PCSK9*	Channel	Name		Signal
	700	0		158
	700	24		2510
	700	48		13700
	700	72		26300

	Channel	Name	Signal	Signal	Signal
	Figure 1E				
PCSK9**	**Channel**	**Name**	Signal	Signal	Signal
	700	PDC #1	16,9	19,9	29,1
	700	PDC #2	20,6	41,9	49,9
	700	PDC #3	12	9,87	9,1
	700	PDC #4	32	66,6	65,3
	700	PDC #5	52,7	76,9	77
PCSK9*	Channel	Name	Signal	Signal	Signal
	700	PDC #1	32,3	43,9	36,2
	700	PDC #2	30,3	26,9	26,6
	700	PDC #3	16,1	26	17,3
	700	PDC #4	80,2	120	94,3
	700	PDC #5	149	108	100
Tubulin	Channel	Name	Signal	Signal	Signal
	800	PDC #1	11300	11300	11300
	800	PDC #2	11600	11600	11600
	800	PDC #3	8170	8170	8170
	800	PDC #4	11700	11700	11700
	800	PDC #5	11900	11900	11900

Table S2. Signal values from the western blots in Figure 2.

		Signals for quantifications in 2C					
Channel	**Antibody/band**	**OVCAR3 – Ctr-siRNA**			**OVCAR3 – PCSK9-siRNA**		
700	PCSK9* SN	1990	1910	4160	670	466	1390
700	PCSK9** CL	433	114	1390	75.7	14.8	605
700	PCSK9* CL	928	525	3170	144	72	947
800	β-tubulin	14500	1020	5340	12800	951	6120
		Signals for quantifications in 2F					
Channel	**Antibody**	**JHOS2 - Ctrl**			**JHOS2 - PCSK9**		
800	AKT	2630	3380	2530	2910	3550	2870
700	pAKT (Ser 473)	611	734	548	958	1030	855
800	MEK1/2	813	741	1320	1020	642	1650
700	pMEK1/2 (Ser217/221)	256	415	407	304	344	532
800	ERK1/2	1430	2230	1070	1920	2620	1470
700	pERK1/2 (Thr202/Tyr204)	1000	3270	1730	811	4010	2220
800	β-tubulin	671	4570	1620	713	3890	1700